

FATTY ACID METABOLISM IN APICOMPLEXAN PARASITES

By

Gustavo A. Afanador

A dissertation submitted to Johns Hopkins University in conformity with the  
requirements for the degree of Doctor of Philosophy

Baltimore, Maryland

January 2014

© 2014 Gustavo A. Afanador

All Rights Reserved

## **Abstract**

*Plasmodium falciparum* and *Toxoplasma gondii* are human parasites that belong to the phylum Apicomplexa and are the causative agents of malaria and toxoplasmosis, respectively. These parasites infect billions of people annually worldwide causing significant morbidity. We made use of biochemical and biophysical methods to better understand essential fatty acid metabolism of these pathogens, such as Fatty Acid Synthesis type II (FAS-II) and lipoate metabolism. The apicoplast, a plastid organelle, harbors the machinery for FAS-II which is essential for the survival of *T. gondii* and for liver stage malaria parasites. A small biocide, triclosan, is known to target the last enzyme in FAS-II with high specificity. Several modifications were made to this scaffold molecule to increase its druggability properties, while retaining specificity. We designed a method to measure the inhibition and IC<sub>50</sub> values of triclosan analogues in 96-well plate format. Also, we modified a thermal shift assay to measure their binding affinity to the enzyme and determine their inhibition mode of action. The FAS-II produces octanoyl-ACP, which is the substrate of downstream enzymes to synthesize lipoate on pyruvate dehydrogenase (PDH). Contrary to the apicoplast, the mitochondrion relies on lipoate scavenged from the host which is essential for the survival of these parasites. In both parasites, two lipoate ligases are localized to the mitochondrion, LipL1 and LipL2. These ligases are believed to catalyze the attachment of lipoate to three lipoate-requiring substrates in the mitochondrion: the H-protein, the branch chain amino acid dehydrogenase (BCDH) and the  $\alpha$ -ketoglutarate dehydrogenase (KDH). We show that LipL1 is the sole lipoate ligase in the mitochondrion with specificity for the H-protein. The BCDH and KDH are lipoylated through a concerted mechanism: LipL1 produces the

conjugate lipoyl-AMP which is transferred to LipL2 to lipoylate the BCDH and KDH. LipL2 is unable to produce the lipoyl-AMP conjugate, but instead acts as a lipoyl-AMP:*N*-lysine lipoyltransferase. The two step LipL1+LipL2 lipoylation mechanism appears to be conserved in most apicomplexan parasites, since the genes encoding both enzymes are conserved. Furthermore, lipoate scavenging shows redox sensitivity for the lipoate redox state -a phenomenon that has not been previously described-. Last, we can target the mitochondrial proteins with lipoate analogues and inhibit their activities, causing cell growth inhibition. The lipoylation mechanism found in apicomplexan parasites differs from that found in metazoans, making it an attractive drug target.

PhD Advisor: Dr. Sean Prigge

Thesis committee: Dr. Daniel Leahy, Dr. Jürgen Bosch, Dr. James Stivers, Dr. Fidel Zavala

Thesis alternate: Dr. Herschel Wade

## **Acknowledgments**

I would like to recognize many individuals that have helped me throughout my scientific career both professionally and personally. I am very grateful to my advisor, Dr. Sean Prigge, for all his help, scientific discussion and guidance. Throughout my years at Hopkins his door was always open whether to discuss results, papers, presentations or for mentoring. I admire his way of thinking, troubleshooting, eloquent writing and communication skills. It has been an incredible opportunity developing as a scientist under his guidance.

I am also thankful for the good scientific discussion provided by my Thesis Advisory Committee throughout graduate school. I particularly want to thank Dr. Jürgen Bosch for his patience and help both at a personal and scientific level. I appreciate his help in my crystallography project, taking time to help me collect and analyze data. I want to recognize Dr. Sandra Gabelli for taking time and training to use the X-ray home source to diffract crystals and for data analysis. I would like to thank two professors in the labs next door, Dr. Fidel Zavala and Dr. Photini Sinnis, for mentoring and providing good advice and insight while looking for post-doctoral opportunities.

I joined the Biophysics Department at Hopkins in 2007 because of the great experiences and training I received during my undergraduate education. I was very fortunate to work at Dr. JoAnne Stubbe lab in the Summer of 2004, this being my first ever research experience. I was exposed at an early stage in an excellent lab, great scientific training and passion for enzymology, which led me to join Dr. Juan López-Garriga as my undergraduate laboratory. At Dr. López-Garriga I was exposed to study

protein function and structure relationship, which was how my interest evolved towards biophysics. I am extremely thankful to both professors for all their help and guidance, and to this day still answer emails and provide mentorship.

My journey in graduate school would not have been the same without the support of friends and lab mates. I have been fortunate to work in a collaborative and relaxed environment. I would like to thank current and past members of the Prigge lab and Prigge-adjacent labs: Maroya Spalding, Jolyn Gisselberg, Teegan Dellibovi-Ragheb, Aleah Roberts, Hugo Jhun, Gundula Bosch, Alfredo Guerra and Daniel Ragheb. In particular, I would like to thank Krista Matthews for all her help, scientific discussion and patience both inside and outside the lab.

Last, I would like to thank my family and friends without whom I would not be here: Arcadio Afanador, Margarita González, Karim and Itamar Afanador, my wonderful niece and nephew, and Aliana Lopez de Victoria.

## Table of Contents

<b>Abstract</b> .....	ii
<b>Acknowledgments</b> .....	iv
<b>Table of Contents</b> .....	vi
<b>List of Tables</b> .....	ix
<b>List of Figures</b> .....	x
<b>List of Abbreviations</b> .....	xii
<b>Chapter 1: Introduction to Lipoate Metabolism</b>	
Introduction to Lipoate.....	1
Lipoate Function in Complexes.....	2
Bacterial Lipoate Metabolism.....	3
Eukaryotic Lipoate Metabolism.....	8
Lipoate Metabolism in Apicomplexa.....	10
References.....	16
Figures.....	26
<b>Chapter 2: <i>Toxoplasma gondii</i> Enoyl Acyl Carrier Protein Inhibition Assay</b>	
Introduction.....	36
Materials and Methods.....	37
References.....	42
Table.....	45
<b>Chapter 3: Discrimination of Potent Inhibitors of <i>Toxoplasma gondii</i> Enoyl-Acyl Carrier Protein Reductase by a Thermal Shift Assay</b>	
Abstract.....	54

Introduction.....	55
Materials and Methods.....	57
Results and Discussion.....	62
Conclusions.....	74
Acknowledgments.....	75
References.....	76
Figures and Tables.....	87

**Chapter 4: Redox-Dependent Lipoylation of Mitochondrial Proteins in *Plasmodium***

*falciparum*

Abstract.....	98
Introduction.....	99
Materials and Methods.....	102
Results.....	111
Discussion.....	118
Conclusions.....	124
Acknowledgments.....	124
References.....	125
Figures and Tables.....	134

**Chapter 5: A New Family of Lipoate Attachment Enzyme Catalyzes Mitochondrial**

Lipoate Metabolism in Malaria Parasites

Abstract.....	148
Introduction.....	149
Materials and Methods.....	152

Results.....	158
Discussion.....	164
Conclusions.....	167
Acknowledgments.....	168
References.....	168
Figures and Tables.....	174
<b>Chapter 6: Conclusion</b>	
References.....	192
Figures.....	197
<b>Appendix I: Crystallization Attempts of <i>Plasmodium falciparum</i> Lipoate Ligase 1....</b>	<b>199</b>
<b>Curriculum vitae.....</b>	<b>210</b>



## List of Tables

<b>Table 2-1.</b> List of percent of inhibition and IC <sub>50</sub> values for triclosan and analogues against recombinant <i>TgENR</i> .....	45
<b>Table 3-1.</b> Inhibitory activity, toxicity and calculated physicochemical properties of 18 substituted triclosan inhibitors of <i>PfENR</i> and <i>MtInhA</i> .....	92
<b>Table 3-2.</b> Kinetic parameters of apicomplexan ENR enzymes.....	94
<b>Table 3-3.</b> Thermal shift assay results for potent inhibitors of <i>TgENR</i> from <b>Table 1</b> and those described elsewhere.....	95
<b>Table 4-1.</b> Primers and plasmids.....	146
<b>Table 5-1.</b> Primers and plasmids.....	182
<b>Table 5-2.</b> Changes in temperature of LipL1 in the presence of different ligands and reducing conditions as measured by thermal shift assay.....	183
<b>Table 5-3.</b> Sequence identity between known lipoate attachment enzymes.....	184
<b>Table A1.</b> Primers used for LipL1 mutants construction.....	209

## List of Figures

<b>Figure 1-1.</b> Different forms of the cofactor 1,2-dithiolane-3-pentanoic acid.....	26
<b>Figure 1-2.</b> Pyruvate Dehydrogenase (PDH) Complex.....	27
<b>Figure 1-3.</b> Different lipoate metabolic pathways.....	28
<b>Figure 1-4.</b> Typical mechanism of lipoate ligases.....	30
<b>Figure 1-5.</b> Lipoate ligases architecture.....	31
<b>Figure 1-6.</b> Conserved lysine is essential for overall ligase activity.....	32
<b>Figure 1-7.</b> Lipoate metabolism of <i>Plasmodium</i> spp. and <i>Toxoplasma gondii</i> .....	33
<b>Figure 1-8.</b> Fatty Acid Synthesis Type II (FAS-II).....	34
<b>Figure 3-1.</b> Thermal Shift Assay results for triclosan and compound 32.....	87
<b>Figure 3-2.</b> Binding and kinetic data for <i>TgENR</i> cofactors.....	88
<b>Figure 3-3.</b> Effect of $\text{NAD}^+$ and inhibitor concentration on the apparent dissociation constant of two <i>TgENR</i> inhibitors.....	89
<b>Figure 3-4.</b> Thermodynamic cycle for formation of the ternary inhibitor/ <i>TgENR</i> / $\text{NAD}^+$ complex.....	90
<b>Figure 3-5.</b> Inhibitor modeling in active site of <i>TgENR</i> .....	91
<b>Figure 4-1.</b> Lipoate synthesis and scavenging pathways.....	134
<b>Figure 4-2.</b> Harmonized LipL2 nucleotide sequence.....	135
<b>Figure 4-3.</b> BCDH and KDH localization and cell-based lipoylation assays.....	136
<b>Figure 4-4.</b> Analysis of <i>lplA</i> -/ <i>lipB</i> - knockout <i>E. coli</i> cell line JEG3.....	138
<b>Figure 4-5.</b> <i>In vitro</i> lipoylation assays.....	139
<b>Figure 4-6.</b> Ligation reactions proceed through an ATP-dependent reaction.....	140
<b>Figure 4-7.</b> Redox dependence of the two lipoylation routes.....	141

<b>Figure 4-8.</b> Modification of BCDH <sub>LD</sub> and KDH <sub>LD</sub> in the presence of THP.....	142
<b>Figure 4-9.</b> 6,8-dichlorooctanoate is attached to all substrates independent of redox environment.....	143
<b>Figure 4-10.</b> Modification of mitochondrial proteins with lipoate analogs.....	144
<b>Figure 4-11.</b> Updated mitochondrial lipoylation pathway for <i>P. falciparum</i> .....	145
<b>Figure 5-1.</b> Evaluation of anti-lipoamide antibodies.....	174
<b>Figure 5-2.</b> LipL1 activity is essential for lipoylation of all substrates.....	175
<b>Figure 5-3.</b> LipL2 activity is essential for lipoylation of the BCDH <sub>LD</sub> and KDH <sub>LD</sub> ....	176
<b>Figure 5-4.</b> Redox dependence of LipL2.....	177
<b>Figure 5-5.</b> LipL2 acts as an <i>N</i> -lysine lipoyltransferase.....	178
<b>Figure 5-6.</b> LipL2-like enzymes are conserved across many apicomplexan parasite species.....	179
<b>Figure 5-7.</b> Updated scheme of mitochondrial lipoate metabolism.....	180
<b>Figure 5-8.</b> Comparison of parasite and mammalian lipoate scavenging mechanisms.....	181
<b>Figure 6-1.</b> The dihydrolipoamide dehydrogenase (E3 subunit of lipoylated complexes) can catalyze the re-oxidation of the lipoyl moiety using NAD <sup>+</sup> .....	197
<b>Figure 6-2.</b> Kinetic analysis of E3 subunit using lipoate as a substrate.....	198
<b>Figure A-1.</b> Expression and purification of full length LipL1.....	205
<b>Figure A-2.</b> Crystallization attempts for full length LipL1.....	207
<b>Figure A-3.</b> d37LipL1 expression and purification attempts.....	208

## List of Abbreviations

6,8-diClO		6,8-dichlorooctanoate
8-BrO		8-bromooctanoate
acetyl-CoA		acetyl coenzyme A
ACP		acyl carrier protein
AMP		adenosine monophosphate
ATP		adenosine triphosphate
<i>Bt</i> or <i>B. taurus</i>	<i>Bos</i>	<i>taurus</i>
BCDH		branch chain amino acid dehydrogenase
<i>Bs</i> or <i>B. subtilis</i>		<i>Bacillus subtilis</i>
CoA		coenzyme A
Crotonyl-CoA		trans-2-butyryl-Coenzyme A
DMSO		dimethyl sulfoxide
DTT		dithiothreitol
E3		dihydrolipoamide dehydrogenase
<i>Ec</i> or <i>E. coli</i>		<i>Escherichia coli</i>
ENR		Enoyl-ACP Reductase
FAS-II		Fatty Acid Synthesis type II
GCV		glycine cleavage system
GFP		green fluorescent protein
GST		glutathione S-transferase
HFF		human foreskin fibroblasts
K <sub>d</sub>		binding constant

KDH	$\alpha$ -ketoglutarate dehydrogenase
LA	lipoic acid or lipoate
LA-AMP	lipoyl-AMP
LD	lipoylation domain
LipA	lipoate synthase
LipB	octanoyl transferase
LplA	lipoate ligase A
MBP	maltose binding protein
NADH	nicotinamide adenine dinucleotide
<i>P. berghei</i> or <i>Pb</i>	<i>Plasmodium berghei</i>
<i>P. falciparum</i> or <i>Pf</i>	<i>Plasmodium falciparum</i>
PDB	protein data bank
PDH	pyruvate dehydrogenase
Sw	solubility in water
<i>T. gondii</i> or <i>Tg</i>	<i>Toxoplasma gondii</i>
TCEP	tris(2-carboxyethyl)phosphine
TEV	tobacco etch virus
THP	tris(hydroxypropyl)phosphine
T <sub>m</sub>	melting temperature
TPSA	topological polar surface area
TSA	thermal shift assay

## **Chapter 1**

### **Introduction to Lipoate Metabolism**

## **Introduction to lipoate**

Lipoate (**Figure 1**) is a highly conserved cofactor involved in several oxidative decarboxylation reactions and one carbon metabolism.<sup>1</sup> This cofactor is a lipophilic molecule with acidic properties, and is involved in the anabolism of fatty acids. Lipoate has a role in catalysis of multienzyme complexes, such as  $\alpha$ -ketoacid dehydrogenases and the glycine cleavage system, involved in intermediate metabolism (**Figure 2**).<sup>1</sup> These enzymes require lipoate to be attached to a conserved lysine of the lipoylation domain, forming an amide linkage.<sup>2,3</sup> This lipoamide acts as a swinging arm shuffling reaction intermediates between different active sites in the multienzyme complexes. Additionally, due to the redox activity of lipoate, it can function as an antioxidant and free-radical scavenger.<sup>4,5</sup> Free living organisms employ different strategies to acquire lipoate including different mechanisms to scavenge or synthesize the cofactor. For microbial pathogens, these strategies impact the virulence of these organisms and the pathogenesis of the diseases they cause.<sup>6</sup> Here I review the function of lipoate in human pathogens with a focus on parasites belonging to the phylum Apicomplexa. Specifically, we look at the mechanism of lipoate scavenging, and the function and specificity of the enzymes involved in scavenging pathways.

## **Lipoate Function in Complexes**

To date, five lipoate requiring enzymes have been described. Three are  $\alpha$ -ketoacid dehydrogenases: pyruvate dehydrogenase (PDH),  $\alpha$ -ketoglutarate dehydrogenase (KDH) and branched chain amino acid  $\alpha$ -ketoacid dehydrogenase (BCDH).<sup>6</sup> These complexes

are composed of multiple copies of three subunits referred to as E1, E2 and E3 (**Figure 2**). A fourth complex, homologous to PDH, is the acetoin dehydrogenase which shares the general architecture of the  $\alpha$ -ketoacid dehydrogenases.<sup>6</sup> The fifth enzyme is the glycine cleavage system (GCV), which has a different architecture and is composed of four loosely associated proteins, called the P-, H-, T-, and L-proteins.<sup>6,7</sup> The GCV proteins are clearly related to those which form the  $\alpha$ -ketoacid dehydrogenases in the sense that the P-protein is homologous to E1 proteins and the L-protein is homologous to E3 proteins. The H-protein and T-protein are homologous to the lipoylation domains and catalytic domains of E2 proteins. Lipoate is attached through an amide bond to a specific lysine in the lipoylation domain (LD). LDs are typically found at the N-terminus of the E2 subunits and in the case of PDH E2 proteins, there can be up to three LDs in tandem.<sup>2,3</sup>

The catalytic cycle of lipoate dependent enzymes begins with lipoamide (lipoate attached to the LD through an amide bond) in the oxidized or close ring form. Lipoamide serves as the substrate for reductive acylation catalyzed by the E1 domain. The catalytic cycle of PDH serves as a good example and is illustrated in **Figure 2**. In the first step, the E1 domain uses its thiamine pyrophosphate cofactor to decarboxylate pyruvate followed by the transfer of the acetyl group to lipoamide on the E2 subunit. The flexible lipoamide group is used to transfer the acetyl group to the catalytic domain of the E2 subunit where it is transferred to coenzyme A. After this step, lipoamide is found in the reduced or open ring form, dihydrolipoamide. The flavin-dependent E3 subunit catalyzes the two-electron oxidation of dihydrolipoamide to lipoamide, forming NADH in the



process (**Figure 2**).<sup>6</sup> The GCV works in a similar fashion where the P-protein acts as the E1 subunit catalyzing the decarboxylation of glycine and formation of aminomethylene-lipoamide on the H-protein. The T-protein catalyzes the transfer of the methylene group to tetrahydrofolate, forming 5,10-methylene-tetrahydrofolate and releasing ammonia. The L-protein then acts as an E3 subunit catalyzing the oxidation of dihydrolipoamide to lipoamide.<sup>6</sup>

These complexes are typically involved in central metabolism in one carbon metabolism. The PDH complex catalyzes the oxidative decarboxylation of pyruvate to acetyl-CoA. Acetyl-CoA feeds into the citric acid cycle (TCA), fatty acid biosynthesis and elongation, and mevalonate pathway of isoprenoid biosynthesis.<sup>6,8</sup> The KDH complex converts  $\alpha$ -ketoglutarate to succinyl-CoA, which can be used in the TCA cycle or be diverted for heme and amino acid biosynthesis.<sup>9,10</sup> The BCDH complex functions as part of the degradation of branch chain amino acids.<sup>6</sup> The branch chain amino acids have to be deaminated by the action of a transaminase. The resulting  $\alpha$ -ketoacids are the substrates of BCDH to generate branch-chain-CoA molecules that can be converted into intermediates of the TCA cycle or used for branch chain fatty acid synthesis. The GCV system catalyzes the reversible decarboxylation of glycine. During glycine catabolism, the GCV produces NADH, CO<sub>2</sub>, NH<sub>3</sub> and the one-carbon donor molecule 5,10-methylene-tetrahydrofolate, which is used for the biosynthesis of some amino acids and nucleotides.<sup>11</sup>

## **Bacterial Lipoate Metabolism**

### *Lipoate Scavenging*

There are two general pathways by which organisms can acquire lipoate: scavenging and biosynthesis (**Figure 3**). The mechanisms for each pathway can differ from organism to organism. Lipoate metabolism has been best characterized in *Escherichia coli* (*E. coli*), which contains both scavenging and synthesis pathways (**Figures 3A and 3C**).<sup>12</sup> When lipoate is present in the media, *E. coli* scavenges the cofactor and a dedicated lipoate ligase (*EcLplA*) catalyzes the attachment of lipoate to the different substrates through an ATP dependent reaction. This enzyme proceeds through a two-step mechanism (**Figure 4**).<sup>13</sup> First, lipoate is activated with ATP forming the intermediate conjugate lipoyl-AMP. Second, the lipoyl moiety of the lipoyl-AMP conjugate is transferred to a conserved lysine of the apo-substrates. The *E. coli* lipoate ligase has been crystallized and found to have two domains, a large N-terminal domain and a small C-terminal domain (**Figure 5**).<sup>13</sup> In the unliganded form, the ligase is found in a conformation where the C-terminal domain folds over the active site. After the adenylation reaction, forming lipoyl-AMP, the C-terminal domain rotates relative to the N-terminal domain by about 180 degrees and the enzyme assumes a more linear stretched conformation. The lipoyl-AMP conjugate assumes a U-shape conformation with the adenine base and the dithiolane ring buried while the linker region containing the phosphate and part of the ribose ring is exposed to solvent in the active site of the ligase. When the ligase is in the linear conformation, it can recognize and bind protein lipoylation substrates (**Figure 5**).<sup>13</sup> Protein substrates are bound in a conformation that orients a specific lysine side chain towards the carbonyl carbon of the lipoyl moiety.

Subsequent attack by the amine of the lysine side chain breaks the phosphodiester bond of the conjugate, forming lipoylated protein and AMP.

It is known that a conserved lysine in the active site of *EcLplA* forms hydrogen bonds with the oxygen of both the lipoyl moiety and the phosphate in lipoyl-AMP (**Figure 6**).<sup>13</sup> This residue has been shown to be essential for both the activation and transfer of lipoate. Mutation of this lysine to alanine in the *EcLplA* resulted in almost complete abolishment of lipoylation in *in vitro* assays.<sup>13</sup> The hydrogen bonds formed between the lysine and lipoyl-AMP make the phosphodiester bond more labile for the apo-substrate to attack this bond and become lipoylated (**Figure 6**).<sup>13</sup>

Other organisms have been studied and found that the mechanism by which lipoate is acquired differs from *E. coli*. An example of this is *Thermoplasma acidophilum*, which has two separate proteins that come together to catalyze the activation of lipoate.<sup>14, 15</sup> Interestingly, these lipoate ligases (*TaLplA* and *TaLplB*) correspond to the N-terminal and C-terminal domains found in *E. coli*, respectively. *T. acidophilum* evolved to have both domains expressed on different genes.<sup>14, 15</sup> The C-terminal domain in *E. coli* and the *LplB* protein in *T. acidophilum* are not catalytically active, but are required for the formation of lipoyl-AMP. *TaLplA* (corresponding to the N-terminal domain in *EcLplA*) is sufficient to catalyze the transfer reaction without the presence of *TaLplB* if it is supplied with lipoyl-AMP.<sup>14-16</sup>

Another bacterium that has been studied for lipoate scavenging is *Chlamydia trachomatis* (*Ct*).<sup>17</sup> *Ct* is an obligate intracellular pathogen causative of sexually transmitted disease Chlamydia.<sup>18</sup> This bacterium presents an interesting scenario for

lipoate metabolism, which resembles what happens in the mitochondrion of Apicomplexa parasites (see below).<sup>17</sup> *Ct* encodes one gene for lipoate biosynthesis, the lipoyl synthase (*CtLipA*) with 47% sequence identity to *EcLipA*. However, *CtLipA* could not complement a lipoylation deficient cell line where *EcLplA* and *EcLipA* were knocked out, making it difficult to assign its function.<sup>17</sup> *C. trachomatis* does encode enzymes believed to be responsible for lipoate scavenging. Contrary to *E. coli*, which contains only one lipoate ligase, *Ct* contains two lipoate ligases: *CtLplA1* and *CtLplA2*, with 30% and 27% sequence identity to *EcLplA*, respectively. Furthermore, *Ct* contains four lipoylation substrates: the PDH, KDH, BCDH and the H-protein. Interestingly, no identifiable components of the GCV have been found in the *Ct* genome except for the H-protein.<sup>19</sup> Overall, this scenario is similar scenario to what we observe in *Plasmodium* spp. and other Apicomplexa which also contain two potential lipoate ligases and an incomplete GCV. Thus far, only *CtLplA1* has been shown to have lipoate ligase activity capable of complementing a lipoylation deficient *E. coli* cell line. It also lipoylates the *CtBCDH* *in vitro* in an ATP-dependent reaction. No activity has been detected for *CtLplA2*; it cannot complement the lipoylation deficient *E. coli* cell line or lipoylate the *CtBCDH* in an *in vitro* reaction.<sup>17</sup>

### *Lipoate Biosynthesis*

An alternative to lipoate scavenging is synthesis of the cofactor. Lipoate synthesis typically proceeds through the sequential action of two separate enzymes (**Figure 3C**). First, an octanoyl transferase (*EcLipB*) transfers the octanoyl moiety from octanoyl-Acyl

Carrier Protein (octanoyl-ACP) to the conserved lysine of the protein substrates.<sup>20</sup> A second enzyme, a lipoyl synthase (*EcLipA*), inserts two sulfur atoms at carbon 6 and 8 to yield the *R*-enantiomer, which is the biologically active form.<sup>21</sup> This pathway is well conserved throughout kingdoms, with two known variations on this theme. One exception is *Bacillus subtilis* (**Figure 3B**),<sup>22, 23</sup> in which a dedicated octanoyl transferase (*BsLipM*) transfers the octanoyl moiety from octanoyl-ACP specifically to the H-protein. A second enzyme (*BsLipM*) is needed to shuffle the octanoyl moiety from the H-protein to other protein substrates.<sup>22, 23</sup> Lastly, a lipoyl synthase (*BsLipA*) catalyzes the sulfur insertion reaction to generate lipoylated proteins.<sup>22, 23</sup>

## **Eukaryotic Lipoate Metabolism**

### *Fungal Lipoate Biosynthesis*

Another known pathway for lipoate biosynthesis is found in *Saccharomyces cerevisiae*,<sup>24, 25</sup> in which an octanoyl transferase (*ScLip2*) transfers the octanoyl moiety from octanoyl-ACP specifically to the H-protein.<sup>24, 25</sup> A second route has been proposed in *S. cerevisiae*, in which octanoyl-ACP is converted to octanoyl-CoA through the action of an acyl-ACP:CoA transferase. Octanoyl-CoA is the substrate of another octanoyl transferase (*ScLip3*) to lipoylate the PDH and KDH in the mitochondria of the fungus.<sup>25</sup> Then, a lipoyl synthase (*ScLip5*) inserts two sulfurs to generate lipoylated substrates for both routes of lipoylation. One possibility, not explored in recent publication, is that *ScLip5* could use octanoyl-ACP as substrate rendering the acyl-ACP:CoA transferase activity redundant. A previous report suggested the need for all four proteins (*ScLip2*,

*ScLip3*, *ScLip5* and H-protein) to remain in a complex to lipoylate the PDH and KDH.<sup>24</sup> Also, the proposed activity of *ScLip5* was to transfer the octanoyl moiety from octanoyl-H-protein, similar to what was observed in *B. subtilis*. These possibilities were not explored in a subsequent publication.<sup>25</sup> Thus, the physiologically relevant lipoylation routes in *Sc* remain unclear.

### *Mammalian Lipoate Metabolism*

Most of the work done to understand mammalian lipoate metabolism has been done in *Bos taurus* (*Bt*) (**Figure 3D**), but homologous enzymes have been identified in humans.<sup>13, 26-30</sup> Lipoate metabolism starts with the scavenging of free lipoate. Lipoate is activated preferentially with GTP, a difference to other systems, by a lipoate activating enzyme (LAE).<sup>29</sup> This LAE was identified to be a medium acyl-CoA synthase with no homology to any described lipoate ligase. The function of this enzyme is to generate lipoyl-GMP, which is taken by an *N*-lysine lipoyltransferase (*BtLipT*) to lipoylate the different substrates.<sup>26-28, 30</sup> The *BtLipT* enzyme is closely related to *EcLplA*, but it cannot catalyze the ligation reaction alone, and it relies on the activity of LAE to supply lipoyl-GMP. *BtLipT* has been crystallized in the presence and absence of lipoyl-AMP in the active site.<sup>13, 26</sup> Interestingly, both structures were found in the stretched conformation that was observed for the *EcLplA*/lipoyl-AMP binary complex (refer to **Figure 5**). Since the stretched conformation is thought to allow protein substrate binding, this may be an indication that *BtLipT* is poised to recruit protein substrates regardless of whether lipoyl-GMP is bound. The bovine lipoylation mechanism is presumably shared by humans and

differs significantly from other described systems including those found in apicomplexan parasites (see below).

## **Lipoate Metabolism in Apicomplexa**

### *Introduction to the phylum Apicomplexa*

The phylum Apicomplexa is comprised of protozoans that are exclusively the intracellular parasites of animals.<sup>6</sup> These protozoans, with some exceptions, contain two endosymbiont organelles: the mitochondrion and the apicoplast. These organelles harbor lipoate scavenging and biosynthesis pathways, respectively.<sup>6, 31-33</sup> The apicoplast is a non-photosynthetic organelle that resulted from the secondary endosymbiosis of a red algae that had previously incorporated a cyanobacterium.<sup>34</sup> As a result, the apicoplast harbors prokaryotic-like metabolic pathways that differ from human pathways, making it an attractive drug target.<sup>34, 35</sup>

Lipoate metabolism and/or downstream pathways are essential for survival of some parasites in this phylum, two of which are *Plasmodium* spp. and *Toxoplasma gondii* (*T. gondii*). Five *Plasmodium* spp. have been identified to cause malaria in humans: *P. falciparum*, *P. vivax*, *P. malariae*, *P. ovale* and *P. knowlesi*.<sup>36-39</sup> *Plasmodium falciparum* (*Pf*) is the deadliest parasite, causing over 1 million deaths annually, primarily affecting children under the age of 5 and pregnant women in sub-Saharan Africa and Southeast Asia.<sup>36-39</sup> *T. gondii* causes toxoplasmosis in humans and infects about one third of the world's population, with most of the deaths occurring in immunocompromised people.<sup>40-</sup>

### *Life cycle of Apicomplexan parasites*

*Plasmodium* spp. have a life cycle comprised of three stages: a sexual stage in the mosquito which serves as the vector for transmission; and two distinct asexual stages in the human host comprised of liver infection followed by the blood stage cycle. After transmission from the mosquito vector, malaria parasites exclusively infect a relatively small (<100) number of liver cells. Over the course of several days, they undergo rapid replication ultimately producing several thousand parasites per infected hepatocyte. These parasites leave the liver and infect erythrocytes beginning the blood stage cycle of the disease. Depending on the species, malaria parasites infect and replicate in red blood cells over the course of 1-2 days. When replication is complete, the erythrocyte ruptures releasing between one and two dozen parasites capable of infecting more erythrocytes. It is the synchronous rupture of erythrocytes during the red blood cell cycle of malaria which causes the debilitating periodic fevers that are the hallmark symptoms of the disease. The World Health Organizations recommends Artemisinin Combination Therapy (ACT) as a treatment of malaria, but treatment failure has been reported in some regions. Increasing drug resistant to current drugs makes it necessary to exploit essential pathways for drug development.<sup>46-48</sup> Drugs targeting the liver stage serve as prophylactic drugs preventing disease, whereas blood stage drugs serve as a treatment of the disease. One pathway that could serve as a target for both liver and blood stages is lipoate metabolism.<sup>31, 35</sup>



The *T. gondii* life cycle is comprised of a sexual phase that only takes place in the primary host (cats of the Felidae family), and an asexual phase that can occur in any warm-blooded animal, including humans.<sup>49, 50</sup> There is no available vaccine to prevent infection in humans. The only available treatments are the antifolate medicines sulfadiazine and pyrimethamine.<sup>42, 44</sup> These medications are effective against tachyzoites, the obligate intracellular form of the parasite in the acute stage of the disease, but they are ineffective against the encysted, latent bradyzoites.<sup>51</sup>

#### *Lipoate in Plasmodium spp.*

Lipoate metabolism has been described in *Plasmodium falciparum* (*Pf*) and *Plasmodium berghei*. *Plasmodium* spp. have been shown to have both synthesis and scavenging pathways (**Figure 7**).<sup>31-33, 52</sup> These pathways are non-redundant and are found in separate compartments. The parasite mitochondrion relies on lipoate scavenged from the host. This was shown by treating *Pf* parasites with radiolabeled lipoate (<sup>35</sup>S-lipoate), where only mitochondrial substrates were modified.<sup>31</sup> Treatment *Pf* parasites with a lipoate analog, 8-bromooctanoate (8-BrO), caused cell death with a MIC<sub>50</sub> of about 400 μM and resulted in dose-dependent reduced lipoylation of the mitochondrial substrates. These results suggested that lipoate scavenging is essential for blood stage parasite growth.<sup>31</sup>

Once lipoate is imported into the mitochondrion there are two candidate lipoate ligases, lipoate ligase 1 (LipL1) and lipoate ligase 2 (LipL2), that could catalyze the attachment of this cofactor to the lipoate requiring substrates through an ATP dependent reaction

(Figure 7).<sup>31, 52, 53</sup> Three possible substrates have been shown or predicted to be in the mitochondrion: the H protein of the GCV and the E2 subunits of the BCDH and KDH.<sup>7, 32</sup> It has been shown that LipL1 can complement a lipoylation deficient *E. coli* cell line, confirming its activity as a ligase. Also, recombinant LipL1 can lipoylate the H-protein in an *in vitro* lipoylation reaction that requires ATP.<sup>31</sup> Presumably, this activity is analogous to the ATP-dependent lipoate ligase reaction catalyzed by *EcLplA*. No activity is known for *P. falciparum* LipL2. It can partially complement a lipoylation deficient *E. coli* cell line, however, only partial growth was observed after four days of incubation, suggesting that it is a poor lipoate ligase.<sup>31</sup> As mentioned earlier, mitochondrial lipoate metabolism in *Plasmodium* spp. appears to be similar to what is observed in *C. trachomatis*. Interestingly, both identified lipoate ligase 2 (LipL2 in *Pf* and LplA2 in *Ct*) are more closely related to each other than to their lipoate ligase 1 counterparts. It would be interesting to determine if both share similar activities and conservation spanning the bacteria and protist kingdoms.

The lipoate synthesis machinery is exclusively localized to the apicoplast.<sup>54, 55</sup> The synthesis pathway in *Plasmodium* spp. follows the same steps as the one described for *E. coli*. Recent studies have shown that many apicoplast pathways are dispensable in the blood stage of malaria parasites.<sup>54, 55</sup> The apicoplast contains a single lipoate requiring protein, the pyruvate dehydrogenase (PDH).<sup>54</sup> This enzyme is responsible for the generation of acetyl-CoA, which feeds into the Fatty Acid Synthesis Type II pathway (FAS-II). The FAS-II pathway is dispensable for blood stage parasite growth, but it is essential for liver stage development and for progression from liver to blood stage.<sup>54</sup> The

PDH activity has also been shown to be essential for liver stage parasite development, making it a candidate target for malaria chemoprophylaxis.

*Plasmodium berghei* (*P. berghei*) is a rodent malaria parasite and cannot infect humans. However, *P. berghei* is well studied because it serves as a model system to study liver stage infection (in mice) which is much more difficult to do with human malaria parasite species. *P. berghei* contains both lipoate scavenging and biosynthesis pathways localized to the mitochondrion and apicoplast, respectively.<sup>55</sup> Similar to *P. falciparum*, treatment of *P. berghei* parasites with 8-BrO resulted in abolished lipoylation of mitochondrial substrates, but not of the apicoplast substrate, PDH. 8-BrO also resulted in reduced ability of the parasites to successfully complete liver stage development.<sup>55</sup> Furthermore, knockout of the LipB enzyme in the apicoplast resulted in sporozoites that are markedly attenuated in their infectivity for mice and arrest in very late liver stage.<sup>55</sup> Together, these results show the importance of lipoate metabolism for parasite development in both liver and blood stages.

#### *Lipoate in Toxoplasma gondii*

*T. gondii* also contains the biosynthesis and scavenging machinery which localize to the apicoplast and the mitochondrion, respectively (**Figure 7**).<sup>56-58</sup> As in *Plasmodium* spp., *T. gondii* relies on lipoate scavenged from the host and contains two lipoate ligase candidates, as well as the same lipoate requiring substrates in the mitochondrion.<sup>58</sup> It is likely that these enzymes share the same functions as in malaria parasites, since these organisms are very similar. Treatment of *T. gondii* parasites with 8-BrO also resulted in

growth inhibition, presumably due to inhibition of key lipoate-dependent proteins in the mitochondrion.<sup>58</sup> Apicoplast metabolism appears to have elevated significance in *T. gondii* compared to *Plasmodium* spp. The only substrate is also the PDH and the lipoate synthesis machinery functions the same way as for *Plasmodium*.<sup>57</sup> The role of the PDH in the apicoplast is also to supply acetyl-CoA to the FAS-II pathway. Contrary to results observed for erythrocytic stage *P. falciparum*, in *T. gondii* the lipoate biosynthesis machinery, PDH activity, and the FAS-II pathway are essential for parasite survival (**Figure 8**).<sup>56</sup>

#### *Fatty Acid Synthesis Type II (FAS-II)*

Because of the essentiality of the FAS-II pathway in *T. gondii*, and the fact that these enzymes do not exist in humans, this pathway has been exploited for drug discovery. Humans have a FAS type I pathway which consist of a single polypeptide with multiple enzymatic domains.<sup>59</sup> The FAS-II elongation pathway consists of four separate enzymes that follow an iterative process beginning with the condensation of malonyl-CoA to the nascent fatty acid bound to ACP (**Figure 8**).<sup>60</sup> The condensation step is followed by reduction, dehydration and a final reduction step. The last enzyme in FAS-II is the Enoyl ACP Reductase (ENR), which is the rate-limiting step and is responsible for the final reductive step in each round of the fatty acid chain elongation, the NADH-dependent reduction of trans-2-enoyl-ACP to acyl-ACP.<sup>60</sup> This enzyme has been well studied and is the target of some antiparasitic and antibacterial compounds including diazaborines, isoniazid and triclosan.<sup>61-63</sup> Triclosan is a very potent inhibitor of *TgENR* with IC<sub>50</sub>

values around 20 nM and MIC<sub>50</sub> around 200 nM for *T. gondii* in culture.<sup>64</sup> Even though triclosan is a potent inhibitor, it is not suitable as a drug due to its poor solubility and drug like properties. As a result, triclosan has served as a scaffold molecule to increase its solubility and make it a more suitable drug.<sup>65, 66</sup>

## References

1. Reed, L. J.; Koike, M.; Levitch, M. E.; Leach, F. R. Studies on the nature and reactions of protein-bound lipoic acid. *J Biol Chem* **1958**, 232, 143-58.
2. Perham, R. N. Swinging arms and swinging domains in multifunctional enzymes: catalytic machines for multistep reactions. *Annu Rev Biochem* **2000**, 69, 961-1004.
3. Reche, P.; Perham, R. N. Structure and selectivity in post-translational modification: attaching the biotinyl-lysine and lipoyl-lysine swinging arms in multifunctional enzymes. *Embo Journal* **1999**, 18, 2673-2682.
4. Roy, S.; Packer, L. Redox regulation of cell functions by alpha-lipoate: biochemical and molecular aspects. *Biofactors* **1998**, 7, 263-7.
5. Arivazhagan, P.; Thilakavathy, T.; Panneerselvam, C. Antioxidant lipoate and tissue antioxidants in aged rats. *J Nutr Biochem* **2000**, 11, 122-7.
6. Spalding, M. D.; Prigge, S. T. Lipoic acid metabolism in microbial pathogens. *Microbiol Mol Biol Rev* **2010**, 74, 200-28.
7. Spalding, M. D.; Allary, M.; Gallagher, J. R.; Prigge, S. T. Validation of a modified method for Bxb1 mycobacteriophage integrase-mediated recombination in

Plasmodium falciparum by localization of the H-protein of the glycine cleavage complex to the mitochondrion. *Mol Biochem Parasitol* **2010**, 172, 156-60.

8. Cronan, J. E.; Zhao, X.; Jiang, Y. Function, attachment and synthesis of lipoic acid in Escherichia coli. *Adv Microb Physiol* **2005**, 50, 103-46.

9. Herbert, A. A.; Guest, J. R. Biochemical and genetic studies with lysine+methionine mutants of Escherichia coli: lipoic acid and alpha-ketoglutarate dehydrogenase-less mutants. *J Gen Microbiol* **1968**, 53, 363-81.

10. Heinemann, I. U.; Jahn, M.; Jahn, D. The biochemistry of heme biosynthesis. *Arch Biochem Biophys* **2008**, 474, 238-51.

11. Douce, R.; Bourguignon, J.; Neuburger, M.; Rebeille, F. The glycine decarboxylase system: a fascinating complex. *Trends Plant Sci* **2001**, 6, 167-76.

12. Morris, T. W.; Reed, K. E.; Cronan, J. E. Lipoic Acid Metabolism in Escherichia-Coli - the Lpla and Lipb Genes Define Redundant Pathways for Ligation of Lipoyl Groups to Apoprotein. *Journal of Bacteriology* **1995**, 177, 1-10.

13. Fujiwara, K.; Maita, N.; Hosaka, H.; Okamura-Ikeda, K.; Nakagawa, A.; Taniguchi, H. Global conformational change associated with the two-step reaction catalyzed by Escherichia coli lipoate-protein ligase A. *J Biol Chem* **2010**, 285, 9971-80.

14. Kim, D. J.; Kim, K. H.; Lee, H. H.; Lee, S. J.; Ha, J. Y.; Yoon, H. J.; Suh, S. W. Crystal structure of lipoate-protein ligase A bound with the activated intermediate: insights into interaction with lipoyl domains. *J Biol Chem* **2005**, 280, 38081-9.

15. McManus, E.; Luisi, B. F.; Perham, R. N. Structure of a putative lipoate protein ligase from *Thermoplasma acidophilum* and the mechanism of target selection for post-translational modification. *J Mol Biol* **2006**, 356, 625-37.
16. Christensen, Q. H.; Cronan, J. E. The *Thermoplasma acidophilum* LplA-LplB complex defines a new class of bipartite lipoate-protein ligases. *J Biol Chem* **2009**, 284, 21317-26.
17. Ramaswamy, A. V.; Maurelli, A. T. *Chlamydia trachomatis* serovar L2 can utilize exogenous lipoic acid through the action of the lipoic acid ligase LplA1. *J Bacteriol* **2010**, 192, 6172-81.
18. Zomorodipour, A.; Andersson, S. G. Obligate intracellular parasites: *Rickettsia prowazekii* and *Chlamydia trachomatis*. *FEBS Lett* **1999**, 452, 11-5.
19. Stephens, R. S.; Kalman, S.; Lammel, C.; Fan, J.; Marathe, R.; Aravind, L.; Mitchell, W.; Olinger, L.; Tatusov, R. L.; Zhao, Q.; Koonin, E. V.; Davis, R. W. Genome sequence of an obligate intracellular pathogen of humans: *Chlamydia trachomatis*. *Science* **1998**, 282, 754-9.
20. Jordan, S. W.; Cronan, J. E. The *Escherichia coli* lipB gene encodes lipoyl (octanoyl)-acyl carrier protein : protein transferase. *Journal of Bacteriology* **2003**, 185, 1582-1589.
21. Miller, J. R.; Busby, R. W.; Jordan, S. W.; Cheek, J.; Henshaw, T. F.; Ashley, G. W.; Broderick, J. B.; Cronan, J. E.; Marletta, M. A. *Escherichia coli* LipA is a lipoyl synthase: In vitro biosynthesis of lipoylated pyruvate dehydrogenase complex from octanoyl-acyl carrier protein. *Biochemistry* **2000**, 39, 15166-15178.

22. Christensen, Q. H.; Martin, N.; Mansilla, M. C.; de Mendoza, D.; Cronan, J. E. A novel amidotransferase required for lipoic acid cofactor assembly in *Bacillus subtilis*. *Mol Microbiol* **2011**, *80*, 350-63.
23. Martin, N.; Christensen, Q. H.; Mansilla, M. C.; Cronan, J. E.; de Mendoza, D. A novel two-gene requirement for the octanoyltransfer reaction of *Bacillus subtilis* lipoic acid biosynthesis. *Mol Microbiol* **2011**, *80*, 335-49.
24. Schonauer, M. S.; Kastaniotis, A. J.; Kursu, V. A.; Hiltunen, J. K.; Dieckmann, C. L. Lipoic acid synthesis and attachment in yeast mitochondria. *J Biol Chem* **2009**, *284*, 23234-42.
25. Hermes, F. A.; Cronan, J. E. The role of the *Saccharomyces cerevisiae* lipoate protein ligase homologue, Lip3, in lipoic acid synthesis. *Yeast* **2013**, *30*, 415-27.
26. Fujiwara, K.; Hosaka, H.; Matsuda, M.; Okamura-Ikeda, K.; Motokawa, Y.; Suzuki, M.; Nakagawa, A.; Taniguchi, H. Crystal structure of bovine lipoyltransferase in complex with lipoyl-AMP. *J Mol Biol* **2007**, *371*, 222-34.
27. Fujiwara, K.; Okamura-Ikeda, K.; Motokawa, Y. Cloning and expression of a cDNA encoding bovine lipoyltransferase. *J Biol Chem* **1997**, *272*, 31974-8.
28. Fujiwara, K.; Okamura-Ikeda, K.; Motokawa, Y. Purification and characterization of lipoyl-AMP:N epsilon-lysine lipoyltransferase from bovine liver mitochondria. *J Biol Chem* **1994**, *269*, 16605-9.
29. Fujiwara, K.; Takeuchi, S.; Okamura-Ikeda, K.; Motokawa, Y. Purification, characterization, and cDNA cloning of lipoate-activating enzyme from bovine liver. *J Biol Chem* **2001**, *276*, 28819-23.



30. Fujiwara, K.; Suzuki, M.; Okumachi, Y.; Okamura-Ikeda, K.; Fujiwara, T.; Takahashi, E.; Motokawa, Y. Molecular cloning, structural characterization and chromosomal localization of human lipoyltransferase gene. *Eur J Biochem* **1999**, *260*, 761-7.
31. Allary, M.; Lu, J. Z.; Zhu, L.; Prigge, S. T. Scavenging of the cofactor lipoate is essential for the survival of the malaria parasite *Plasmodium falciparum*. *Mol Microbiol* **2007**, *63*, 1331-44.
32. Gunther, S.; McMillan, P. J.; Wallace, L. J.; Muller, S. *Plasmodium falciparum* possesses organelle-specific alpha-keto acid dehydrogenase complexes and lipoylation pathways. *Biochem Soc Trans* **2005**, *33*, 977-80.
33. McMillan, P. J.; Stimmler, L. M.; Foth, B. J.; McFadden, G. I.; Muller, S. The human malaria parasite *Plasmodium falciparum* possesses two distinct dihydrolipoamide dehydrogenases. *Mol Microbiol* **2005**, *55*, 27-38.
34. Lim, L.; McFadden, G. I. The evolution, metabolism and functions of the apicoplast. *Philos Trans R Soc Lond B Biol Sci* **2010**, *365*, 749-63.
35. Storm, J.; Muller, S. Lipoic acid metabolism of *Plasmodium*--a suitable drug target. *Curr Pharm Des* **2012**, *18*, 3480-9.
36. Mudhune, S. A.; Okiro, E. A.; Noor, A. M.; Zurovac, D.; Juma, E.; Ochola, S. A.; Snow, R. W. The clinical burden of malaria in Nairobi: a historical review and contemporary audit. *Malar J* **2011**, *10*, 138.

37. Okiro, E. A.; Al-Taiar, A.; Reyburn, H.; Idro, R.; Berkley, J. A.; Snow, R. W. Age patterns of severe paediatric malaria and their relationship to Plasmodium falciparum transmission intensity. *Malaria Journal* **2009**, *8*.
38. Okiro, E. A.; Bitira, D.; Mbabazi, G.; Mpimbaza, A.; Alegana, V. A.; Talisuna, A. O.; Snow, R. W. Increasing malaria hospital admissions in Uganda between 1999 and 2009. *Bmc Medicine* **2011**, *9*.
39. Okiro, E. A.; Mutheu, J.; Gething, P. W.; Juma, E.; Snow, R. W. The Changing Patterns of Malaria Admissions since 1999 at 18 Hospitals across Kenya. *American Journal of Tropical Medicine and Hygiene* **2009**, *81*, 54-54.
40. Boyer, K.; Marcinak, J.; McLeod, R. *Toxoplasma gondii (Toxoplasmosis)*. 3rd ed.; Churchill Livingstone: New York, 2009.
41. McLeod, R.; Boyer, K.; Karrison, T.; Kasza, K.; Swisher, C.; Roizen, N.; Jalbrzikowski, J.; Remington, J.; Heydemann, P.; Noble, A. G.; Mets, M.; Holfels, E.; Withers, S.; Latkany, P.; Meier, P. Outcome of treatment for congenital toxoplasmosis, 1981-2004: the National Collaborative Chicago-Based, Congenital Toxoplasmosis Study. *Clin Infect Dis* **2006**, *42*, 1383-94.
42. McLeod, R.; Khan, A. R.; Noble, G. A.; Latkany, P.; Jalbrzikowski, J.; Boyer, K. Severe sulfadiazine hypersensitivity in a child with reactivated congenital toxoplasmic chorioretinitis. *Pediatr Infect Dis J* **2006**, *25*, 270-2.
43. Olariu, T. R.; Remington, J. S.; McLeod, R.; Alam, A.; Montoya, J. G. Severe congenital toxoplasmosis in the United States: clinical and serologic findings in untreated infants. *Pediatr Infect Dis J* **2011**, *30*, 1056-61.

44. Remington, J. S.; McLeod, R.; Thulliez, P.; Desmonts, G. *Toxoplasmosis*. 7th ed.; Elsevier Saunders: Philadelphia, 2011.
45. Swisher, C. N.; Boyer, K.; McLeod, R. Congenital toxoplasmosis. The Toxoplasmosis Study Group. *Semin Pediatr Neurol* **1994**, 1, 4-25.
46. Fidock, D. A.; Eastman, R. T.; Ward, S. A.; Meshnick, S. R. Recent highlights in antimalarial drug resistance and chemotherapy research. *Trends Parasitol* **2008**, 24, 537-44.
47. Hay, S. I.; Guerra, C. A.; Gething, P. W.; Patil, A. P.; Tatem, A. J.; Noor, A. M.; Kabaria, C. W.; Manh, B. H.; Elyazar, I. R.; Brooker, S.; Smith, D. L.; Moyeed, R. A.; Snow, R. W. A world malaria map: Plasmodium falciparum endemicity in 2007. *PLoS Med* **2009**, 6, e1000048.
48. Phyto, A. P.; Nkhoma, S.; Stepniewska, K.; Ashley, E. A.; Nair, S.; McGready, R.; ler Moo, C.; Al-Saai, S.; Dondorp, A. M.; Lwin, K. M.; Singhasivanon, P.; Day, N. P.; White, N. J.; Anderson, T. J.; Nosten, F. Emergence of artemisinin-resistant malaria on the western border of Thailand: a longitudinal study. *Lancet* **2012**, 379, 1960-6.
49. Dubey, J. P. The history of Toxoplasma gondii--the first 100 years. *J Eukaryot Microbiol* **2008**, 55, 467-75.
50. Dubey, J. P.; Lindsay, D. S.; Speer, C. A. Structures of Toxoplasma gondii tachyzoites, bradyzoites, and sporozoites and biology and development of tissue cysts. *Clin Microbiol Rev* **1998**, 11, 267-99.
51. Montoya, J. G.; Liesenfeld, O. Toxoplasmosis. *Lancet* **2004**, 363, 1965-76.

52. Wrenger, C.; Muller, S. The human malaria parasite *Plasmodium falciparum* has distinct organelle-specific lipoylation pathways. *Mol Microbiol* **2004**, *53*, 103-13.
53. Gunther, S.; Wallace, L.; Patzewitz, E. M.; McMillan, P. J.; Storm, J.; Wrenger, C.; Bissett, R.; Smith, T. K.; Muller, S. Apicoplast lipoic acid protein ligase B is not essential for *Plasmodium falciparum*. *PLoS Pathog* **2007**, *3*, e189.
54. Pei, Y.; Tarun, A. S.; Vaughan, A. M.; Herman, R. W.; Soliman, J. M.; Erickson-Wayman, A.; Kappe, S. H. *Plasmodium* pyruvate dehydrogenase activity is only essential for the parasite's progression from liver infection to blood infection. *Mol Microbiol* **2010**, *75*, 957-71.
55. Falkard, B.; Kumar, T. R.; Hecht, L. S.; Matthews, K. A.; Henrich, P. P.; Gulati, S.; Lewis, R. E.; Manary, M. J.; Winzeler, E. A.; Sinnis, P.; Prigge, S. T.; Heussler, V.; Deschermeier, C.; Fidock, D. A key role for lipoic acid synthesis during *Plasmodium* liver stage development. *Cell Microbiol* **2013**.
56. Roberts, C. W.; McLeod, R.; Rice, D. W.; Ginger, M.; Chance, M. L.; Goad, L. J. Fatty acid and sterol metabolism: potential antimicrobial targets in apicomplexan and trypanosomatid parasitic protozoa. *Mol Biochem Parasitol* **2003**, *126*, 129-42.
57. Thomsen-Zieger, N.; Schachtner, J.; Seeber, F. Apicomplexan parasites contain a single lipoic acid synthase located in the plastid. *FEBS Lett* **2003**, *547*, 80-6.
58. Crawford, M. J.; Thomsen-Zieger, N.; Ray, M.; Schachtner, J.; Roos, D. S.; Seeber, F. *Toxoplasma gondii* scavenges host-derived lipoic acid despite its de novo synthesis in the apicoplast. *EMBO J* **2006**, *25*, 3214-22.

59. Magnuson, K.; Jackowski, S.; Rock, C. O.; Cronan, J. E., Jr. Regulation of fatty acid biosynthesis in *Escherichia coli*. *Microbiol Rev* **1993**, *57*, 522-42.
60. Massengo-Tiasse, R. P.; Cronan, J. E. Diversity in enoyl-acyl carrier protein reductases. *Cell Mol Life Sci* **2009**, *66*, 1507-17.
61. Grassberger, M. A.; Turnowsky, F.; Hildebrandt, J. Preparation and antibacterial activities of new 1,2,3-diazaborine derivatives and analogues. *J Med Chem* **1984**, *27*, 947-53.
62. Rozwarski, D. A.; Grant, G. A.; Barton, D. H.; Jacobs, W. R., Jr.; Sacchettini, J. C. Modification of the NADH of the isoniazid target (InhA) from *Mycobacterium tuberculosis*. *Science* **1998**, *279*, 98-102.
63. Ward, W. H.; Holdgate, G. A.; Rowsell, S.; McLean, E. G.; Pauptit, R. A.; Clayton, E.; Nichols, W. W.; Colls, J. G.; Minshull, C. A.; Jude, D. A.; Mistry, A.; Timms, D.; Camble, R.; Hales, N. J.; Britton, C. J.; Taylor, I. W. Kinetic and structural characteristics of the inhibition of enoyl (acyl carrier protein) reductase by triclosan. *Biochemistry* **1999**, *38*, 12514-25.
64. McLeod, R.; Muench, S. P.; Rafferty, J. B.; Kyle, D. E.; Mui, E. J.; Kirisits, M. J.; Mack, D. G.; Roberts, C. W.; Samuel, B. U.; Lyons, R. E.; Dorris, M.; Milhous, W. K.; Rice, D. W. Triclosan inhibits the growth of *Plasmodium falciparum* and *Toxoplasma gondii* by inhibition of apicomplexan Fab I. *Int J Parasitol* **2001**, *31*, 109-13.
65. Cheng, G.; Muench, S. P.; Zhou, Y.; Afanador, G. A.; Mui, E. J.; Fomovska, A.; Lai, B. S.; Prigge, S. T.; Woods, S.; Roberts, C. W.; Hickman, M. R.; Lee, P. J.; Leed, S. E.; Auschwitz, J. M.; Rice, D. W.; McLeod, R. Design, synthesis, and biological activity

of diaryl ether inhibitors of *Toxoplasma gondii* enoyl reductase. *Bioorg Med Chem Lett* **2013**, 23, 2035-43.

66. Stec, J.; Fomovska, A.; Afanador, G. A.; Muench, S. P.; Zhou, Y.; Lai, B. S.; El Bissati, K.; Hickman, M. R.; Lee, P. J.; Leed, S. E.; Auschwitz, J. M.; Sommerville, C.; Woods, S.; Roberts, C. W.; Rice, D.; Prigge, S. T.; McLeod, R.; Kozikowski, A. P. Modification of triclosan scaffold in search of improved inhibitors for enoyl-acyl carrier protein (ACP) reductase in *Toxoplasma gondii*. *ChemMedChem* **2013**, 8, 1138-60.

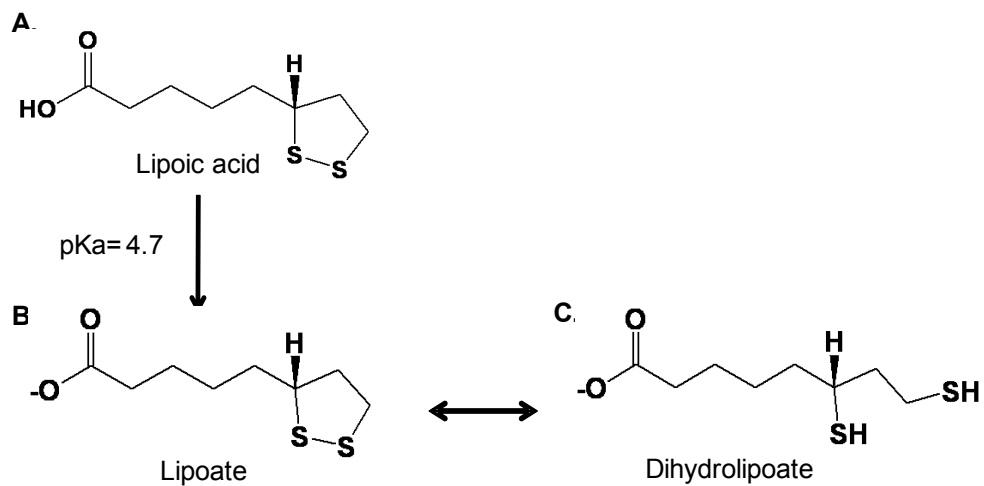
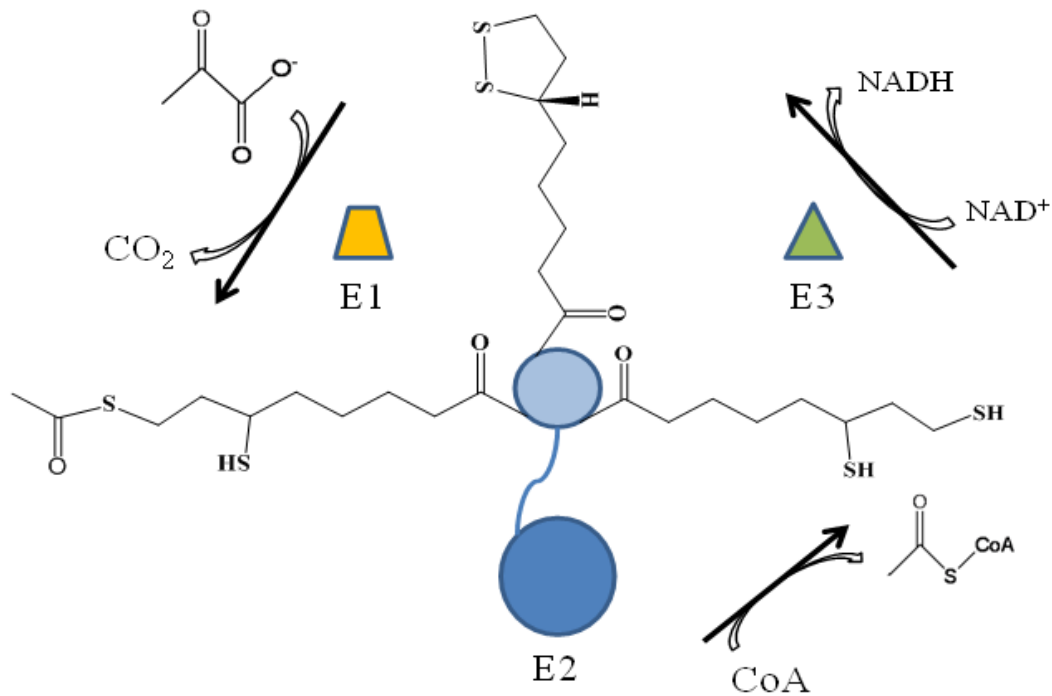


**Figure 1** – Different forms of the cofactor 1,2-dithiolane-3-pentanoic acid. A) Lipoic acid (protonated form). B) Lipoate (deprotonated) which is the form found in solution at neutral pH. C) Dihydrolipoate (reduced form of the dithiolane ring).



### Pyruvate Dehydrogenase

**Figure 2** – Pyruvate Dehydrogenase (PDH) Complex. PDH is one of five complexes that require lipoate for its function. PDH is composed of three subunits named: E1, E2 and E3. The E1 subunit catalyzes the decarboxylation of pyruvate using its thiamine pyrophosphate cofactor. The E2 subunit is composed of an N-terminal lipoyl domain and C-terminal catalytic domain. The E1 domain then catalyzes the reductive acetylation of the lipoamide on the E2 lipoyl domain. The acetyl-lipoamide product is then shuttled from the E1 subunit to the E2 catalytic domain where the acetyl group is transferred to coenzyme A (CoA) forming acetyl-CoA. The E3 subunit oxidizes the reduced form of lipoamide, dihydrolipoamide, in a NAD<sup>+</sup> dependent reaction and the catalytic cycle can be repeated.



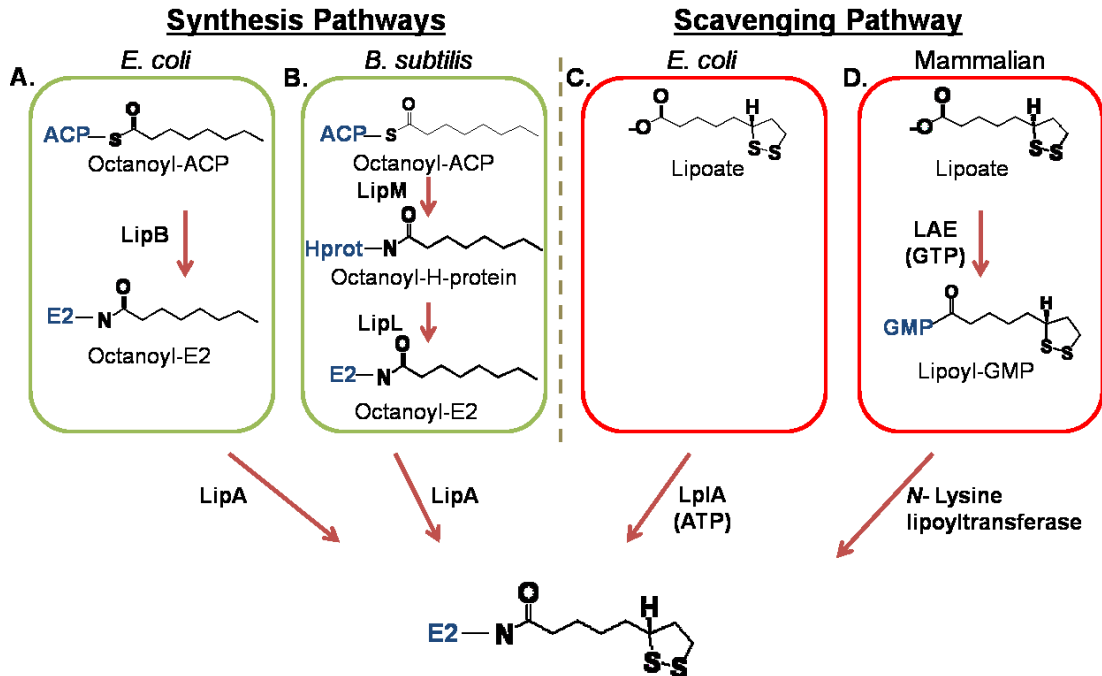
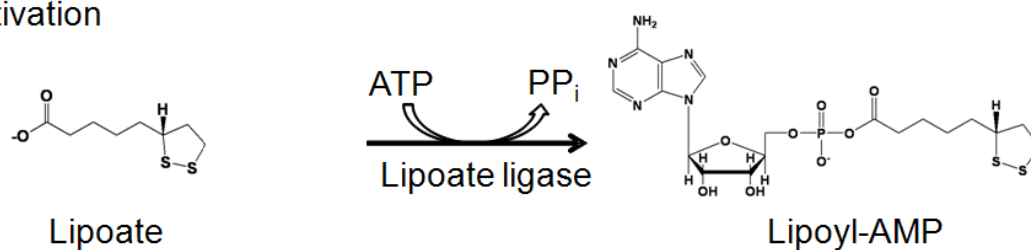


**Figure 3** – Different lipoate metabolic pathways. A) In *E. coli*, lipoate synthesis starts by transferring the octanoyl moiety from octanoyl-ACP to the different lipoate requiring substrates (E2 proteins) by the action of an octanoyl transferase (*EcLipB*). A second enzyme, lipoyl synthase (*EcLipA*), inserts two sulfurs atoms at carbon 6 and 8 to generate the lipoyl-substrates. B) *B. subtilis* lipoate synthesis also starts with the action of an octanoyl transferase (*BsLipM*), but with specificity for only the H-protein. A second enzyme, *BsLipL*, shuffles the octanoyl moiety to the other substrates. Last, a lipoyl synthase (*BsLipA*) generates the lipoyl moiety similar to *E. coli*. C) *E. coli* also has a scavenging pathway in which a dedicated lipoate ligase (*EcLplA*) takes free lipoate and activates it with ATP, generating lipoyl-AMP, and then transferring the lipoyl moiety to the protein substrates. D) In mammalian organisms lipoate is activated by a lipoate activating enzyme, a medium acyl-CoA synthase, through a GTP dependant reaction. The formed conjugate, lipoyl-GMP is the substrate for an *N*-lysine lipoyltransferase to lipoylate the different substrates.

### A. Activation



### B. Transfer

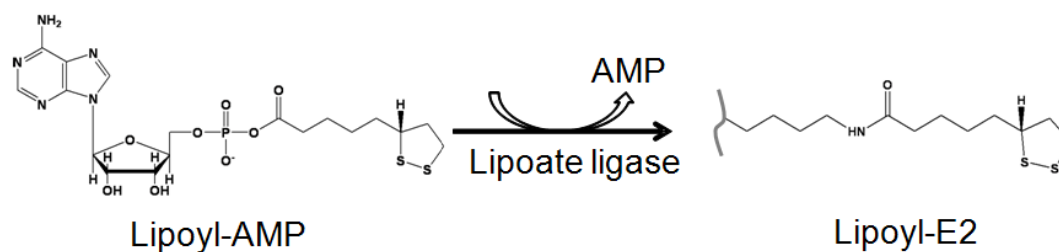


**Figure 4** – Typical mechanism of lipoate ligases. A) The first step is an adenylation reaction, in which lipoate is activated with ATP, generating the lipoyl-AMP conjugate. B) The lipoyl moiety from the conjugate is then transferred to a specific lysine of the different lipoate requiring substrates.

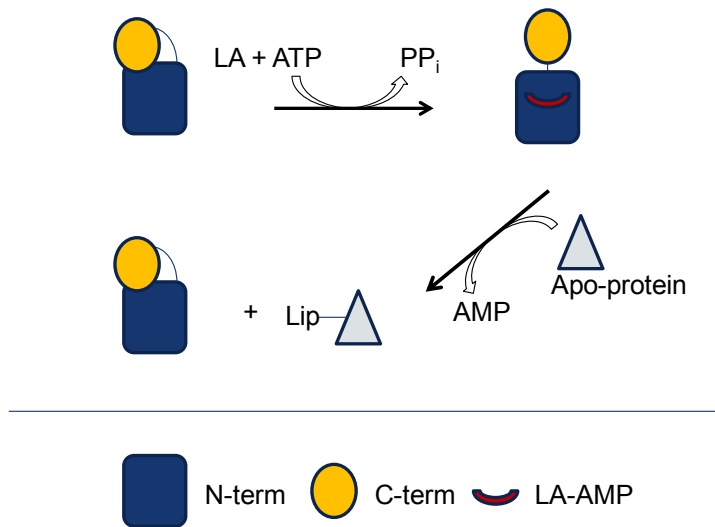


**Figure 5** – Lipoyl transferase architecture. Lipoyl transferases have two domains: a large N-terminal domain and a small C-terminal domain. The active site is found in the N-terminal domain where the lipoate, ATP and lipoyl-AMP are bound. In the unliganded form, the C-terminal adopts a bent conformation. Upon activation of lipoate, lipoyl-AMP formation, three conformational changes occur: 1) an adenylate binding loop becomes ordered protecting the AMP portion of lipoyl-AMP; 2) a second loop, called the lipoyl binding loop, folds over the lipoyl moiety; and 3) the C-terminal domain rotates relative to the N-terminal domain adopting a more linear conformation. This stretched conformation is how the enzyme recognizes the apo-substrate proteins. The  $\epsilon$ -amino group of the lysine of apo-substrates is positioned to attack to the carbonyl group of the lipoyl-AMP. After the transfer reaction is completed, the ligase assumes the relaxed or bent conformation, releasing lipoylated protein and AMP.

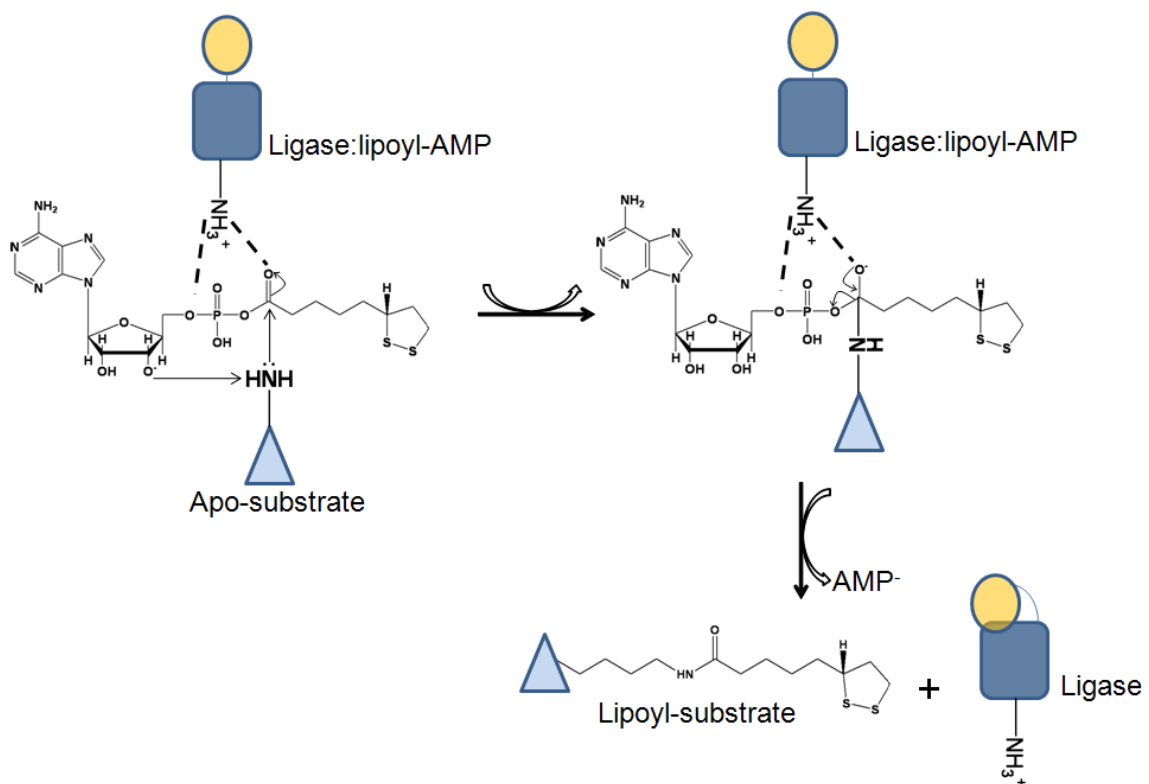


**Figure 6** – Conserved lysine is essential for overall ligase activity. It has been shown for *EcLplA* that a conserved lysine (K133) assembles the ATP and lipoate in the active site, forming hydrogen bonds with the carboxyl group of lipoate and the ribose and phosphate of ATP (not shown). This facilitates the nucleophilic attack of the carboxyl group of lipoate on the  $\alpha$ -phosphorous atom of ATP, forming lipoyl-AMP. Upon formation of lipoyl-AMP, the conjugate assumes a U-shaped conformation in the active site. The K133 remains hydrogen bonded with the carbonyl group and ribose moiety of lipoyl-AMP, helping to orient the conjugate in the active site. K133 also facilitates nucleophilic attack by the incoming lysine of the apo-substrates through stabilization of the resulting oxyanion.

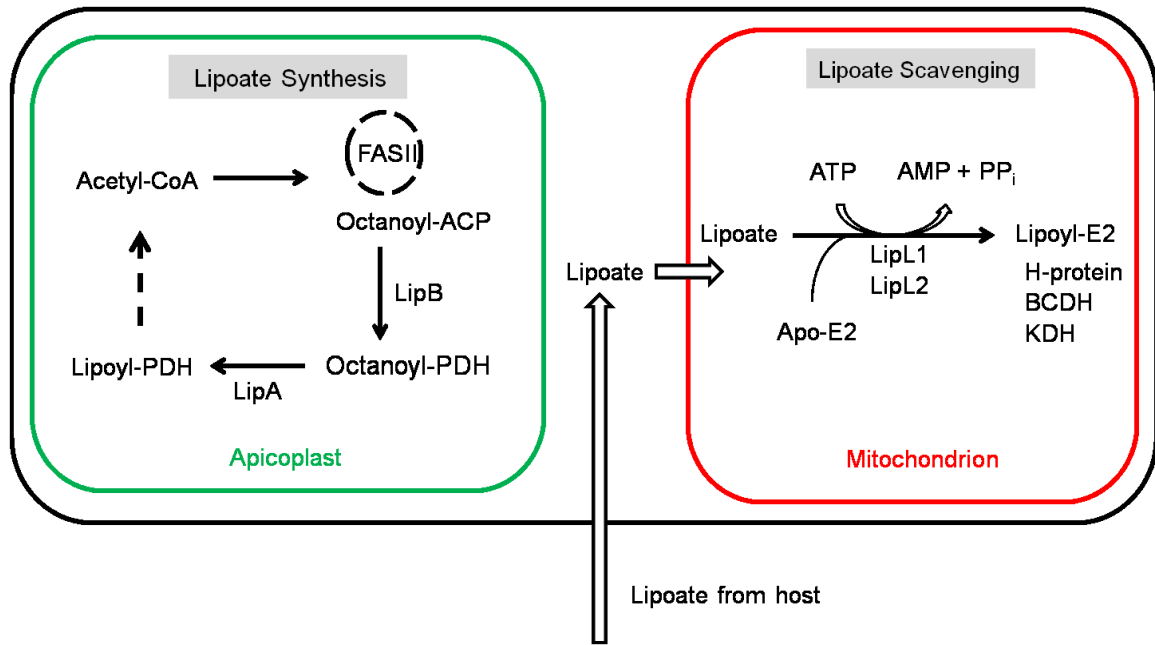


**Figure 7** – Lipoate metabolism of *Plasmodium* spp. and *Toxoplasma gondii*. Both parasites contain lipoate scavenging and synthesis pathways. These pathways are localized in distinct organelles and have been shown to be non-redundant. The mitochondrion relies on lipoate scavenged from the host involving the import of lipoate and its attachment to the different apo-substrates in an ATP dependent reaction by a lipoate ligase (LipL1 and/or LipL2). The apicoplast relies on lipoate synthesis for the sole substrate, pyruvate dehydrogenase (PDH). Lipoate is synthesized on the PDH by the action of two enzymes, octanoyl transferase (LipB) and lipoyl synthase (LipA). Lipoyl-PDH functions to generate acetyl-CoA, which feeds into the Fatty Acid Synthesis Type II pathway (FAS-II).

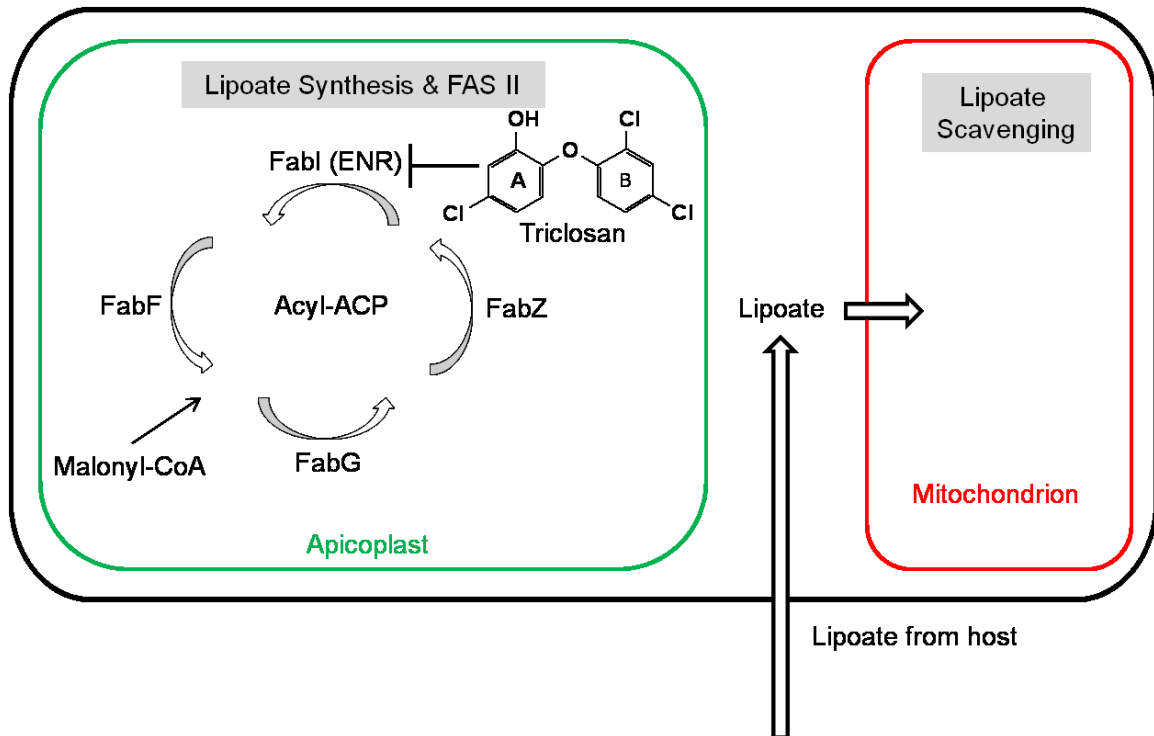


**Figure 8** – Fatty Acid Synthesis Type II (FAS-II). The FAS-II pathway is located in the apicoplast organelle and is essential for *Toxoplasma gondii* survival. FAS-II starts with the condensation of malonyl-CoA to a nascent acyl-ACP chain in an iterative process involving four separate enzymes. The last and rate-limiting step is catalyzed by FabI or Enoyl Acyl-Carrier Protein (ACP) Reductase (ENR). This enzyme is the target of different inhibitors including the biocide triclosan.

## Chapter 2

### *Toxoplasma gondii* Enoyl-Acyl Carrier Protein Inhibition Assay

The methods described in this chapter were used to generate data for the following publications:

*Antimicrob. Agents Chemother.*, 56, 266-2682 (2012).

*ChemMedChem*, 8, 442-461 (2013).

*Bioorg. Med. Chem. Lett.*, 23, 2035-2043 (2013).

*Bioorg. Med. Chem. Lett.*, 23, 3551-3555 (2013).

*ChemMedChem*, 8, 1138-1160 (2013).

*Biochemistry*, 52:9155-9166 (2013).



## Introduction

*Toxoplasma gondii* (*T. gondii*) is a protozoan parasite that belongs to the phylum Apicomplexa.<sup>1-3</sup> *T. gondii* contains a plastid organelle called the apicoplast that harbors plant-like pathways that differ from human pathways.<sup>4-6</sup> Several medicinal studies are looking for essential pathways that can serve as drug targets.<sup>7-9</sup> One such pathway is the Fatty Acid Synthesis type II (FAS-II) found in the apicoplast of *T. gondii*.<sup>10</sup> Contrary to the type II pathway found in *T. gondii*, humans rely on a type I pathway which is encoded in a single polypeptide chain. The biosynthesis of fatty acids is an iterative process starting with the condensation of malonyl-CoA to a nascent fatty acid chain that is covalently bound to the Acyl Carrier Protein (ACP). A total of four enzymes are found in FAS-II pathways, with the final reductive step in each round of fatty acid elongation catalyzed by the Enoyl-ACP Reductase (ENR). ENR catalyzes the NADH-dependent reduction of trans-2-enoyl-ACP to acyl-ACP.<sup>9,10</sup> The *T. gondii* ENR (*TgENR*) protein has been studied and found to be essential for parasite survival.<sup>9</sup>

Many inhibitors of bacterial and parasitic ENR enzymes have been previously described including diazaborines, isoniazid and triclosan (Table 1).<sup>9,11</sup> Triclosan is a very potent inhibitor of the *TgENR* enzyme with a low nanomolar IC<sub>50</sub> value; it also inhibits parasite growth in the low micromolar range. Regardless of its potency, triclosan is unsuitable for oral administration due to its poor pharmacokinetic properties, especially low solubility. Triclosan has served as a scaffold molecule in medicinal chemistry studies focused on increasing its solubility and improving the Absorption, Distribution, Metabolism, Excretion and Toxicity (ADMET) properties.<sup>7,8</sup> As part of a collaborative

effort focused on *TgENR* as a drug target, we developed a medium-throughput assay to assess potential inhibitors. Although trans-2-enoyl-ACP species are the physiological substrates for *TgENR*, the enzyme will catalyze the reduction of trans-2-enoyl-Coenzyme A species as well. We used trans-2-butyryl-Coenzyme A (crotonyl-CoA) since it is the cheapest ENR substrate commercially available. Using this substrate, we developed a kinetic assay of *TgENR* activity based on monitoring the absorbance of the NADH cofactor as it is consumed over the course of the reaction. We adapted this assay to function in 96-well plate format and ultimately assessed the activity of ~8,000 compounds.

We first expressed and purified recombinant *TgENR* as described previously.<sup>12</sup> An assay of *TgENR* enzymatic activity used previously<sup>13</sup> was adapted for use in 96-well plates. The activity of *TgENR* was monitored by consumption of NADH at a wavelength of 340 nm with an extinction coefficient of  $6220 \text{ M}^{-1}\text{cm}^{-1}$ . We monitored the NADH consumption throughout the experiment using a SpectraMax M2 plate reader. This machine measures the absorption in each well of the plate every 35 seconds for a total of 15 minutes. Each well contained a reaction with a final volume of 100  $\mu\text{L}$  in 96-well Corning UV plates. Each well contained a final concentration of 100  $\mu\text{M}$  Crotonyl-CoA (Sigma), 100  $\mu\text{M}$  NADH, 5 nM of *TgENR* and 1% DMSO. Initial screening was done with potential inhibitors (dissolved in DMSO) at a final concentration of 1  $\mu\text{M}$ . Dilution series were subsequently used to determine  $\text{IC}_{50}$  values for successful inhibitors.

## **Materials and Methods**

### *Reagent preparation*

1. 1mM Crotonyl-CoA: Stock solutions of 10 mM Crotonyl-CoA (in water) were stored at -80 degrees in aliquots of 100  $\mu$ L. A total of 900  $\mu$ L of dH<sub>2</sub>O was added to an aliquot immediately prior to use bringing it to the 1 mM working concentration.
2. Crotonyl-CoA plate: A total of 83  $\mu$ L of 1 mM of Crotonyl-CoA were pipetted into each well of the first row of a V-bottom plate (Costar 3896) to serve as the source material for a 96-well assay plate.
3. Drug plate:
  - a. In a different V-bottom plate, 20  $\mu$ L of DMSO was added to each of the eight wells in the first column of the plate to serve as baseline controls.
  - b. In columns 2-11, 20  $\mu$ L of 100  $\mu$ M compound diluted in DMSO (Sigma) were added to each well.
  - c. The eight wells in column 12 contained a dilution series of the inhibitor triclosan (in DMSO) starting with 10  $\mu$ M and ending with 610 pM (dilutions by factors of 4).
4. TgENR enzyme: The TgENR was stored in 10  $\mu$ L aliquots at a concentration of 0.5 mg/mL at -80 degrees for single use to avoid freeze/thaw cycles. Thawed enzyme was stored on ice.
5. 1 mM NADH: Aliquots of 120  $\mu$ L of 10 mM NADH stock solution were stored at -80 degrees for single use. This material must be used fairly soon after thawing since NADH oxidizes in solutions exposed to air. A total of 1080  $\mu$ L of dH<sub>2</sub>O

was added to this aliquot to generate the 1mM NADH working solution which was kept on ice.

#### *Assay plate preparation*

1. A 12-well multichannel pipette was used to transfer 10  $\mu\text{L}$  of 1 mM Crotonyl-CoA from the first row of the Crotonyl-CoA plate to each row of a UV-plate (Sigma).
2. Using a 12-well multichannel pipette, a total of 1  $\mu\text{L}$  of each drug was transferred from the drug plate to the UV-plate row by row. Each row was pipetted twice to run the samples in duplicates at a final concentration of 1  $\mu\text{M}$ . It was important at this step to make sure that bubbles are not formed while pipetting the drugs.
3. The reaction buffer (9.5 mL of 127 mM Phosphate, 190 mM NaCl, pH 7.5) was then mixed with 1.2 mL of 1 mM NADH and 4  $\mu\text{L}$  of 0.5 mg/mL *TgENR* in a 15 mL conical tube. This reaction mixture was then transferred to a v-bottom reservoir.
4. Then a total of 89  $\mu\text{L}$  of reaction mixture was added to the assay plate to yield a final concentration of 5nM *TgENR*, 100 mM Na/K Phosphate and 150 mM NaCl buffer pH 7.5 and 100  $\mu\text{M}$  NADH. The reaction mixture was added row by row (with a brief with pipetting up and down) with a 12-channel pipettor to initiate the assay. The assay plate was then loaded on the SpectraMax M2 plate reader and the absorbance in each well was monitored at room temperature.

### *Plate reader and assay*

1. The SpectraMax plate reader measures the absorption at 340 nm for 15 minutes with measurements being made for each well in the 96-well plate every 35 seconds. The slopes were calculated by the program in the SpectraMax M2, and analyzed using Excel. Because we were monitoring the NADH consumption, the slopes had a negative value. In general, using the time frame of 50-200 seconds to calculate the slopes was ideal for the amount of enzymatic activity that we observed.
2. The first column of each plate contained blank reactions with 1% DMSO which served as baseline activities for each row of the assay plate.
3. The last column of each plate contained the potent inhibitor triclosan which served as a positive control for *Tg*ENR inhibition.
4. The enzymatic activity was determined by comparing the slopes of the absorbance curves for each drug ( $m_{\text{drug}}$ ) to those of the baselines ( $m_{\text{blank}}$ ) in the first column of the plate.
5. The percent of inhibition was calculated using the following equation. Each compound was screened in duplicates in the same assay at 1  $\mu\text{M}$  final concentration.

$$\% \text{ inhibition at } 1 \mu\text{M} = \left( \frac{m_{\text{drug}} - m_{\text{blank}}}{m_{\text{blank}}} \right) * -100$$

To determine the reproducibility and quality of the assay, we calculated the Z-factor. The Z-factor<sup>14</sup> is a statistic value that describes the quality of the assay, with values between 0.5 and 1 being an excellent assay.

$$Z = 1 - \frac{(3\sigma_s - 3\sigma_c)}{|\mu_s - \mu_c|}$$

Where  $\sigma_s$  is the standard deviation of the sample,  $\sigma_c$  is the standard deviation of the control,  $\mu_s$  is the mean of the library sample and  $\mu_c$  is the mean of the library control. For the assay previously described, the Z-value was calculated from positive and negative control data spanning 25 plates and was found to be 0.65.

As mentioned previously, all compounds were initially screened in duplicate at a concentration of 1  $\mu$ M. The compounds with significant inhibition, >90%, were further analyzed to determine their IC<sub>50</sub> values. The IC<sub>50</sub> values were determined in triplicate with each replicate consisting of 11 inhibitor concentrations ranging from 10  $\mu$ M to 170 pM (serial dilutions by factors of 3), following the same protocol as described above. After obtaining the percent of inhibition for each concentration, a nonlinear regression analysis was performed using GraphPad Prism software. The output of GraphPad Prism gives the IC<sub>50</sub> value as well as a 95% confidence interval for each measurement. The table below was modified from different publications, which include the compound synthesis and other biological tests.<sup>7, 8, 15, 16</sup>

## References

1. Hill, D.; Dubey, J. P. *Toxoplasma gondii*: transmission, diagnosis and prevention. *Clin Microbiol Infect* **2002**, 8, 634-40.
2. McLeod, R.; Boyer, K.; Karrison, T.; Kasza, K.; Swisher, C.; Roizen, N.; Jalbrzikowski, J.; Remington, J.; Heydemann, P.; Noble, A. G.; Mets, M.; Holfels, E.;

- Withers, S.; Latkany, P.; Meier, P. Outcome of treatment for congenital toxoplasmosis, 1981-2004: the National Collaborative Chicago-Based, Congenital Toxoplasmosis Study. *Clin Infect Dis* **2006**, 42, 1383-94.
3. Boyer, K.; Marcinak, J.; McLeod, R. *Toxoplasma gondii (Toxoplasmosis)*. 3rd ed.; Churchill Livingstone: New York, 2009.
  4. Roberts, C. W.; McLeod, R.; Rice, D. W.; Ginger, M.; Chance, M. L.; Goad, L. J. Fatty acid and sterol metabolism: potential antimicrobial targets in apicomplexan and trypanosomatid parasitic protozoa. *Mol Biochem Parasitol* **2003**, 126, 129-42.
  5. McFadden, G. I.; Reith, M. E.; Munholland, J.; Lang-Unnasch, N. Plastid in human parasites. *Nature* **1996**, 381, 482.
  6. Kohler, S.; Delwiche, C. F.; Denny, P. W.; Tilney, L. G.; Webster, P.; Wilson, R. J.; Palmer, J. D.; Roos, D. S. A plastid of probable green algal origin in Apicomplexan parasites. *Science* **1997**, 275, 1485-9.
  7. Stec, J.; Fomovska, A.; Afanador, G. A.; Muench, S. P.; Zhou, Y.; Lai, B. S.; El Bissati, K.; Hickman, M. R.; Lee, P. J.; Leed, S. E.; Auschwitz, J. M.; Sommerville, C.; Woods, S.; Roberts, C. W.; Rice, D.; Prigge, S. T.; McLeod, R.; Kozikowski, A. P. Modification of triclosan scaffold in search of improved inhibitors for enoyl-acyl carrier protein (ACP) reductase in *Toxoplasma gondii*. *ChemMedChem* **2013**, 8, 1138-60.
  8. Cheng, G.; Muench, S. P.; Zhou, Y.; Afanador, G. A.; Mui, E. J.; Fomovska, A.; Lai, B. S.; Prigge, S. T.; Woods, S.; Roberts, C. W.; Hickman, M. R.; Lee, P. J.; Leed, S. E.; Auschwitz, J. M.; Rice, D. W.; McLeod, R. Design, synthesis, and biological activity

of diaryl ether inhibitors of *Toxoplasma gondii* enoyl reductase. *Bioorg Med Chem Lett* **2013**, 23, 2035-43.

9. McLeod, R.; Muench, S. P.; Rafferty, J. B.; Kyle, D. E.; Mui, E. J.; Kirisits, M. J.; Mack, D. G.; Roberts, C. W.; Samuel, B. U.; Lyons, R. E.; Dorris, M.; Milhous, W. K.; Rice, D. W. Triclosan inhibits the growth of *Plasmodium falciparum* and *Toxoplasma gondii* by inhibition of apicomplexan Fab I. *Int J Parasitol* **2001**, 31, 109-13.

10. Muench, S. P.; Prigge, S. T.; McLeod, R.; Rafferty, J. B.; Kirisits, M. J.; Roberts, C. W.; Mui, E. J.; Rice, D. W. Studies of *Toxoplasma gondii* and *Plasmodium falciparum* enoyl acyl carrier protein reductase and implications for the development of antiparasitic agents. *Acta Crystallogr D Biol Crystallogr* **2007**, 63, 328-38.

11. Zuther, E.; Johnson, J. J.; Haselkorn, R.; McLeod, R.; Gornicki, P. Growth of *Toxoplasma gondii* is inhibited by aryloxyphenoxypropionate herbicides targeting acetyl-CoA carboxylase. *Proc Natl Acad Sci U S A* **1999**, 96, 13387-92.

12. Muench, S. P.; Prigge, S. T.; Zhu, L.; Kirisits, M. J.; Roberts, C. W.; Wernimont, S.; McLeod, R.; Rice, D. W. Expression, purification and preliminary crystallographic analysis of the *Toxoplasma gondii* enoyl reductase. *Acta Crystallogr Sect F Struct Biol Cryst Commun* **2006**, 62, 604-6.

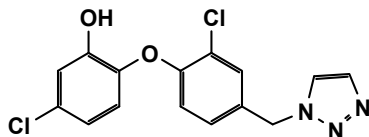
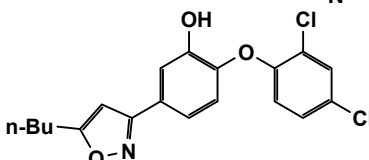
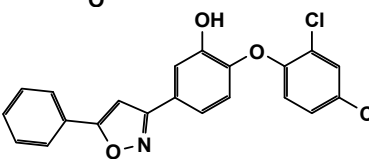
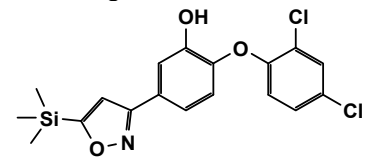
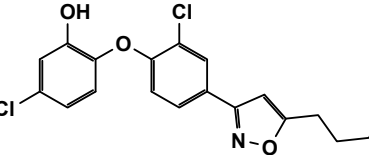
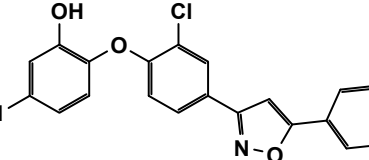
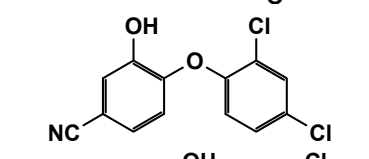
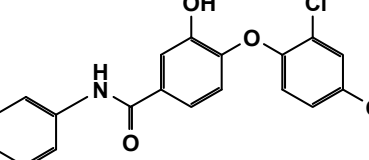
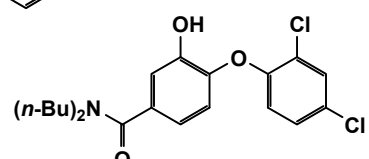
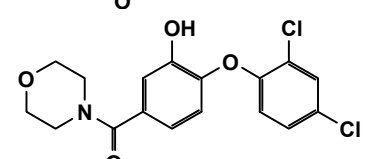
13. Tipparaju, S. K.; Muench, S. P.; Mui, E. J.; Ruzheinikov, S. N.; Lu, J. Z.; Hutson, S. L.; Kirisits, M. J.; Prigge, S. T.; Roberts, C. W.; Henriquez, F. L.; Kozikowski, A. P.; Rice, D. W.; McLeod, R. L. Identification and development of novel inhibitors of *Toxoplasma gondii* enoyl reductase. *J Med Chem* **2010**, 53, 6287-300.

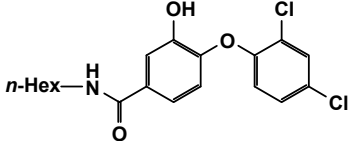
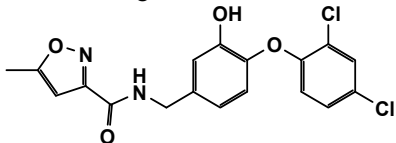
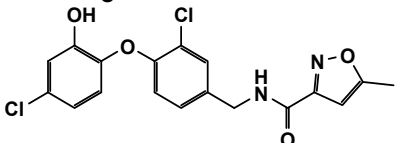
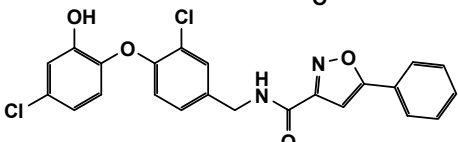
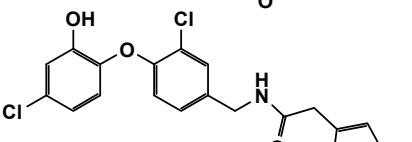
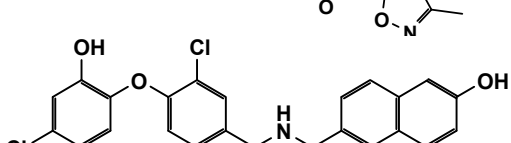
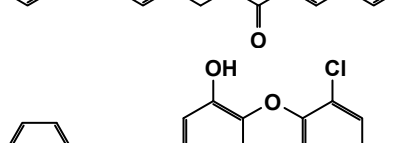
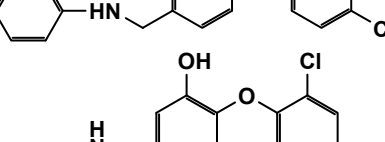
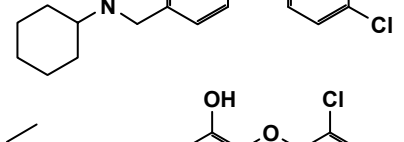
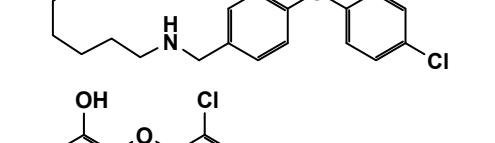


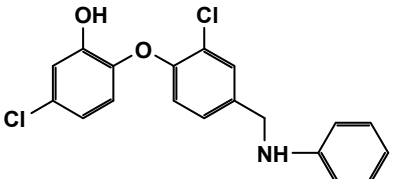
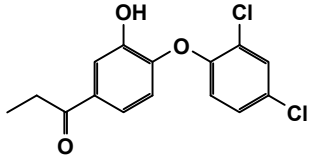
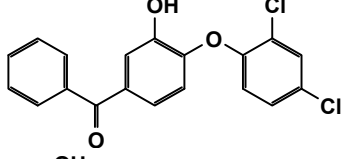
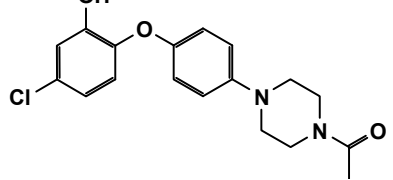
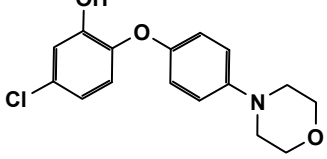
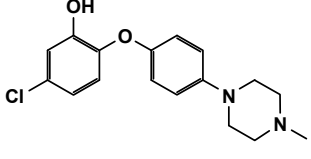
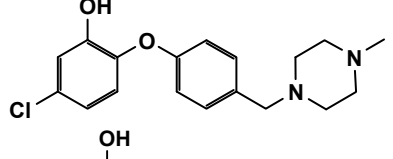
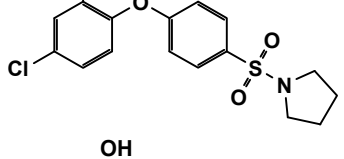
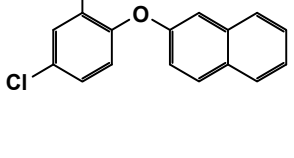
14. Zhang, J. H.; Chung, T. D.; Oldenburg, K. R. A Simple Statistical Parameter for Use in Evaluation and Validation of High Throughput Screening Assays. *J Biomol Screen* **1999**, 4, 67-73.
15. Schrader, F. C.; Glinca, S.; Sattler, J. M.; Dahse, H. M.; Afanador, G. A.; Prigge, S. T.; Lanzer, M.; Mueller, A. K.; Klebe, G.; Schlitzer, M. Novel type II fatty acid biosynthesis (FAS II) inhibitors as multistage antimalarial agents. *ChemMedChem* **2013**, 8, 442-61.
16. Muench, S. P.; Stec, J.; Zhou, Y.; Afanador, G. A.; McPhillie, M. J.; Hickman, M. R.; Lee, P. J.; Leed, S. E.; Auschwitz, J. M.; Prigge, S. T.; Rice, D. W.; McLeod, R. Development of a triclosan scaffold which allows for adaptations on both the A- and B-ring for transport peptides. *Bioorg Med Chem Lett* **2013**, 23, 3551-5.

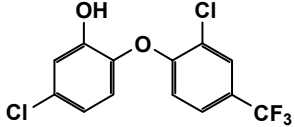
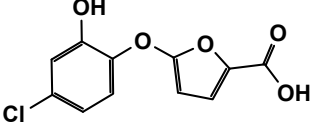
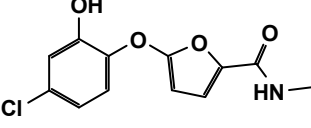
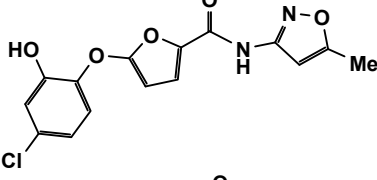
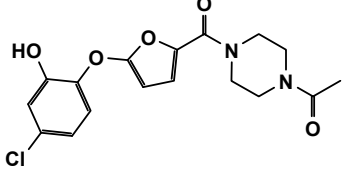
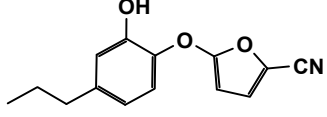
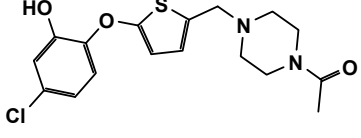
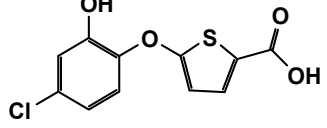
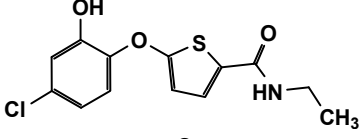
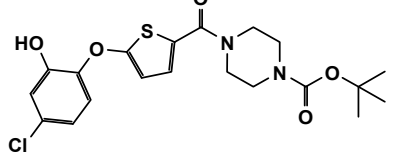
**Table 1.** List of percent of inhibition and IC<sub>50</sub> values for triclosan and analogues against recombinant *Tg*ENR.

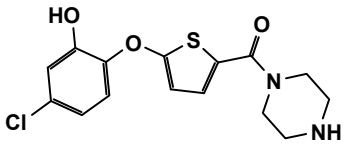
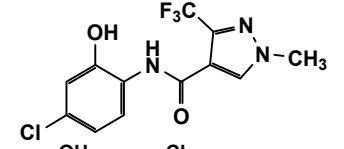
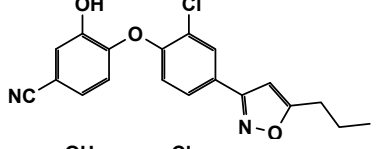
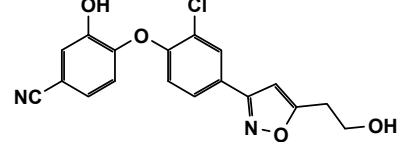
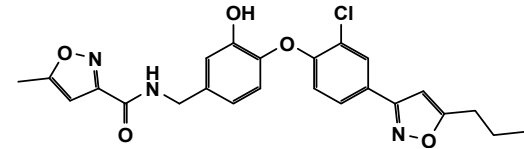
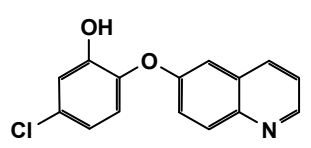
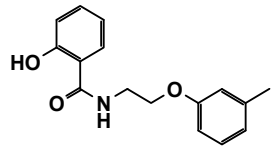
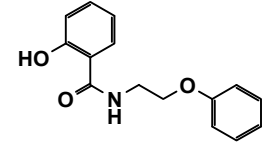
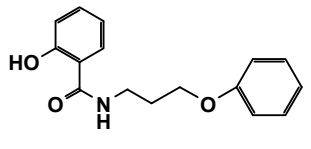
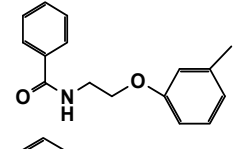
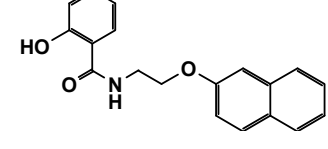
Compound	Structure	% Inhibition at 1 μM	IC <sub>50</sub> (nM)	95% Conf Interval (nM)
Triclosan		97	17	13-22
1		12		
2		94	38	30-48
3		93	54	43-68
4		93	130	87-206
5		90	43	35-54
6		82		

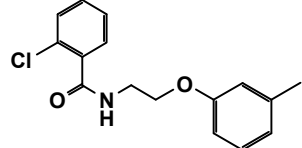
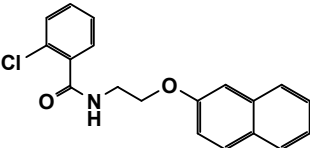
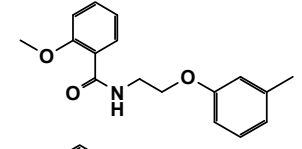
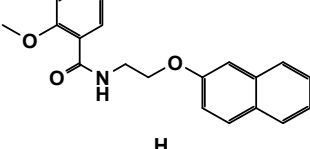
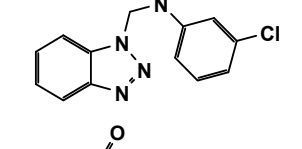
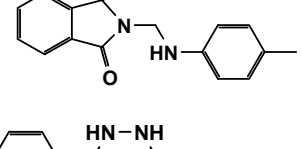
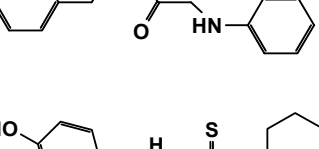
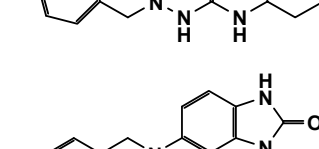
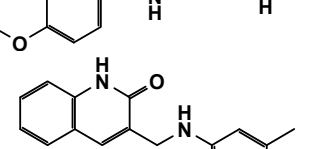
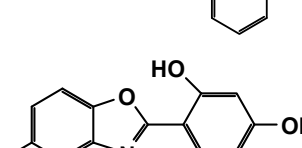

7		91	27	22-34
8		59		
9		40		
10		25		
11		92	22	16-30
12		88	41	31-56
13		97	24	16-36
14		7		
15		44		
16		43		

17		30		
18		96	19	17-21
19		88	100	79-126
20		80		
21		96	33	27-40
22		89		
23		96	130	98-174
24		34		
25		16		
26		25		

27		94	31	26-37
28		85	380	300-481
29		78	750	487-1150
30		81	225	171-296
31		74		
32		25		
33		32		
34		78		
35		91	41	31-54

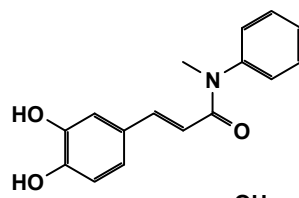
36		95	30	25-37
37		79		
38		46		
39		90	58	42-79
40		45		
41		82		
42		73	965	523-1780
43		48		
44		75		
45		76		

46		60		
47		27		
48		94	29	23-36
49		94	34	29-40
50		89	137	104-181
51		87	135	100-184
52		10		
53		21		
54		28		
55		31		
56		36		

57		41
58		58
59		59
60		71
61		86
62		11
63		15
64		20
65		34
66		36
67		46

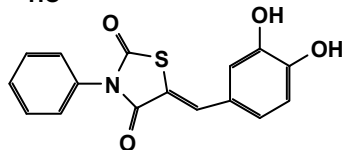


68



60

69



80

## **Chapter 3**

### **Discrimination of Potent Inhibitors of *Toxoplasma gondii* Enoyl-Acyl Carrier Protein Reductase by a Thermal Shift Assay**

Adapted from *Biochemistry*, 52:9155-9166 (2013).

## Abstract

Many microbial pathogens rely on a Fatty Acid Synthesis Type II (FAS-II) pathway which is distinct from the type I pathway found in humans. Enoyl-Acyl Carrier Protein Reductase (ENR) is an essential FAS-II pathway enzyme and the target of a number of antimicrobial drug discovery efforts. The biocide triclosan is established as a potent inhibitor of ENR and has been the starting point for medicinal chemistry studies. We evaluated a series of triclosan analogs for their ability to inhibit the growth of *Toxoplasma gondii*, a pervasive human pathogen, and its ENR enzyme (*TgENR*). Several compounds were identified that inhibited *TgENR* at low nanomolar concentrations, but could not be further differentiated due to the limited dynamic range of the *TgENR* activity assay. Thus, we adapted a thermal shift assay (TSA) to directly measure the dissociation constant ( $K_d$ ) of the most potent inhibitors identified in this study as well as inhibitors from previous studies. Furthermore, the TSA allowed us to determine the mode of action of these compounds in the presence of NADH or NAD<sup>+</sup> cofactors. We found that all of the inhibitors bind to a *TgENR*/NAD<sup>+</sup> complex, but that they differed in their dependence on NAD<sup>+</sup> concentration. Ultimately, we were able to identify compounds which bind to the *TgENR*/NAD<sup>+</sup> complex in the low femtomolar range. This shows how TSA data combined with enzyme inhibition, parasite growth inhibition data and ADMET predictions allow for better discrimination between potent ENR inhibitors for future medicine development.

## Introduction

*Toxoplasma gondii* is an obligate intracellular, protozoan parasite that infects about one third of the world's population, causing substantial morbidity and mortality.<sup>1-6</sup> The life cycle of *T. gondii* is comprised of a sexual phase that only takes place in the primary host (cats of the Felidae family), and an asexual phase that can occur in any warm-blooded animal, including humans.<sup>7,8</sup> Currently there is no available vaccine to prevent infection in humans, and only the antifolate medicines sulfadiazine and pyrimethamine are typically used for treatment of *T. gondii* in humans.<sup>2,9</sup> Sulfonamides are associated with hypersensitivity, and pyrimethamine with bone marrow toxicity. Even though these medications are effective against tachyzoites, the obligate intracellular form of the parasite in the acute stage of the disease, they are ineffective against the encysted, latent bradyzoites. There is no available treatment to eliminate bradyzoites in humans.<sup>10</sup> *T. gondii* infection in immunocompetent individuals is generally asymptomatic and self-limiting, whereas in immunocompromised people, *T. gondii* infection can cause eye and brain disease such as toxoplasmic encephalitis, chorioretinitis and in severe cases can be fatal.<sup>11,12</sup> Pregnant women are especially at risk because the parasite can be transmitted from mother to fetus, and can lead to congenital toxoplasmosis that may result in abortion, neonatal death, or fetal abnormalities.<sup>2,9,13-18</sup>

*T. gondii* parasites contain a plastid organelle, called the apicoplast, which harbors plant-like metabolic pathways.<sup>19</sup> One pathway that resides in the apicoplast is the machinery for a Fatty Acid Synthesis Type II (FAS-II) pathway which is prokaryotic-like.<sup>20,21</sup> The FAS-II pathway in *T. gondii* has been shown to be essential for parasite survival making it an attractive target for drug discovery efforts.<sup>22-26</sup> In malaria parasites,

a similar FAS-II pathway is critical for liver stage development<sup>27, 28</sup> and is thought to have an important role in the synthesis of lipoic acid.<sup>29</sup> In contrast to the type II pathway, humans rely on a distinct type I pathway for bulk fatty acid synthesis, which is encoded in a single polypeptide chain.<sup>30</sup> Fatty acid biosynthesis is an iterative process involving the condensation of malonyl-CoA with a nascent fatty acid chain that is covalently bound to Acyl Carrier Protein (ACP). The enzyme Enoyl-ACP Reductase (ENR) is responsible for the final reductive step in each round of fatty acid chain elongation, the NADH-dependent reduction of trans-2-enoil-ACP to acyl-ACP.<sup>31</sup> Many inhibitors of bacterial and parasitic ENR enzymes have been previously described including diazaborines, isoniazid and triclosan.<sup>32-34</sup> It has been shown that triclosan inhibits *Tg*ENR with an IC<sub>50</sub> value of less than 20 nM in an *in vitro* inhibition assay using pure recombinant *Tg*ENR.<sup>35</sup> Triclosan also inhibits growth of *T. gondii* parasites with an IC<sub>50</sub> of about 200 nM, presumably due to its inhibition of the FAS-II pathway.<sup>23</sup>

Even though triclosan is a potent inhibitor of *Tg*ENR, it has limitations including poor bioavailability and impairment of muscle contractility that prevent it from being a safe and effective medicine.<sup>36</sup> Instead, triclosan has been exploited as a scaffold to generate a series of analogues, many of which are also potent inhibitors of *Tg*ENR.<sup>35, 37-39</sup> In this study, we report the inhibitory properties of a set of 2'-, 4'-, 5- and 6-substituted triclosan analogues developed as inhibitors of *Plasmodium falciparum* ENR (*Pf*ENR) and *Mycobacterium tuberculosis* ENR (*Mt*InhA).<sup>27, 40-43</sup> Several of these compounds inhibited *Tg*ENR at low nanomolar concentrations, the lowest concentrations that we are able to assess in our enzymatic activity assay. To further characterize the inhibitory properties of these compounds and potent inhibitors from previous medicinal chemistry

efforts<sup>37,39</sup> we employed a thermal shift assay (TSA). Using this assay, we were able to confirm the mode of action for all of the compounds as binding to the *Tg*ENR/NAD<sup>+</sup> complex rather than to the *Tg*ENR/NADH complex or to *Tg*ENR alone. Combined with thermodynamic parameters determined by differential scanning calorimetry, we calculated dissociation constants<sup>44-46</sup> for NAD<sup>+</sup> and NADH binding to *Tg*ENR as well as for inhibitor binding to the *Tg*ENR/NAD<sup>+</sup> complex. The K<sub>d</sub> values we determined range from 6 mM (for NAD<sup>+</sup> binding to *Tg*ENR) to 6.3 fM (for compound 19 binding to the *Tg*ENR/NAD<sup>+</sup> complex), highlighting the large dynamic range of the TSA. Consequently, TSA results combined with enzyme and parasite inhibition data provide a better basis to differentiate between potent ENR inhibitors.

## **Materials and Methods**

### *Compound Preparation and Synthesis*

Compounds were designed and synthesized as described by Alan Kozikowski<sup>37,39</sup> and Jacobus Pharmaceutical Inc.<sup>27,40-43</sup> The purity of compounds 1-4,<sup>43</sup> 5-10,<sup>40</sup> 11-14,<sup>41,42</sup> 15-18,<sup>27</sup> 19-29,<sup>39</sup> and 30-32<sup>37</sup> was >95% as determined by HPLC and the identity of each compound was verified by high resolution mass spectrometry. The compounds were initially dissolved in DMSO at a concentration of 10 mM, and further diluted to required concentrations in culture media (described below). For cell proliferation assays the final concentration of DMSO was not more than 0.1%, whereas for the *in vitro* *Tg*ENR enzyme assay the DMSO concentration was 1%.

### *Parasite and Cell Culture*

The strain of *T. gondii* parasites used in this set of experiments was a modified type I RH strain which expresses yellow fluorescent protein (RH-YFP), kindly provided by Dr. Boris Striepen (University of Georgia). Parasites were maintained in confluent monolayers of Human Foreskin Fibroblast (HFF) cells at 37 °C and 5% CO<sub>2</sub> in culture medium consisting of Iscove's Modified Dulbecco's Medium supplemented with 10% Fetal Calf Serum, 1% Glutamax, and 1% Penicillin-Streptomycin-Fungizone (Invitrogen).

#### *In vitro Challenge Assay*

Growth inhibition of *T. gondii* was assessed as previously described.<sup>39</sup> Host cells containing RH-YFP parasites were lysed by double passage through a 25g needle, and separated from the parasites by filtration and centrifugation. Confluent monolayers of HFF cells in 96-well plates (Falcon 96 Optilux Flat-bottom) were infected with 3,500 parasites per well. Parasites were allowed to infect host cells for one hour, after which experimental compounds and control solutions were added. Seventy-two hours later, the parasite burden was assessed by measuring relative fluorescence using a Synergy H4 Hybrid Reader (BioTek) and Gen5 1.10 software. All compounds and control solutions were tested in triplicate exemplars. Biological replicates of each experiment were performed twice for compound 17 and three times for all other compounds. The compounds were tested in a dilution series from 10 μM to 0.01 μM concentrations as described previously.<sup>39</sup> In each assay, these results were compared with those for DMSO control and triclosan. Other internal controls included a curve obtained with varying concentrations of parasites to confirm that each assay detected differing numbers of

parasites, and cultures treated with a known inhibitory concentration of pyrimethamine and sulfadiazine as a positive control. Inhibitory index was calculated as:

$$\frac{[\text{RFU}_{(\text{compound})} \times \text{RFU}_{(\text{control fibroblasts})}]}{[\text{RFU}_{(\text{DMSO control})} \times \text{RFU}_{(\text{control fibroblasts})}]} \times 100$$
. MIC<sub>50</sub> is defined as the compound concentration required to inhibit replication by 50%.

#### *Human cell proliferation assay*

Potential cytotoxic effects of the compounds were assessed using Cell Proliferation Reagent WST-1 (Roche), which measures the metabolic activity of viable cells. Confluent HFF cells in 96-well plates were treated under the same conditions as in the challenge assay described above, except that the cells were not infected with parasites. After 72 hours, the cells were incubated with WST-1 reagent for 1-2 hrs, and cell viability was assessed by measuring the absorbance at 420 nm of the final colored product, which correlates directly with cell number. All samples were tested in triplicate in at least two biological replicates.

#### *Inhibition of TgENR activity in vitro and enzymatic assay*

Recombinant TgENR was purified as described previously.<sup>47</sup> A 96-well plate assay was used to measure the inhibition of TgENR as described previously.<sup>37, 39</sup> Briefly, a SpectraMax M2 plate reader was used to monitor the activity of TgENR by consumption of NADH ( $\epsilon_{340} = 6220 \text{ M}^{-1} \text{ cm}^{-1}$ ). Reactions were carried out in a final volume of 100  $\mu\text{L}$  in 96 well Corning UV plates. A reaction mixture was used containing 100  $\mu\text{M}$  crotonyl-CoA (Sigma), 1  $\mu\text{L}$  of DMSO (or compounds dissolved in DMSO), 5nM TgENR, 100 mM Na/K Phosphate pH 7.5 150 mM NaCl and 100  $\mu\text{M}$  NADH. The



enzymatic activity was determined by comparing the slopes of the absorbance curves for each well to those of the blanks in the first column of the plate. Each compound was measured in duplicate at 1  $\mu\text{M}$  final concentration. Potent inhibitors (>90% inhibition at 1  $\mu\text{M}$ ) were further analyzed to determine  $\text{IC}_{50}$  values in triplicate. Nonlinear regression analysis was performed using GraphPad Prism software.

To calculate the  $K_m$  and  $k_{\text{cat}}$  values for NADH and Crotonyl-CoA we followed a method described previously.<sup>25</sup> The  $K_m$  and  $k_{\text{cat}}$  were determined at variable concentrations of NADH (0–0.5 mM) in triplicate and a fixed concentration of crotonyl-CoA (100  $\mu\text{M}$ ). The  $K_m$  and  $k_{\text{cat}}$  for Crotonyl-CoA were determined at concentrations ranging from 0.8–150  $\mu\text{M}$  and a fixed concentration of NADH (100 $\mu\text{M}$ ). Kinetic parameters were calculated by fitting the initial velocity data to the Michaelis–Menten equation using GraphPad Prism software.

#### *Thermal Shift Assay (TSA) and binding constant calculations*

A real-time PCR (RT-PCR) instrument, in the presence of Sypro Orange (an environmentally sensitive fluorescent dye), was used to monitor the thermal unfolding of *TgENR* alone or in the presence of ligands. The TSA was modified from previous reports<sup>44–46</sup> to measure the thermal melting temperature ( $T_m$ ) of *TgENR*. Real-time PCR tube strips (Eppendorf) were used to hold 31  $\mu\text{L}$  mixtures containing final concentrations of 2  $\mu\text{M}$  *TgENR*, 20  $\mu\text{M}$  inhibitor and 100  $\mu\text{M}$  cofactor. The reactions were set up with a 28  $\mu\text{L}$  mixture of *TgENR* and buffer (20 mM HEPES pH 7.5, 100 mM NaCl) to which 1  $\mu\text{L}$  of water (or cofactor dissolved in water), 1  $\mu\text{L}$  DMSO (or inhibitor dissolved in DMSO), and 1  $\mu\text{L}$  of Sypro Orange (Sigma, Product Number S-5692 at a final

concentration of 5X) was added. The reaction mixture was incubated in the RT-PCR machine (Applied Biosystems, Step One Plus Real-Time PCR System) for 2 minutes at 20 °C followed by 0.2 °C increases in the temperature every 10 seconds until a final temperature of 80 °C was reached. During the thermal scan, fluorescence was monitored using a pre-defined TAMRA filter in which an increase in Sypro Orange fluorescence was observed upon thermal denaturation of *TgENR*. The derivative of the fluorescence curve was used to determine the  $T_m$  (as seen in **Figure 1**). The initial  $T_m$  in the absence of ligands, but in the presence of DMSO, served as the baseline temperature ( $T_o$ ) for determining temperature shifts ( $\Delta T_m$ ). All measurements were made in triplicate.

#### *Calculation of binding constant ( $K_d$ )*

The  $T_m$  values obtained in the TSA were used to calculate the dissociation constant ( $K_d$ ) as described by Mei-Chu Lo and coworkers.<sup>44</sup> The dissociation constant at the melting temperature was calculated using the equation

$$K_{d(T_m)} = \frac{[L_{T_m}]}{\exp\left\{\frac{-\Delta H_{T_o}}{R} \left(\frac{1}{T_m} - \frac{1}{T_o}\right) + \frac{\Delta C_{pT_o}}{R} \left[\ln\left(\frac{T_m}{T_o}\right) + \frac{T_o}{T_m} - 1\right]\right\}}$$

in which  $T_o$  is the melting temperature of *TgENR* with no ligands (baseline),  $T_m$  is the melting temperature of *TgENR* in complex with one or more ligands,  $R$  is the gas constant,  $\Delta H$  is the enthalpy of protein unfolding,  $\Delta C_p$  is the heat capacity change on protein unfolding, and  $[L_{T_m}]$  is the free ligand concentration at  $T_m$ . The two thermodynamic parameters ( $\Delta H$  and  $\Delta C_p$ ) were measured by Differential Scanning Calorimetry. A temperature scan of 0.33 mg/mL *TgENR* from 10 to 65 °C at 1 °C/min was monitored using a VP-DSC microcalorimeter (MicroCal). The change in heat

capacity ( $\Delta C_{pT_0}$ ) of 3.8 kcal/K/mol was estimated from the difference in baselines between the baselines of the denatured and native states. The enthalpy ( $\Delta H_{T_0}$ ) was obtained from the area under the curve yielding a value of 228.7 kcal/mol. The dissociation constant at the melting temperature was normalized to temperature T (37 °C) using the equation

$$K_{d(T)} = \frac{K_{d(T_m)}}{\exp\left(\frac{-\Delta H_{L(T)}}{R} \left(\frac{1}{T} - \frac{1}{T_m}\right)\right)}$$

in which  $\Delta H_{L(T)}$  is the van't Hoff enthalpy of binding at temperature T, estimated to be -15 kcal/mol.<sup>44, 48</sup>

### *Molecular Docking*

Molecular docking studies were performed using AutoDock 4.2,<sup>49</sup> SwissPDB Viewer<sup>50</sup> and MacroModel version 8.1 (Schrodinger, LLC, New York, NY, 2012) in conjunction with the X-ray crystal structures of *T. gondii* ENR in complex with inhibitors triclosan (PDB ID: 202S)<sup>51</sup> and benzimidazole (PDB ID: 1LX6)<sup>52</sup> available from the Brookhaven Protein DataBank. A 10 Å radius of the active site was used to dock the synthesized molecules with a grid box margin of 62. All other docking parameters were left as default. The obtained docking poses were analyzed using PyMol.

## **Results and Discussion**

*Parasite inhibition, host cell cytotoxicity, and inhibition of TgENR enzymatic activity*

A structure-based approach was adopted by Freundlich and colleagues to develop 2'-, 4'-, 5- and 6-substituted triclosan analogues against *Pf*ENR and *Mt*InhA.<sup>27, 40-43</sup> In the present study, we evaluated 18 of these analogues against *Toxoplasma gondii*. The triclosan analogues were first tested for efficacy against *T. gondii* tachyzoites *in vitro*. Triclosan was also included in the assay for a direct comparison. Type 1 RH tachyzoites that express Yellow Fluorescent Protein (RH-YFP) were used, allowing parasite proliferation to be assessed by means of a fluorometric assay, since relative fluorescence is directly correlated with parasite viability. A seventy-two hour end-point was chosen to allow slow acting compounds to take effect. Seven compounds emerged as the most effective inhibitors of *T. gondii* tachyzoites: 5, 8, 9, 10, 15, 16 and 17 (**Table 1**). These compounds demonstrated an efficacy equivalent to triclosan (MIC<sub>50</sub> of 2.8 μM), with MIC<sub>50</sub> values ranging from 1.6-3.5 μM. The compounds were also tested for cytotoxic activity against Human Foreskin Fibroblast host cells and exhibited no cytotoxic effects at the highest concentration tested (10 μM). These results demonstrate that inhibition of parasite growth at lower concentrations did not result from killing the host cells, however, since we did not reach the MIC<sub>50</sub> for inhibition of host cell proliferation, we do not know the overall selectivity of our compounds.

The triclosan analogues were also screened in duplicate at 1 μM for inhibition of *Tg*ENR in an *in vitro* inhibition assay. Those analogues with significant inhibitory activity (>90 % at 1 μM) were subsequently assayed in triplicate to determine their IC<sub>50</sub> values (**Table 1**). A total of six analogues were potent inhibitors of *Tg*ENR with IC<sub>50</sub> values of less than 23 nM, similar to that of triclosan (15 nM). None of the compounds with 2'-substitutions proved to have significant inhibitory activity. This result is

consistent with a lack of potent activity against *Pf*ENR.<sup>43</sup> Based on the current crystal structures of *Tg*ENR and *Pf*ENR bound to triclosan,<sup>51</sup> the 2'-triclosan analogues are unlikely to be effective since added bulk at this position will likely result in severe steric clashes with the NAD<sup>+</sup> cofactor (see docking results for further details). Potent inhibitors of *Tg*ENR with IC<sub>50</sub> values in the low nanomolar range were found with substitutions at the 4'-, 5-, and 6- positions of triclosan. Previous medicinal chemistry efforts targeting *Tg*ENR led to the discovery of several potent 4'-triclosan and 5-triclosan analogues.<sup>37, 39</sup> The activities of 6-triclosan analogues have not previously been described against *T. gondii*. However, as shown in **Table 1**, 6-triclosan analogues such as 15 and 17 can be inhibitors of *Tg*ENR enzymatic activity and parasite growth.

#### *Thermal Shift Assay (TSA)*

Our current study of 18 triclosan analogues yielded six compounds with *Tg*ENR IC<sub>50</sub> values in the low nanomolar range (< 23 nM). These IC<sub>50</sub> values are similar to that of triclosan (15 nM) and approach the low nanomolar concentrations of *Tg*ENR enzyme used in our activity assay. Because of this we could not determine which of the six compounds is the most potent or how they compare to triclosan with currently available assays. In addition we have 14 inhibitors discovered in previous studies<sup>37, 39</sup> which also inhibit *Tg*ENR with IC<sub>50</sub> values lower than 100 nM, making 20 compounds in total. In an attempt to differentiate between these inhibitors, we adapted a thermal shift assay (TSA)<sup>44-46</sup> to further characterize the binding of the compounds to *Tg*ENR.

A significant advantage of TSA over several other biophysical techniques, such as NMR, mass spectrometry or calorimetry, is that it can be done with higher throughput

without requiring large amounts of protein.<sup>44-46, 48, 53-55</sup> This method has been previously employed for screening conditions which stabilize proteins;<sup>46, 56, 57</sup>  $K_d$  calculations for proteins with one or two ligands,<sup>44, 45, 48, 55</sup> as well as to determine the mode of action of ligand binding.<sup>55</sup> Calculations of  $K_d$  values by TSA have been favorably compared to measurements done by other biophysical techniques.<sup>44</sup>

We used the TSA to measure the melting temperature ( $T_m$ ) of *TgENR* alone, in binary complex with NADH or  $NAD^+$  cofactor, or in a ternary complex with triclosan (or analogues) and NADH or  $NAD^+$  bound. Using a real time PCR machine to accurately control the temperature, we monitored the thermal denaturation of *TgENR* in the presence of the environmentally sensitive dye Sypro Orange. The TSA method consists of monitoring the fluorescence of the dye which has a higher quantum yield when it interacts with hydrophobic amino acids exposed upon *TgENR* unfolding. As shown in **Figure 1**, the derivative of the fluorescence intensity is marked by a sharp minimum at the  $T_m$ . A shift in thermal stability occurs upon formation of a ligand complex and the magnitude of the shift in  $T_m$  depends on the affinity of the ligand for *TgENR*. The observed change in  $T_m$  ( $\Delta T_m = T_m(\text{ligand}) - T_o(\text{no ligand})$ ) is used to calculate the binding constant ( $K_d$ ) of the ligand.<sup>44, 46</sup> TSA can be particularly useful for proteins such as *TgENR* which have multiple ligand binding sites and can bind inhibitors and cofactor molecules. In cases like this, the relative stability of the protein with different combinations of ligands can be used to determine the mode of action of an inhibitor.<sup>55</sup>

*TgENR* binary complex with NADH or  $NAD^+$

We studied the  $\Delta T_m$  of *Tg*ENR with increasing concentrations of NADH or NAD<sup>+</sup> (**Figure 2A**). Each data point with a nonzero  $\Delta T_m$  allowed us to calculate independent  $K_d$  values for these ligands. For NADH,  $K_d$  values of 26  $\mu\text{M}$  ( $\Delta T_m = 0.4\text{ C}$ ) and 21  $\mu\text{M}$  ( $\Delta T_m = 1.7\text{ C}$ ) were measured, and for NAD<sup>+</sup> the  $K_d$  values were 6 mM ( $\Delta T_m = 0.4\text{ C}$ ) and 6 mM ( $\Delta T_m = 1.6\text{ C}$ ). The  $K_d$  values resulting from the larger temperature shifts are likely to be the most accurate (21  $\mu\text{M}$  for NADH and 6 mM for NAD<sup>+</sup>). The  $K_d$  for NADH binding to *Tg*ENR is similar to the value obtained for *Pf*ENR with a  $K_d$  for NADH of 51.6  $\mu\text{M}$ <sup>58</sup> and that of *E. coli* ENR with a  $K_d$  for NADH of 5.4  $\mu\text{M}$ .<sup>32</sup> The  $K_d$  for NAD<sup>+</sup> could not be determined for *Pf*ENR, except in the presence of triclosan, yielding an artificially low value of 15  $\mu\text{M}$ <sup>58</sup>, whereas the  $K_d$  of NAD<sup>+</sup> for *Ec*ENR was determined to be 1.8 mM.<sup>32</sup> The kinetic parameters for *Tg*ENR were calculated by using the enzymatic activity assay at 11 different concentrations of NADH and Crotonyl-CoA in triplicate, with the highest concentration of 500  $\mu\text{M}$  and dilutions by factors of two for NADH and 0.8-150  $\mu\text{M}$  for Crotonyl-CoA. **Figure 2B** shows a Michaelis-Menten plot for *Tg*ENR with a  $k_{\text{cat}}$  of 12  $\text{s}^{-1}$  and  $K_m$  of 20  $\mu\text{M}$  for NADH; for Crotonyl-CoA,  $k_{\text{cat}}$  is 26  $\text{s}^{-1}$  and  $K_m$  is 40  $\mu\text{M}$  (**Figure 2C**). These values are similar to those of ENR enzymes from the apicomplexan parasites *Eimeria tenella* and *Plasmodium falciparum* (**Table 2**).<sup>25, 59, 60</sup> Although  $K_m$  values cannot be equated with dissociation constants, the  $K_m$  values for NADH are consistent with the 21  $\mu\text{M}$   $K_d$  value determined by TSA.

#### *Inhibitor mode of action determined by TSA*

The mode of action of ENR inhibition by triclosan has been well studied in several systems, including apicomplexan parasites, plants and bacteria. Triclosan is an

uncompetitive inhibitor with respect to  $\text{NAD}^+$  and forms a tight ternary triclosan/ $\text{NAD}^+$ /ENR complex. Consistent with this mechanism of action, we observed a large shift in  $T_m$  when *Tg*ENR was analyzed by TSA in the presence of triclosan and  $\text{NAD}^+$ , but not in the absence of the cofactor (**Figure 1A**). Interestingly, we also observed a small shift in  $T_m$  when triclosan was added to *Tg*ENR in the presence of NADH (**Figure 1A**). Triclosan has an apparent  $K_d$  value of 186  $\mu\text{M}$  for the *Tg*ENR/NADH complex, an affinity that is probably too weak to have physiological significance since this value is 100,000 times larger than the  $K_d$  of triclosan binding to the *Tg*ENR/ $\text{NAD}^+$  complex (1.3 nM at 100  $\mu\text{M}$   $\text{NAD}^+$  listed in **Table 3**). The apparent weak binding of triclosan to the *Tg*ENR/NADH complex is consistent with reports of ternary triclosan/NADH complexes formed by ENR enzymes from *E. coli*,<sup>61</sup> *Haemophilus influenzae*<sup>62</sup> and *Pseudomonas aeruginosa*.<sup>63</sup>

Potent inhibition of ENR enzymes with triclosan is due to the slow formation of a tight ternary triclosan/ $\text{NAD}^+$ /ENR complex. *Pf*ENR is 50% identical to *Tg*ENR and serves as a good example of this phenomenon. Triclosan binds to the *Pf*ENR/ $\text{NAD}^+$  complex with relatively low affinity (53 nM) followed by the slow ( $0.055 \text{ s}^{-1}$  forward rate constant) formation of a tight binding complex with an overall inhibition constant of 96 pM.<sup>64</sup> The tight binding complex involves the formation of an  $\alpha$ -helix over the inhibitor binding site, a feature that was observed in the crystal structure of *Tg*ENR co-crystallized with triclosan and  $\text{NAD}^+$ , making it very likely that triclosan inhibits *Tg*ENR through the same mechanism as described for other ENR enzymes.<sup>51</sup> The slow kinetics of inhibition appear to be responsible for the artificially high 15 nM  $\text{IC}_{50}$  value of triclosan shown in **Table 1**. The  $\text{IC}_{50}$  value approaches the theoretical limit (half of the 5 nM *Tg*ENR



concentration) when the enzyme is preincubated with triclosan and  $\text{NAD}^+$  allowing the inhibitory complex to form prior to initiating the assay. In the TSA experiments, there is a total incubation time of about 30 minutes from the time the experiment is set up to the time it reaches  $T_m$ . This allows enough time for triclosan to form the tight ternary complex. To confirm this, we set up TSA experiments as explained in the Methods section, but allowed 2 hours of pre-incubation. This pre-incubation time did not affect the  $K_d$  of triclosan for the enzyme (data not shown). To determine the reproducibility of the TSA measurements, we measured the  $T_m$  in four experiments in triplicates on different days for *TgENR* alone, in binary complex with NADH and  $\text{NAD}^+$  and in the ternary complex *TgENR*/ $\text{NAD}^+$ /triclosan. The standard deviation of these measurements was 0.40, 0.56, 0.36 and 0.37 degree Celsius, respectively.

All of our potent inhibitors were also tested by TSA for binding to the *TgENR*/ $\text{NAD}^+$  complex, the *TgENR*/NADH complex, or *TgENR* alone. In all cases, the inhibitors displayed a similar mode of action as that of triclosan, forming a tight complex with *TgENR*/ $\text{NAD}^+$ . **Figure 1B** shows the TSA results for 32, a compound that differs significantly from the structure of triclosan, but displays a similar  $T_m$  shift profile and thus the same mode of action as triclosan, binding exclusively to the *TgENR*/ $\text{NAD}^+$  complex. As shown in **Figure 1**, the presence of 100  $\mu\text{M}$   $\text{NAD}^+$  alone (orange curves) or 20  $\mu\text{M}$  inhibitor alone (green curves) does not shift the  $T_m$  of *TgENR* and thus, the  $\Delta T_m$  observed in the presence of inhibitor and  $\text{NAD}^+$  is due to the formation of the ternary complex.

*Effect of  $\text{NAD}^+$  concentration on inhibitor affinity*

In TSA experiments we can control the concentration of the cofactors NADH and NAD<sup>+</sup>. By contrast, in the enzymatic assay NADH is constantly being consumed and NAD<sup>+</sup> is formed over the course of the reaction. For TSA, we used 100 μM NADH, the concentration used as the starting point in the enzymatic assay. As described above, this concentration is well above the 21 μM K<sub>d</sub> of NADH, ensuring that the majority of *TgENR* forms a binary *TgENR*/NADH complex during the TSA experiments. The same is not true for NAD<sup>+</sup>. In the TSA experiments described above, 100 μM NAD<sup>+</sup> was used whereas the K<sub>d</sub> is 6 mM. Under these conditions, the fraction of enzyme found as a binary *TgENR*/NAD<sup>+</sup> complex is very small (~1.6%).

We then analyzed the binding of two inhibitors, triclosan and 32, to better understand how NAD<sup>+</sup> concentration affects the apparent K<sub>d</sub> values determined by TSA. We determined K<sub>d</sub> values for both inhibitors at eight concentrations of NAD<sup>+</sup> ranging from 2.7 μM to 6 mM. As shown in **Figure 3A**, the apparent K<sub>d</sub> for these inhibitors decreases as the concentration of NAD<sup>+</sup> increases, until reaching a plateau while approaching the K<sub>d</sub> of NAD<sup>+</sup> (6 mM). The apparent dissociation constant of triclosan ranges from 18 μM (at a NAD<sup>+</sup> concentration of 2.7 μM) to 20 fM (at a NAD<sup>+</sup> concentration of 6 mM), despite the fact that NAD<sup>+</sup> is in stoichiometric excess to *TgENR* (2 μM) throughout this concentration range. Similarly, the K<sub>d</sub> values for compound 32 vary from 51 μM to 689 fM over the same range of NAD<sup>+</sup> concentrations. These results underscore the need to consider cofactor concentration when comparing K<sub>d</sub> values for uncompetitive inhibitors like triclosan. For example, a K<sub>d</sub> value of 32 nM was reported for triclosan binding to *PfENR*<sup>58</sup> which is similar to the value of 1.3 nM listed in **Table 3** for *TgENR*. However, the K<sub>d</sub> for *PfENR* was determined with 250 μM NAD<sup>+</sup> and the equivalent K<sub>d</sub> value for

*TgENR* is 105 pM. In a similar experiment, we determined the  $K_d$  values for triclosan and compound 32 at seven concentrations ranging from 450 nM to 333  $\mu$ M, while keeping  $[NAD^+]$  constant at 100  $\mu$ M. As expected, we found that the  $K_d$  values for both compounds decrease as we increase the inhibitor concentration (**Figure 3B**).

We determined the  $K_d$  values for our most potent *TgENR* inhibitors in the presence of 6 mM  $NAD^+$  and compared these values with those determined at 100  $\mu$ M  $NAD^+$  (**Table 3**). The higher  $NAD^+$  concentration increased the apparent affinity of all of our inhibitors, however, the factor by which the affinity increased was not uniform across the compound series (**Table 3**). The  $K_d$  of 25 decreased by a factor of 2,300,000 when  $NAD^+$  concentrations were increased, whereas the  $K_d$  of 30 only decreased by a factor of 11,000. Even between similar compounds such as 28 and 29 there were differences in the dependence of  $K_d$  on  $NAD^+$  concentrations. These differences may reflect the ability of some inhibitors to bind more tightly to *TgENR* in the absence of  $NAD^+$ . In the thermodynamic cycle shown in **Figure 4A**, these inhibitors would have smaller  $K_i$  values and larger  $\alpha$  values corresponding to less selectivity between binding to the *TgENR*/ $NAD^+$  complex *versus* *TgENR* alone.

We did not detect the binding of any inhibitor to *TgENR* when we used 20  $\mu$ M inhibitor concentrations, however,  $K_i$  values could be well above this level. We screened for inhibitor binding at higher concentrations of inhibitor (111  $\mu$ M and 333  $\mu$ M) but found that most compounds did not have measureable binding or interfered with the TSA at these concentrations. Compound 29, however, appeared to bind with a dissociation constant ( $K_i$ ) of 0.8 mM (**Figure 4B**). This value of  $K_i$  allows us to estimate the parameter  $\alpha$  if we can measure the affinity of compound 29 for the E• $NAD$  complex

( $\alpha K_i$ ) shown in **Figure 4A**. The  $K_d$  of compound 29 in the presence of 6 mM  $\text{NAD}^+$  is 116 pM (**Table 3**). We can estimate  $\alpha K_i$  using the equation for the binding of uncompetitive inhibitors

$$K_i^{\text{app}} = \alpha K_i \left( 1 + \frac{K_{\text{NAD}}}{[\text{NAD}]} \right)$$

in which  $K_i^{\text{app}}$  is the observed dissociation constant of the inhibitor at any concentration of  $\text{NAD}^+$  and  $K_{\text{NAD}}$  is the  $K_d$  of  $\text{NAD}^+$ . Since the 6 mM concentration of  $\text{NAD}^+$  used in the TSA equals  $K_{\text{NAD}}$ , this equation reduces to:

$$\alpha K_i = \frac{K_i^{\text{app}}}{2} = 58 \text{ pM}$$

Similar estimations of  $\alpha K_i$  can be made for all of the compounds with measured  $K_d$  values at 6 mM  $\text{NAD}^+$  (**Table 3**). The parameter  $\alpha$  describing the selectivity of compound 29 for the binary complex would then be  $7 \times 10^{-8}$ . The parameter  $\alpha$  is presumably related to the ratio of  $K_d$  values shown in **Table 3** in the sense that both numbers provide an indication of how dependent an inhibitor is on binding to the binary *Tg*ENR/ $\text{NAD}^+$  complex. This phenomenon may help to guide the selection of the best inhibitors. The  $\text{NAD}^+$  concentration has been measured in different cell types, including mouse erythrocytes and mammalian cells with values of 368  $\mu\text{M}$  and a range of 300-800  $\mu\text{M}$ , respectively.<sup>65-69</sup> Although the concentration of  $\text{NAD}^+$  in the apicoplast of *T. gondii* has not been measured, it is also likely to be well below the 6 mM  $K_d$  value. Therefore, at any given time, most *Tg*ENR molecules will not have  $\text{NAD}^+$  bound. Indeed, the large discrepancy between the  $\text{MIC}_{50}$  values in Table 1 and the extremely tight binding properties of some of the compounds in Table 3 may be an indication that  $\text{NAD}^+$  levels are low in the apicoplast organelle.

### *Inhibitor affinity to the TgENR/NAD<sup>+</sup> complex*

The twenty compounds that we examined by TSA all had IC<sub>50</sub> values of less than 100 nM in the TgENR enzyme activity assay (**Table 3**). The calculated K<sub>d</sub> values at the two NAD<sup>+</sup> concentrations can be used to identify the most potent compounds and how dependent inhibitor binding is on NAD<sup>+</sup> concentration (**Table 3**). A total of six compounds showed K<sub>d</sub> values of less than 10 nM with 100 μM NAD<sup>+</sup>, and less than 100 fM with 6 mM NAD<sup>+</sup> (5, 9, 10, 15, 19 and 27). From analyzing these compounds, it is clear that tight binding inhibitors can contain small substituents at the 4'-position (as in compound 5), the 5-position (as in compound 19), or the 6-position (as in compound 15). As described previously<sup>37,39</sup>, bulky substituents at the 4'- and 5-positions are accommodated by the TgENR active site. Compound 27 contains a large isoxazole ring at the 5-position while compounds 9 and 10 contain a benzylamino moiety. The 6-position triclosan analogues have not been described previously for TgENR. We show that modifications at this position are well tolerated as seen for compounds 15 and 17 (see modeling data below).

Overall, three compounds (5, 9 and 19) appear to bind to the TgENR/NAD<sup>+</sup> complex as well as triclosan or better. These compounds differ, however, in terms of how dependent the dissociation constants are on NAD<sup>+</sup> concentration. The ratio of K<sub>d</sub> values determined at low and high NAD<sup>+</sup> concentrations is 250,000 for compound 19, whereas this ratio is only 30,000 for compound 9 (**Table 3**). As discussed above, the reduced dependence of compound 9 on NAD<sup>+</sup> concentration could reflect the ability of this compound to bind weakly to TgENR, adding an additional route to forming the ternary

inhibitor/*Tg*ENR/NAD<sup>+</sup> complex. By contrast, compound 19 may be more dependent on binding to a preformed *Tg*ENR/NAD<sup>+</sup> complex. In this sense, compound 9 could prove to be a more exciting scaffold for further modification. Since a variety of substituents are tolerated at the 5-position, these are possible additions that could improve the properties of compound 9. Similarly, small groups such as those found in compounds 15 and 17 could be added to the 6-position.

### *Inhibitor Modeling*

In order to further understand the different binding properties of the various inhibitors studied, molecular modeling was carried out using the *Tg*ENR crystal structure and the molecular docking software AutoDock.<sup>49</sup> The least effective triclosan analogues contained modifications on the B-ring at the 2'-position. The close proximity of the NAD<sup>+</sup> cofactor to this position on the B-ring is likely to cause a significant steric clash upon inhibitor binding (**Figure 5A**). The addition of a 5-methyl-3-carboxamide-isoxazole group to the A- or B- rings of triclosan resulted in a marked difference in their K<sub>d</sub> values. The presence of this group at the 5-position on the A-ring (compound 27) produced a very potent inhibitor (K<sub>d</sub> = 33 fM with 6 mM NAD<sup>+</sup>), whereas this modification at the 4'-position on the B-ring gave inhibitor 29 with 3,500 fold less affinity (K<sub>d</sub> = 116 pM with 6 mM NAD<sup>+</sup>).

Molecular modeling was used to rationalize this difference in affinity. Modeling in AutoDock suggested that the isoxazole group, and other large substituents<sup>37, 39</sup> can be tolerated within the hydrophobic pocket surrounding the A-ring due to the mobile alpha helix. Conversely, the positioning of this group on the B-ring extends towards the

solvent exposed entrance to the binding site, and should be able to accommodate such a substituent. However, sampling the potential ligand conformations in AutoDock exposed a steric clash between the 4'-methylisoxazole of compound 29 and Phe243 (*TgENR* numbering) due to the rigid nature of the 5-methyl-3-carboxamide-isoxazole group. The addition of a methylene group between the amide and isoxazole ring (compound 28) decreased the  $K_d$  by about two orders of magnitude, perhaps because the additional flexibility alleviated this steric clash.

The most promising inhibitors discovered to date have a modification at the 6-position on the A-ring. Considering the extra bulk of the nitrile (compound 15) and the hydroxymethyl (compound 17) moieties, the initial steric clash observed between these substituents and Tyr179 must be alleviated through the movement about C $\beta$ . This result is corroborated through further modeling studies whereby the conserved Tyr179 residue can rotate to accommodate the 6-substituents within the heart of the binding site (**Figure 5B**).

## Conclusions

We evaluated a series of triclosan analogues as inhibitors of *Toxoplasma gondii*. The 4'- and 5-substituted triclosan analogues are effective inhibitors of parasite growth and *TgENR* enzymatic activity. Compounds with modifications at the 2'-position did not show inhibitory activity against *TgENR* due to steric clashes with either the NAD<sup>+</sup> cofactor or the top of the binding pocket. Modifications in the 6-position were well tolerated and displayed good inhibitory activity against the parasite and the *TgENR* enzyme. Six compounds which inhibited *TgENR* with IC<sub>50</sub> values in the low nanomolar

range were identified, but could not be further differentiated due to the limited dynamic range of the *Tg*ENR activity assay. A thermal shift assay was employed to further characterize these compounds as well as 14 other potent inhibitors from previous studies.<sup>37,39</sup> All 20 compounds share the same mode of action and form a ternary complex with *Tg*ENR and NAD<sup>+</sup>, but do not bind significantly to the *Tg*ENR/NADH complex or to *Tg*ENR alone. The apparent K<sub>d</sub> values for the inhibitors were strongly affected by NAD<sup>+</sup> concentration and reached a plateau as the NAD<sup>+</sup> concentration approached the 6 mM K<sub>d</sub> of NAD<sup>+</sup>. By comparing the apparent K<sub>d</sub> values of the inhibitors at low and high NAD<sup>+</sup> concentrations, we could identify potent compounds which are less dependent on NAD<sup>+</sup> binding. Ultimately, we were able to identify six compounds which bind to the *Tg*ENR/NAD<sup>+</sup> complex in the low femtomolar range with affinities similar to or exceeding that of triclosan (5, 9, 10, 15, 19 and 27). Additionally, four of these compounds inhibit the growth of *T. gondii* parasites with equal or better potency than triclosan (5, 9, 10 and 15). TSA data combined with enzyme inhibition and parasite growth inhibition data allow for better discrimination between potent ENR inhibitors, and therefore provide an excellent method for better selection of promising lead compounds.

### **Acknowledgments**

The authors thank Jürgen Bosch for helpful discussions about the TSA. Cell growth inhibition data in **Table 1** were determined by Alina Fomovska. Physicochemical properties calculations from **Table 1** were performed by Gang Cheng. Differential



scanning calorimetry was done by Arne Schon. Molecular docking simulations (Discussion and **Figure 5**) were done by Stephen Muench and Martin McPhillie.

## References

1. Hill, D.; Dubey, J. P. *Toxoplasma gondii*: transmission, diagnosis and prevention. *Clin Microbiol Infect* **2002**, *8*, 634-40.
2. McLeod, R.; Boyer, K.; Karrison, T.; Kasza, K.; Swisher, C.; Roizen, N.; Jalbrzikowski, J.; Remington, J.; Heydemann, P.; Noble, A. G.; Mets, M.; Holfels, E.; Withers, S.; Latkany, P.; Meier, P. Outcome of treatment for congenital toxoplasmosis, 1981-2004: the National Collaborative Chicago-Based, Congenital Toxoplasmosis Study. *Clin Infect Dis* **2006**, *42*, 1383-94.
3. Boyer, K.; Marcinak, J.; McLeod, R. *Toxoplasma gondii (Toxoplasmosis)*. 3rd ed.; Churchill Livingstone: New York, 2009.
4. Hill, D.; Coss, C.; Dubey, J. P.; Wroblewski, K.; Sautter, M.; Hosten, T.; Munoz-Zanzi, C.; Mui, E.; Withers, S.; Boyer, K.; Hermes, G.; Coyne, J.; Jagdis, F.; Burnett, A.; McLeod, P.; Morton, H.; Robinson, D.; McLeod, R. Identification of a sporozoite-specific antigen from *Toxoplasma gondii*. *J Parasitol* **2011**, *97*, 328-37.
5. Boyer, K.; Hill, D.; Mui, E.; Wroblewski, K.; Karrison, T.; Dubey, J. P.; Sautter, M.; Noble, A. G.; Withers, S.; Swisher, C.; Heydemann, P.; Hosten, T.; Babiarz, J.; Lee, D.; Meier, P.; McLeod, R. Unrecognized ingestion of *Toxoplasma gondii* oocysts leads to congenital toxoplasmosis and causes epidemics in North America. *Clin Infect Dis* **2011**, *53*, 1081-9.

6. Desmonts, G.; Couvreur, J. Congenital toxoplasmosis. A prospective study of 378 pregnancies. *N Engl J Med* **1974**, 290, 1110-6.
7. Dubey, J. P.; Lindsay, D. S.; Speer, C. A. Structures of *Toxoplasma gondii* tachyzoites, bradyzoites, and sporozoites and biology and development of tissue cysts. *Clin Microbiol Rev* **1998**, 11, 267-99.
8. Dubey, J. P. The history of *Toxoplasma gondii*--the first 100 years. *J Eukaryot Microbiol* **2008**, 55, 467-75.
9. Remington, J. S.; McLeod, R.; Thulliez, P.; Desmonts, G. *Toxoplasmosis*. 7th ed.; Elsevier Saunders: Philadelphia, 2011.
10. Montoya, J. G.; Liesenfeld, O. Toxoplasmosis. *Lancet* **2004**, 363, 1965-76.
11. Luft, B. J.; Remington, J. S. Toxoplasmic encephalitis in AIDS. *Clin Infect Dis* **1992**, 15, 211-22.
12. Porter, S. B.; Sande, M. A. Toxoplasmosis of the central nervous system in the acquired immunodeficiency syndrome. *N Engl J Med* **1992**, 327, 1643-8.
13. Swisher, C. N.; Boyer, K.; McLeod, R. Congenital toxoplasmosis. The Toxoplasmosis Study Group. *Semin Pediatr Neurol* **1994**, 1, 4-25.
14. Olariu, T. R.; Remington, J. S.; McLeod, R.; Alam, A.; Montoya, J. G. Severe congenital toxoplasmosis in the United States: clinical and serologic findings in untreated infants. *Pediatr Infect Dis J* **2011**, 30, 1056-61.
15. McLeod, R.; Mack, D. G.; Boyer, K.; Mets, M.; Roizen, N.; Swisher, C.; Patel, D.; Beckmann, E.; Vitullo, D.; Johnson, D.; et al. Phenotypes and functions of lymphocytes in congenital toxoplasmosis. *J Lab Clin Med* **1990**, 116, 623-35.

16. McGee, T.; Wolters, C.; Stein, L.; Kraus, N.; Johnson, D.; Boyer, K.; Mets, M.; Roizen, N.; Beckman, J.; Meier, P.; et al. Absence of sensorineural hearing loss in treated infants and children with congenital toxoplasmosis. *Otolaryngol Head Neck Surg* **1992**, *106*, 75-80.
17. McAuley, J.; Boyer, K. M.; Patel, D.; Mets, M.; Swisher, C.; Roizen, N.; Wolters, C.; Stein, L.; Stein, M.; Schey, W.; et al. Early and longitudinal evaluations of treated infants and children and untreated historical patients with congenital toxoplasmosis: the Chicago Collaborative Treatment Trial. *Clin Infect Dis* **1994**, *18*, 38-72.
18. McLeod, R.; Khan, A. R.; Noble, G. A.; Latkany, P.; Jalbrzikowski, J.; Boyer, K. Severe sulfadiazine hypersensitivity in a child with reactivated congenital toxoplasmic chorioretinitis. *Pediatr Infect Dis J* **2006**, *25*, 270-2.
19. Roberts, C. W.; McLeod, R.; Rice, D. W.; Ginger, M.; Chance, M. L.; Goad, L. J. Fatty acid and sterol metabolism: potential antimicrobial targets in apicomplexan and trypanosomatid parasitic protozoa. *Mol Biochem Parasitol* **2003**, *126*, 129-42.
20. McFadden, G. I.; Reith, M. E.; Munholland, J.; Lang-Unnasch, N. Plastid in human parasites. *Nature* **1996**, *381*, 482.
21. Kohler, S.; Delwiche, C. F.; Denny, P. W.; Tilney, L. G.; Webster, P.; Wilson, R. J.; Palmer, J. D.; Roos, D. S. A plastid of probable green algal origin in Apicomplexan parasites. *Science* **1997**, *275*, 1485-9.
22. Zuther, E.; Johnson, J. J.; Haselkorn, R.; McLeod, R.; Gornicki, P. Growth of *Toxoplasma gondii* is inhibited by aryloxyphenoxypropionate herbicides targeting acetyl-CoA carboxylase. *Proc Natl Acad Sci U S A* **1999**, *96*, 13387-92.

23. McLeod, R.; Muench, S. P.; Rafferty, J. B.; Kyle, D. E.; Mui, E. J.; Kirisits, M. J.; Mack, D. G.; Roberts, C. W.; Samuel, B. U.; Lyons, R. E.; Dorris, M.; Milhous, W. K.; Rice, D. W. Triclosan inhibits the growth of *Plasmodium falciparum* and *Toxoplasma gondii* by inhibition of apicomplexan Fab I. *Int J Parasitol* **2001**, 31, 109-13.
24. Ben Mamoun, C.; Prigge, S. T.; Vial, H. Targeting the Lipid Metabolic Pathways for the Treatment of Malaria. *Drug Dev Res* **2010**, 71, 44-55.
25. Lu, J. Z.; Muench, S. P.; Allary, M.; Campbell, S.; Roberts, C. W.; Mui, E.; McLeod, R. L.; Rice, D. W.; Prigge, S. T. Type I and type II fatty acid biosynthesis in *Eimeria tenella*: enoyl reductase activity and structure. *Parasitology* **2007**, 134, 1949-62.
26. Mazumdar, J.; E, H. W.; Masek, K.; C, A. H.; Striepen, B. Apicoplast fatty acid synthesis is essential for organelle biogenesis and parasite survival in *Toxoplasma gondii*. *Proc Natl Acad Sci U S A* **2006**, 103, 13192-7.
27. Yu, M.; Kumar, T. R.; Nkrumah, L. J.; Coppi, A.; Retzlaff, S.; Li, C. D.; Kelly, B. J.; Moura, P. A.; Lakshmanan, V.; Freundlich, J. S.; Valderramos, J. C.; Vilcheze, C.; Siedner, M.; Tsai, J. H.; Falkard, B.; Sidhu, A. B.; Purcell, L. A.; Gratraud, P.; Kremer, L.; Waters, A. P.; Schiehsler, G.; Jacobus, D. P.; Janse, C. J.; Ager, A.; Jacobs, W. R., Jr.; Sacchettini, J. C.; Heussler, V.; Sinnis, P.; Fidock, D. A. The fatty acid biosynthesis enzyme FabI plays a key role in the development of liver-stage malarial parasites. *Cell Host Microbe* **2008**, 4, 567-78.
28. Vaughan, A. M.; O'Neill, M. T.; Tarun, A. S.; Camargo, N.; Phuong, T. M.; Aly, A. S.; Cowman, A. F.; Kappe, S. H. Type II fatty acid synthesis is essential only for malaria parasite late liver stage development. *Cell Microbiol* **2009**, 11, 506-20.

29. Falkard, B.; Kumar, T. R.; Hecht, L. S.; Matthews, K. A.; Henrich, P. P.; Gulati, S.; Lewis, R. E.; Manary, M. J.; Winzeler, E. A.; Sinnis, P.; Prigge, S. T.; Heussler, V.; Deschermeier, C.; Fidock, D. A key role for lipoic acid synthesis during Plasmodium liver stage development. *Cell Microbiol* **2013**.
30. Magnuson, K.; Jackowski, S.; Rock, C. O.; Cronan, J. E., Jr. Regulation of fatty acid biosynthesis in Escherichia coli. *Microbiol Rev* **1993**, *57*, 522-42.
31. Massengo-Tiasse, R. P.; Cronan, J. E. Diversity in enoyl-acyl carrier protein reductases. *Cell Mol Life Sci* **2009**, *66*, 1507-17.
32. Ward, W. H.; Holdgate, G. A.; Rowsell, S.; McLean, E. G.; Pauptit, R. A.; Clayton, E.; Nichols, W. W.; Colls, J. G.; Minshull, C. A.; Jude, D. A.; Mistry, A.; Timms, D.; Camble, R.; Hales, N. J.; Britton, C. J.; Taylor, I. W. Kinetic and structural characteristics of the inhibition of enoyl (acyl carrier protein) reductase by triclosan. *Biochemistry* **1999**, *38*, 12514-25.
33. Rozwarski, D. A.; Grant, G. A.; Barton, D. H.; Jacobs, W. R., Jr.; Sacchettini, J. C. Modification of the NADH of the isoniazid target (InhA) from Mycobacterium tuberculosis. *Science* **1998**, *279*, 98-102.
34. Grassberger, M. A.; Turnowsky, F.; Hildebrandt, J. Preparation and antibacterial activities of new 1,2,3-diazaborine derivatives and analogues. *J Med Chem* **1984**, *27*, 947-53.
35. Tipparaju, S. K.; Muench, S. P.; Mui, E. J.; Ruzheinikov, S. N.; Lu, J. Z.; Hutson, S. L.; Kirisits, M. J.; Prigge, S. T.; Roberts, C. W.; Henriquez, F. L.; Kozikowski, A. P.; Rice, D. W.; McLeod, R. L. Identification and development of novel inhibitors of Toxoplasma gondii enoyl reductase. *J Med Chem* **2010**, *53*, 6287-300.

36. Cherednichenko, G.; Zhang, R.; Bannister, R. A.; Timofeyev, V.; Li, N.; Fritsch, E. B.; Feng, W.; Barrientos, G. C.; Schebb, N. H.; Hammock, B. D.; Beam, K. G.; Chiamvimonvat, N.; Pessah, I. N. Triclosan impairs excitation-contraction coupling and Ca<sup>2+</sup> dynamics in striated muscle. *Proc Natl Acad Sci U S A* **2012**, 109, 14158-63.
37. Cheng, G.; Muench, S. P.; Zhou, Y.; Afanador, G. A.; Mui, E. J.; Fomovska, A.; Lai, B. S.; Prigge, S. T.; Woods, S.; Roberts, C. W.; Hickman, M. R.; Lee, P. J.; Leed, S. E.; Auschwitz, J. M.; Rice, D. W.; McLeod, R. Design, synthesis, and biological activity of diaryl ether inhibitors of *Toxoplasma gondii* enoyl reductase. *Bioorg Med Chem Lett* **2013**, 23, 2035-43.
38. Samuel, B. U.; Hearn, B.; Mack, D.; Wender, P.; Rothbard, J.; Kirisits, M. J.; Mui, E.; Wernimont, S.; Roberts, C. W.; Muench, S. P.; Rice, D. W.; Prigge, S. T.; Law, A. B.; McLeod, R. Delivery of antimicrobials into parasites. *Proc Natl Acad Sci U S A* **2003**, 100, 14281-6.
39. Stec, J.; Fomovska, A.; Afanador, G. A.; Muench, S. P.; Zhou, Y.; Lai, B. S.; El Bissati, K.; Hickman, M. R.; Lee, P. J.; Leed, S. E.; Auschwitz, J. M.; Sommerville, C.; Woods, S.; Roberts, C. W.; Rice, D.; Prigge, S. T.; McLeod, R.; Kozikowski, A. P. Modification of triclosan scaffold in search of improved inhibitors for enoyl-acyl carrier protein (ACP) reductase in *Toxoplasma gondii*. *ChemMedChem* **2013**, 8, 1138-60.
40. Freundlich, J. S.; Anderson, J. W.; Sarantakis, D.; Shieh, H. M.; Yu, M.; Valderramos, J. C.; Lucumi, E.; Kuo, M.; Jacobs, W. R., Jr.; Fidock, D. A.; Schiehsler, G. A.; Jacobus, D. P.; Sacchetti, J. C. Synthesis, biological activity, and X-ray crystal structural analysis of diaryl ether inhibitors of malarial enoyl acyl carrier protein

reductase. Part 1: 4'-substituted triclosan derivatives. *Bioorg Med Chem Lett* **2005**, 15, 5247-52.

41. Freundlich, J. S.; Wang, F.; Tsai, H. C.; Kuo, M.; Shieh, H. M.; Anderson, J. W.; Nkrumah, L. J.; Valderramos, J. C.; Yu, M.; Kumar, T. R. S.; Valderramos, S. G.; Jacobs, W. R.; Schiehser, G. A.; Jacobus, D. P.; Fidock, D. A.; Sacchettini, J. C. X-ray structural analysis of plasmodium falciparum enoyl acyl carrier protein reductase as a pathway toward the optimization of Triclosan antimalarial efficacy. *Journal of Biological Chemistry* **2007**, 282, 25436-25444.

42. Freundlich, J. S.; Wang, F.; Vilcheze, C.; Gulten, G.; Langley, R.; Schiehser, G. A.; Jacobus, D. P.; Jacobs, W. R., Jr.; Sacchettini, J. C. Triclosan derivatives: towards potent inhibitors of drug-sensitive and drug-resistant Mycobacterium tuberculosis. *ChemMedChem* **2009**, 4, 241-8.

43. Freundlich, J. S.; Yu, M.; Lucumi, E.; Kuo, M.; Tsai, H. C.; Valderramos, J. C.; Karagyozov, L.; Jacobs, W. R., Jr.; Schiehser, G. A.; Fidock, D. A.; Jacobus, D. P.; Sacchettini, J. C. Synthesis and biological activity of diaryl ether inhibitors of malarial enoyl acyl carrier protein reductase. Part 2: 2'-substituted triclosan derivatives. *Bioorg Med Chem Lett* **2006**, 16, 2163-9.

44. Lo, M. C.; Aulabaugh, A.; Jin, G.; Cowling, R.; Bard, J.; Malamas, M.; Ellestad, G. Evaluation of fluorescence-based thermal shift assays for hit identification in drug discovery. *Anal Biochem* **2004**, 332, 153-9.

45. Matulis, D.; Kranz, J. K.; Salemme, F. R.; Todd, M. J. Thermodynamic stability of carbonic anhydrase: measurements of binding affinity and stoichiometry using ThermoFluor. *Biochemistry* **2005**, 44, 5258-66.

46. Niesen, F. H.; Berglund, H.; Vedadi, M. The use of differential scanning fluorimetry to detect ligand interactions that promote protein stability. *Nat Protoc* **2007**, 2, 2212-21.
47. Muench, S. P.; Prigge, S. T.; Zhu, L.; Kirisits, M. J.; Roberts, C. W.; Wernimont, S.; McLeod, R.; Rice, D. W. Expression, purification and preliminary crystallographic analysis of the *Toxoplasma gondii* enoyl reductase. *Acta Crystallogr Sect F Struct Biol Cryst Commun* **2006**, 62, 604-6.
48. Pantoliano, M. W.; Petrella, E. C.; Kwasnoski, J. D.; Lobanov, V. S.; Myslik, J.; Graf, E.; Carver, T.; Asel, E.; Springer, B. A.; Lane, P.; Salemme, F. R. High-density miniaturized thermal shift assays as a general strategy for drug discovery. *J Biomol Screen* **2001**, 6, 429-40.
49. Goodsell, D. S.; Morris, G. M.; Olson, A. J. Automated docking of flexible ligands: applications of AutoDock. *J Mol Recognit* **1996**, 9, 1-5.
50. Guex, N.; Peitsch, M. C. SWISS-MODEL and the Swiss-PdbViewer: an environment for comparative protein modeling. *Electrophoresis* **1997**, 18, 2714-23.
51. Muench, S. P.; Prigge, S. T.; McLeod, R.; Rafferty, J. B.; Kirisits, M. J.; Roberts, C. W.; Mui, E. J.; Rice, D. W. Studies of *Toxoplasma gondii* and *Plasmodium falciparum* enoyl acyl carrier protein reductase and implications for the development of antiparasitic agents. *Acta Crystallogr D Biol Crystallogr* **2007**, 63, 328-38.
52. Miller, W. H.; Seefeld, M. A.; Newlander, K. A.; Uzinskas, I. N.; Burgess, W. J.; Heerding, D. A.; Yuan, C. C.; Head, M. S.; Payne, D. J.; Rittenhouse, S. F.; Moore, T. D.; Pearson, S. C.; Berry, V.; DeWolf, W. E., Jr.; Keller, P. M.; Polizzi, B. J.; Qiu, X.;



- Janson, C. A.; Huffman, W. F. Discovery of aminopyridine-based inhibitors of bacterial enoyl-ACP reductase (FabI). *J Med Chem* **2002**, 45, 3246-56.
53. Todd, M. J. Affinity assays for decrypting protein targets of unknown function. *Drug Discovery Today: Technologies* **2005**, 2, 267–273.
54. Cummings, M. D.; Farnum, M. A.; Nelen, M. I. Universal screening methods and applications of ThermoFluor. *J Biomol Screen* **2006**, 11, 854-63.
55. Lea, W. A.; Simeonov, A. Differential scanning fluorometry signatures as indicators of enzyme inhibitor mode of action: case study of glutathione S-transferase. *PLoS One* **2012**, 7, e36219.
56. Vedadi, M.; Niesen, F. H.; Allali-Hassani, A.; Fedorov, O. Y.; Finerty, P. J., Jr.; Wasney, G. A.; Yeung, R.; Arrowsmith, C.; Ball, L. J.; Berglund, H.; Hui, R.; Marsden, B. D.; Nordlund, P.; Sundstrom, M.; Weigelt, J.; Edwards, A. M. Chemical screening methods to identify ligands that promote protein stability, protein crystallization, and structure determination. *Proc Natl Acad Sci U S A* **2006**, 103, 15835-40.
57. Ericsson, U. B.; Hallberg, B. M.; Detitta, G. T.; Dekker, N.; Nordlund, P. ThermoFluor-based high-throughput stability optimization of proteins for structural studies. *Anal Biochem* **2006**, 357, 289-98.
58. Kapoor, M.; Mukhi, P. L.; Surolia, N.; Suguna, K.; Surolia, A. Kinetic and structural analysis of the increased affinity of enoyl-ACP (acyl-carrier protein) reductase for triclosan in the presence of NAD<sup>+</sup>. *Biochem J* **2004**, 381, 725-33.
59. Perozzo, R.; Kuo, M.; Sidhu, A.; Valiyaveetil, J. T.; Bittman, R.; Jacobs, W. R., Jr.; Fidock, D. A.; Sacchettini, J. C. Structural elucidation of the specificity of the

antibacterial agent triclosan for malarial enoyl acyl carrier protein reductase. *Journal of Biological Chemistry* **2002**, *277*, 13106-14.

60. Kapoor, M.; Dar, M. J.; Surolia, A.; Surolia, N. Kinetic determinants of the interaction of enoyl-ACP reductase from *Plasmodium falciparum* with its substrates and inhibitors. *Biochem Biophys Res Commun* **2001**, *289*, 832-7.

61. Sivaraman, S.; Sullivan, T. J.; Johnson, F.; Novichenok, P.; Cui, G.; Simmerling, C.; Tonge, P. J. Inhibition of the bacterial enoyl reductase FabI by triclosan: a structure-reactivity analysis of FabI inhibition by triclosan analogues. *J Med Chem* **2004**, *47*, 509-18.

62. Marcinkeviciene, J.; Jiang, W.; Kopcho, L. M.; Locke, G.; Luo, Y.; Copeland, R. A. Enoyl-ACP reductase (FabI) of *Haemophilus influenzae*: steady-state kinetic mechanism and inhibition by triclosan and hexachlorophene. *Arch Biochem Biophys* **2001**, *390*, 101-8.

63. Lee, J. H.; Park, A. K.; Chi, Y. M.; Moon, J. H.; Lee, K. S. Crystallization and preliminary X-ray crystallographic studies of enoyl-acyl carrier protein reductase (FabI) from *Pseudomonas aeruginosa*. *Acta Crystallogr Sect F Struct Biol Cryst Commun* **2011**, *67*, 214-6.

64. Kapoor, M.; Reddy, C. C.; Krishnasastri, M. V.; Surolia, N.; Surolia, A. Slow-tight-binding inhibition of enoyl-acyl carrier protein reductase from *Plasmodium falciparum* by triclosan. *Biochem J* **2004**, *381*, 719-24.

65. Yamada, K.; Hara, N.; Shibata, T.; Osago, H.; Tsuchiya, M. The simultaneous measurement of nicotinamide adenine dinucleotide and related compounds by liquid

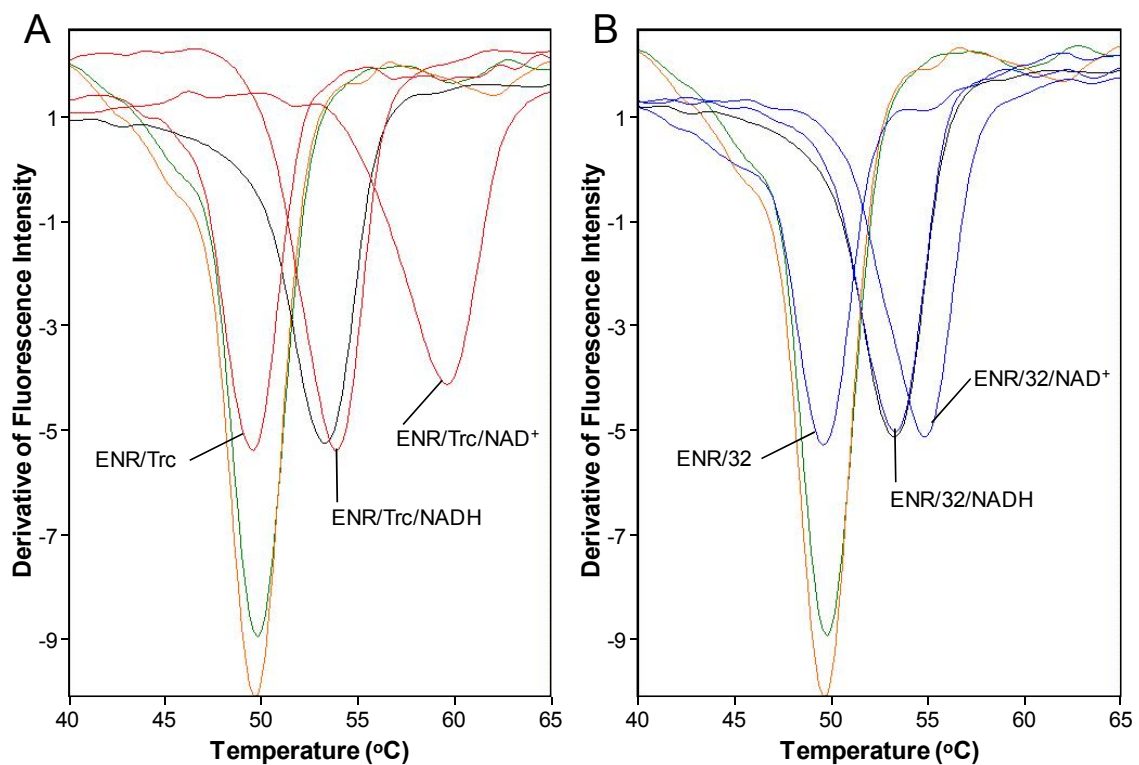
chromatography/electrospray ionization tandem mass spectrometry. *Anal Biochem* **2006**, 352, 282-5.

66. Houtkooper, R. H.; Canto, C.; Wanders, R. J.; Auwerx, J. The secret life of NAD<sup>+</sup>: an old metabolite controlling new metabolic signaling pathways. *Endocr Rev* **2010**, 31, 194-223.

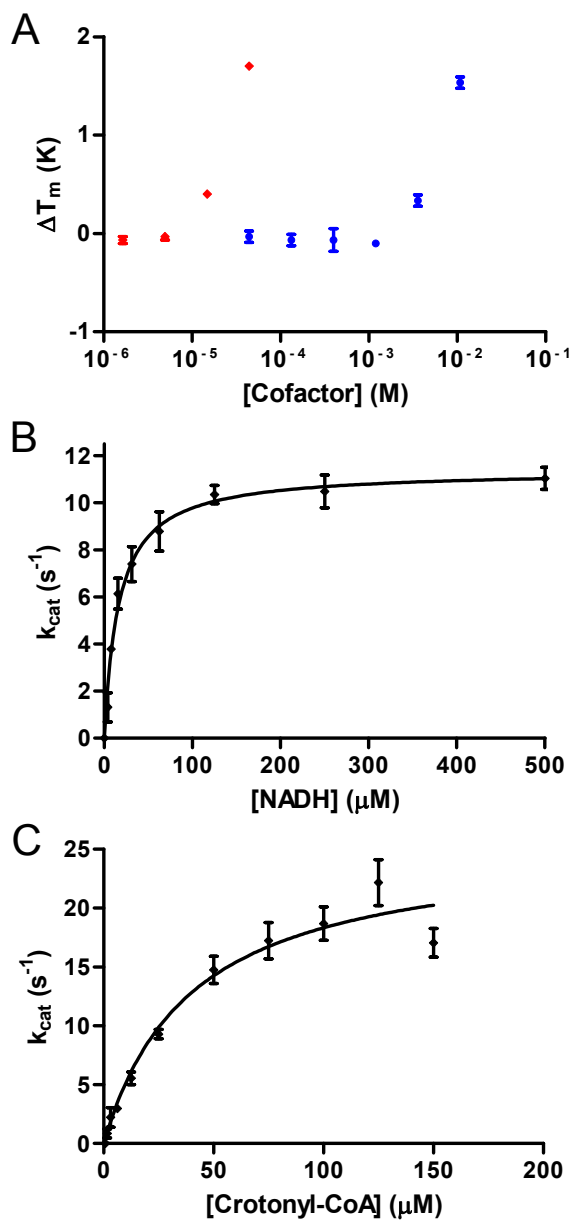
67. Yang, H.; Yang, T.; Baur, J. A.; Perez, E.; Matsui, T.; Carmona, J. J.; Lamming, D. W.; Souza-Pinto, N. C.; Bohr, V. A.; Rosenzweig, A.; de Cabo, R.; Sauve, A. A.; Sinclair, D. A. Nutrient-sensitive mitochondrial NAD<sup>+</sup> levels dictate cell survival. *Cell* **2007**, 130, 1095-107.

68. Wilhelm, F.; Hirrlinger, J. The NAD<sup>+</sup> /NADH redox state in astrocytes: independent control of the NAD<sup>+</sup> and NADH content. *J Neurosci Res* **2011**, 89, 1956-64.

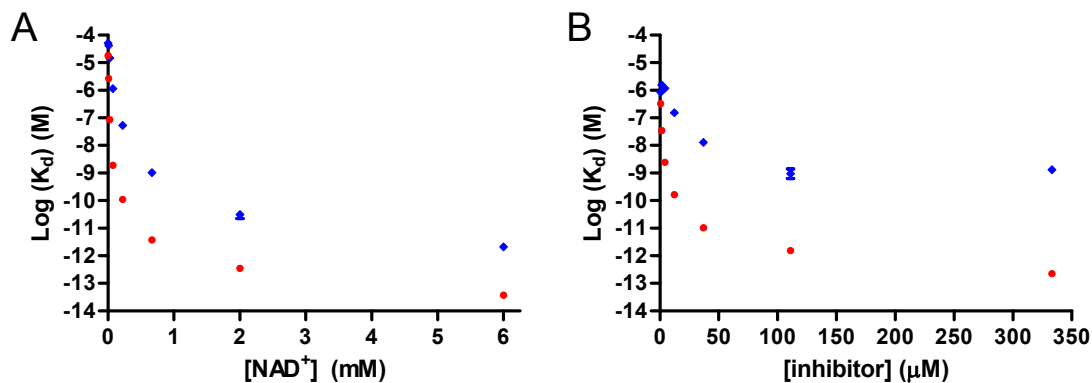
69. Hara, N.; Yamada, K.; Shibata, T.; Osago, H.; Hashimoto, T.; Tsuchiya, M. Elevation of cellular NAD levels by nicotinic acid and involvement of nicotinic acid phosphoribosyltransferase in human cells. *J Biol Chem* **2007**, 282, 24574-82.



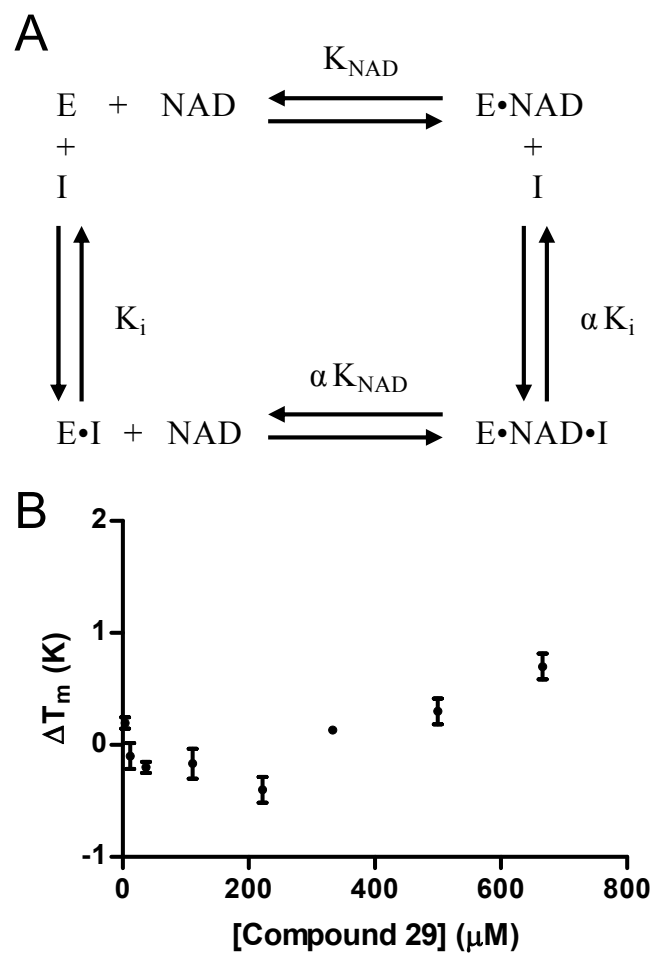
**Figure 1.** Thermal Shift Assay results for triclosan (red curves) and compound 32 (blue curves). The derivatives of the fluorescence intensity curves are shown with the minima defining the melting temperatures ( $T_m$ ). Enzyme alone – green; Enzyme/NADH – black; Enzyme/NAD<sup>+</sup> - orange.



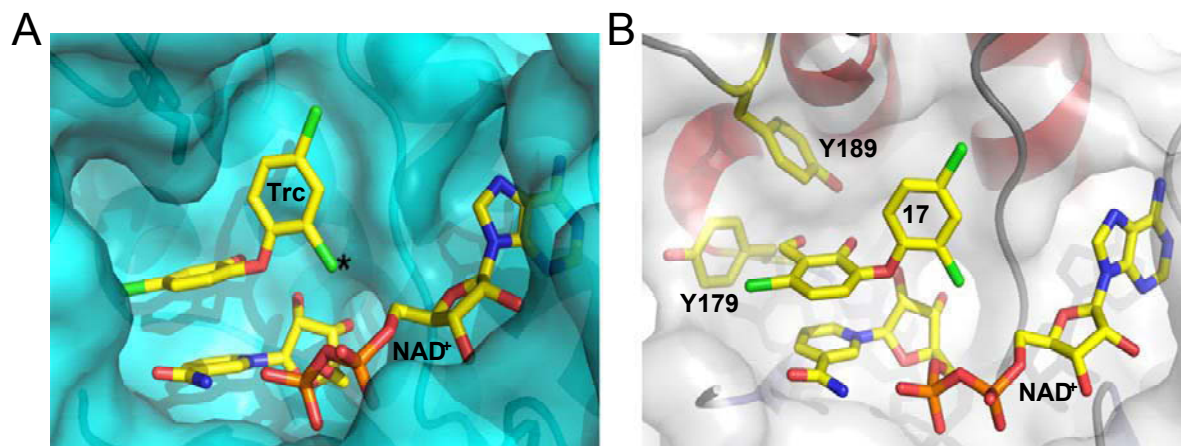
**Figure 2.** Binding and kinetic data for *TgENR* cofactors. A) Thermal Shift Assay results for the binding of NADH (red) and NAD<sup>+</sup> (blue) to *TgENR*. B) Kinetic analysis of *TgENR* with NADH cofactor. C) Kinetic analysis of *TgENR* with Crotonyl-CoA cofactor. Error bars represent the standard deviation from triplicate measurements.



**Figure 3.** Effect of  $\text{NAD}^+$  and inhibitor concentration on the apparent dissociation constant of two *TgENR* inhibitors. Thermal Shift Assay was used to determine apparent  $K_d$  values for triclosan (red) and compound 32 (blue) at different concentrations of  $\text{NAD}^+$  and inhibitor. A) The apparent dissociation constants reach a plateau as  $\text{NAD}^+$  concentrations approach 6 mM (the  $K_d$  of  $\text{NAD}^+$ ). B) The apparent dissociation constants decrease as the inhibitor concentration increases to 333  $\mu\text{M}$ , the highest concentration we were able to measure. Error bars represent the standard deviation of triplicate measurements.



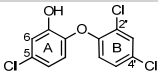
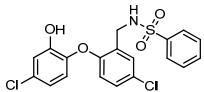
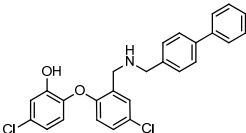
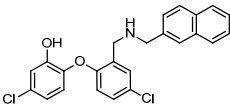
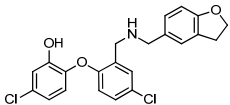
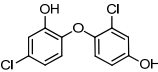
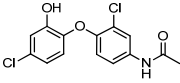
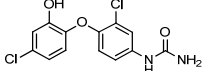
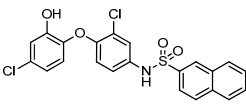
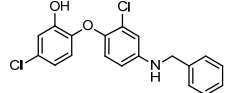
**Figure 4.** Thermodynamic cycle for formation of the ternary inhibitor/*Tg*ENR/ $\text{NAD}^+$  complex. The parameter  $\alpha$  describes the selectivity of inhibitor binding for the *Tg*ENR/ $\text{NAD}^+$  complex ( $E \cdot \text{NAD}$ ) and the selectivity of  $\text{NAD}^+$  binding to the inhibitor/*Tg*ENR complex ( $E \cdot I$ ).

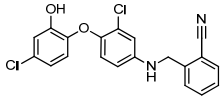
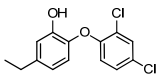
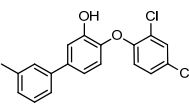
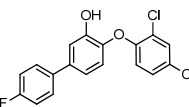
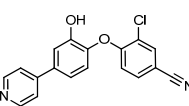
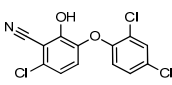
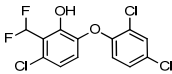
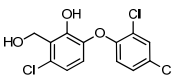
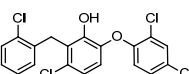


**Figure 5.** Inhibitor modeling in active site of *TgENR*. A) The NAD<sup>+</sup>/triclosan binding pocket of *TgENR* from a crystal structure (PDB ID: 202S)<sup>51</sup> Ligands NAD<sup>+</sup> and triclosan are shown in stick format colored by atom type. Modification of the 2' atom (marked with an asterisk) results in decreased affinity (see compounds 1, 2, 3 and 4) due to steric clashes with the NAD<sup>+</sup> cofactor and the binding pocket. B) Molecular modeling of inhibitor 17 showing the position of the additional OH group and its close proximity to the two fully conserved active site Tyr residues.



**Table 1.** Inhibitory activity, toxicity and calculated physicochemical properties of 18 substituted triclosan inhibitors of *Pf*ENR and *Mt*InhA.

Compd.	Structure	Cell Growth Inhibition		<i>Tg</i> ENR Inhibition			Physicochemical Properties (ACD/Labs) <sup>c</sup>		
		<i>T. gondii</i> MIC <sub>50</sub> ( $\mu$ M) <sup>a</sup>	HFF MIC <sub>50</sub> ( $\mu$ M) <sup>b</sup>	Inhibition at 1 $\mu$ M (%) <sup>c</sup>	IC <sub>50</sub> (nM)	95% Conf. Interval (nM)	clogP <sup>d</sup>	TPSA [ $\text{\AA}^2$ ]	Sw (mg/L)
Triclosan		2.8 $\pm$ 0.2	>10	98 $\pm$ 2	15	7-33	5.53	53.25	4.6 <sup>f</sup>
1		>10	>10	13 $\pm$ 13	nd		5.59	84.01	2.2
2		>10	>10	14 $\pm$ 7	nd		7.46	41.49	0.52
3		>10	>10	22 $\pm$ 2	nd		6.74	41.49	0.33
4		>10	>10	28 $\pm$ 5	nd		5.63	50.72	4.2
5		3.1 $\pm$ 0.3	>10	97 $\pm$ 2	3	2-5	4.44	49.69	140
6		10	>10	73 $\pm$ 5	nd		4.09	58.56	12
7		>10	>10	74 $\pm$ 3	nd		3.82	84.58	7.4
8		3.0 $\pm$ 0.8	>10	45 $\pm$ 4	nd		6.62	84.01	0.077
9		3.5 $\pm$ 0.4	>10	98 $\pm$ 2	13	10-16	6.06	41.19	1.0

10		1.6 ± 0.3	>10	96 ± 0	16	13-20	5.64	65.28	2.1
11		>10	>10	97 ± 1	8	7-9	5.55	29.46	2.5
12		>10	>10	78 ± 1	nd		5.82	49.69	2.8
13		>10	>10	80 ± 2	nd		5.53	49.69	4.6
14		>10	>10	41 ± 1	nd		3.82	66.14	6.9
15		2.9 ± 0.4	>10	95 ± 1	18	16-20	5.33	53.25	7.3
16		2.7 ± 0.6	>10	87 ± 2	nd		5.67	29.46	1.9
17		2.8 ± 0.7	>10	92 ± 0	23	19-26	4.44	49.69	21
18		>10	>10	81 ± 1	nd		8.26	29.46	0.024

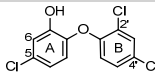
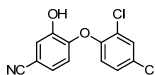
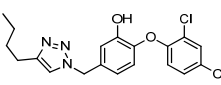
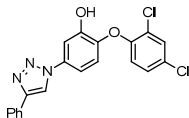
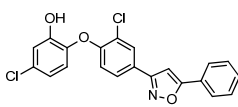
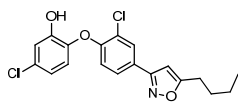
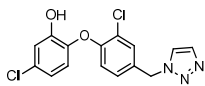
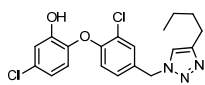
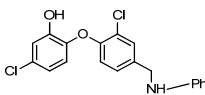
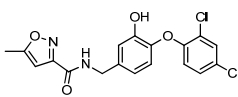
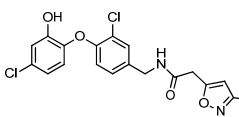
<sup>a</sup>MIC<sub>50</sub> of *T. gondii* growth with SEM from assays conducted in at least two independent trials each with triplicate measurements. <sup>b</sup>Growth inhibition of human foreskin fibroblasts (HFF). <sup>c</sup>Standard deviation from duplicate measurements. <sup>d</sup>Calculated by ChemDraw Ultra 7.0. <sup>e</sup>These data were predicted by ADMET suite 5.0 (ACD/Labs). TPSA = topological polar surface area; Sw = solubility in water; <sup>f</sup>The actual water solubility for triclosan is 12 mg/L at 20°C, according to US EPA - Reregistration Eligibility Decision (RED) for Triclosan.

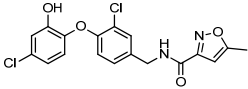
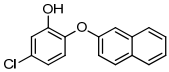
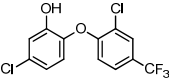
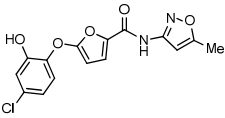
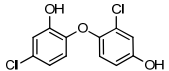
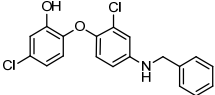
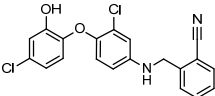
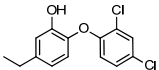
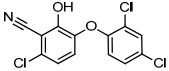
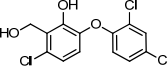
**Table 2.** Kinetic parameters of apicomplexan ENR enzymes.

NADH					
Organism	$K_m$ ( $\mu\text{M}$ )	Std. Error ( $\mu\text{M}$ ) <sup>b</sup>	$k_{\text{cat}}$ ( $\text{s}^{-1}$ )	Std. Error ( $\text{s}^{-1}$ ) <sup>b</sup>	Reference
<i>Eimeria tenella</i>	60		11		Lu <i>et al.</i> <sup>25</sup>
<i>Plasmodium falciparum</i>	30		49		Perozzo <i>et al.</i> <sup>59</sup>
<i>Toxoplasma gondii</i> <sup>a</sup>	20	3.5	12	0.5	This Study <sup>a</sup>
Crotonyl-CoA					
Organism	$K_m$ ( $\mu\text{M}$ )	Std. Error ( $\mu\text{M}$ ) <sup>b</sup>	$k_{\text{cat}}$ ( $\text{s}^{-1}$ )	Std. Error ( $\text{s}^{-1}$ ) <sup>b</sup>	Reference
<i>Eimeria tenella</i>	40		6		Lu <i>et al.</i> <sup>25</sup>
<i>Plasmodium falciparum</i>	48		10		Perozzo <i>et al.</i> <sup>59</sup>
<i>Toxoplasma gondii</i> <sup>a</sup>	40	6.7	26	1.6	This Study <sup>a</sup>

<sup>a</sup>Kinetic measurements were determined in triplicate and the data were analyzed with GraphPad Prism software. <sup>b</sup>Standard error as reported in GraphPad Prism software.

**Table 3.** Thermal shift assay results for potent inhibitors of *Tg*ENR from **Table 1** and those described elsewhere.<sup>37, 39</sup>

Compd.	Structure	<i>Tg</i> ENR Inhibition		Thermal Shift Assay				
		IC <sub>50</sub> (nM)	95% Conf. Interval (nM)	K <sub>d</sub> (nM) at 100 μM <sup>a</sup>		K <sub>d</sub> (fM) at 6 mM <sup>b</sup>		NAD <sup>+</sup> K <sub>d</sub> Ratio <sup>c</sup>
Triclosan		15	13-22	1.3	± 0.7	20	± 3	62,000
19		24	16-36	1.6	± 0.8	6.3	± 1	250,000
20 <sup>d</sup>		38	30-48	nd		nd		nd
21 <sup>d</sup>		54	43-68	nd		nd		nd
22 <sup>d</sup>		28	22-36	nd		nd		nd
23 <sup>d</sup>		18	14-24	nd		nd		nd
24		26	23-41	680	± 200	2,000	± 300	350,000
25		43	35-54	600	± 30	257	± 40	2,300,000
26		31	26-37	560	± 50	1,800	± 400	310,000
27		19	17-21	6.9	± 2	33	± 5	210,000
28		33	27-40	460	± 5	826	± 90	550,000

29		100	79-126	19,000	± 9,000	116,000	± 50	170,000
30		41	31-54	9,700	± 1,000	887,000	± 100,000	11,000
31		30	25-34	480	± 60	5,300	± 2,000	90,000
32		58	42-79	440	± 30	689	± 40	630,000
5		3	2-5	2.1	± 2	20	± 1	110,000
9		13	10-16	0.8	± 0.2	27.5	± 6	30,000
10		16	13-20	7.3	± 0.2	68.9	± 70	110,000
11		8	7-9	170	± 100	1,000	± 3,000	170,000
15		18	16-20	9.9	± 1	27.5	± 6	360,000
17		23	19-26	210	± 60	939	± 200	220,000

<sup>a</sup>K<sub>d</sub> of inhibitor at a NAD<sup>+</sup> concentration of 100 μM with standard deviation from triplicate measurements. <sup>b</sup>K<sub>d</sub> of inhibitor at a NAD<sup>+</sup> concentration of 6 mM with standard deviation from triplicate measurements. <sup>c</sup>Ratio of K<sub>d</sub> at 100 μM NAD<sup>+</sup> to K<sub>d</sub> at 6 mM NAD<sup>+</sup>. <sup>d</sup>These compounds interfered with the TSA.

## **Chapter 4**

### **Redox-Dependent Lipoylation of Mitochondrial Proteins in *Plasmodium falciparum***

Adapted from paper submitted to *Molecular Microbiology*, December 2013

## **Abstract**

Lipoate scavenging from the human host is essential for malaria parasite survival.

Scavenged lipoate is covalently attached to three parasite proteins: the H-protein and the E2 subunits of branched chain amino acid dehydrogenase (BCDH) and  $\alpha$ -ketoglutarate dehydrogenase (KDH). We show mitochondrial localization for the E2 subunits of BCDH and KDH, similar to previously localized H-protein, demonstrating that all three lipoylated proteins reside in the parasite mitochondrion. The lipoate ligase 1, LipL1, has been shown to reside in the mitochondrion and it catalyzes the lipoylation of the H-protein; however, we show that LipL1 alone cannot lipoylate BCDH or KDH. A second mitochondrial protein with homology to lipoate ligases, LipL2, does not show ligase activity and is not capable of lipoylating any of the mitochondrial substrates. Instead, BCDH and KDH are lipoylated through a novel mechanism requiring both LipL1 and LipL2. This mechanism is sensitive to redox conditions where BCDH and KDH are exclusively lipoylated under strong reducing conditions in contrast to the H-protein which is preferentially lipoylated under less reducing conditions. Thus, malaria parasites contain two different routes of mitochondrial lipoylation, an arrangement that has not been described for any other organism.

## Introduction

*Plasmodium falciparum* (*Pf*) is the deadliest of five apicomplexan parasite species capable of causing malaria in humans.<sup>1-4</sup> *Plasmodium* spp. first invade the liver and undergo a single round of replication. This phase is asymptomatic, in contrast to the erythrocytic stage of the parasite life cycle, which is characterized by a cyclical fever corresponding to multiple rounds of parasite replication within red blood cells.

Increasing resistance to current drugs that target erythrocytic stage parasites makes it necessary to characterize pathways that are essential for parasite survival.<sup>5-8</sup> One such pathway believed to be essential for malaria parasites is lipoate metabolism.<sup>9-11</sup> The parasite contains two organelles that harbor non-redundant pathways for lipoate metabolism: the apicoplast -a plastid organelle- and the mitochondrion.<sup>9, 11, 12</sup> The apicoplast contains a lipoate biosynthesis pathway that is critical for liver stage parasite development, but is dispensable in the erythrocytic stage.<sup>13-15</sup> The mitochondrion relies on lipoate scavenging from the host, which has been proposed to be essential for parasite survival during the erythrocytic stage.<sup>9, 10, 16</sup>

Lipoate is an essential cofactor for aerobic metabolism in oxidative decarboxylation reactions of 2-oxoacid complexes. Each complex is comprised of three subunits named E1, E2 and E3, except for glycine cleavage system which does not form a stable complex.<sup>17</sup> Lipoate is attached to a conserved lysine residue of a small lipoyl domain (LD) through an amide bond, serving as a swinging arm to shuffle reaction intermediates between active sites.<sup>18, 19</sup> LDs are typically found at the N-terminus of the E2-subunit of the 2-oxoacid dehydrogenase complexes. The H-protein of the glycine cleavage system (GCV) functions as a LD. Lipoate shuffles the decarboxylated acid from the E1 subunit



through a thioester linkage to the core of the E2-subunit where the acyl thioester is converted to the corresponding Coenzyme-A (CoA) thioester by thioester exchange. The dihydrolipoamide is oxidized to lipoamide by the dihydrolipoamide dehydrogenase (E3 subunit) to reset the catalytic cycle. The glycine cleavage system works in a similar fashion, but instead of three subunits it is composed of four loosely associated proteins: the P-protein (corresponding to the E1 subunit), the H-protein (lipoyl domain), the T-protein (core of E2-subunit) and the L-protein, which is the E3 subunit.<sup>20</sup>

Lipoate metabolism has been best characterized in *Escherichia coli* (*E. coli*), which has both biosynthetic and scavenging pathways (**Figures 1A and 1C**). In *E. coli*, unlike in *Plasmodium* spp., these two pathways have been shown to be redundant.<sup>21</sup> Lipoate biosynthesis starts with an octanoyl transferase (*EcLipB*), which transfers the octanoyl group from octanoyl-Acyl Carrier Protein (octanoyl-ACP) to a conserved lysine of the lipoate requiring proteins.<sup>22</sup> Then a lipoyl synthase (*EcLipA*) inserts two sulfur atoms in positions C6 and C8 of the octanoyl group to produce the lipoyl moiety (**Figure 1A**).<sup>23</sup> The scavenging pathway uses a lipoate ligase (*EcLplA*) to attach lipoate to LDs in an ATP-dependent reaction (**Figure 1C**).<sup>21, 24</sup>

Lipoate synthesis in the apicoplast of *Pf* follows the same pathway as the biosynthetic pathway described for *E. coli*.<sup>11, 25</sup> However, less is known about the mechanism of lipoate metabolism in the parasite mitochondrion, which relies on lipoate scavenged from the host.<sup>9</sup> Once lipoate is imported into the mitochondrion, there are two candidate enzymes, lipoate ligase 1 (LipL1) and lipoate ligase 2 (LipL2), which could catalyze the attachment of free lipoate to the lipoate requiring proteins. LipL1 and LipL2, which have both been localized to the mitochondrion,<sup>15, 26</sup> share about 21% sequence identity and are

unlikely to be paralogs.<sup>9</sup> Three lipoate requiring proteins have been localized or predicted to be in the mitochondrion: branched chain amino acid dehydrogenase (BCDH),  $\alpha$ -ketoglutarate dehydrogenase (KDH), and the H-protein of the GCV.<sup>12</sup> The H-protein has been previously localized to the mitochondrion<sup>20</sup> and LipL1 can lipoylate the H-protein in an ATP-dependent reaction.<sup>9</sup> There is no known activity for LipL2 in the *Pf* mitochondrion, and no mechanism to lipoylate E2-BCDH or E2-KDH has yet been described.

It has been proposed that lipoate scavenged from red blood cells is essential to the parasite.<sup>10</sup> The halogenated compound 8-bromooctanoate (8-BrO) causes parasite growth inhibition and reduced lipoylation of lipoate requiring proteins in the mitochondrion is observed.<sup>9</sup> The reliance on scavenged lipoate makes this an attractive process to target with therapeutics. Yet, several questions remain unanswered: what is the compartmentalization of BCDH and KDH substrates; why does the parasite possess two non-paralogous lipoate ligases; what is their activity and substrate specificity against the three possible lipoate requiring substrates in the mitochondrion; and last, how does 8-BrO inhibit parasite growth?

Here we present mitochondrial localization data for the E2 subunits of BCDH and KDH in *Pf*. We show that LipL1 is the only active lipoate ligase in the parasite mitochondrion modifying the H-protein through an ATP-dependent reaction; however LipL1 does not recognize the other substrates, BCDH and KDH. LipL2 does not exhibit ligase activity against any of the mitochondrial substrates. Interestingly, both LipL1 and LipL2 are required in an ATP-dependent reaction to lipoylate BCDH and KDH. These two mitochondrial lipoylation pathways show dependence on the lipoate redox state. The

H-protein can be lipoylated under all conditions tested, but increased lipoylation is observed under less reducing conditions. In contrast to the H-protein, BCDH and KDH are only lipoylated under strong reducing conditions. Last, a lipoate analog that mimics the reduced form, 6,8-dichlorooctanoate (6,8-diClO), causes blood stage parasite growth inhibition similar to 8-BrO. 6,8-diClO can be scavenged by the parasite and attached to BCDH and KDH in the mitochondrion. Modification with 6,8-diClO or 8-BrO leads to irreversible inactivation of these mitochondrial enzymes and subsequent parasite death.

## **Materials and Methods**

### *Expression plasmids*

The malaria genome resource PlasmoDB<sup>48</sup> was used to identify the genes encoding the E2 subunits of BCDH (PF3D7\_0303700) and KDH (PF3D7\_1320800). Nucleotides encoding the first 30 amino acids of both proteins were amplified from cDNA extracted from erythrocytic stage *Plasmodium falciparum* 3D7 parasites using primers BCDH<sub>30</sub>.AvrII.F and BCDH<sub>30</sub>.BsiWI.R or KDH<sub>30</sub>.AvrII.F and KDH<sub>30</sub>.BsiWI.R (**Table 1**). The BCDH<sub>30</sub> and KDH<sub>30</sub> amplicons were digested with *AvrII* and *BsiWI* and ligated into parasite transfection plasmid pRL2<sup>49</sup> in frame with GFP, generating plasmids pRL2-BCDH<sub>30</sub>GFP and pRL2-KDH<sub>30</sub>GFP. Plasmid pRL2 is a variant of pLN<sup>27</sup> in which the calmodulin promoter has been replaced with the weaker ribosomal protein L2 promoter.<sup>50</sup>

Ampicillin-resistant plasmid pGEXT<sup>51</sup> was used to express lipoylation domains with an amino-terminal glutathione *S*-transferase (GST) tag. The nucleotides encoding the lipoylation domain of BCDH (residues V34-L139) and KDH (residues I35-N152) were amplified using primers BCDH.BamHI.F100 and BCDH.EcoRI.R417 or

KDH.BamHI.F103 and KDH.EcoRI.R456 (**Table 1**). The BCDH<sub>LD</sub> and KDH<sub>LD</sub> amplicons were digested with *EcoRI* and *BamHI* and ligated into pGEXT, generating plasmids pGEXT-BCDH<sub>LD</sub> and pGEXT-KDH<sub>LD</sub>.

A kanamycin-resistant expression plasmid, pGEXTK, was generated by subcloning the kanamycin cassette from plasmid pRK586<sup>52</sup> into the *BspHI* sites of pGEXT using primers Kan.BspHI.F and Kan.BspHI.R (**Table 1**). The nucleotides encoding BCDH<sub>LD</sub> and KDH<sub>LD</sub> were subcloned from pGEXT to pGEXTK using *BamHI* and *Sall*, generating plasmids pGEXTK-BCDH<sub>LD</sub> and pGEXTK-KDH<sub>LD</sub>. Nucleotides encoding residues E35-K200 (lacking the predicted N-terminal mitochondrial transit peptide) of the H-protein (PF3D7\_1132900) were amplified from an expression plasmid similar to pMA007<sup>9</sup> with primers Hprot.BamHI.F and Hprot.Sall.R (**Table 1**). The resulting amplicon was digested with *BamHI* and *Sall*, and ligated into pGEXTK, generating plasmid pGEXTK-Hprot.

Expression plasmid pMALcHT<sup>9, 53</sup> was used to express lipoylation enzymes as maltose binding protein (MBP) fusion proteins with a linker region composed of a tobacco etch virus (TEV) protease cut site followed by a six histidine affinity tag. Plasmid pMA006<sup>9</sup> expressing LipL1 (PF3D7\_1314600) was renamed pMALcHT-LipL1 for this study. A codon harmonized gene (**Figure 2**) encoding LipL2 (PF3D7\_0923600) was synthesized by GeneArt and ligated to pMALcHT using the *EcoRI* and *HindIII* sites, generating pMALcHT-LipL2. The gene encoding *E. coli* lipoylation ligase, *EcLplA*, was amplified from BL21 gDNA with primers LplA.BamHI.F and LplA.Sall.R (**Table 1**), digested with *BamHI* and *Sall*, and ligated to pMALcHT, generating pMALcHT-LplA.

*Construction of lplA-/lipB- E. coli (JEG3 strain)*

In order to construct the JEG3 cell line a *lipB-* *E. coli* strain was obtained from the Keio deletion collection (Keio JW5089). The kanamycin resistance cassette was removed by transforming JW5089 cells with the ampicillin resistant pCP20 Flp recombinase plasmid.<sup>54</sup> Colonies were selected on kanamycin and ampicillin and incubated at 30 degrees. One colony was transferred to liquid LB medium without antibiotic and incubated overnight at 42 degrees in order to induce the loss of the pCP20 plasmid. Colonies were selected on LB agar plates followed by replica plating on LB plates containing LB alone, ampicillin, or kanamycin to screen for colonies which had successfully lost both the kanamycin resistance cassette and the pCP20 plasmid. This kanamycin sensitive *lipB-* strain was called JEG1. Primers LplA.H.F and LplA.H.R (**Table 1**) were designed based on the homologous regions flanking the *lplA* gene originally described by Baba and coworkers.<sup>28</sup> These primers were used to amplify the kanamycin cassette flanked by FRT sites which had previously been inserted into the *lplA* locus in *lplA* - Keio strain JW4349. JEG1 cells were transformed with plasmid pKD46 which expresses  $\lambda$  Red recombinase (GenBank Accession number AY048746).<sup>29</sup> Chemically competent JEG1/pKD46 cells were prepared and transformed with 400 ng of the PCR product generated above and grown in SOC medium with 1 mM L-arabinose for 2 hours at 37 degrees, after which they were selected with kanamycin on LB agar plates. Three colonies were screened for the *lplA* deletion by PCR using primers specific for the kanamycin cassette (K1.int.F and K2.int.R, **Table 1**) in combination with primers upstream and downstream of *lplA* (LplA.U and LplA.D, **Table 1**). This *lipB-*: Kan<sup>S</sup>, *lplA-*: Kan<sup>R</sup> line was called JEG2. A kanamycin sensitive line was generated as

described above using the pCP20 plasmid and called JEG3. Primers LipB.U and LipB.D (**Table 1**) flanking the *lipB* locus were used in conjunction with primers LplA.U and LplA.D to verify the deletion of both genes in strain JEG3.

#### *Parasite culture for protein localization*

*P. falciparum* asexual blood stage cultures were maintained at 2% hematocrit in complete medium consisting of RPMI 1640 medium with L-glutamine (Gibco) supplemented with 10% human serum (Interstate Blood Bank, Memphis, TN), 25 mM HEPES, 0.24% NaHCO<sub>3</sub>, and 12.5 µg/ml hypoxanthine.<sup>55</sup> Site-specific integration mediated by the mycobacteriophage Bxb1 integrase was used to generate cell lines with the pRL2-BCDH<sub>30</sub>GFP and pRL2-KDH<sub>30</sub>GFP plasmids described above that were integrated into the attB locus of Dd2<sup>attB</sup> parasites.<sup>27</sup> Transfection of parasites was conducted as described previously.<sup>20</sup> Cell lines were analyzed for integration at the attB site by PCR analysis of genomic DNA using primers that flank the 5' and 3' integration sites. Parasites were imaged on a Nikon Eclipse E800 epifluorescence microscope. For live fluorescence, cells were incubated with 100 nM MitoTracker CMX-Ros (Invitrogen) and 1 µg/ml Hoechst 33258 to visualize parasite mitochondria and nuclei.

#### *Protein expression and purification*

Plasmid pMALcHT-LipL1 was transformed into BL21-Star (DE3) cells (Invitrogen) and co-transformed with the pRIL plasmid isolated from BL21-CodonPlus-RIL cells (Agilent) and plasmid pRL586 encoding the Tobacco Etch Virus (TEV) protease,<sup>52</sup> as previously described.<sup>9</sup> These cells produce LipL1 fused to an amino-terminal six

histidine-tag. Transformed cells were grown to mid-log phase, and the expression of recombinant proteins was induced by the addition of 0.4 mM IPTG. Cells were harvested after growth for 10 h at 20°C. LipL1 was purified by metal chelate chromatography followed by cation exchange chromatography; LipL1 was further purified by gel filtration. Plasmid pMALcHT-LipL2 was transformed into BL21-Star (DE3) and co-transformed with the pRIL plasmid. These cells produce LipL2 fused to an amino-terminal MBP. LipL2 was affinity purified using Amylose resin (NEB #E8021).

The plasmids pGEXT-BCDH<sub>LD</sub>, pGEXT-KDH<sub>LD</sub> or pGEXTK-Hprot were transformed into JEG3 cells containing the pRIL plasmid. These cells produced BCDH<sub>LD</sub>, KDH<sub>LD</sub> or the H-protein in the apo-form (non-lipoylated) with an amino-terminal GST fusion protein. The proteins were purified by GSTrap FF chromatography (GE Healthcare). All cultures were grown and harvested as described for LipL1, with the exception that JEG3 cultures were supplemented with 5 mM sodium succinate, 5 mM sodium acetate and 1% glucose. All purifications were conducted with 20 mM HEPES, 100 mM NaCl at pH 7.5 as the base buffer. For GST purifications, 1 mM DTT was used during the steps of lysis and purification. The concentration of proteins after purification was determined by Bradford assay.

#### *Cell-based lipoylation assay*

The JEG3 lipoylation deficient *E. coli* strain was transformed with the pRIL plasmid and grown in LB medium supplemented with 1% glucose as a carbon source and 35 µg ml<sup>-1</sup> chloramphenicol. Sodium succinate (5 mM) and sodium acetate (5 mM) were added to bypass the requirement for KDH and PDH activity respectively. JEG3/pRIL was

transformed with a plasmid expressing a candidate lipoate ligase (either pMALcHT-LipL1, pMALcHT-LipL2 or pMALcHT-*Ec*LplA) and a plasmid expressing a lipoylation substrate (pGEXTK-BCDH<sub>LD</sub> or pGEXTK-KDH<sub>LD</sub>) and selected using 100 µg ml<sup>-1</sup> ampicillin and 50 µg ml<sup>-1</sup> kanamycin. Transformants were grown in LB medium and supplemented as described above with the addition of 200 µM *R*-lipoic acid (Sigma). Plasmids pGEXTK-BCDH<sub>LD</sub> and pGEXTK-KDH<sub>LD</sub> were also transformed into BL21-Star (DE3) cells containing the pRIL plasmid and maintained in LB medium containing 35 µg ml<sup>-1</sup> chloramphenicol and 50 µg ml<sup>-1</sup> kanamycin. For the cell-based assay 20 mL cultures were grown to mid-log phase at 37 degrees and induced with 0.4 mM IPTG for 10 hours at 20 degrees. Cells were harvested by centrifugation and resuspended with 0.5 mL of buffer containing 20 mM HEPES, 100 mM NaCl at pH 7.5 and lysed by sonication. The cell lysates were clarified by centrifugation at 16,000 g and the supernatants were collected and resolved by SDS-PAGE (Invitrogen). Lipoylated proteins were visualized by western blot as described in lipoate ligase assay section.

#### *Synthesis of 6,8-dichlorooctanoic acid (6,8-diClO)*

The preparation of 6,8-diClO was carried out using the ester hydrolysis conditions previously reported for similar analogs.<sup>56</sup> All reagents were obtained from commercial sources. A solution of ethyl 6,8-dichlorooctanoate (500 mg, 2 mmol) in EtOH (1 mL) was added to a suspension of LiOH (72 mg, 3.0 mmol) in 50:50 EtOH/water (1 mL) at room temperature. The mixture was stirred at room temperature and monitored by thin layer chromatography (CH<sub>2</sub>Cl<sub>2</sub>) until the ester hydrolysis reaction appeared to be complete (2 h). Water was added (20 mL), and the resulting mixture was extracted with



EtOAc (3 × 10 mL). The aqueous layer containing the product was acidified to pH 2 using 1N HCl, and extracted with EtOAc (3 × 20 mL). 6,8-Dichlorooctanoic acid was obtained as an oil (386 mg, 88%,  $R_f = 0.76$  in  $\text{CH}_2\text{Cl}_2$ ). NMR characterization was performed on a 400 MHz Varian instrument. Chemical shifts are reported in parts per million from tetramethylsilane. HRMS characterization was carried out at the University of Illinois Mass Spectrometry Lab using ES ionization.  $^1\text{H}$  NMR ( $\text{CDCl}_3$ )  $\delta$  4.10 (m, 1H); 3.70 (m, 2H); 2.37 (t, 2H); 2.11 (m, 2H); 1.76 (q, 2H); 1.65 (m, 3H), 1.50 (m, 1H). HRMS: calcd. for  $\text{C}_8\text{H}_{14}\text{O}_2\text{Cl}_2$ :  $m/z$  235.0277  $[\text{M} + \text{Na}]^+$ ; found: 235.0269.

#### *Lipoate ligase assay*

Purified LipL1 or LipL2 (1  $\mu\text{M}$ ) was incubated in reaction buffer (100 mM Na/K Phosphate buffer, 150 mM NaCl at pH 7.5) containing 2 mM ATP, 2 mM  $\text{MgCl}_2$ , 5 mM TCEP, 200  $\mu\text{M}$  *R*-lipoic acid and 10  $\mu\text{M}$  apo-protein substrate: H-protein,  $\text{BCDH}_{\text{LD}}$ , or  $\text{KDH}_{\text{LD}}$ . After incubation at 37 degrees for 1 hour, the reactions were terminated with the addition of gel loading buffer and analyzed by SDS-PAGE followed by transfer to nitrocellulose membrane. The membranes were blocked with 5% milk in PBS for 30 minutes, and probed with 1:5000 rabbit polyclonal  $\alpha$ -LA (Calbiochem) for 2 hours in 1% milk/PBS at room temperature. The membrane was washed with 1xPBS three times and then probed with 1:5000 donkey  $\alpha$ -Rabbit IgG horseradish peroxidase (HRP) secondary antibody (GE Healthcare) in 1% milk/PBS overnight at 4 degrees. The membranes were visualized with enhanced chemiluminescence (ECL) western substrate (Pierce) and exposed to film.

All lipoylation assays were conducted similarly using the same protein concentrations and base buffer. Where indicated, ATP was omitted from the reaction and 5 mM of DTT or water was used instead of TCEP. *R*-lipoic acid was substituted with 200  $\mu$ M 6,8-dichlorooctanoate or 200  $\mu$ M 8-bromooctanoate where indicated, and in these reactions 1:5000 rabbit polyclonal  $\alpha$ -6,8-diClO was used as the primary probe for western blots.

#### *Amidotransferase assay*

Lipoylated H-protein (Holo H-protein) was generated by co-transforming pGEXTK-Hprot and pMALcHT-LipL1 in JEG3 cells containing the pRIL plasmid. These cells express the H-protein with an amino-terminal GST tag and LipL1 with an amino-terminal MBP. One liter cultures were grown to mid-log phase and induced with 0.4 mM IPTG for 10 hours at 20 degrees. Cells were harvested as described above and Holo H-protein was purified by affinity chromatography using a GSTrap FF column (GE Healthcare), followed by anion exchange using a MonoQ column (Pharmacia). The protein concentration was determined by Bradford assay. A final concentration of 10  $\mu$ M of Holo H-protein was used in all assays, in the presence of 1  $\mu$ M of LipL1 and/or LipL2 and 10  $\mu$ M of BCDH<sub>LD</sub> or KDH<sub>LD</sub>, 2 mM MgCl<sub>2</sub>, 5 mM TCEP in 100 mM Na/K Phosphate buffer, 150 mM NaCl at pH 7.5. The reactions were incubated and analyzed as described in the lipoate ligase assay.

#### *Production of rabbit $\alpha$ -6,8-diClO antiserum*

Compound 6,8-diClO was conjugated to keyhole limpet hemocyanin using the Imject EDC mcKLH Spin Kit (Pierce). Antibodies to the conjugate were generated in rabbits

using the standard protocol of the custom antibody service Cocalico Biologicals (Reamstown, PA). The resulting antiserum was used in western blots where indicated with the label  $\alpha$ -6,8-diClO to probe for proteins modified with either 8-bromooctanoate or 6,8-dichlorooctanoate.

*Parasite culture for 6,8-diClO growth inhibition assay and labeling*

All *Plasmodium falciparum* parasite lines for these experiments were grown as previously described<sup>9</sup> with the following exceptions: complete media was supplemented with 10% Albumax (Gibco) and parasites were maintained under a 3% O<sub>2</sub> and 3% CO<sub>2</sub> gas mixture. To assess parasite growth in the presence of 6,8-diClO, Dd2<sup>attB</sup> parasites were synchronized with 5% sorbitol<sup>57</sup> and seeded into 6-well plates at 0.05% parasitemia. Parasites were treated with 0, 25, 100, 400, and 1000  $\mu$ M 6,8-diClO. All dilutions of 6,8-diClO were prepared in DMSO so that the final amount of DMSO in the parasite culture was 0.05%. For all experiments culture media and drug were added fresh each day. Blood smears were made every other day to monitor parasitemia.

For western blot analysis, asynchronous 3D7 parasites were seeded at 1% parasitemia and treated with 10  $\mu$ M 6,8-diClO, 2  $\mu$ M *R*-lipoic acid in 10% EtOH or vehicle for three days. Parasites were isolated from red blood cells using 0.5% saponin in PBS as previously described.<sup>9</sup> Parasite pellets were resuspended in RIPA Buffer (Boston BioProducts) supplemented with protease inhibitors (Complete Mini EDTA-free, Roche) and lysed by vigorous vortexing. Insoluble debris was pelleted at 10,000 g and total protein of the supernatant was measured by Bradford assay. Loading dye was added to the supernatant and samples were boiled for 5 min at 95 degrees and separated on a 4–

12% gradient gel (Invitrogen) by SDS-PAGE. Western blots were conducted as described above using 1:5000 rabbit  $\alpha$ -6,8-diClO or 1:1000 rabbit  $\alpha$ -LA (Calbiochem) as the primary probes. Membranes were stripped and re-probed with 1:10,000 mouse  $\alpha$ -PfHsp70<sup>58</sup> as a loading control.

## Results

### *The E2 subunits of BCDH and KDH localize to the parasite mitochondrion*

To better understand lipoylation in the mitochondrion of *Plasmodium falciparum* (*Pf*), we first investigated the localization of the two lipoylated substrates predicted to be mitochondrial: the E2 subunits of BCDH and KDH.<sup>12</sup> The E1 $\beta$  subunit of BCDH and the shared E3 subunit have been previously localized to the mitochondrion in *Pf*, showing that components of 2-oxoacid dehydrogenase reside in this compartment.<sup>12</sup> The E2-BCDH of *Plasmodium berghei* has been localized to the mitochondrion.<sup>14</sup> To confirm the localization of the *Pf*E2 proteins, we generated constructs in which the first 30 amino acids containing the predicted mitochondrial targeting sequence of E2-BCDH and E2-KDH were fused to green fluorescent protein (GFP). The transgene was inserted into the *Pf*cg6 locus by mycobacteriophage integrase mediated recombination<sup>20,27</sup> and GFP fluorescence from these parasites was analyzed by live microscopy. For both E2-GFP transgenic parasite lines, we observed GFP fluorescence in an organelle with branched-like morphology that co-localized with the mitochondrial marker MitoTracker (**Figure 3A**). We confirmed expression of these constructs by western blot (**Figure 3B**). These results demonstrate that the lipoylated E2 subunits of BCDH and KDH, in addition to the

H-protein, reside in the mitochondrion with the previously localized lipoate attachment enzymes, LipL1 and LipL2.<sup>15, 26</sup>

*Neither LipL1 nor LipL2 lipoylate BCDH<sub>LD</sub> or KDH<sub>LD</sub> in a cell-based lipoylation assay*

The lipoate attachment enzymes LipL1 and LipL2 are predicted to be lipoate ligases based on sequence homology to the *E. coli* lipoate ligase (*EcLplA*).<sup>9</sup> LipL1 can complement a lipoylation deficient *E. coli* cell line (TM136) in minimal media by adding exogenous lipoate, demonstrating its activity as a ligase.<sup>9</sup> LipL2 has been shown to have similar activity in TM136 cells but cell growth required four days of incubation, making this datum less conclusive.<sup>9</sup> An additional factor complicating these experiments involves the low level of endogenous lipoylation that remains in the TM136 line. Apparently, transposon disruption of the *lplA* gene does not completely ablate lipoate ligase activity in TM136 (**Figure 4**). Therefore, we used a lambda red recombination system<sup>28, 29</sup> to generate an *E. coli* *lplA* and *lipB* deletion line (*lplA*-/*lipB*-) that is completely deficient in lipoylation activity (**Figure 4**). We used this new strain (JEG3) to conduct cell-based lipoylation assays. The lipoylation domains of BCDH and KDH (BCDH<sub>LD</sub> and KDH<sub>LD</sub>, respectively) were subcloned into a pGEX vector expressing GST (glutathione *S*-transferase) fusion proteins. To validate that BCDH<sub>LD</sub> and KDH<sub>LD</sub> are competent lipoylation substrates, we expressed each domain in wild type BL21 cells and found that they were lipoylated by *E. coli* lipoylation enzymes when visualized by western blot using an antibody against lipoic acid ( $\alpha$ -LA) (**Figure 3C**). We next subcloned LipL1, LipL2 and *EcLplA* into a pMAL vector expressing MBP (maltose binding protein) fusion proteins. We co-expressed each LD in the JEG3 cell line with

either *Pf*ligase or *Ec*LplA. We found that the *Ec*LplA was sufficient to lipoylate BCDH<sub>LD</sub> and KDH<sub>LD</sub> (**Figure 3D, lanes 1-2**), but neither substrate was lipoylated in our *in vitro* cell-based assay by either putative *Pf*ligase when visualized by western blot (**Figure 3D, lanes 3-6**). The lack of activity against BCDH<sub>LD</sub> and KDH<sub>LD</sub> was surprising since LipL1 is competent to lipoylate *Ec*KDH and *Ec*PDH (**Figure 3D, lanes 3-4**) and LipL2 apparently lipoylates *Ec*PDH, albeit poorly (**Figure 3D, lanes 5-6**).

*LipL1 has substrate specific lipoate ligase activity*

To verify the unexpected behavior of LipL1 and LipL2, we decided to study the activity of purified recombinant enzymes. The BCDH<sub>LD</sub> and KDH<sub>LD</sub> lipoylation domains and truncated H-protein, lacking the N-terminal transit peptide, were expressed as GST fusion proteins in the lipoylation deficient JEG3 cell line and purified in the apo form. We tested recombinant LipL1 and LipL2 alone against each apo substrate in the presence or absence of ATP, and visualized lipoylation by western blot. As shown in **Figure 5A**, LipL1 is an active ligase only against the H-protein in an ATP-dependent reaction (**top panel, lanes 1-2**) in agreement with a previous report in which full length H-protein was used.<sup>9</sup> We also found that ATP is the preferred nucleotide used by LipL1 with minor activity observed with GTP (**Figure 6A**). Consistent with results observed in the cell-based assay, LipL1 did not catalyze the lipoylation of BCDH<sub>LD</sub> or KDH<sub>LD</sub> (**Figure 5A, top panel, lanes 3-6**). Similarly, we found that LipL2 did not lipoylate any of the *Pf* substrates in our *in vitro* ligation assay (**Figure 5A, lower panel**). These results, along with those from the *in vitro* cell-based assay, show that BCDH<sub>LD</sub> and KDH<sub>LD</sub> are lipoylated by *E. coli* lipoylation enzymes, but not by either candidate *Pf*lipoate ligase.

LipL1 appears to be the only lipoate ligase with the H-protein as its only parasite substrate.

*Neither LipL1 nor LipL2 acts as an amidotransferase*

Lipoate metabolism has also been described in other systems such as *Bacillus subtilis*.<sup>30,31</sup> In *B. subtilis*, an enzyme similar to *E. coli* LipB (*BsLipM*) specifically octanoylates the H-protein, but does not modify other protein substrates (**Figure 1B**). An amidotransferase is then required to transfer octanoyl (or possibly lipoyl) groups from the H-protein to the remaining four lipoate-dependent proteins in *B. subtilis*.<sup>30,31</sup> We tested whether LipL1 or LipL2 could act as an amidotransferase in an assay in which the only lipoate source is the holo H-protein. We generated holo H-protein by expressing the *Pf* H-protein and LipL1 in the *E. coli* lipoylation deficient JEG3 cell line. The H-protein was then purified in the holo form by GST affinity chromatography. We tested the transferase activity of either LipL1 or LipL2 and found that neither enzyme can act as an amidotransferase (**Figure 5B, lanes 1-6**). Even when LipL1 and LipL2 are combined in the same reaction, they are unable to transfer lipoyl groups from the H-protein to either BCDH<sub>LD</sub> or KDH<sub>LD</sub> (**Figure 5B, lanes 7-9**). Thus, neither enzyme appears to be a lipoyl amidotransferase. We did not test LipL1 or LipL2 for the octanoyl amidotransferase activity observed in *B. subtilis* because there is no known source of octanoyl groups (fatty acid biosynthesis or degradation pathways) in the parasite mitochondrion.

*LipL1 and LipL2 are both required to lipoylate BCDH<sub>LD</sub> and KDH<sub>LD</sub> in a ligation reaction*

We next tested whether both LipL1 and LipL2 are required to ligate free lipoate to BCDH<sub>LD</sub> or KDH<sub>LD</sub> in our *in vitro* ligation assay. In these reactions, equimolar amounts of LipL1 and LipL2 were combined with substrate in the presence or absence of ATP. As shown in **Figure 5C**, both enzymes are required to lipoylate BCDH<sub>LD</sub> and KDH<sub>LD</sub> in an ATP-dependent ligation reaction (**Figure 6B**). Thus, LipL1 and LipL2 function together as a lipoate ligase for both substrates. Taken together, our results suggest two different routes by which the mitochondrial substrates of *Pf* are lipoylated: one in which LipL1 alone is sufficient to lipoylate the H-protein, and a second route in which both LipL1 and LipL2 are necessary to lipoylate BCDH and KDH.

*The two lipoylation routes differ in their redox dependence*

The lipoylation assays described in the previous sections were performed using tris(2-carboxyethyl)phosphine (TCEP) as reducing agent. As observed, all substrates can be modified in the presence of TCEP, but we found that the two lipoylation routes differed in their redox dependence. In order to better understand this effect we tested three reducing agents, dithiothreitol (DTT), TCEP, and tris(hydroxypropyl)phosphine (THP) in our *in vitro* ligation assay. We first tested the lipoylation of the H-protein by LipL1 in the presence and absence of the reducing agents. As seen in **Figure 7A**, the H-protein can be lipoylated by LipL1 under oxidizing or reducing conditions, albeit at different levels. There was enhanced activity of LipL1 under reducing conditions with DTT as compared to no reducing agent, perhaps because reducing agents in general help to protect lipoate from oxidative damage under aerobic conditions. However, the strong reducing agents TCEP and THP resulted in lower LipL1 activity compared to the weaker



reducing agent DTT. The lower activity of LipL1 in the phosphine reducing agents may have to do with the ability of agents like TCEP to reduce the dithiolane ring of lipoate.<sup>32</sup>

We next tested the activity of both LipL1 and LipL2 in lipoylating BCDH<sub>LD</sub> and KDH<sub>LD</sub> under different reducing environments. In contrast to the H-protein, BCDH<sub>LD</sub> and KDH<sub>LD</sub> are not lipoylated in the absence of reducing agents or under reducing conditions with DTT (**Figure 7B, lanes 5-8**). The LipL1/LipL2 reaction only occurs in the presence of the strong reducing agents TCEP (**Figure 7B, lane 9**) or THP (**Figure 8, top panel**). However, it is not clear from these results whether these strong reducing agents are acting on the lipoate redox state or affecting the enzymes (LipL1 and/or LipL2) and/or protein substrates (BCDH<sub>LD</sub> and KDH<sub>LD</sub>).

*6,8-dichlorooctanoate (6,8-diClO) is a non-redox sensitive lipoate analog*

To test whether the phosphine reducing agents are acting on lipoate or the proteins we used a non-redox sensitive lipoate analog, 6,8-dichlorooctanoate (6,8-diClO), which mimics the reduced form of lipoate (**Figure 5A**). We generated antiserum that is specific for proteins modified with 6,8-diClO and show that LipL1 can use 6,8-diClO as a substrate to modify the H-protein (**Figure 9B, lower panel, lane 3**). As shown in **Figure 9B**,  $\alpha$ -LA antibodies and the  $\alpha$ -6,8-diClO antiserum are specific for their respective substrates, even when the western blots are significantly overexposed. Using these reagents we tested the different lipoylation routes and their redox dependence in our *in vitro* assay.

When 6,8-diClO was used as a substrate to modify the H-protein, DTT was no longer the most favorable reducing agent and LipL1 activity appeared to be independent of

redox conditions (**Figure 9C**). The lower activity with TCEP (also observed in **Figure 7A**) probably results from the instability of TCEP in phosphate buffer rather than a redox effect.<sup>33, 34</sup> The other strong reducing agent THP only decreased LipL1 activity relative to DTT when lipoate, but not 6,8-diClO was used as a substrate, indicating a redox-specific effect on lipoate itself (**compare lanes 3 & 7 from Figures 7A and 9C**). A similar phenomenon was observed for the lipoylation of BCDH<sub>LD</sub> and KDH<sub>LD</sub>. LipL1 and LipL2 modified these substrates with 6,8-diClO independent of the redox environment (**Figures 9D and 8, bottom panel**). These results demonstrate that the requirement for the strong phosphine reducing agents in the LipL1/LipL2 lipoylation reactions is actually a requirement for reduced lipoate in these reactions and that the proteins themselves do not need to be reduced in order to be functional (**Figure 9A**). The redox state of lipoate appears to be important for the lipoylation of the different mitochondrial substrates. BCDH and KDH are only modified when lipoate is in the reduced state, while the H-protein shows increased lipoylation under less reducing conditions.

#### *Lipoate analogs are scavenged and attached to mitochondrial substrates*

We have previously shown that the lipoate analog 8-BrO inhibits the growth of blood stage *Pf* and that treatment with 8-BrO reduces the lipoylation of the three substrates found in the mitochondrion of *Pf*.<sup>9</sup> From these results, it was not clear whether 8-BrO blocked lipoate import, activation and transfer of lipoate, or if attachment of 8-BrO to the mitochondrial substrates inhibited their activity. We know from the above experiments that 6,8-diClO can be attached to all mitochondrial substrates in our *in vitro* assay (see

**Figures 9C and 9D).** To determine if 8-BrO can be attached to the parasite proteins, we used the  $\alpha$ -6,8-diClO antiserum, which also recognizes proteins modified with 8-BrO. As shown in **Figure 10A**, 8-BrO can be attached to all three mitochondrial substrates in an ATP-dependent reaction in our *in vitro* assay, suggesting that both lipoate analogs can potentially share a similar mode of action in malaria parasites.

We also treated asexual blood stage parasites with 6,8-diClO at different concentrations as done previously for 8-BrO<sup>9</sup>. We found that 6,8-diClO significantly inhibits parasite growth at a concentration of 100  $\mu$ M (**Figure 10B**), similar to growth inhibition results observed for 8-BrO. To determine whether this lipoate analog is attached to mitochondrial proteins in the parasites, we treated cultured parasites with 0 or 10  $\mu$ M 6,8-diClO and probed the lysates with  $\alpha$ -6,8-diClO antiserum. Both E2-BCDH and E2-KDH were modified with 6,8-diClO, demonstrating that this compound can be imported into parasites and used by the mitochondrial lipoylation enzymes (**Figure 10C**). In parallel experiments, we were able to detect lipoylated E2-BCDH, E2-KDH, and E2-PDH in parasites treated with lipoate (**Figure 10C**). Lipoylation of E2-PDH is independent of lipoate scavenging, consistent with the finding that lipoate is synthesized in the apicoplast.<sup>12</sup> We were unable to detect modification of the H-protein by either substrate, possibly due to low expression levels of this protein in the parasite.

## **Discussion**

The mitochondrion of *Plasmodium falciparum* (*Pf*) relies on lipoate scavenging from the host. Treatment of parasites with the lipoate analog 8-bromooctanoate (8-BrO) inhibited parasite growth and specifically blocked the lipoylation of mitochondrial

proteins.<sup>9</sup> These results indicated that lipoate scavenging is essential for the survival of malaria parasites and that the lipoylation machinery in the parasite mitochondrion would likewise be essential. *Plasmodium* spp. possess two putative lipoate ligases in the genome (LipL1 and LipL2) that are believed to catalyze the attachment of free lipoate to the lipoate requiring proteins in an ATP-dependent reaction. In *Pf*, LipL1 was localized to the mitochondrion<sup>26</sup> while LipL2 was reportedly found in the mitochondrion as well as the apicoplast organelle.<sup>15</sup> Although the role of LipL2 in the apicoplast is not well defined, both LipL1 and LipL2 are involved in the lipoylation of three proteins in the mitochondrion of malaria parasites. We have previously shown that one of these proteins, the H-protein, is mitochondrial<sup>20</sup>, and in this work we confirmed the mitochondrial localization of the E2 subunits of BCDH and KDH (**Figure 3A**). Thus, the mitochondrion of erythrocytic stage *Pf* contains two putative lipoate ligases responsible for the lipoylation of three protein substrates.

It was previously shown that LipL1 can catalyze the attachment of lipoate to full length H-protein in an ATP-dependent reaction<sup>9</sup> and it was assumed that LipL1 could lipoylate all of the mitochondrial substrates. Attempts to disrupt *Pf*LipL1 and the *P. berghei* ortholog failed<sup>16</sup> reinforcing the idea that lipoate scavenging is essential for blood stage malaria parasites and that LipL1 plays a key role in this process. In the present study, we observed lipoylation of the H-protein by LipL1, and found that it preferentially uses ATP as a nucleotide substrate (**Figure 6A**). These properties make LipL1 lipoate ligase activity similar to that of its *E. coli* ortholog, *EcLplA*. However, LipL1 is unable to lipoylate *Pf*BCDH and KDH (**Figures 3D and 5A**), while *EcLplA* is able to lipoylate both parasite proteins (**Figure 3D**). It is possible that LipL1 has an unusual specificity

for the H-protein. However, the ability of LipL1 to lipoylate the *Ec*PDH and *Ec*KDH when expressed in *E. coli* (**Figure 3D**) indicates that LipL1 is not highly specific for its substrates. Instead, the *Pf*BCDH and KDH may have unique features that are not recognized by LipL1. As shown in **Figures 3 and 5**, LipL2 does not have lipoate ligase activity with respect to any of the three parasite protein substrates.

The specificity of LipL1 for the H-protein is reminiscent of the lipoylation pathways described for *B. subtilis* (**Figure 1B**). In *B. subtilis*, an amidotransferase (LipL) with homology to lipoate ligases shuffles the lipoyl or octanoyl moiety from the H-protein to the other protein substrates.<sup>30,31</sup> We tested LipL1 or LipL2 alone, or in complex in an amidotransferase assay using lipoyl-H-protein as substrate (parasites lack a pathway to generate octanoyl-H-protein), but did not detect any transfer of lipoyl groups to either BCDH or KDH (**Figure 5B**). We also considered a recent report showing that a lipoate ligase homolog in *Saccharomyces cerevisiae* (Lip3) transfers octanoyl groups from octanoyl-CoA to protein substrates followed by sulfur insertion by a lipoyl synthase (Lip5).<sup>35</sup> We did not test LipL1 or LipL2 for this type of octanoyl transferase activity since the mitochondrion of malaria parasites does not contain a lipoyl synthase or a biochemical pathway likely to produce octanoyl-CoA.

The lipoylation of BCDH and KDH occurs through a novel mechanism requiring both LipL1 and LipL2 (**Figure 5C**). However, the role that each protein plays is unknown. It is likely that LipL1 is responsible for at least activating lipoate, forming lipoyl-adenylate since this is the initial step catalyzed by LipL1 in the lipoylation of the H-protein. The role of LipL2 is less clear. It is possible that LipL2 catalyzes the transfer of lipoyl groups from lipoyl-adenylate to BCDH and KDH. It is also possible that LipL2 does not have a

catalytic role, but instead acts as an effector helping to recruit protein substrates that would otherwise not be recognized by LipL1. In either case, the LipL1/LipL2 reaction defines a second lipoylation pathway in the parasite mitochondrion (**Figure 11**). Attempts to disrupt the gene encoding *Pf*LipL2 have so far been unsuccessful,<sup>10</sup> suggesting that this second lipoylation pathway is essential for the survival of blood stage malaria parasites.

The two mitochondrial lipoylation pathways are sensitive to redox conditions (**Figure 11**). Lipoylation of H-protein by LipL1 in the first pathway is significantly enhanced in the presence of DTT, but is less active in the presence of strong reducing agents such as TCEP and THP (**Figure 7A**). The decreased lipoylation of H-protein in the presence of TCEP as compared to THP is likely due to the reactivity of TCEP in phosphate buffer.<sup>33,</sup><sup>34</sup> In contrast to the first pathway, the lipoylation of BCDH and KDH by the second pathway only occurs in the presence of TCEP or THP (**Figures 7B and 8**). The redox potential for both DTT and lipoate has been measured to be -0.33 V and -0.32 V, respectively.<sup>36,37</sup> Currently, there is no measurement of redox potential for TCEP or THP, but experimental data show that TCEP readily reduces both DTT and lipoate.<sup>32</sup> In the absence of reducing agent, lipoate is found in the oxidized, closed-ring form, but upon reduction with TCEP or THP it presumably adopts the open-ring dihydrolipoate form (**Figure 9A**). We synthesized a structural analog (6,8-diClO) of dihydrolipoate and used this compound to probe the redox requirements of the second lipoylation pathway. Using 6,8-diClO as a substrate, all three proteins were modified regardless of the redox conditions (**Figures 9C and 9D**). This demonstrates that the second pathway requires dihydrolipoate, and that the LipL1 and LipL2 enzymes are not themselves sensitive to

redox conditions. These results have interesting connotations for how lipoylation may work and why two different routes are needed in the mitochondrion of a malaria parasite.

Our results suggest that dihydrolipoate is needed in the mitochondrion for the lipoylation of BCDH and KDH. Therefore, the redox potential of the parasite mitochondrion needs to be highly reducing or the parasites must employ a mechanism to reduce lipoate to dihydrolipoate. While there is no measurement of the redox potential for the *Plasmodium* mitochondrion, the redox potential of the mitochondrion of HeLa cells has been reported to be -0.36 V.<sup>37</sup> This value is more reducing than that of lipoate, and it might be sufficient to reduce lipoate to dihydrolipoate and/or maintain lipoate in the reduced state. *Pf* has two redox systems: the glutathione and thioredoxin systems.<sup>38</sup> Six proteins from these systems have been localized to the mitochondrion: thioredoxin reductase (TrxR - dually localized to cytosol and mitochondrion), thioredoxin-like protein 2 (Tlp2), peroxiredoxin (Prx1m), glutaredoxin-like protein (Glp3), and peroxidase-like thioredoxin peroxidase (TPX<sub>G1</sub> – localized to the cytosol, mitochondria and apicoplast).<sup>38, 39</sup> These proteins are likely involved in maintaining the redox potential of the mitochondrion and/or defending against oxidative stress. It would be interesting to determine whether any of these proteins have the additional role of reducing lipoate. In addition to these redox systems, the dihydrolipoamide dehydrogenase (E3 subunit of mitochondrial dehydrogenase complexes, PF3D7\_1232200) likely recognizes free lipoate and reduces it. This has been observed for mammalian systems, in which lipoate is converted to dihydrolipoate in a NADH-dependent reaction in isolated mitochondrion.<sup>36,</sup>

40, 41

Inhibition of parasite growth by 8-BrO<sup>9</sup> or 6,8-diClO (**Figure 10B**) indicates that one or more of the lipoate-dependent proteins in the mitochondrion are essential. It is not clear, however, which of the three possible candidates is likely to have an essential role during the erythrocytic stages of parasite development. Two of the proteins, BCDH and KDH, are thought to be involved in central metabolism. The BCDH is so named because of its similarity to the branched chain amino acid dehydrogenases found in other organisms, however, malaria parasites do not appear to possess other enzymes required for the catabolism of branched chain amino acids.<sup>42</sup> In light of this fact, it has been proposed that BCDH could act as a mitochondrial pyruvate dehydrogenase to produce acetyl-CoA likely required for acetylation reactions in the organelle.<sup>42, 43</sup> A recent survey of protein acetylation in *Pf* found 421 sites in 230 proteins distributed throughout multiple subcellular compartments.<sup>44</sup> Deletion of the gene encoding the E1 subunit of the KDH complex led to accumulation of 2-oxoglutarate and reduction of succinyl-CoA, establishing the role of KDH in the parasite TCA cycle.(Akhil Vaidya, manuscript in submission). While this result shows that KDH activity (and the TCA cycle) is dispensable in blood stage parasites, it is possible that the lipoylated E2-KDH subunit has an additional, essential role in the parasite independent of the TCA cycle in maintaining the redox potential of the mitochondrion (see below). Even though our results suggest an important role for either or both BCDH and KDH in parasite survival, we cannot rule out the essentiality of the H-protein.

The H-protein is perhaps the most puzzling of the three lipoylated mitochondrial proteins. It is unlikely to function as part of a glycine cleavage system due to the lack of an identifiable P-protein in the parasite genome.<sup>45</sup> Rather than its traditional metabolic



role, the H-protein could have a role in maintaining redox balance by reacting with the thioredoxin-like protein 2 (Tlp2).<sup>12</sup> Tlp2 and TrxR are the only thioredoxin and reductase localized to the mitochondrion, but recombinant TrxR does not reduce Tlp2 *in vitro*, raising the possibility that there is another mechanism to reduce Tlp2.<sup>46</sup> In conjunction with the dihydrolipoamide dehydrogenase (E3 subunit), the H-protein, or perhaps one of the other lipoylated proteins, could be involved in such a mechanism. The KDH in *Mycobacterium tuberculosis* has been shown to participate in this kind of redox system<sup>47</sup> and a similar pathway has been proposed for malaria parasites.<sup>12</sup>

## Conclusions

In the current study we show that lipoate metabolism in the mitochondrion of *Pf* follows two lipoylation routes (**Figure 11**). In the first route, lipoylation of H-protein is catalyzed solely by the lipoate ligase LipL1. In the second route, both LipL1 and LipL2 are required to lipoylate the BCDH and KDH. The two lipoylation routes are dependent on the redox state of lipoate, a phenomenon that has not been observed previously in any other system. Furthermore, we show that all three mitochondrial substrates can be modified by lipoate analogs (8-BrO and 6,8-diClO) suggesting that the lethality of these compounds results from their attachment to essential parasite proteins by lipoylation enzymes. Our results suggest that one or more of the mitochondrial protein substrates and by extension, LipL1 and LipL2, are essential for parasite survival making mitochondrial lipoylation in *Plasmodium* an attractive target for therapeutic intervention.

## Acknowledgments

We thank Swetha Velivela and Marina Allary for help with the initial cloning of the lipoylation substrates. We also thank John Cronan for *E. coli* strain TM136 and the National BioResource Project (NIG, Japan) for strains JW5089 and JW4349. Plasmids pKD46 and pCP20 were provided by the Yale University CGSC (Coli Genetic Stock Center) which is supported by NSF program DBI-0742708. We also thank Roger McMacken for the gift of rabbit  $\alpha$ -*EcHsp70* antiserum and Nirbhay Kumar for mouse  $\alpha$ -*PfHsp70* antiserum.

Construction of *E. coli* cell line JEG3 and **Figure 4** were done by Jolyn Gisselberg. Maroya Spalding generated the transgenic parasites shown in **Figure 3** and collected the data for this figure. Parasite experiments presented in **Figures 10B and 10C** were conducted by Krista Matthews. The compound 6,8-dichlorooctanoate was synthesized in the laboratory of Caren Freel Meyers.

## References

1. Mudhune, S. A.; Okiro, E. A.; Noor, A. M.; Zurovac, D.; Juma, E.; Ochola, S. A.; Snow, R. W. The clinical burden of malaria in Nairobi: a historical review and contemporary audit. *Malar J* **2011**, 10, 138.
2. Okiro, E. A.; Al-Taiar, A.; Reyburn, H.; Idro, R.; Berkley, J. A.; Snow, R. W. Age patterns of severe paediatric malaria and their relationship to Plasmodium falciparum transmission intensity. *Malaria Journal* **2009**, 8.
3. Okiro, E. A.; Bitira, D.; Mbabazi, G.; Mpimbaza, A.; Alegana, V. A.; Talisuna, A. O.; Snow, R. W. Increasing malaria hospital admissions in Uganda between 1999 and 2009. *Bmc Medicine* **2011**, 9.

4. Okiro, E. A.; Mutheu, J.; Gething, P. W.; Juma, E.; Snow, R. W. The Changing Patterns of Malaria Admissions since 1999 at 18 Hospitals across Kenya. *American Journal of Tropical Medicine and Hygiene* **2009**, 81, 54-54.
5. Fidock, D. A.; Eastman, R. T.; Ward, S. A.; Meshnick, S. R. Recent highlights in antimalarial drug resistance and chemotherapy research. *Trends Parasitol* **2008**, 24, 537-44.
6. Hay, S. I.; Guerra, C. A.; Gething, P. W.; Patil, A. P.; Tatem, A. J.; Noor, A. M.; Kabaria, C. W.; Manh, B. H.; Elyazar, I. R.; Brooker, S.; Smith, D. L.; Moyeed, R. A.; Snow, R. W. A world malaria map: Plasmodium falciparum endemicity in 2007. *PLoS Med* **2009**, 6, e1000048.
7. Dondorp, A. M.; Fairhurst, R. M.; Slutsker, L.; Macarthur, J. R.; Breman, J. G.; Guerin, P. J.; Wellems, T. E.; Ringwald, P.; Newman, R. D.; Plowe, C. V. The threat of artemisinin-resistant malaria. *N Engl J Med* **2011**, 365, 1073-5.
8. Phyto, A. P.; Nkhoma, S.; Stepniewska, K.; Ashley, E. A.; Nair, S.; McGready, R.; ler Moo, C.; Al-Saai, S.; Dondorp, A. M.; Lwin, K. M.; Singhasivanon, P.; Day, N. P.; White, N. J.; Anderson, T. J.; Nosten, F. Emergence of artemisinin-resistant malaria on the western border of Thailand: a longitudinal study. *Lancet* **2012**, 379, 1960-6.
9. Allary, M.; Lu, J. Z.; Zhu, L.; Prigge, S. T. Scavenging of the cofactor lipoate is essential for the survival of the malaria parasite Plasmodium falciparum. *Mol Microbiol* **2007**, 63, 1331-44.
10. Storm, J.; Muller, S. Lipoic acid metabolism of Plasmodium--a suitable drug target. *Curr Pharm Des* **2012**, 18, 3480-9.

11. Spalding, M. D.; Prigge, S. T. Lipoic acid metabolism in microbial pathogens. *Microbiol Mol Biol Rev* **2010**, 74, 200-28.
12. Gunther, S.; McMillan, P. J.; Wallace, L. J.; Muller, S. Plasmodium falciparum possesses organelle-specific alpha-keto acid dehydrogenase complexes and lipoylation pathways. *Biochem Soc Trans* **2005**, 33, 977-80.
13. Pei, Y.; Tarun, A. S.; Vaughan, A. M.; Herman, R. W.; Soliman, J. M.; Erickson-Wayman, A.; Kappe, S. H. Plasmodium pyruvate dehydrogenase activity is only essential for the parasite's progression from liver infection to blood infection. *Mol Microbiol* **2010**, 75, 957-71.
14. Falkard, B.; Kumar, T. R.; Hecht, L. S.; Matthews, K. A.; Henrich, P. P.; Gulati, S.; Lewis, R. E.; Manary, M. J.; Winzeler, E. A.; Sinnis, P.; Prigge, S. T.; Heussler, V.; Deschermeier, C.; Fidock, D. A key role for lipoic acid synthesis during Plasmodium liver stage development. *Cell Microbiol* **2013**.
15. Gunther, S.; Wallace, L.; Patzewitz, E. M.; McMillan, P. J.; Storm, J.; Wrenger, C.; Bissett, R.; Smith, T. K.; Muller, S. Apicoplast lipoic acid protein ligase B is not essential for Plasmodium falciparum. *PLoS Pathog* **2007**, 3, e189.
16. Gunther, S.; Matuschewski, K.; Muller, S. Knockout studies reveal an important role of Plasmodium lipoic acid protein ligase A1 for asexual blood stage parasite survival. *PLoS One* **2009**, 4, e5510.
17. Reed, L. J.; Koike, M.; Levitch, M. E.; Leach, F. R. Studies on the nature and reactions of protein-bound lipoic acid. *J Biol Chem* **1958**, 232, 143-58.
18. Perham, R. N. Swinging arms and swinging domains in multifunctional enzymes: catalytic machines for multistep reactions. *Annu Rev Biochem* **2000**, 69, 961-1004.

19. Reche, P.; Perham, R. N. Structure and selectivity in post-translational modification: attaching the biotinyl-lysine and lipoyl-lysine swinging arms in multifunctional enzymes. *Embo Journal* **1999**, *18*, 2673-2682.
20. Spalding, M. D.; Allary, M.; Gallagher, J. R.; Prigge, S. T. Validation of a modified method for Bxb1 mycobacteriophage integrase-mediated recombination in *Plasmodium falciparum* by localization of the H-protein of the glycine cleavage complex to the mitochondrion. *Mol Biochem Parasitol* **2010**, *172*, 156-60.
21. Morris, T. W.; Reed, K. E.; Cronan, J. E. Lipoic Acid Metabolism in *Escherichia Coli* - the *LplA* and *LipB* Genes Define Redundant Pathways for Ligation of Lipoyl Groups to Apoprotein. *Journal of Bacteriology* **1995**, *177*, 1-10.
22. Jordan, S. W.; Cronan, J. E. The *Escherichia coli* *lipB* gene encodes lipoyl (octanoyl)-acyl carrier protein : protein transferase. *Journal of Bacteriology* **2003**, *185*, 1582-1589.
23. Miller, J. R.; Busby, R. W.; Jordan, S. W.; Cheek, J.; Henshaw, T. F.; Ashley, G. W.; Broderick, J. B.; Cronan, J. E.; Marletta, M. A. *Escherichia coli* *LipA* is a lipoyl synthase: In vitro biosynthesis of lipoylated pyruvate dehydrogenase complex from octanoyl-acyl carrier protein. *Biochemistry* **2000**, *39*, 15166-15178.
24. Fujiwara, K.; Maita, N.; Hosaka, H.; Okamura-Ikeda, K.; Nakagawa, A.; Taniguchi, H. Global conformational change associated with the two-step reaction catalyzed by *Escherichia coli* lipoyl-protein ligase A. *J Biol Chem* **2010**, *285*, 9971-80.
25. Foth, B. J.; Stimmler, L. M.; Handman, E.; Crabb, B. S.; Hodder, A. N.; McFadden, G. I. The malaria parasite *Plasmodium falciparum* has only one pyruvate

- dehydrogenase complex, which is located in the apicoplast. *Mol Microbiol* **2005**, 55, 39-53.
26. Wrenger, C.; Muller, S. The human malaria parasite *Plasmodium falciparum* has distinct organelle-specific lipoylation pathways. *Mol Microbiol* **2004**, 53, 103-13.
27. Nkrumah, L. J.; Muhle, R. A.; Moura, P. A.; Ghosh, P.; Hatfull, G. F.; Jacobs, W. R., Jr.; Fidock, D. A. Efficient site-specific integration in *Plasmodium falciparum* chromosomes mediated by mycobacteriophage Bxb1 integrase. *Nat Methods* **2006**, 3, 615-21.
28. Baba, T.; Ara, T.; Hasegawa, M.; Takai, Y.; Okumura, Y.; Baba, M.; Datsenko, K. A.; Tomita, M.; Wanner, B. L.; Mori, H. Construction of *Escherichia coli* K-12 in-frame, single-gene knockout mutants: the Keio collection. *Mol Syst Biol* **2006**, 2, 2006 0008.
29. Datsenko, K. A.; Wanner, B. L. One-step inactivation of chromosomal genes in *Escherichia coli* K-12 using PCR products. *Proc Natl Acad Sci U S A* **2000**, 97, 6640-5.
30. Christensen, Q. H.; Martin, N.; Mansilla, M. C.; de Mendoza, D.; Cronan, J. E. A novel amidotransferase required for lipoic acid cofactor assembly in *Bacillus subtilis*. *Mol Microbiol* **2011**, 80, 350-63.
31. Martin, N.; Christensen, Q. H.; Mansilla, M. C.; Cronan, J. E.; de Mendoza, D. A novel two-gene requirement for the octanoyltransfer reaction of *Bacillus subtilis* lipoic acid biosynthesis. *Mol Microbiol* **2011**, 80, 335-49.
32. Burns, J. A.; Butler, J. C.; Moran, J.; Whitesides, G. M. Selective Reduction of Disulfides by Tris(2-Carboxyethyl)Phosphine. *Journal of Organic Chemistry* **1991**, 56, 2648-2650.

33. Hansen, R. E.; Winther, J. R. An introduction to methods for analyzing thiols and disulfides: Reactions, reagents, and practical considerations. *Anal Biochem* **2009**, 394, 147-58.
34. Svagera, Z.; Hanzlikova, D.; Simek, P.; Husek, P. Study of disulfide reduction and alkyl chloroformate derivatization of plasma sulfur amino acids using gas chromatography-mass spectrometry. *Anal Bioanal Chem* **2012**, 402, 2953-63.
35. Schonauer, M. S.; Kastaniotis, A. J.; Kursu, V. A.; Hiltunen, J. K.; Dieckmann, C. L. Lipoic acid synthesis and attachment in yeast mitochondria. *J Biol Chem* **2009**, 284, 23234-42.
36. Haramaki, N.; Han, D.; Handelman, G. J.; Tritschler, H. J.; Packer, L. Cytosolic and mitochondrial systems for NADH- and NADPH-dependent reduction of alpha-lipoic acid. *Free Radic Biol Med* **1997**, 22, 535-42.
37. Hanson, G. T.; Aggeler, R.; Oglesbee, D.; Cannon, M.; Capaldi, R. A.; Tsien, R. Y.; Remington, S. J. Investigating mitochondrial redox potential with redox-sensitive green fluorescent protein indicators. *J Biol Chem* **2004**, 279, 13044-53.
38. Jortzik, E.; Becker, K. Thioredoxin and glutathione systems in *Plasmodium falciparum*. *Int J Med Microbiol* **2012**, 302, 187-94.
39. Chaudhari, R.; Narayan, A.; Patankar, S. A novel trafficking pathway in *Plasmodium falciparum* for the organellar localization of glutathione peroxidase-like thioredoxin peroxidase. *FEBS J* **2012**, 279, 3872-88.
40. Constantinescu, A.; Pick, U.; Handelman, G. J.; Haramaki, N.; Han, D.; Podda, M.; Tritschler, H. J.; Packer, L. Reduction and transport of lipoic acid by human erythrocytes. *Biochem Pharmacol* **1995**, 50, 253-61.

41. Arner, E. S.; Nordberg, J.; Holmgren, A. Efficient reduction of lipoamide and lipoic acid by mammalian thioredoxin reductase. *Biochem Biophys Res Commun* **1996**, 225, 268-74.
42. Seeber, F.; Limenitakis, J.; Soldati-Favre, D. Apicomplexan mitochondrial metabolism: a story of gains, losses and retentions. *Trends in Parasitology* **2008**, 24, 468-478.
43. Cobbold, S. A.; Vaughan, A. M.; Lewis, I. A.; Painter, H. J.; Camargo, N.; Perlman, D. H.; Fishbaugher, M.; Healer, J.; Cowman, A. F.; Kappe, S. H.; Llinas, M. Kinetic flux profiling elucidates two independent acetyl-CoA biosynthetic pathways in *Plasmodium falciparum*. *J Biol Chem* **2013**.
44. Miao, J.; Lawrence, M.; Jeffers, V.; Zhao, F.; Parker, D.; Ge, Y.; Sullivan, W. J., Jr.; Cui, L. Extensive lysine acetylation occurs in evolutionarily conserved metabolic pathways and parasite-specific functions during *Plasmodium falciparum* intraerythrocytic development. *Mol Microbiol* **2013**, 89, 660-75.
45. Salcedo, E.; Sims, P. F. G.; Hyde, J. E. A glycine-cleavage complex as part of the folate one-carbon metabolism of *Plasmodium falciparum*. *Trends in Parasitology* **2005**, 21, 406-411.
46. Nickel, C.; Rahlfs, S.; Deponete, M.; Koncarevic, S.; Becker, K. Thioredoxin networks in the malarial parasite *Plasmodium falciparum*. *Antioxid Redox Signal* **2006**, 8, 1227-39.
47. Rezaie, T.; Child, A.; Hitchings, R.; Brice, G.; Miller, L.; Coca-Prados, M.; Heon, E.; Krupin, T.; Ritch, R.; Kreutzer, D.; Crick, R. P.; Sarfarazi, M. Adult-onset primary open-angle glaucoma caused by mutations in optineurin. *Science* **2002**, 295, 1077-9.



48. Bahl, A.; Brunk, B.; Crabtree, J.; Fraunholz, M. J.; Gajria, B.; Grant, G. R.; Ginsburg, H.; Gupta, D.; Kissinger, J. C.; Labo, P.; Li, L.; Mailman, M. D.; Milgram, A. J.; Pearson, D. S.; Roos, D. S.; Schug, J.; Stoeckert, C. J., Jr.; Whetzel, P. PlasmoDB: the Plasmodium genome resource. A database integrating experimental and computational data. *Nucleic Acids Res* **2003**, *31*, 212-5.
49. Gisselberg, J. E.; Dellibovi-Ragheb, T. A.; Matthews, K. A.; Bosch, G.; Prigge, S. T. The Suf Iron-Sulfur Cluster Synthesis Pathway Is Required for Apicoplast Maintenance in Malaria Parasites. *PLoS Pathog* **2013**, *9*, e1003655.
50. Balabaskaran Nina, P.; Morrisey, J. M.; Ganesan, S. M.; Ke, H.; Pershing, A. M.; Mather, M. W.; Vaidya, A. B. ATP synthase complex of Plasmodium falciparum: dimeric assembly in mitochondrial membranes and resistance to genetic disruption. *J Biol Chem* **2011**, *286*, 41312-22.
51. Delli-Bovi, T. A.; Spalding, M. D.; Prigge, S. T. Overexpression of biotin synthase and biotin ligase is required for efficient generation of sulfur-35 labeled biotin in E. coli. *BMC Biotechnol* **2010**, *10*, 73.
52. Kapust, R. B.; Waugh, D. S. Controlled intracellular processing of fusion proteins by TEV protease. *Protein Expr Purif* **2000**, *19*, 312-8.
53. Muench, S. P.; Rafferty, J. B.; McLeod, R.; Rice, D. W.; Prigge, S. T. Expression, purification and crystallization of the Plasmodium falciparum enoyl reductase. *Acta Crystallogr D Biol Crystallogr* **2003**, *59*, 1246-8.
54. Cherepanov, P. P.; Wackernagel, W. Gene disruption in Escherichia coli: TcR and KmR cassettes with the option of Flp-catalyzed excision of the antibiotic-resistance determinant. *Gene* **1995**, *158*, 9-14.

55. Trager, W.; Jensen, J. B. Continuous culture of *Plasmodium falciparum*: its impact on malaria research. *Int J Parasitol* **1997**, *27*, 989-1006.
56. Woster, P. M.; Black, A. Y.; Duff, K. J.; Coward, J. K.; Pegg, A. E. Synthesis and biological evaluation of S-adenosyl-1,12-diamino-3-thio-9-azadodecane, a multisubstrate adduct inhibitor of spermine synthase. *J Med Chem* **1989**, *32*, 1300-7.
57. Lambros, C.; Vanderberg, J. P. Synchronization of *Plasmodium falciparum* erythrocytic stages in culture. *J Parasitol* **1979**, *65*, 418-20.
58. Kumar, N.; Zheng, H. Evidence for epitope-specific thymus-independent response against a repeat sequence in a protein antigen. *Immunology* **1998**, *94*, 28-34.

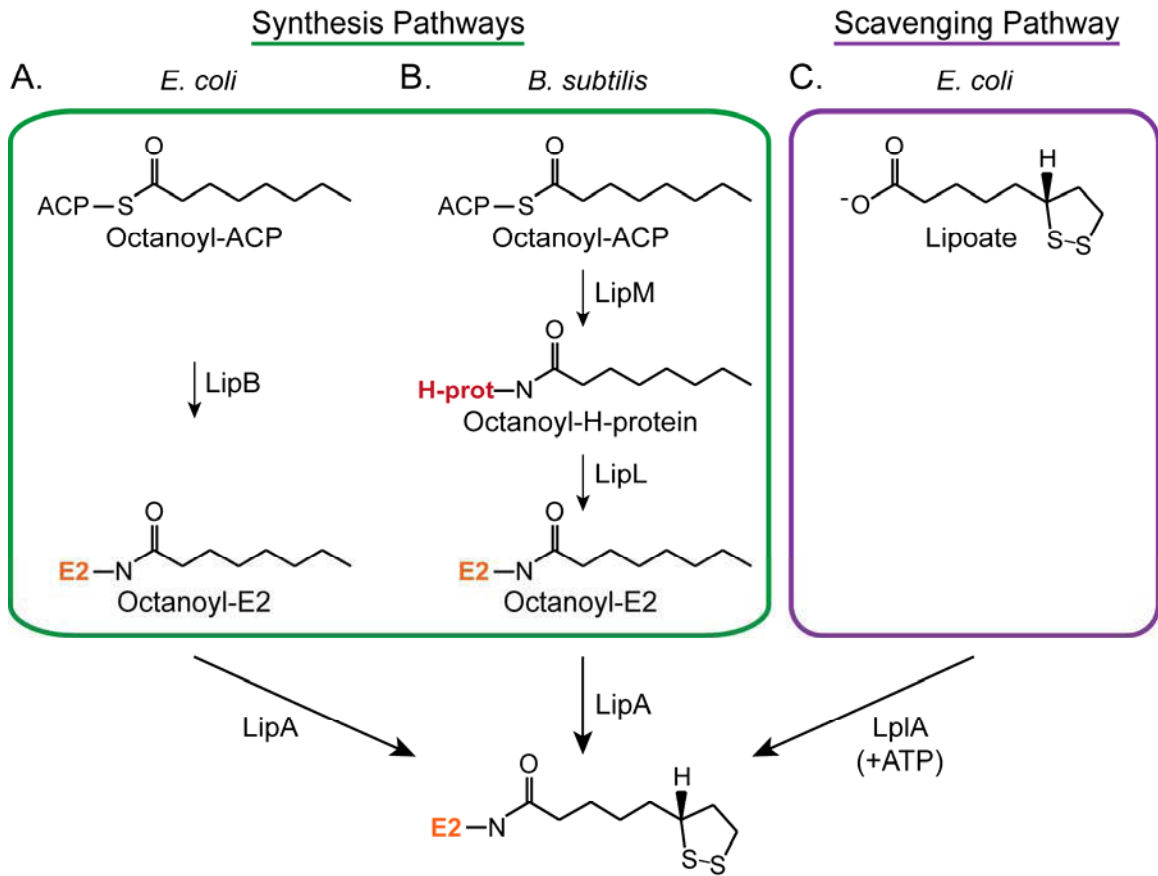


**Figure 1.** Lipoate synthesis and scavenging pathways. A) Lipoate synthesis as observed in *E. coli*. Octanoyl groups from octanoyl-ACP (acyl carrier protein) are transferred to E2 proteins (and the H-protein) by an octanoyltransferase (LipB) followed by the insertion of sulfur atoms by a lipoyl synthase (LipA). B) Lipoate synthesis as observed in *B. subtilis*. Octanoyl groups are transferred specifically to the H-protein by octanoyltransferase (LipM) and are subsequently distributed to the E2 proteins by an amidotransferase (LipL). As in *E. coli*, sulfur insertion is catalyzed by a lipoyl synthase (LipA). C) Lipoate scavenging as observed in *E. coli*. Lipoate scavenged from the external environment is attached to E2 proteins (and the H-protein) by an ATP-dependent lipoyl synthase (LplA).

Harmonized LipL2 nucleotide sequence.

ATGCGCATCATTAAGTGTCTAGATCAGATTTTCCGGCCGGTACTGCCGAATGTGAACATT  
AACACATTCAGAAGAACAACAAAAAATTAATATCCTCTATTTTCATCGATGTATCAAAATTT  
CATGTGTTTGAACAACCTTCTGCTGGAAGAGAGCCTGTTTCGGATTAGCAACAACACCACC  
GAAGGCCTGAATAACATTGGTTTTGTAATCGTGAACAACACCTGCCAAGAAATGAACGAG  
TCGAAAGGCAATGAATGTATCTTTAACAACAAGAAATGCGTCATTCTGGGTATCAGCAAC  
AAAATTAAGATCATATTAAGATACGAACTATATCAAAGAAAACAAAATTTCACTGATC  
AAACGCTTTACCGCGGTGGCACGATTTACATTAACAAAAACAGCCTGCTGGTTTTCTCTG  
ATTCTCCACATAAATTTGAAAAAACAACAAAAATCTATCCGAGCAACATCACAGAATGG  
TCCTATAACTATTTCTACAACACCTCAAAACAGATTTATGATAAAACCCAGATTAATAAC  
GAAAAAACTCCCTGAATAAAAACCATATCTTATTTAACCAGTATTTTAACTATTATGAA  
AACGATTATGTGTATAAAGATTATGATGAACATAACAAAAACATAATCCTGAAAAAGTC  
GGCGGTAACGCACAGAGCTTCGCCCGTAACTATTTGTCGATCACACGAGCTATATTTGG  
ACCTGCGATTACAAGGAAATGAACAACATTTCTGCTGAACCCGTCAAAGCAGCCGATTTAC  
CGTAACAAACGCAAACATCAGCACTTTCTTCAAAGCATAAACTGTGCCTTCATGATGAT  
ATTCACACCCCAAACATTTTTATCGAAAACTGATCAAACATATTAACACATAATTAAT  
TATAAAAACATCACGGATCAGCATGATTACTGGTTCTTTAATAAAATCAACCTGAAAAAC  
ATCAACGATCATATTTCTGCGTAACTCAGAACACTTTGATGATATTTATGTAGCGGATATG  
AACTTGCTGCAGTGTATCTTTAATTATTATAACAACAGCAGCTTGTTCAACAACATGCGC  
AGTACGTATTTCTGGATTTAGAGGGAAAAAAGTTAGTGATCGGTATTACGATATTCCG  
ACCTATTTTCTCTAATAA

Harmonized LipL2 amino acid sequence.

MRI I KCLDQI FRPVL PNVNINNI QKNKKINILYFIDVSKFHVFEQLLLEESLFRISNNTT  
EGLNNI GFVIVNNTCEEMNESKGN ECI FNNKKCVILGISNKIKDHIKDTNYIKENKISLI  
KRFTGGGTIYINKNSLLVSLILPHKFEKNKKIYPSNITEWSYNYFYNTSKQIYDKTQINN  
EKNSLNKNHILFNQYFNYYENDYVYKDYDEHNKNIILKKVGGNAQSFARNYFVHHTSYIW  
TCDYKEMNNILLNPSKQPIYRNKRKHQHFLQSIKLCLHDDIHTPNIFIEKLIKHIKHIIN  
YKNITDQHDYWFNKNLNKNINDHILRNSEHFDDIYVADMNLLQCIFNYNNSSSLFNMR  
STYFLDLEGKKVSDRYDYDIPTYFL--

**Figure 2.** Nucleotide and amino acid sequence for synthetic harmonized LipL2 based on gene PF3D7\_0923600.

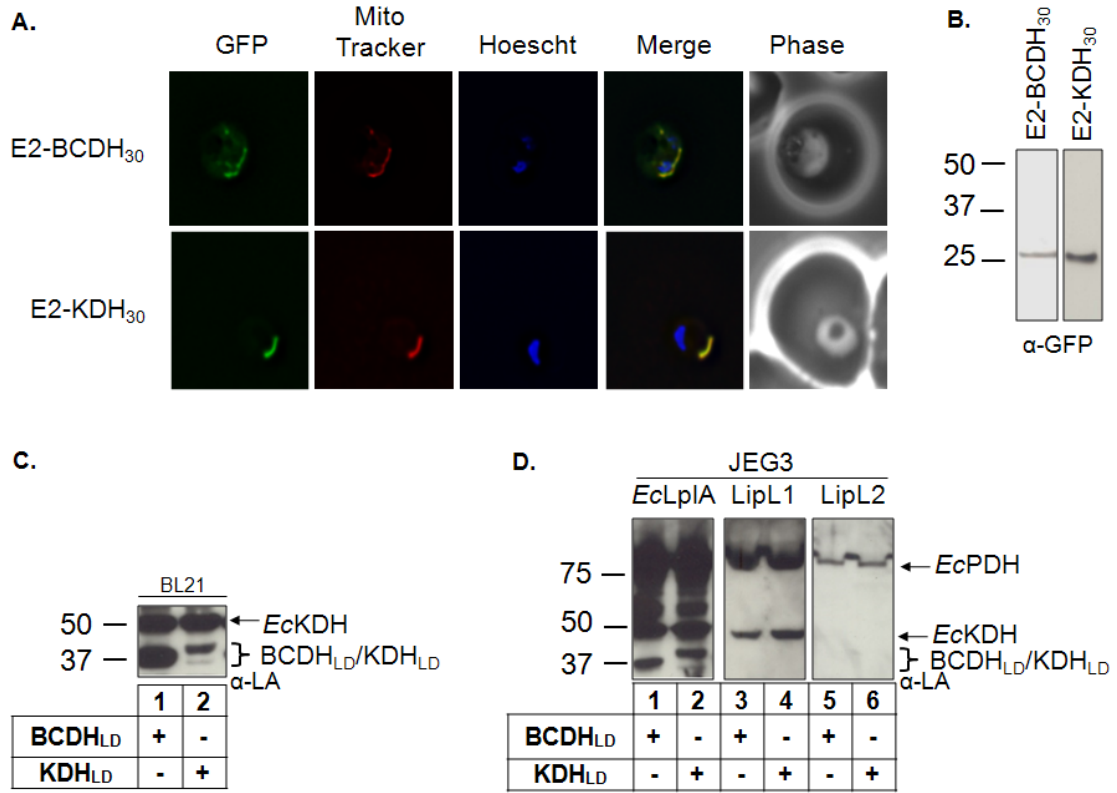


**Figure 3.** BCDH and KDH localization and cell-based lipoylation assays.

A) Epifluorescent images of live *P. falciparum* erythrocytic-stage parasites expressing GFP fused to either the BCDH leader peptide (E2-BCDH<sub>30</sub>) or the KDH leader peptide (E2-KDH<sub>30</sub>). The parasites were stained with MitoTracker to identify mitochondria and Hoescht to identify nuclei. Image z-stacks were deconvolved and then presented as a single combined image. In both cases, GFP fluorescence co-localizes with MitoTracker to the mitochondrion. B) Expression of the E2-BCDH<sub>30</sub>-GFP and E2-KDH<sub>30</sub>-GFP constructs. An  $\alpha$ -GFP western blot of parasite lysates identifies both proteins with the predicted molecular mass. C) Lipoylation of BCDH<sub>LD</sub> and KDH<sub>LD</sub> in BL21 *E. coli*. The lipoylation domains (LD) of both the E2-BCDH and the E2-KDH are lipoylated in anti-lipoate ( $\alpha$ -LA) western blots of bacterial lysate, verifying that these constructs act as lipoylation substrates. D) Cell-based assay of lipoate ligase activity. Lipoylation deficient JEG3 cells were used to test the activity of three candidate lipoate ligases (*EcLplA*, LipL1 and LipL2) with two lipoylation substrates (BCDH<sub>LD</sub> and KDH<sub>LD</sub>). *E. coli* lipoate ligase (*EcLplA*) is sufficient to lipoylate BCDH<sub>LD</sub> and KDH<sub>LD</sub>, whereas neither LipL1 nor LipL2 lipoylate either parasite substrate.

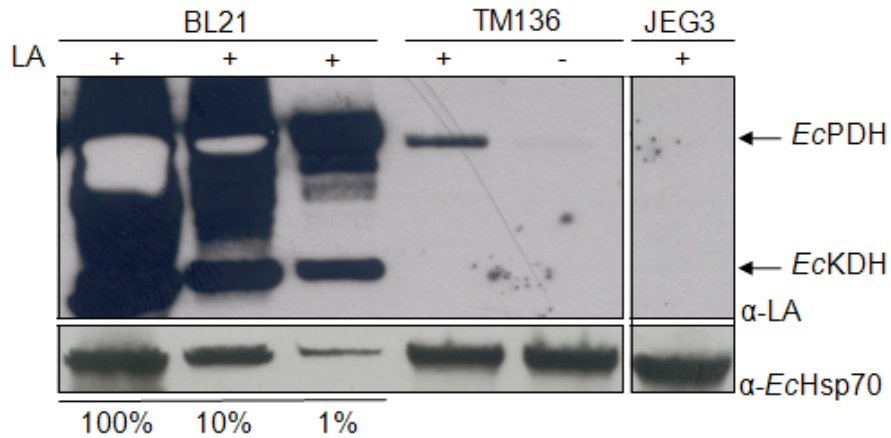


**Figure 4.** Analysis of *lplA*-/*lipB*- knockout *E. coli* cell line JEG3. Cultures of three different *E. coli* cell lines (BL21, TM136 and JEG3) were normalized by OD<sub>600</sub> before analysis by western blot using antibodies specific for lipoylated proteins ( $\alpha$ -LA) and antiserum specific for *E. coli* Hsp70 ( $\alpha$ -Hsp70) as a loading control. Lipoate (LA) was added to the cultures grown in minimal medium (containing succinate and acetate) to assess lipoate ligase activity which is still present in the TM136 *lplA*-/*lipB*- disruption cell line, but not the JEG3 *lplA*-/*lipB*- knockout cell line.

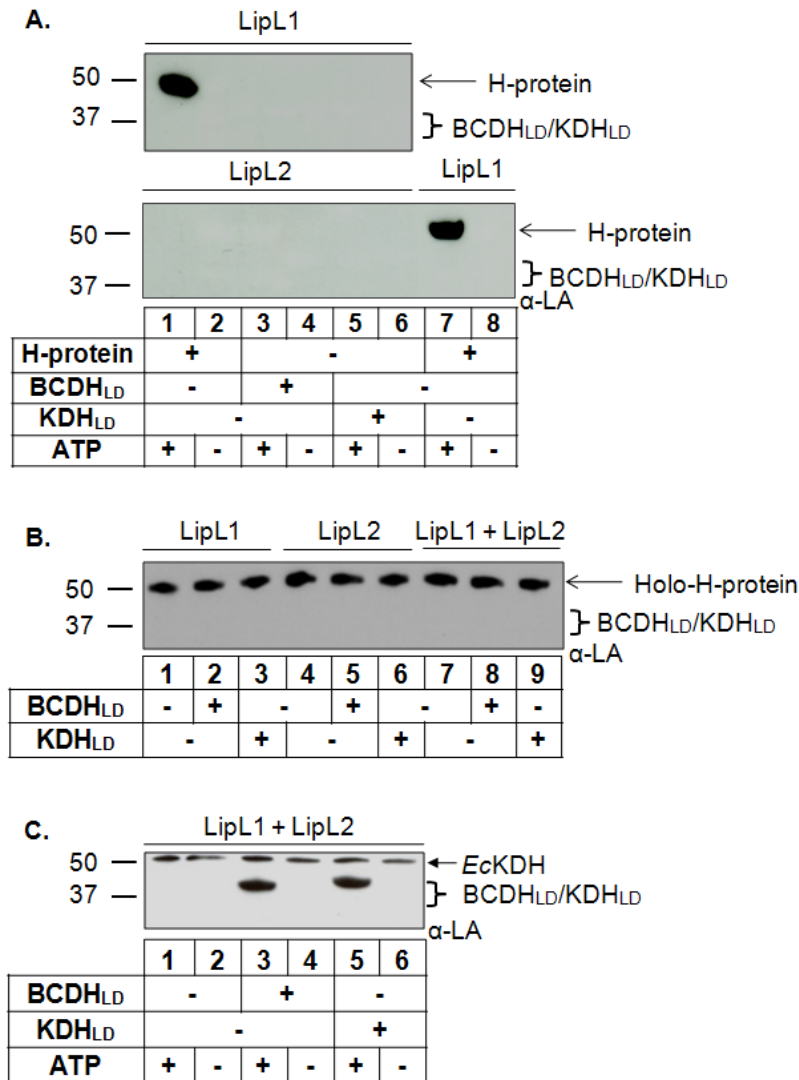


**Figure 5.** *In vitro* lipoylation assays. A) Lipoylation activity. Western blot analysis shows that LipL1 is an ATP-dependent lipoylation enzyme only when H-protein is used as substrate, while LipL2 does not display lipoylation activity with any substrate. B) Lipoyl amidotransferase activity. Western blot analysis shows that LipL1 and LipL2 are not able to transfer lipoyl groups from Holo-H-protein to either BCDH<sub>LD</sub> or KDH<sub>LD</sub>. C) Combined LipL1 + LipL2 lipoylation activity. Both LipL1 and LipL2 are needed for lipoylation of BCDH<sub>LD</sub> and KDH<sub>LD</sub> in an ATP-dependent lipoylation reaction. The asterisk (\*) marks a minor population of *E. coli* E2-KDH found in purified LipL2.



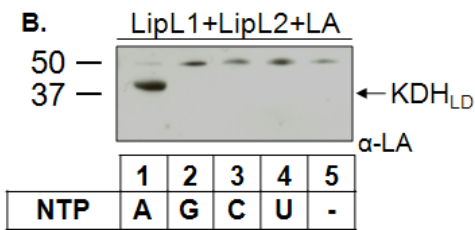
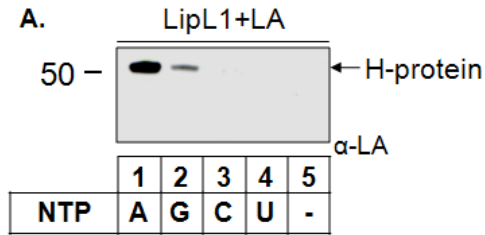


**Figure 6.** Ligation reactions proceed through an ATP-dependent reaction. A) Western blot analysis of ligation reactions catalyzed by LipL1 showing that the H-protein is preferentially lipoylated using ATP (A) as a nucleotide source with minor activity observed for GTP (G), but not for CTP (C) or UTP (U). B) Western blot analysis of ligation reactions catalyzed by LipL1 and LipL2 showing that the  $KDH_{LD}$  is preferentially lipoylated using ATP (A).

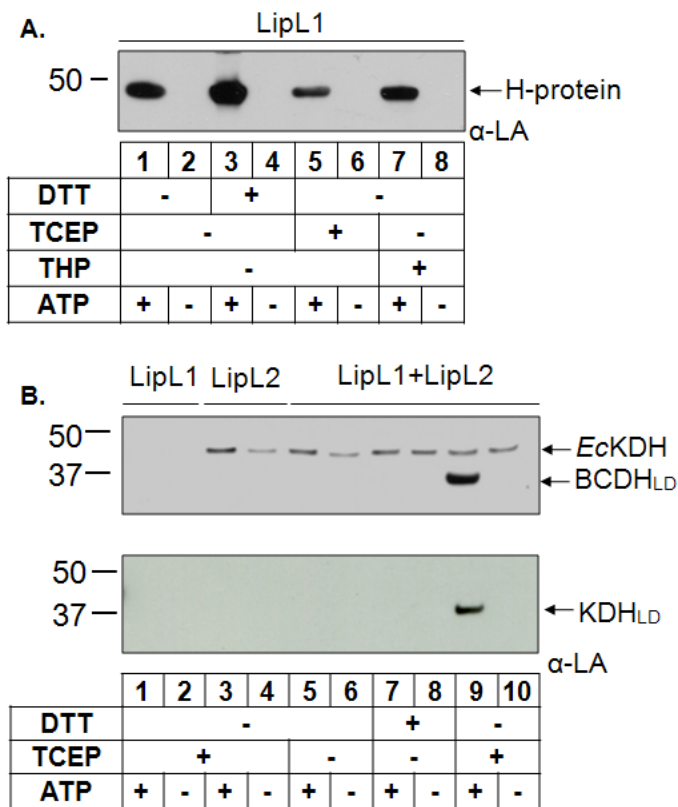


**Figure 7.** Redox dependence of the two lipoylation routes. A) Redox dependence of H-protein lipoylation. Western blot analysis shows that lipoylation of the H-protein by LipL1 is enhanced in the presence of DTT. B) Dependence of the LipL1 + LipL2 reaction on strong reducing conditions. Western blots show that lipoylation of  $BCDH_{LD}$  and  $KDH_{LD}$  occur only in the presence of the strong reducing agent TCEP. The asterisk (\*) marks a minor population of *E. coli* E2-KDH found in purified LipL2

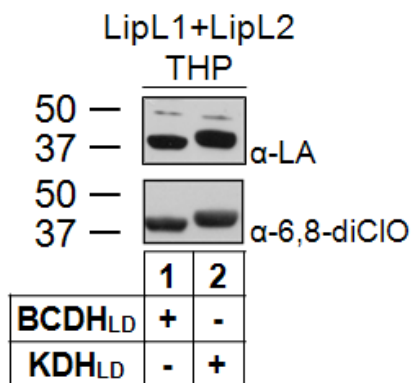


**Figure 8.** Modification of BCDH<sub>LD</sub> and KDH<sub>LD</sub> in the presence of THP

LipL1 and LipL2 can modify both substrates with LA (top panel) or 6,8-diClO (lower panel) in a coupled reaction in the presence of the strong reducing agent THP similar to the results with TCEP (see **Figure 4B**).

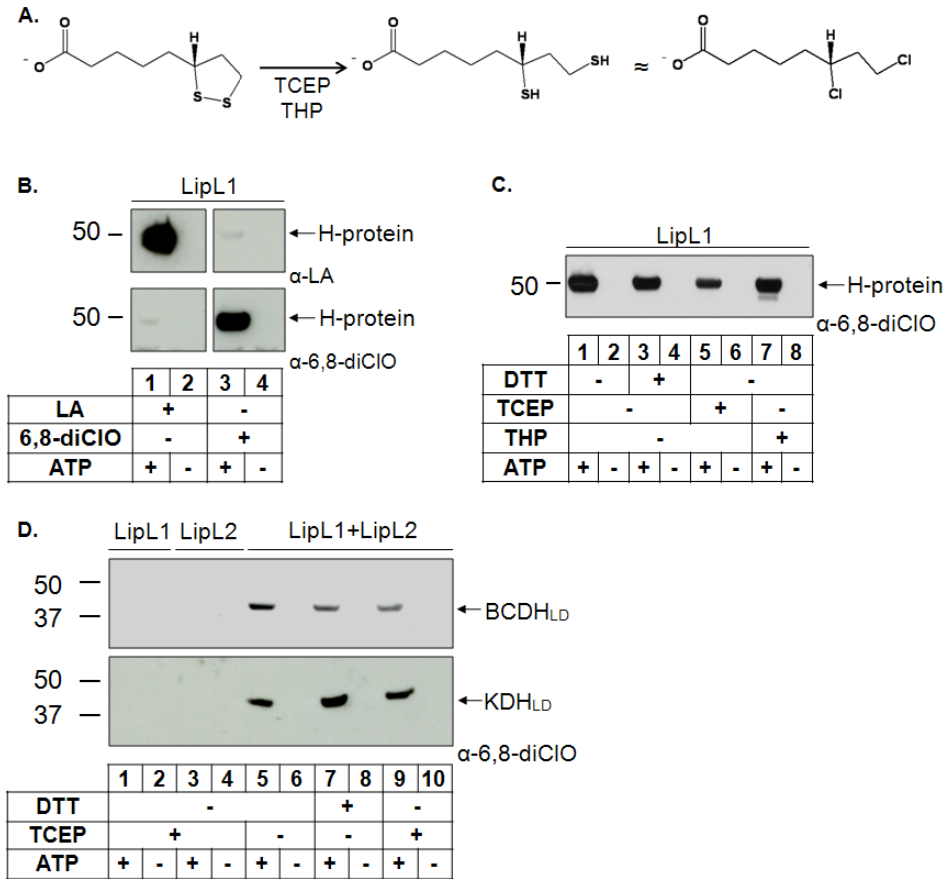


**Figure 9.** 6,8-dichlorooctanoate is attached to all substrates independent of redox environment. A) Redox states of lipoate. The oxidized ring form of lipoate is reduced to the dihydrolipoate form by treatment with TCEP or THP. 6,8-Dichlorooctanoate (6,8-diClO) mimics the dihydrolipoate form. B) Modification of the H-protein by lipoate and 6,8-diClO. LipL1 catalyzes the attachment of lipoate as shown in the  $\alpha$ -LA western blot (top panels) and 6,8-diClO as shown in the  $\alpha$ -6,8-diClO western blot (bottom panels). The  $\alpha$ -LA antibodies and the  $\alpha$ -6,8-diClO antiserum show very little cross-reactivity. C) Effect of reducing conditions on the enzymatic activity of LipL1 against the H-protein. The H-protein is modified by 6,8-diClO independent of the redox environment. D) Effect of reducing conditions on the enzymatic activity of LipL1 + LipL2. BCDH<sub>LD</sub> and KDH<sub>LD</sub> are modified by 6,8-diClO independent of the redox environment.

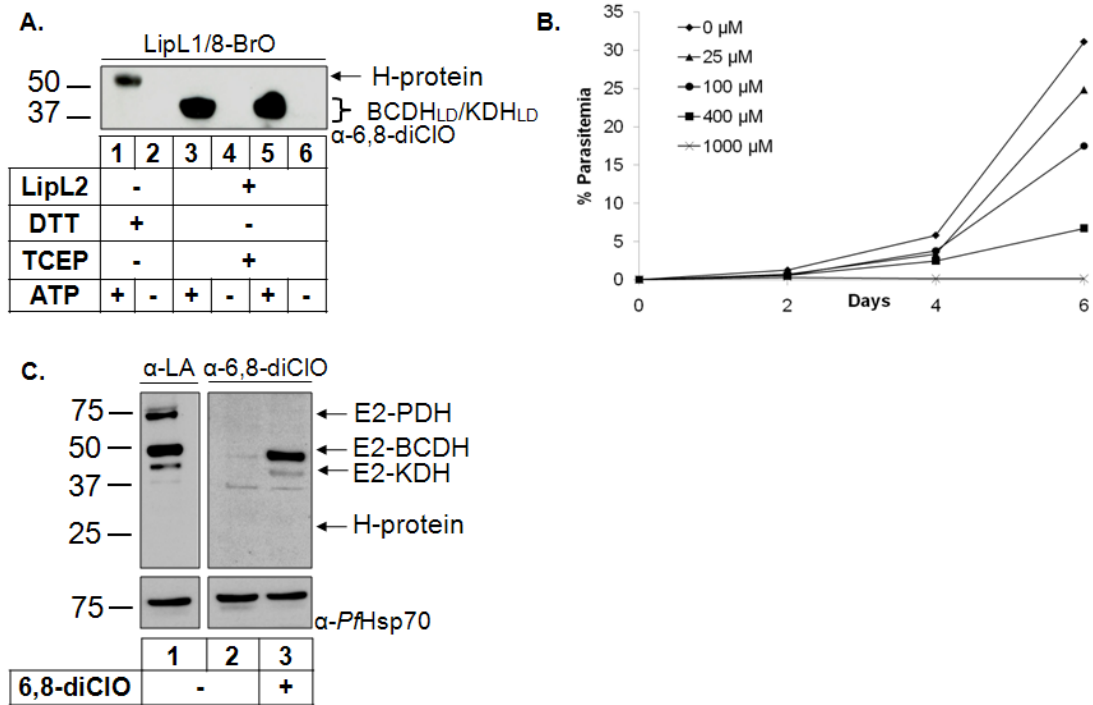


**Figure 10.** Modification of mitochondrial proteins with lipoate analogs. A) Attachment of 8-bromooctanoate (8-BrO) to lipoylation substrates *in vitro*. An  $\alpha$ -6,8-diClO western blot shows that LipL1 can attach 8-BrO to the H-protein and that LipL1+LipL2 can attach 8-BrO to BCDH<sub>LD</sub> and KDH<sub>LD</sub>. B) Growth inhibition of *P. falciparum* treated with 6,8-diClO. The lipoate analog 6,8-diClO inhibits blood stage parasite growth in a dose-dependent manner. C) Uptake and attachment of LA and 6,8-diClO in parasite culture. Western blot analysis of parasite lysate shows that treatment of *P. falciparum* parasites with either 6,8-diClO or LA results in the modification of E2-BCDH and E2-KDH. Lipoylated E2-PDH is derived from a synthesis pathway in the apicoplast and not from lipoate scavenging.

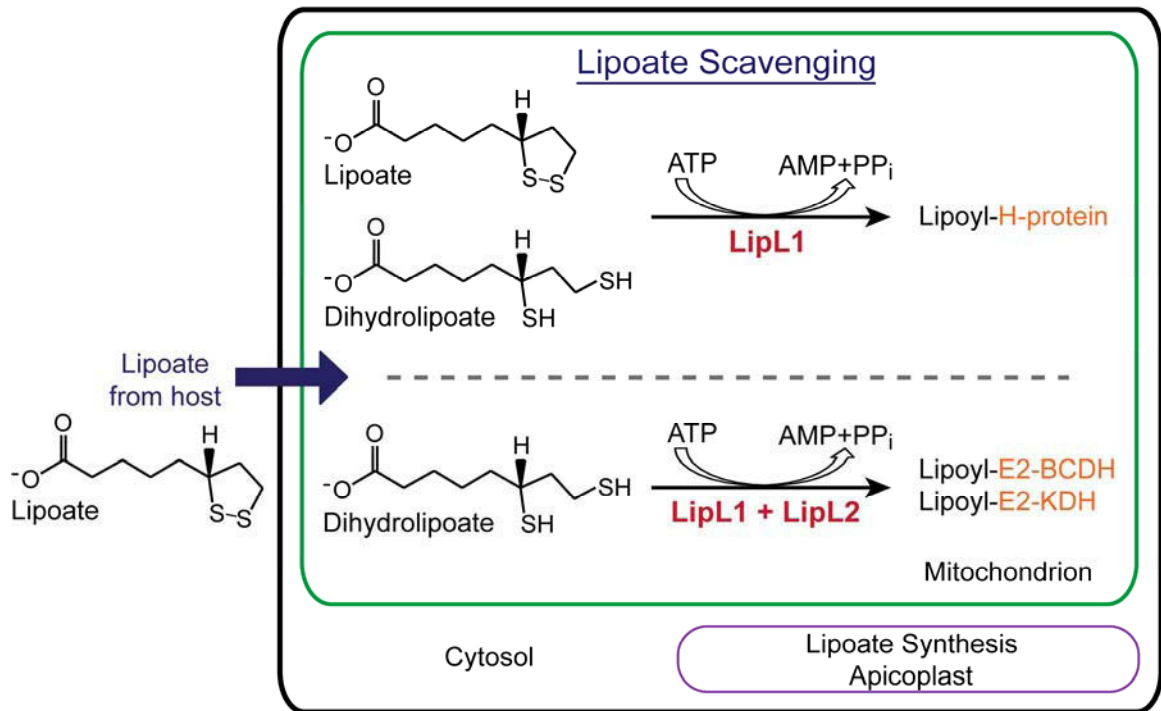


**Figure 11.** Updated mitochondrial lipoylation pathway for *Plasmodium falciparum*. The mitochondrion relies on lipoate scavenging from the host while the apicoplast contains an isolated lipoate synthesis pathway. Our data suggests that there are two routes for lipoylation of protein substrates in the mitochondrion. The H-protein is solely lipoylated by LipL1 in an ATP-dependent reaction; this activity is enhanced under less reducing conditions. Both LipL1 and LipL2 are needed for lipoylation of the E2 domains of BCDH (E2-BCDH) and KDH (E2-KDH) in an ATP-dependent reaction which only occurs under strong reducing conditions.

**Table 1.** Primers and plasmids used in this study.

Plasmid	Primer Name	Primer Sequence
pMALcHT-LipL1	n/a	pMA006 as described in <sup>9</sup>
pMALcHT-LipL2	n/a	none - excised using <i>EcoRI</i> and <i>HindIII</i> from synthesized gene
pMALcHT -LplA	LplA.BamHI.F	<u>GGTGGTGGATCC</u> <b><i>ATGTCCACATTACGCCTGCTCATCTC</i></b>
	LplA.SalI.R	<b><i>GGTGGTGTCTGACCTACCTTACAGCCCCCGCCATC</i></b>
pGEXT-BCDH <sub>LD</sub>	BCDH.BamHI.F100	<u>GGCGGCGGATCC</u> <b><i>GTGAAATGCAAATTATTTGATATAGG</i></b>
	BCDH.EcoRI.R417	<b><i>GGCGGCGAATTCCTTATAAACTTAAATCACTTTCACCATC</i></b>
pGEXT-KDH <sub>LD</sub>	KDH.BamHI.F103	<u>GGCGGCGGATCC</u> <b><i>ATTGAAGGATCACTTAAGAGATATTTTC</i></b>
	KDH.EcoRI.R456	<b><i>GGCGGCGAATTCCTTAATTTAATTGATTAAATGTATAATTATTTTC</i></b>
pGEXTK	Kan.BspHI.F	<b><i>GGTGGTTCATGAGGATGGCTTCTTGCCGCAAGG</i></b>
	Kan.BspHI.R	<b><i>GGTGGTTCATGACGCCCGCGGCAACCGAG</i></b>
pGEXTK-BCDH <sub>LD</sub>	n/a	none - excised using <i>BamHI</i> and <i>SalI</i> from pGEXT-BCDH <sub>LD</sub>
pGEXTK-KDH <sub>LD</sub>	n/a	none - excised using <i>BamHI</i> and <i>SalI</i> from pGEXT-KDH <sub>LD</sub>
pGEXTK-Hprot	Hprot.BamHI.F	<u>GGTGGTGGATCC</u> <b><i>GAATATATAAAAATTGAGGATGGAAATTTGAAC</i></b>
	Hprot.SalI.R	<b><i>GGTGGTGTCTGACCTTATTTCCCCCTTGCCCTTTATTTTC</i></b>
pRL2-BCDH <sub>30</sub> GFP	BCDH <sub>30</sub> .AvrII.F	<u>GGTGGTGCTAGCC</u> <b><i>TAGGATGTTTTGTGAAGAATGTACTAAACGTGC</i></b>
	BCDH <sub>30</sub> .BsiWI.R	<b><i>GGTGGTCTGACGATGTATTGCACTCGTGTTCAGGTAATG</i></b>
pRL2-KDH <sub>30</sub> GFP	KDH <sub>30</sub> .AvrII.F	<u>GGTGGTCCTAGG</u> <b><i>ATGACAAAGAATCTTGTATTTGATTAATAAATC</i></b>
	KDH <sub>30</sub> .BsiWI.R	<b><i>GGTGGTCTGACGATTATACTTATGGTTAAAAATGTTCTATTAATAAATTTT</i></b>
	LplA.H.F	<u>AAAGCGAGAAAAAAGAGTGACCCATTACTACAAGAAAGGAAATCGTTATG</u>
	LplA.H.R	<u>AAGAGAAAGTTGCCCGCATGGGCGGGTAACTACCTTACAGCCCCCGCCAT</u>
	K1.int.F	<u>AGGCTATTCGGCTATGACTG</u>
	K2.int.R	<u>GCAGTTCATTCAGGGCACCG</u>
	LplA.U	<u>CTGGCGAAAGCGTCGAAGTG</u>
	LplA.D	<u>GCGTGATGCTGCCATTGAGG</u>
	LipB.U	<u>AGTGTAATTGGGCCATTGATGTATGG</u>
	LipB.D	<u>CCCCTTTACTCATTCTCCACGGAGATGCCG</u>

The annealing portions of these sequences are underlined, endonuclease sites are marked by boldface type, and italics marks relevant start and stop codons.

## **Chapter 5**

### **A New Family of Lipoate Attachment Enzyme Catalyzes Mitochondrial Lipoate Metabolism in Malaria Parasites**



## **Abstract**

Mitochondrial lipoate metabolism is essential for the survival of malaria parasites. The parasite mitochondrion contains two enzymes (LipL1 and LipL2) that catalyze the attachment of lipoate to three lipoate requiring substrates: the H-protein of the glycine cleavage system, the E2-subunits of branch chain amino acid dehydrogenase (BCDH) and  $\alpha$ -ketoglutarate dehydrogenase (KDH). Previous work showed that these substrates are lipoylated through two routes in an ATP dependent reaction with different redox sensitivity. LipL1 is sufficient to lipoylate the H-protein in a ligation reaction using oxidized or reduced lipoate. Lipoylation of the BCDH and KDH requires both LipL1 and LipL2 in a ligation reaction, using exclusively reduced lipoate as substrate. Herein we show that LipL1 has two activities that are essential for lipoylation of all mitochondrial substrates. First, LipL1 functions as a lipoate ligase capable of lipoylating the H-protein. Second, it functions as a lipoate activating enzyme to generate lipoyl-AMP using reduced lipoate as substrate. LipL2 is not a ligase; instead it acts as an *N*-lysine lipoyltransferase, using lipoyl-AMP as substrate. Also, LipL2 is the only enzyme that recognizes BCDH and KDH. Furthermore, LipL2 represents a new family of lipoate attachment enzymes conserved in malaria parasites. Mitochondrial lipoylation in malaria parasites differs from other described systems making it an attractive drug target.

## Introduction

*Plasmodium falciparum* (*Pf*) is an apicomplexan parasite that causes malaria in humans.<sup>1-4</sup> The parasite's life cycle consists of three stages: mosquito, liver and erythrocytic stage. The erythrocytic or red blood cell stage corresponds to the symptomatic phase. Several drugs have been designed against this stage, but increased drug resistance makes it necessary to exploit pathways that are essential for parasite survival.<sup>3,5-7</sup> One pathway that is essential for parasite survival is lipoate metabolism.<sup>8,9</sup> *Pf* contains two organelles that harbor two non-redundant pathways for lipoate metabolism: the apicoplast and the mitochondrion.<sup>9-12</sup> The apicoplast contains the machinery needed for lipoate biosynthesis, which has been shown to be essential for progression from liver to erythrocytic stage.<sup>10</sup> In contrast to the apicoplast, the mitochondrion relies on lipoate scavenged from the host, which has been shown to be essential for parasite survival during both liver and erythrocytic stage.<sup>8,9,13</sup>

The cofactor lipoate is essential for aerobic metabolism in oxidative decarboxylation reactions of 2-oxoacid complexes comprised of three subunits named E1, E2 and E3, and for glycine cleavage.<sup>14</sup> Lipoate is covalently bound to a specific lysine residue of a small lipoylation domain (LD) through an amide bond, forming lipoamide.<sup>15,16</sup> The LDs are typically found at the N-terminus of the E2-subunit of the 2-oxoacid dehydrogenase complexes. The H-protein of the glycine cleavage system (GCV) functions as the LD.<sup>17</sup> Lipoamide serves as a swinging arm to shuffle reaction intermediates between active sites of the different subunits in the multienzyme complexes. Lipoamide shuffles the decarboxylated acid from the E1 subunit through a thioester linkage to the core of the E2 subunit where the acyl thioester is converted to the corresponding coenzyme-A (CoA)

thioester by thioester exchange. Upon completion of this step, the lipoate is found in the reduced state (dihydrolipoamide). The dihydrolipoamide is oxidized to lipoamide by the dihydrolipoamide dehydrogenase (E3 subunit) to reset the catalytic cycle. The glycine cleavage system works in a similar fashion, but instead of three subunits it is composed of four loosely associated proteins: the P-protein (corresponding to the E1 subunit), the H-protein (lipoylation domain), the T-protein (core of E2 subunit) and the L-protein, which is the E3 subunit.<sup>17</sup>

Lipoate metabolism has been well characterized in *E. coli*. *E. coli* possesses the machinery for both biosynthesis and scavenging pathways. In *E. coli*, unlike in *Plasmodium*, these two pathways have been shown to be redundant.<sup>18</sup> Lipoate biosynthesis starts with an octanoyl transferase (*EcLipB*), which transfers the octanoyl group from octanoyl-Acyl Carrier Protein (octanoyl-ACP) to a conserved lysine of the lipoate requiring proteins.<sup>19</sup> Then a lipoyl synthase (*EcLipA*) inserts two sulfur atoms in positions C6 and C8 of the octanoyl group to produce the lipoyl moiety.<sup>20</sup> The second pathway is through lipoate scavenging, where a dedicated lipoate ligase (*EcLplA*) ligates the lipoyl group to lipoate requiring substrates in an ATP dependent reaction.<sup>18,21</sup> The *EcLplA* catalyzes the lipoate attachment by a two-step reaction. First, lipoate is activated with ATP, forming a lipoyl-AMP intermediate that remains bound to the enzyme. Upon binding of a protein substrate, the lipoyl moiety is transferred to a conserved substrate lysine residue.

The *EcLplA* crystal structure has been determined and shown to be a two-domain protein consisting of a large N-terminal domain and a small C-terminal domain.<sup>21</sup> Upon activation of lipoate (lipoyl-AMP formation), the *EcLplA* undergoes a conformational

change and the lipoyl-AMP adopts a U-shaped conformation at the bifurcated active site.<sup>21,22</sup> A conserved lysine residue in the *Ec*LplA has been shown to be essential for catalysis, and mutation of this residue resulted in almost completely abolished overall lipoylation.<sup>21</sup>

Lipoate synthesis in the apicoplast of *Pf* follows the same pathway as the biosynthesis pathway described for *E. coli*.<sup>10,23</sup> The parasite mitochondrion relies on lipoate scavenged from the host, which has been shown to proceed through two routes (Chapter 4). The parasite has two enzymes, lipoate ligase 1 (LipL1) and lipoate ligase 2 (LipL2), that are responsible for lipoylation of the mitochondrial substrates. Three lipoylated substrates have been localized to the mitochondrion: the branched chain amino acid dehydrogenase (BCDH), the  $\alpha$ -ketoglutarate dehydrogenase (KDH), and the H-protein of the GCV.<sup>17</sup> LipL1 appears to be the only active ligase in the mitochondrion being sufficient for lipoylation of the H-protein. Both LipL1 and LipL2 are needed for lipoylation of the BCDH and KDH. These two routes show different dependence on the lipoate redox state: the H-protein is lipoylated when lipoate is oxidized or reduced; whereas the BCDH and KDH are only lipoylated when lipoate is fully reduced. It has been previously shown that by treating parasites with lipoate analogues, 8-bromooctanoate or 6,8-dichlorooctanoate, we can inhibit the activity of the mitochondrial lipoylation substrates and cause cell death. These results make lipoate scavenging an interesting pathway to dissect for drug discovery. Of particular interest are the individual mechanistic roles of LipL1 and LipL2 in the combined reaction. Since both enzymes are homologous to lipoate ligases, either could be responsible for activating lipoate to lipoyl-

AMP, recognition of protein substrates, or transfer of the lipoyl group to the protein substrates.

Here we present data which show that LipL1 is the only lipoate ligase in the parasite mitochondrion and is the only enzyme responsible for lipoylation of the H-protein. Lipoylation of the BCDH and KDH proceeds through a concerted mechanism in which LipL1 acts as a lipoate activating enzyme producing lipoyl-AMP. LipL2 is not a ligase, instead it acts as an *N*-lysine lipoyltransferase taking the lipoyl-AMP formed by LipL1 and transferring the lipoyl moiety to BCDH and KDH. LipL2 cannot catalyze this reaction to lipylate the H-protein. Both LipL1 and LipL2 possess a conserved lysine residue, across LipL1-like and LipL2-like enzymes respectively, that is essential for their overall activity. Last, LipL2 appears to represent a new family of lipoate attachment enzymes that is conserved across most apicomplexans. We present *in vitro* lipoylation data to support these findings.

## **Materials and Methods**

### *Lipoyl-AMP synthesis*

All reagents were obtained from commercial suppliers and used without further purification unless stated. Acetonitrile was distilled after drying on CaH<sub>2</sub> then stored over 3Å molecular sieves. Yields of all reactions refer to the purified products. <sup>1</sup>H spectra were acquired on a Bruker Avance III 500 spectrometer operating at 500 MHz. Chemical shift values are reported as δ (ppm) relative to DMSO at δ 2.50 ppm. The purity of synthesized compounds was analyzed by HPLC (Beckman Gold Nouveau System Gold) on a C<sub>18</sub> column (Grace Alltima 3 μm C<sub>18</sub> analytical Rocket® column, 53 mm × 7 mm) using

triethylammonium acetate buffer (50 mM, pH 6) and methanol as eluent, flow rate 3 mL/min, and detection at 260 nm.

Procedures for synthesis of Lipoic Acid-Adenosine Monophosphate Mixed Anhydrides were based on Reed et al. (1958), with modifications.<sup>14</sup>

(R)-5-(1,2-dithiolan-3-yl)pentanoic (((2R,3S,4R,5R)-5-(6-amino-9H-purin-9-yl)-3,4-dihydroxytetrahydrofuran-2-yl)methyl phosphoric) anhydride monosodium salt (Lipoyl-AMP). *R*-Lipoic acid (0.500 g, 2.42 mmol) was dissolved in acetonitrile (2.5 mL) and added to a solution of dicyclohexylcarbodiimide (0.250 g, 1.21 mmol) in acetonitrile (0.9 mL) and stirred at room temperature for 30 minutes. The resulting suspension was then transferred to a conical tube and centrifuged (5 minutes, 4000 rpm) to pellet the solid.

The supernatant containing the *R*-lipoic acid anhydride was added to a solution of adenosine monophosphate monohydrate (0.442 g, 1.21 mmol) in pyridine (3.68 mL) and water (7.81 mL) at 0°C. After stirring at 0°C for 50 minutes, water (10 mL) was added and the solution was transferred to a separatory funnel where it was washed with ice cold diethyl ether (2 x 10 mL) and then ice cold chloroform (2 x 10 mL). The aqueous layer was collected and acetone was added to precipitate residual adenosine monophosphate, which was removed by centrifugation (5 minutes, 4000 rpm). The supernatant was condensed under reduced pressure and then redissolved in a minimum volume of water and loaded on a C<sub>18</sub> solid phase extraction column and washed with water (10 mL) and then eluted with acetonitrile. Condensation *in vacuo* yielded the desired product in 96% purity (0.006 g, 0.01 mmol, 1% yield). <sup>1</sup>H NMR (500 MHz, DMSO-d<sub>6</sub>) δ 8.57 (s, 1H), 8.31 (s, 1H), 5.94 (d, *J* = 5.62 Hz, 1H), 4.57 (t, *J* = 5.38 Hz, 1H), 4.18 (dd, *J* = 3.42, 4.65 Hz, 1H), 4.04 - 4.15 (m, 10H), 3.53 - 3.64 (m, 1H), 3.13 - 3.22 (m, 1H), 3.05 - 3.13 (m,

1H), 2.35 - 2.44 (m, 1H), 2.36 (t,  $J = 7.21$  Hz, 2H), 2.20 (t,  $J = 7.21$  Hz, 1H), 1.80 - 1.91 (m, 1H), 1.58 - 1.69 (m, 1H), 1.44 - 1.58 (m, 4H), 1.28 - 1.41 (m, 2H)

*Expression plasmids, protein expression and purification*

Cloning, expression and purification of the lipoylation domains of BCDH and KDH (BCDH<sub>LD</sub> and KDH<sub>LD</sub> respectively), the H-protein, as well as LipL1 and LipL2 were previously described in Chapter 4.

The lipoylation enzymes were clone into the expression plasmid pMALcHT which encodes a maltose binding protein (MBP) followed by a linker region composed of a tobacco etch virus (TEV) protease cut site followed by a six histidine affinity tag. Plasmid pMALcHT-LipL1 (Chapter 4) was mutated by site directed mutagenesis to generate pMALcHT-LipL1<sub>K160A</sub> using primers listed in **Table 1**. Plasmid pMALcHT-LipL1<sub>K160A</sub> was transformed into BL21-Star (DE3) cells (Invitrogen) and co-transformed with the pRIL plasmid isolated from BL21-CodonPlus-RIL cells (Agilent) and plasmid pRL586 encoding the Tobacco Etch Virus (TEV) protease, as described in Chapter 4. These cells produce LipL1<sub>K160A</sub> fused to an amino-terminal six histidine-tag. These cells were grown to mid-log phase, and protein expression was induced by the addition of 0.4 mM IPTG. Cells were harvested after growth for 10 h at 20°C. LipL1<sub>K160A</sub> was purified by metal chelate chromatography followed by cation exchange chromatography.

Plasmid pMALcHT-LipL2, codon optimized ligase (Chapter 4), was mutated by site directed mutagenesis using primers listed in **Table 1** to generate pMALcHT-LipL2<sub>C93A</sub>, pMALcHT-LipL2<sub>C276A</sub> and pMALcHT-LipL2<sub>K219A</sub>. Plasmids pMALcHT-LipL2<sub>C93A</sub>, pMALcHT-LipL2<sub>C276A</sub> and pMALcHT-LipL2<sub>K219A</sub> were transformed into BL21-Star

(DE3) and co-transformed with the pRIL plasmid. These cells produce LipL2 fused to an amino-terminal MBP. LipL2<sub>C93A</sub>, LipL2<sub>C276A</sub> and LipL2<sub>K219A</sub> were purified using Amylose resin (NEB #E8021).

Plasmid pMALcHT-PbLipL2 (PBANKA\_082459) was cloned from *Plasmodium berghei* ANKA genomic DNA (a gift from the Photini Sinnis Lab) using primers PbLipL2.fwd and PbLipL2.rev listed in **Table 1**. Similar to LipL2 constructs, pMALcHT-PbLipL2 was transformed into BL21-Star (DE3) and co-transformed with the pRIL plasmid. These cells produce PbLipL2 fused to an amino-terminal MBP, which was purified using Amylose resin.

#### *Lipoylation assays*

Purified LipL1, LipL2 or mutants (1  $\mu$ M), was incubated in reaction buffer (100 mM Na/K Phosphate buffer, 150 mM NaCl at pH 7.5) containing 2 mM ATP, 2 mM MgCl<sub>2</sub>, 5 mM TCEP, 200  $\mu$ M *R*-lipoic acid and 10  $\mu$ M apo-protein substrate: H-protein, BCDH<sub>LD</sub>, or KDH<sub>LD</sub>. The reactions were incubated at 37 degrees for 1 hour and quenched with the addition of gel loading buffer and resolved by SDS-PAGE followed by transfer to nitrocellulose membrane. The membranes were blocked with 5% milk in PBS for 30 minutes, and probed with 1:5000 rabbit polyclonal  $\alpha$ -LA<sub>891</sub> for 1 hour in 1% milk/PBS at room temperature. The membrane was washed with 1xPBS three times and then probed with 1:5000 donkey  $\alpha$ -Rabbit IgG horseradish peroxidase (HRP) secondary antibody (GE Healthcare) in 1% milk/PBS overnight at 4 degrees. The membranes were visualized with enhanced chemiluminescence (ECL) western substrate (Pierce) and exposed to film.



All lipoylation assays were conducted similarly using the same protein concentrations and base buffer. Where indicated, ATP was omitted from the reaction and 5 mM of DTT, 5 mM THP or water was used instead of TCEP. *R*-lipoic acid was substituted with 1 or 10  $\mu$ M *R*-lipoyl-AMP as the sole lipoate source, with no ATP added.

#### *Cell-based lipoylation assay*

The JEG3 lipoylation deficient *E. coli* strain (Chapter 4) was transformed with the pRIL plasmid and grown in LB medium supplemented with 1% glucose as a carbon source and 35  $\mu$ g ml<sup>-1</sup> chloramphenicol. Sodium succinate (5 mM) and sodium acetate (5 mM) were added to bypass the requirement for KDH and PDH activity respectively. JEG3/pRIL was transformed with a plasmid expressing a candidate lipoate ligase (either pMALcHT-LipL1 or pMALcHT-LipL1<sub>K160A</sub>) and selected using 100  $\mu$ g ml<sup>-1</sup> ampicillin and 35  $\mu$ g ml<sup>-1</sup> chloramphenicol. Transformants were grown in LB medium and supplemented as described above with the addition of 200  $\mu$ M *R*-lipoic acid (Sigma). For the cell-based assay 20 mL cultures were grown to mid-log phase at 37 degrees and induced with 0.4 mM IPTG for 10 hours at 20 degrees. Cells were harvested by centrifugation and resuspended with 0.5 mL of buffer containing 20 mM HEPES, 100 mM NaCl at pH 7.5 and lysed by sonication. The cell lysates were clarified by centrifugation at 16,000 g and the supernatants were collected and resolved by SDS-PAGE (Invitrogen). Lipoylated proteins were visualized by western blot as described in the lipoylation assays section.

#### *Thermal Shift Assay*

We followed a method described previously,<sup>24</sup> with some modifications. Real-time PCR tube strips (Eppendorf) were used to hold 31  $\mu$ L mixtures containing final concentrations of 1  $\mu$ M LipL1, 10  $\mu$ M of ligand (*R*-LA, *R*-LA-AMP or 6,8-diClO) diluted in DMSO. The reactions were set up with a 29  $\mu$ L mixture of LipL1, buffer (100 mM Phosphate pH 7.5, 150 mM NaCl and 2 mM MgCl<sub>2</sub>) and Sypro Orange (Sigma, Product Number S-5692 at a final concentration of 5X) to which 1  $\mu$ L of DMSO (or ligand) and 1  $\mu$ L of water or (DTT or TCEP diluted in water) were added. The reaction mixture was incubated in the RT-PCR machine (Applied Biosystems, Step One Plus Real-Time PCR System) for 2 minutes at 20 °C followed by 0.2 °C increases in the temperature every 10 seconds until a final temperature of 80 °C was reached. During the thermal scan, fluorescence was monitored using a pre-defined TAMRA filter in which an increase in Sypro Orange fluorescence was observed upon thermal denaturation of LipL1. The derivative of the fluorescence curve was used to determine the  $T_m$ . The initial  $T_m$  in the absence of ligand, but in the presence of DMSO, served as the baseline temperature ( $T_0$ ) for determining temperature shifts ( $\Delta T_m$ ). All measurements were made in triplicate.

#### *Production of rabbit $\alpha$ -LA 891 antibodies and test*

*R*-lipoic acid was conjugated to keyhole limpet hemocyanin using the Imject EDC mcKLH Spin Kit (Pierce). Antibodies to the conjugate were generated in rabbits using the standard protocol of the custom antibody service Cocalico Biologicals (Reamstown, PA). Specific antibodies were purified from serum using a holo-H-protein affinity column. A 1 mL NHS-activated HP column (GE Healthcare) was activated with 1 mM HCl according to the manufacturer's instructions. Immediately after activation, 13.5 mg

of *E. coli* H-protein in 4 mL of reaction buffer (100 mM NaCO<sub>3</sub>H, 500 mM NaCl pH 8.3) was pumped through the column at a constant rate of 0.1 mL/min. H-protein was circulated through the column for 2 hrs at room temperature at which point the release of N-hydroxysuccinimide reaction product was quantified by absorbance at 260 nM ( $\epsilon = 8600 \text{ M}^{-1} \text{ cm}^{-1}$ ). The column was subsequently washed and blocked according to the manufacturer's directions. Rabbit antiserum (6 mL) was circulated over the affinity column at room temperature for 1.5 hrs at 0.25 mL/min. Nonspecific proteins were washed from the column with 10 mL of PBS followed by elution in 4 mL of 50 mM glycine pH 1.9. A total of 0.68 mg of specific IgG was concentrated to 0.68 mg/mL and stored at -80°C in storage buffer (PBS, 50% glycerol, 0.02% NaN<sub>3</sub>). The specific polyclonal antibodies were labeled  $\alpha$ -LA<sub>891</sub>. To test this new reagent, we generated lipoylated PfH-protein using LipL1, R-LA and ATP in a lipoate ligase reaction, as described above. The resulting reaction mixture was used to compare  $\alpha$ -LA<sub>891</sub> to commercially available  $\alpha$ -LA (Calbiochem) by western blot (**Figure 1**).

#### *Sequence identity and alignments*

The eukaryotic pathogen database<sup>25</sup>, including PlasmoDB, ToxoDB and PiroplasmaDB, and the Wellcome Trust Sanger Institute for *Eimeria tenella*<sup>26</sup> were used for BLAST homology search of LipL2-like enzymes. Amino acid sequence identity was calculated by using the program STRETCHER<sup>27</sup>, and sequence alignments were performed with the programs CLUSTALW2<sup>28</sup> and ESPRIPT 2.<sup>9,29</sup>

## **Results**

*Active LipL1 is needed for lipoylation of all lipoylation substrates*

*Pf* mitochondrial lipoylation proceeds through two different routes. LipL1 is sufficient to lipoylate the H-protein in an ATP dependent reaction, whereas both LipL1 and LipL2 are needed to lipoylate the BCDH<sub>LD</sub> and KDH<sub>LD</sub>. It is possible that LipL1 and LipL2 are lipoylating the BCDH<sub>LD</sub> and KDH<sub>LD</sub> through a concerted mechanism or by forming a heteromeric complex. First, we wanted to determine whether LipL1 plays a catalytic role in the lipoylation of the BCDH<sub>LD</sub> and KDH<sub>LD</sub>. To test this we produced an inactive mutant of LipL1 (LipL1<sub>K160A</sub>) based on sequence homology to the *E. coli* lipoate ligase (*EcLplA*). Substitution of this lysine residue in *EcLplA* results in an enzyme that cannot transfer lipoyl groups and cannot form the lipoyl-AMP intermediate.<sup>21</sup> When we expressed LipL1<sub>K160A</sub> in the *lplA*-/*lipB*- *E. coli* cell line, we observed no lipoylation of the *E. coli* substrates, which confirms the phenotype of this mutant (**Figure 2A**). We then expressed and purified recombinant LipL1<sub>K160A</sub> and tested its activity in our *in vitro* ligation assay. We found that this mutant cannot lipoylate the H-protein (**Figure 2B, lanes 1-2**). We also found that BCDH<sub>LD</sub> and KDH<sub>LD</sub> are not lipoylated in the presence of LipL1<sub>K160A</sub> and LipL2 (**Fig. 2B, lanes 3-6**). These results indicate that LipL1 has a catalytic role in the lipoylation of BCDH<sub>LD</sub> and KDH<sub>LD</sub>; it either catalyzes the activation of the lipoyl-AMP conjugate, the transfer of the lipoyl group, or both.

In order to determine whether LipL1<sub>K160A</sub> inhibits the activation or transfer reaction, we synthesized the intermediate, lipoyl-AMP, and used it as the sole lipoate source in our *in vitro* assays. As seen in **Figure 2C**, LipL1<sub>K160A</sub> failed to lipoylate the H-protein using lipoyl-AMP (lane 1), confirming that this mutant cannot catalyze the transfer reaction. When we combined LipL1<sub>K160A</sub> and LipL2 using the BCDH<sub>LD</sub> and KDH<sub>LD</sub> as substrates,

we observed lipoylation of both substrates when using lipoyl-AMP (**Figure 2C, lanes 2-5**). These data suggest that the role of LipL1 in the LipL1+LipL2 reaction is to catalyze the activation reaction generating lipoyl-AMP and that LipL2 is not capable of producing the conjugate. Instead, it appears that LipL2 catalyzes the lipoyl transfer reaction, however, it is not clear whether LipL1 is required for a non-catalytic role such as substrate recognition.

#### *LipL2 functions as a lipoyltransferase*

From our previous results, we can conclude that LipL1 is the only enzyme capable of activating lipoate to form the LA-AMP intermediate, whereas LipL2 seems to be essential for the transfer reaction. In order to determine whether LipL2 is sufficient to catalyze the transfer reaction, we tested LipL2 in the absence of LipL1 using the synthesized LA-AMP as the sole source of lipoate. We found that LipL2 cannot lipoylate the H-protein, but it can recognize and lipoylate BCDH<sub>LD</sub> or KDH<sub>LD</sub> when lipoyl-AMP is supplied (**Figure 3**). These results show that LipL2 acts independently as a lipoyltransferase against BCDH<sub>LD</sub> and KDH<sub>LD</sub>. Combining these data with the above results, we can conclude that LipL1 forms the LA-AMP conjugate and can recognize either the H-protein as a lipoylation substrate or LipL2 as a lipoylation partner enzyme. LipL2 acts as a lipoyltransferase, binding LA-AMP produced by LipL1 and recognizing BCDH<sub>LD</sub> or KDH<sub>LD</sub> As lipoylation substrates.

#### *LipL2 is not redox sensitive*

Given the lipoyltransferase activity of LipL2 and that the lipoylation of BCDH<sub>LD</sub> and KDH<sub>LD</sub> is strictly gated by the redox state of lipoate, we hypothesized that LipL2 must be a redox-sensitive enzyme. To test this, we incubated LipL2 with lipoyl-AMP in the presence or absence of different reducing agents (DTT, TCEP and THP) and tested the lipoyl transfer reaction with each of the three mitochondrial substrates. We found, as seen in **Figure 3**, that LipL2 does not recognize the H-protein under any redox conditions (**lanes 1-4**), thus confirming that H-protein is only lipoylated by LipL1. Surprisingly, LipL2 did not show sensitivity to the redox state of lipoyl-AMP as both BCDH<sub>LD</sub> and KDH<sub>LD</sub> are lipoylated under all reducing conditions tested (**Figure 3, lanes 5-12**). This result was puzzling given that the lipoylation of both BCDH<sub>LD</sub> and KDH<sub>LD</sub> occurs only in the presence of strong reducing conditions (eg. TCEP and THP, Chapter 4).

Since LipL2 is not redox sensitive, we predict that LipL1 must be responsible for the redox sensitive behavior of the coupled LipL1+LipL2 reaction. It is possible that lipoyl-AMP or dihydrolipoyl-AMP have different binding affinity to LipL1, thus determining the fate of the conjugate. By using the thermal shift assay,<sup>24</sup> we found that oxidized lipoate and lipoyl-AMP bind tightly to LipL1; whereas dihydrolipoate, dihydrolipoyl-AMP, and the reduced state analog 6,8-diClO bind with less relative affinity to LipL1 (**Table 2**). This phenomenon may be the result of conformational changes in LipL1 such as those observed for *EcLplA* rather than simply differences in binding affinity. These conformational changes would then dictate whether LipL1 would recruit LipL2.

*A conserved lysine is essential for LipL2 activity*

We wanted to further characterize the activity of LipL2 against the parasite substrates by mutational analysis. Transfer reactions are typically catalyzed through a cysteine or lysine residue. In *Bacillus subtilis*, an octanoyl transferase (*BsLipL*) catalyzes the transfer of the octanoyl moiety through a cysteine on which the octanoyl moiety is covalently attached.<sup>30,31</sup> We attempted to produce an inactive mutant of LipL2 by mutating the only two cysteines that are conserved across all *Plasmodium* species (C93 and C276). The recombinant LipL2 mutants (LipL2<sub>C93A</sub> and LipL2<sub>C276A</sub>) were tested in our *in vitro* assays. We found that the BCDH<sub>LD</sub> and KDH<sub>LD</sub> were still lipoylated (**Figure 5B, lanes 1-3 and 5-7**), suggesting that LipL2 does not require a cysteine for activity and does not transfer lipoate through a thioester intermediate.

In other systems, such as *E. coli* and mammalian, the transfer of the lipoyl moiety from lipoyl-AMP is facilitated by a lysine residue in the active site.<sup>32-35</sup> This is the case for LipL1 as discussed above. But unlike LipL1, LipL2 shares low sequence identity to *EcLplA* and *Bos taurus* N-lysine lipoyltransferase (*BtLipT*) (**Table 3**) and does not have an apparent conserved lysine residue when aligned to other known enzymes. In fact, only the highly conserved lipoate binding motif is found in all of these enzymes, whereas the ATP binding motif is not conserved in LipL2-like enzymes (**Figure 6A**). However, we observed a cluster of residues that seems to define the LipL2-like family of enzymes (**Figure 6A, black line**) and includes two well-conserved lysine residues. We generated homology models of LipL2 using the program iTasser<sup>36</sup> to better understand where these residues could be located relative to the active site. The models generated by iTasser were based on the *BtLipT* structure (PDB<sub>id</sub>: 2E5A) which may be significant since the bovine enzyme is also a lipoyltransferase which is not capable of activating lipoate to

LA-AMP. The structure of *BtLipT* contains a conserved active site lysine (**Figure 5A**) which aligns structurally with one of the lysine residues conserved in LipL2-like enzymes (**Figure 6A, blue box**). In *BtLipT*, this lysine is essential for the transfer reaction.<sup>32, 33</sup> We proceeded to mutate this lysine residue in LipL2 (LipL2<sub>K219A</sub>) and tested the recombinant protein in our *in vitro* assay. LipL2<sub>K219A</sub> is inactive in our assay when reacted in the presence of LipL1 in an ATP dependent reaction, thus confirming that this residue is essential for LipL2 activity (**Figure 5B, lanes 4 and 8**). Furthermore, LipL2<sub>K219A</sub> alone is unable to use lipoyl-AMP as a substrate (**Figure 4C**), thus confirming that this residue is involved in the transfer reaction. Taken together, LipL2 is an *N*-lysine lipoyltransferase similar to the *BtLipT*.<sup>32, 33</sup>

#### *LipL2 is a new family of lipoate transfer enzymes*

LipL2 acts as an *N*-lysine lipoyltransferase with low sequence identity to previously described lipoate attachment enzymes (**Table 3**). Sequence alignment of apicomplexan LipL2-like enzymes shows a conserved cluster of residues that might be important for recognition and binding of lipoyl-AMP, which is not conserved in other lipoate attachment enzymes (**Figure 6A**). This cluster of residues maps logically to the active site in our structure homology model for LipL2. Is this “LipL2” activity conserved in other Apicomplexa parasites as well? In order to investigate this, we cloned and expressed *Plasmodium berghei* LipL2 (*PbLipL2*) and tested its activity in our *in vitro* assay. We found that *PbLipL2* can use lipoyl-AMP as a substrate and lipoylate the *Pf* substrates BCDH<sub>LD</sub> and KDH<sub>LD</sub> but not the H-protein (**Figure 6B**). This result suggests



that LipL2-like enzymes act as *N*-lysine lipoyltransferases throughout the phylum Apicomplexa.

## Discussion

*Plasmodium falciparum* mitochondrial lipoylation relies on lipoate scavenged from the host. After lipoate is imported to the mitochondrion there are two enzymes, LipL1 and LipL2, which attach lipoate to the different substrates.<sup>9</sup> We previously showed that there are two routes by which the substrates are modified. First, LipL1 appears to be the only active ligase and is sufficient to lipoylate the H-protein through an ATP dependent reaction. Second, both LipL1 and LipL2 are needed to lipoylate the BCDH and KDH also in an ATP dependent reaction. Last, lipoylation shows redox sensitivity: the H-protein is lipoylated under different redox conditions; whereas the BCDH and KDH are only lipoylated under strong reducing conditions (eg. Tris(2-carboxyethyl)phosphine (TCEP) or tris(hydroxypropyl)phosphine (THP) conditions) demonstrating the need for dihydrolipoate in order for these substrates to be lipoylated. From these previous results it was not clear if lipoylation of the BCDH and KDH proceeds through a concerted mechanism or by LipL1 and LipL2 forming a complex. Also, the specific role of these enzymes in the parasite was not addressed.

In order to understand the specific activity of these enzymes in the parasite we proceeded to mutate a conserved lysine residue in LipL1 (K160A). We found that this mutation blocked lipoylation of all substrates. This establishes that active LipL1 is needed for lipoylation of all substrates and is likely to be an essential enzyme. LipL1<sub>K160A</sub> is unable to catalyze the transfer reaction using the H-protein as substrate

(**Figure 2C, lane 1**). While in the presence of LipL2, both BCDH and KDH were still lipoylated. We concluded that LipL1 is the only active lipoate ligase in the parasite mitochondrion, and that LipL2 activity is essential for the lipoylation of BCDH and KDH. Thus, with respect to the H-protein, LipL1 behaves like the *E. coli* lipoate ligase (Chapter 4).

However, the lipoylation of the BCDH and KDH is more akin to the bovine system in which a lipoate activating enzyme (LAE) activates the free lipoate with GTP, and an *N*-lysine lipoyltransferase (*BtLipT*) then transfers lipoate from the formed conjugate (lipoyl-GMP) to the substrates (**Figure 8**).<sup>32-34, 37, 38</sup> In *Pf*, we show that LipL1 acts as the LAE and that LipL2 acts as the *N*-lysine lipoyltransferase to lipoylate the BCDH and KDH, but with some differences between the systems. First, LipL1 has dual activity: 1) as a ligase being sufficient to lipoylate the H-protein and 2) as a LAE forming the lipoyl-AMP conjugate. In mammalian systems a medium chain acyl-CoA synthase has been identified to act as the LAE (**Figure 8**).<sup>38</sup> Second, mammalian systems use GTP to activate lipoate,<sup>38</sup> whereas *Pf* uses only ATP. One last difference, and the most striking, is the difference in the dependence on the redox state of lipoate. The LAE can recognize the oxidized form of lipoate and pass the conjugate to *BtLipT*; the assays were performed in the presence of 0.5 mM DTT.<sup>33</sup> The reactions were not carried out under strong reducing conditions (TCEP or THP containing buffer), making difficult to conclude if the bovine system could lipoylate the substrate using dihydrolipoate as substrate. By contrast, we have shown that *Pf* can only lipoylate the BCDH and KDH when lipoate is in the reduced state. This is the first system in which this redox dependent lipoylation activity has been reported.

LipL1 behaves similar to *EcLplA* (29% identity),<sup>9</sup> but it shows different substrate specificity. Furthermore, LipL1 has 26 % sequence identity to the bovine *N*-lysine lipoyltransferase, but they share no similar activities. The second *Pf* enzyme, LipL2, has low sequence identity to LipL1 (21%) as well as to *EcLplA* (12%), and no ligase activity.<sup>9</sup> LipL2, structurally and functionally, seems to resemble the *BtLipT* despite the fact that they share low sequence identity (17%). Based on our assays, LipL2 is not a ligase, but instead it acts as an *N*-lysine lipoyltransferase (**Figure 5C**) similar to the *BtLipT* as described above.

The BCDH and KDH are only lipoylated by using dihydrolipoate as substrate, thus we hypothesized that LipL2 has a requirement for dihydrolipoyl-AMP for its activity. We found that LipL2 can recognize both lipoyl-AMP and dihydrolipoyl-AMP to lipoylate the BCDH and KDH. Therefore, we suggest that LipL1 must have some redox sensitivity for the lipoate redox state. We found that lipoate and lipoyl-AMP bind to LipL1 with different affinities depending on their redox state. The oxidized species bind relatively tighter to the enzyme than the reduced form. We also found that 6,8-diClO (dihydrolipoate analog) binds less tightly to LipL1, with similar affinity as dihydrolipoate. The binding affinity of reduced lipoyl-AMP might be important for transfer of the conjugate to LipL2. Still, this might not be sufficient given that LipL1 can modify the H-protein under different reducing conditions with both lipoate and 6,8-diClO (Chapter 4). Perhaps, the adenylation of dihydrolipoate triggers a conformational change on LipL1 that could be recognized by LipL2 and thus allow LipL2 to obtain the conjugate. The relatively low binding affinity of dihydrolipoate-AMP could facilitate this transfer.

Both LipL1 and LipL2 are well conserved among apicomplexan parasites, suggesting that perhaps this mechanism of lipoate metabolism is not unique to *Plasmodium*. We tested the activity of a rodent malaria parasite (*Plasmodium berghei*) LipL2 against the *Pf* substrates and found that this enzyme has lipoyltransferase activity. Similar to *Pf*, the *Plasmodium berghei* genome also encodes a LipL1 enzyme. These results suggest that the mechanism of lipoylation found in *Plasmodium falciparum* is shared in other malaria parasites and could be distributed broadly across other apicomplexan parasite species.

## Conclusions

In the current study we expand the understanding of mitochondrial lipoylation in *Pf*. The parasite contains two lipoate attachment enzymes (LipL1 and LipL2) and three lipoate requiring substrates (H-protein, BCDH and KDH). These substrates are lipoylated through two routes with different redox sensitivity (**Figure 7**). We show that LipL1 is the sole lipoate ligase and it is responsible for lipoylation of the H-protein in an ATP dependent reaction. The BCDH and KDH are lipoylated through a concerted mechanism. LipL1 acts as a lipoate activating enzyme to generate lipoyl-AMP by using reduced lipoate as a substrate. The intermediate lipoyl-AMP is the substrate of LipL2 to lipoylate the BCDH and KDH. LipL2 is not a ligase as previously proposed; instead it acts as an *N*-lysine lipoyltransferase. We show that LipL2 is not sensitive to the redox state of lipoyl-AMP. It seems that LipL1, upon activation of lipoate or dihydrolipoate, decides the fate of the formed conjugate. Either to lipoylate the H-protein or pass the conjugate to LipL2. Last, LipL2 is part of a new family of attachment enzymes that is conserved throughout apicomplexan parasites. We show that *Plasmodium berghei* LipL2

also acts as a lipoyltransferase with the same pattern of substrate specificity. *Pf* mitochondrial lipoylation shows differences to previously described systems, including those found in mammals, making it an attractive drug target (**Figure 8**).

### **Acknowledgements**

Synthesis of lipoyl-AMP was performed by David Bartee of the Caren Freel Meyers lab. Cloning of *Plasmodium berghei* LipL2 was done by Krista Matthews.

### **References**

1. Mudhune, S. A.; Okiro, E. A.; Noor, A. M.; Zurovac, D.; Juma, E.; Ochola, S. A.; Snow, R. W. The clinical burden of malaria in Nairobi: a historical review and contemporary audit. *Malar J* **2011**, 10, 138.
2. Okiro, E. A.; Al-Taiar, A.; Reyburn, H.; Idro, R.; Berkley, J. A.; Snow, R. W. Age patterns of severe paediatric malaria and their relationship to *Plasmodium falciparum* transmission intensity. *Malaria Journal* **2009**, 8.
3. Okiro, E. A.; Bitira, D.; Mbabazi, G.; Mpimbaza, A.; Alegana, V. A.; Talisuna, A. O.; Snow, R. W. Increasing malaria hospital admissions in Uganda between 1999 and 2009. *Bmc Medicine* **2011**, 9.
4. Okiro, E. A.; Mutheu, J.; Gething, P. W.; Juma, E.; Snow, R. W. The Changing Patterns of Malaria Admissions since 1999 at 18 Hospitals across Kenya. *American Journal of Tropical Medicine and Hygiene* **2009**, 81, 54-54.

5. Dondorp, A. M.; Fairhurst, R. M.; Slutsker, L.; Macarthur, J. R.; Breman, J. G.; Guerin, P. J.; Wellems, T. E.; Ringwald, P.; Newman, R. D.; Plowe, C. V. The threat of artemisinin-resistant malaria. *N Engl J Med* **2011**, *365*, 1073-5.
6. Fidock, D. A.; Eastman, R. T.; Ward, S. A.; Meshnick, S. R. Recent highlights in antimalarial drug resistance and chemotherapy research. *Trends Parasitol* **2008**, *24*, 537-44.
7. Phyo, A. P.; Nkhoma, S.; Stepniewska, K.; Ashley, E. A.; Nair, S.; McGready, R.; ler Moo, C.; Al-Saai, S.; Dondorp, A. M.; Lwin, K. M.; Singhasivanon, P.; Day, N. P.; White, N. J.; Anderson, T. J.; Nosten, F. Emergence of artemisinin-resistant malaria on the western border of Thailand: a longitudinal study. *Lancet* **2012**, *379*, 1960-6.
8. Storm, J.; Muller, S. Lipoic acid metabolism of Plasmodium--a suitable drug target. *Curr Pharm Des* **2012**, *18*, 3480-9.
9. Allary, M.; Lu, J. Z.; Zhu, L.; Prigge, S. T. Scavenging of the cofactor lipoate is essential for the survival of the malaria parasite Plasmodium falciparum. *Mol Microbiol* **2007**, *63*, 1331-44.
10. Foth, B. J.; Stimmler, L. M.; Handman, E.; Crabb, B. S.; Hodder, A. N.; McFadden, G. I. The malaria parasite Plasmodium falciparum has only one pyruvate dehydrogenase complex, which is located in the apicoplast. *Mol Microbiol* **2005**, *55*, 39-53.
11. Gunther, S.; McMillan, P. J.; Wallace, L. J.; Muller, S. Plasmodium falciparum possesses organelle-specific alpha-keto acid dehydrogenase complexes and lipoylation pathways. *Biochem Soc Trans* **2005**, *33*, 977-80.

12. Wrenger, C.; Muller, S. The human malaria parasite *Plasmodium falciparum* has distinct organelle-specific lipoylation pathways. *Mol Microbiol* **2004**, *53*, 103-13.
13. Falkard, B.; Kumar, T. R.; Hecht, L. S.; Matthews, K. A.; Henrich, P. P.; Gulati, S.; Lewis, R. E.; Manary, M. J.; Winzeler, E. A.; Sinnis, P.; Prigge, S. T.; Heussler, V.; Deschermeier, C.; Fidock, D. A key role for lipoic acid synthesis during *Plasmodium* liver stage development. *Cell Microbiol* **2013**.
14. Reed, L. J.; Koike, M.; Levitch, M. E.; Leach, F. R. Studies on the nature and reactions of protein-bound lipoic acid. *J Biol Chem* **1958**, *232*, 143-58.
15. Perham, R. N. Swinging arms and swinging domains in multifunctional enzymes: catalytic machines for multistep reactions. *Annu Rev Biochem* **2000**, *69*, 961-1004.
16. Reche, P.; Perham, R. N. Structure and selectivity in post-translational modification: attaching the biotinyl-lysine and lipoyl-lysine swinging arms in multifunctional enzymes. *Embo Journal* **1999**, *18*, 2673-2682.
17. Spalding, M. D.; Allary, M.; Gallagher, J. R.; Prigge, S. T. Validation of a modified method for Bxb1 mycobacteriophage integrase-mediated recombination in *Plasmodium falciparum* by localization of the H-protein of the glycine cleavage complex to the mitochondrion. *Mol Biochem Parasitol* **2010**, *172*, 156-60.
18. Morris, T. W.; Reed, K. E.; Cronan, J. E. Lipoic Acid Metabolism in *Escherichia Coli* - the *LplA* and *LipB* Genes Define Redundant Pathways for Ligation of Lipoyl Groups to Apoprotein. *Journal of Bacteriology* **1995**, *177*, 1-10.
19. Jordan, S. W.; Cronan, J. E. The *Escherichia coli* *lipB* gene encodes lipoyl (octanoyl)-acyl carrier protein : protein transferase. *Journal of Bacteriology* **2003**, *185*, 1582-1589.

20. Miller, J. R.; Busby, R. W.; Jordan, S. W.; Cheek, J.; Henshaw, T. F.; Ashley, G. W.; Broderick, J. B.; Cronan, J. E.; Marletta, M. A. Escherichia coli LipA is a lipoyl synthase: In vitro biosynthesis of lipoylated pyruvate dehydrogenase complex from octanoyl-acyl carrier protein. *Biochemistry* **2000**, *39*, 15166-15178.
21. Fujiwara, K.; Maita, N.; Hosaka, H.; Okamura-Ikeda, K.; Nakagawa, A.; Taniguchi, H. Global conformational change associated with the two-step reaction catalyzed by Escherichia coli lipoyl-protein ligase A. *J Biol Chem* **2010**, *285*, 9971-80.
22. Kim, D. J.; Kim, K. H.; Lee, H. H.; Lee, S. J.; Ha, J. Y.; Yoon, H. J.; Suh, S. W. Crystal structure of lipoyl-protein ligase A bound with the activated intermediate: insights into interaction with lipoyl domains. *J Biol Chem* **2005**, *280*, 38081-9.
23. Pei, Y.; Tarun, A. S.; Vaughan, A. M.; Herman, R. W.; Soliman, J. M.; Erickson-Wayman, A.; Kappe, S. H. Plasmodium pyruvate dehydrogenase activity is only essential for the parasite's progression from liver infection to blood infection. *Mol Microbiol* **2010**, *75*, 957-71.
24. Afanador, G. A.; Muench, S. P.; McPhillie, M.; Fomovska, A.; Schon, A.; Zhou, Y.; Cheng, G.; Stec, J.; Freundlich, J. S.; Shieh, H. M.; Anderson, J. W.; Jacobus, D. P.; Fidock, D. A.; Kozikowski, A. P.; Fishwick, C. W.; Rice, D. W.; Freire, E.; McLeod, R.; Prigge, S. T. Discrimination of Potent Inhibitors of Toxoplasma gondii Enoyl-Acyl Carrier Protein Reductase by a Thermal Shift Assay. *Biochemistry* **2013**, *52*, 9155-66.
25. Aurrecoechea, C.; Brestelli, J.; Brunk, B. P.; Fischer, S.; Gajria, B.; Gao, X.; Gingle, A.; Grant, G.; Harb, O. S.; Heiges, M.; Innamorato, F.; Iodice, J.; Kissinger, J. C.; Kraemer, E. T.; Li, W.; Miller, J. A.; Nayak, V.; Pennington, C.; Pinney, D. F.; Roos, D. S.; Ross, C.; Srinivasamoorthy, G.; Stoeckert, C. J., Jr.; Thibodeau, R.; Treatman, C.;



- Wang, H. EuPathDB: a portal to eukaryotic pathogen databases. *Nucleic Acids Res* **2010**, 38, D415-9.
26. Ling, K. H.; Rajandream, M. A.; Rivaille, P.; Ivens, A.; Yap, S. J.; Madeira, A. M.; Mungall, K.; Billington, K.; Yee, W. Y.; Bankier, A. T.; Carroll, F.; Durham, A. M.; Peters, N.; Loo, S. S.; Isa, M. N.; Novaes, J.; Quail, M.; Rosli, R.; Nor Shamsudin, M.; Sobreira, T. J.; Tivey, A. R.; Wai, S. F.; White, S.; Wu, X.; Kerhornou, A.; Blake, D.; Mohamed, R.; Shirley, M.; Gruber, A.; Berriman, M.; Tomley, F.; Dear, P. H.; Wan, K. L. Sequencing and analysis of chromosome 1 of *Eimeria tenella* reveals a unique segmental organization. *Genome Res* **2007**, 17, 311-9.
27. Myers, E. W.; Miller, W. Optimal alignments in linear space. *Comput Appl Biosci* **1988**, 4, 11-7.
28. Thompson, J. D.; Gibson, T. J.; Higgins, D. G. Multiple sequence alignment using ClustalW and ClustalX. *Curr Protoc Bioinformatics* **2002**, Chapter 2, Unit 2.3.
29. Gouet, P.; Courcelle, E.; Stuart, D. I.; Metz, F. ESPript: analysis of multiple sequence alignments in PostScript. *Bioinformatics* **1999**, 15, 305-8.
30. Christensen, Q. H.; Martin, N.; Mansilla, M. C.; de Mendoza, D.; Cronan, J. E. A novel amidotransferase required for lipoic acid cofactor assembly in *Bacillus subtilis*. *Mol Microbiol* **2011**, 80, 350-63.
31. Martin, N.; Christensen, Q. H.; Mansilla, M. C.; Cronan, J. E.; de Mendoza, D. A novel two-gene requirement for the octanoyltransfer reaction of *Bacillus subtilis* lipoic acid biosynthesis. *Mol Microbiol* **2011**, 80, 335-49.

32. Fujiwara, K.; Hosaka, H.; Matsuda, M.; Okamura-Ikeda, K.; Motokawa, Y.; Suzuki, M.; Nakagawa, A.; Taniguchi, H. Crystal structure of bovine lipoyltransferase in complex with lipoyl-AMP. *J Mol Biol* **2007**, *371*, 222-34.
33. Fujiwara, K.; Okamura-Ikeda, K.; Motokawa, Y. Purification and characterization of lipoyl-AMP:N epsilon-lysine lipoyltransferase from bovine liver mitochondria. *J Biol Chem* **1994**, *269*, 16605-9.
34. Fujiwara, K.; Suzuki, M.; Okumachi, Y.; Okamura-Ikeda, K.; Fujiwara, T.; Takahashi, E.; Motokawa, Y. Molecular cloning, structural characterization and chromosomal localization of human lipoyltransferase gene. *Eur J Biochem* **1999**, *260*, 761-7.
35. Fujiwara, K.; Toma, S.; Okamura-Ikeda, K.; Motokawa, Y.; Nakagawa, A.; Taniguchi, H. Crystal structure of lipoate-protein ligase A from Escherichia coli. Determination of the lipoic acid-binding site. *J Biol Chem* **2005**, *280*, 33645-51.
36. Zhang, Y. I-TASSER server for protein 3D structure prediction. *BMC Bioinformatics* **2008**, *9*, 40.
37. Fujiwara, K.; Okamura-Ikeda, K.; Motokawa, Y. Cloning and expression of a cDNA encoding bovine lipoyltransferase. *J Biol Chem* **1997**, *272*, 31974-8.
38. Fujiwara, K.; Takeuchi, S.; Okamura-Ikeda, K.; Motokawa, Y. Purification, characterization, and cDNA cloning of lipoate-activating enzyme from bovine liver. *J Biol Chem* **2001**, *276*, 28819-23.

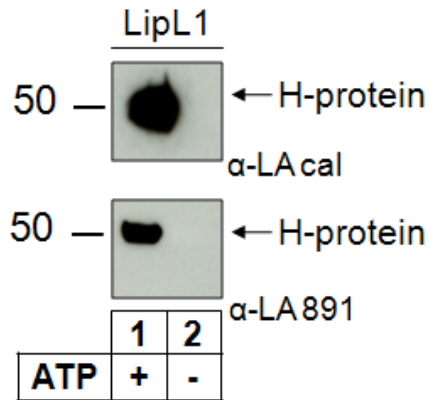


**Figure 1.** Evaluation of anti-lipoamide antibodies. We tested the specificity of commercially available rabbit polyclonal antiserum (Calbiochem) and purified rabbit IgG (bottom panel). We found that both reagents have the same specificity against lipoylated proteins when tested in an *in vitro* reaction of LipL1 against the H-protein. These reactions were performed under reducing conditions containing DTT.

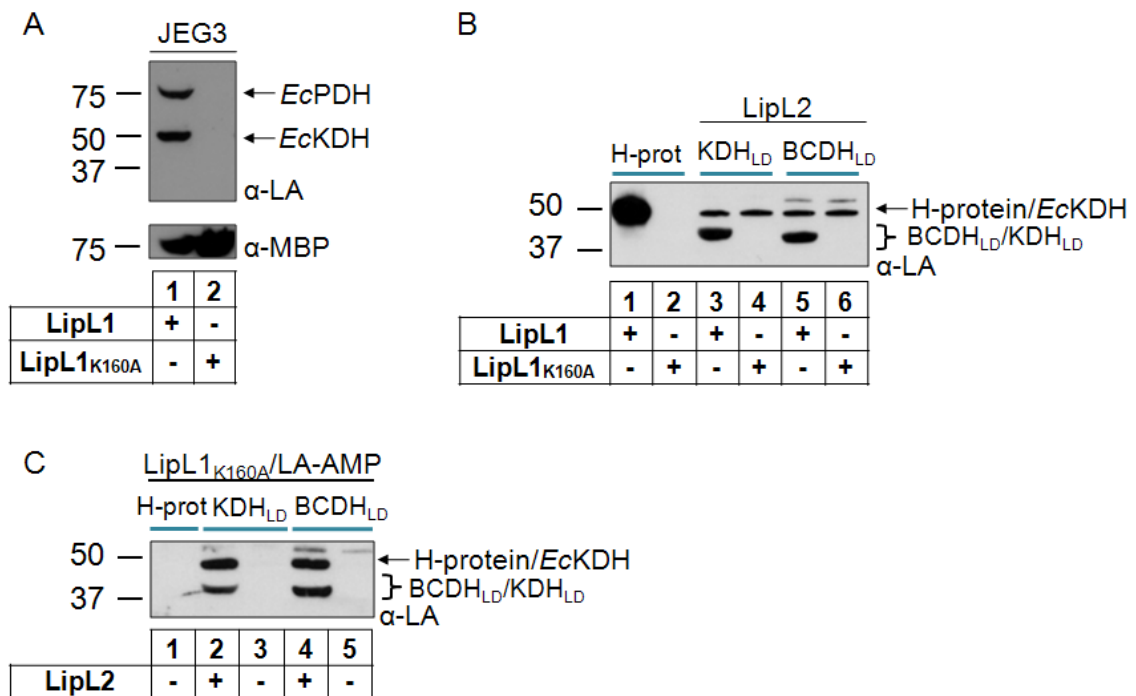


**Figure 2.** LipL1 activity is essential for lipoylation of all substrates. A) LipL1 can complement a lipoylation deficient *E. coli* cell line, whereas LipL1<sub>K160A</sub> fails to lipoylate *E. coli* proteins *in vivo*. B) LipL1<sub>K160A</sub> fails to lipoylate all three mitochondrial lipoylation substrates in *in vitro* assays. C) LipL1<sub>K160A</sub> cannot use lipoyl-AMP as substrate to lipoylate the H-protein; this mutant does not prevent lipoylation of the BCDH<sub>LD</sub> and KDH<sub>LD</sub> in the presence of LipL2. H-protein reactions were performed under DTT conditions; BCDH<sub>LD</sub> and KDH<sub>LD</sub> were performed under TCEP containing conditions.

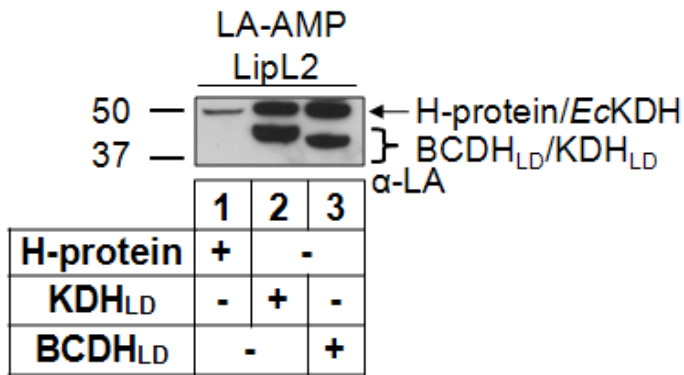


**Figure 3.** LipL2 activity is essential for lipoylation of the BCDH<sub>LD</sub> and KDH<sub>LD</sub>. LipL2 acts as a lipoyltransferase by using lipoyl-AMP as substrate to lipoylate the BCDH<sub>LD</sub> and KDH<sub>LD</sub>, but it cannot lipoylate the H-protein. These reactions were performed under TCEP containing conditions.

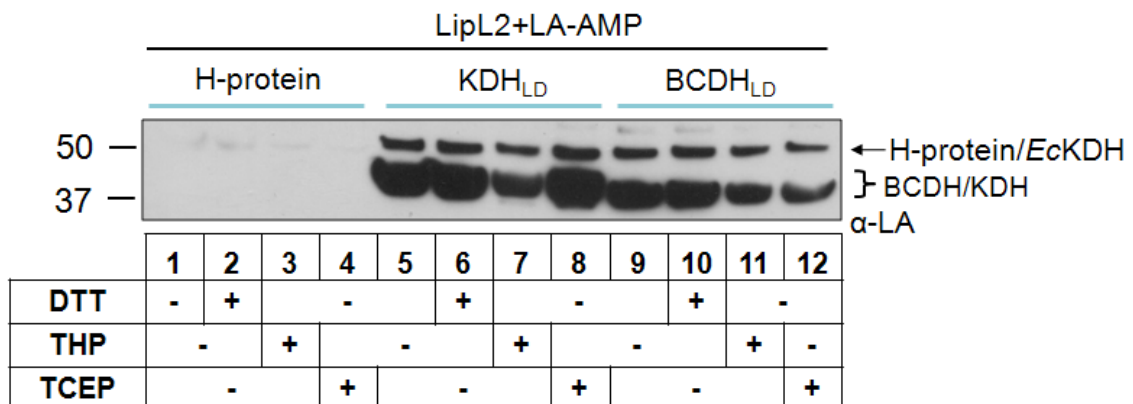


**Figure 4.** Redox dependence of LipL2. LipL2 does not recognize the H-protein under any redox conditions. The BCDH<sub>LD</sub> and KDH<sub>LD</sub> are lipoylated independent of the reducing potential, thus showing LipL2 is not responsible for the redox sensitivity previously observed in the LipL1+LipL2 reaction.

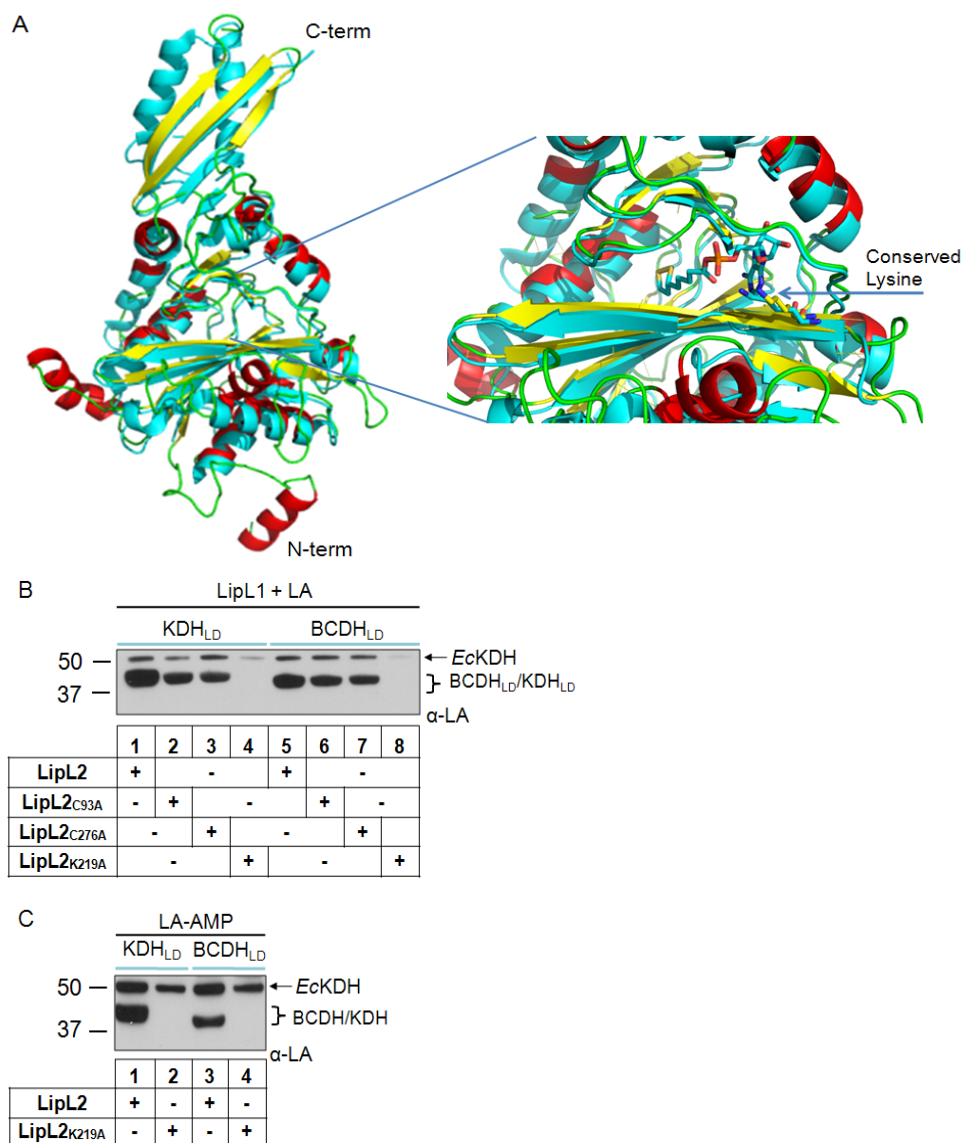


**Figure 5.** LipL2 acts as an *N*-lysine lipoyltransferase. A) LipL2 iTasser homology model (yellow and red) using the structure of the bovine lipoyltransferase (PDB<sub>id</sub>: 2E5A) as a template (cyan). The active site shows conservation of residues that could be essential for activity, including a conserved lysine in lipoyl attachment enzymes involved in overall activity. B) Mutational analysis of LipL2 shows that Lys219 is essential for LipL2 activity. C) LipL2<sub>K219A</sub> is unable to use lipoyl-AMP as substrate. These reactions were performed under THP containing conditions.

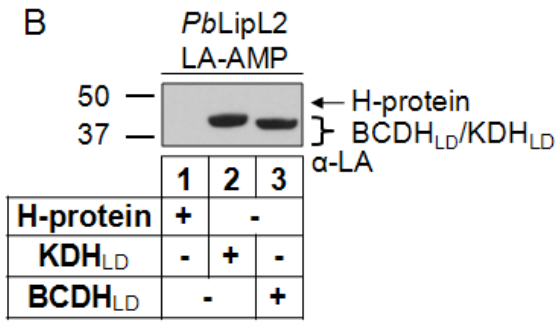
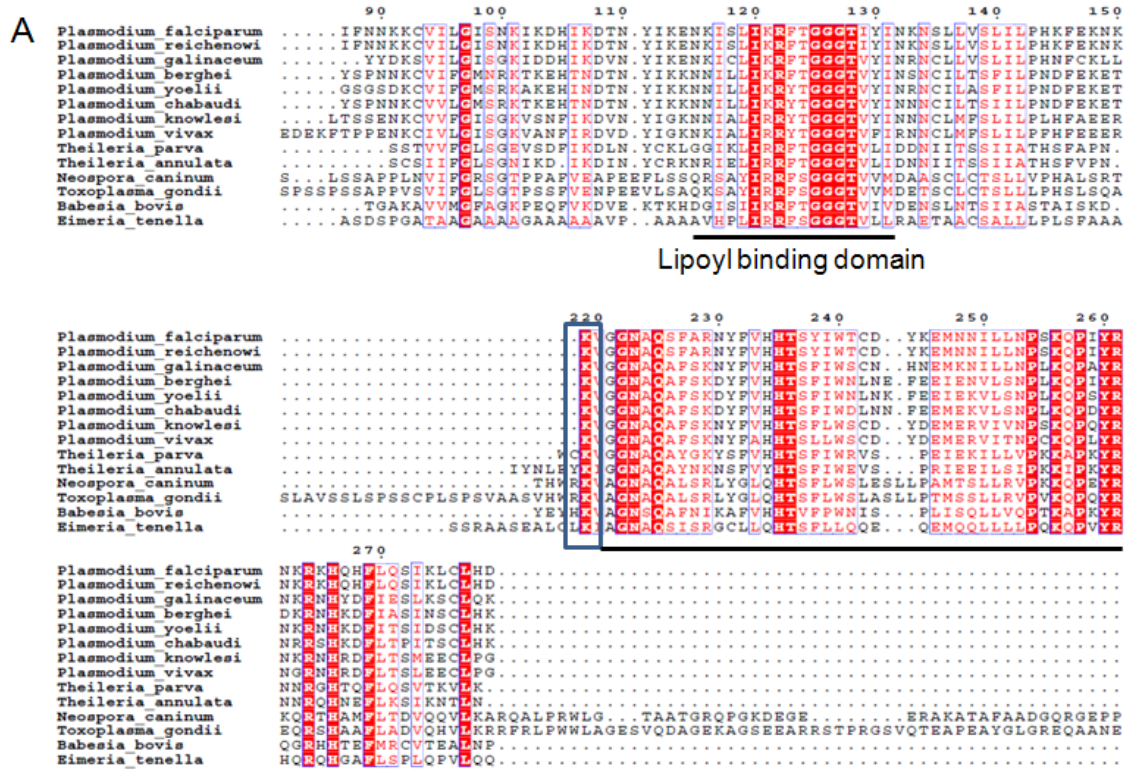


**Figure 6.** LipL2-like enzymes are conserved across many apicomplexan parasite species. A) Sequence alignment of apicomplexan LipL2-like enzymes. The conserved lipoyl binding domain is underlined. Conserved lysine 219 is highlighted by a dark blue box. B) *Plasmodium berghei* LipL2 shows similar activity and specificity to *Pf*LipL2. *Pb*LipL2 catalyzes the lipoyltransferase reaction for substrates *Pf*BCDH<sub>LD</sub> and *Pf*KDH<sub>LD</sub>, but not for the *Pf*H-protein. These reactions were performed in TCEP containing conditions.



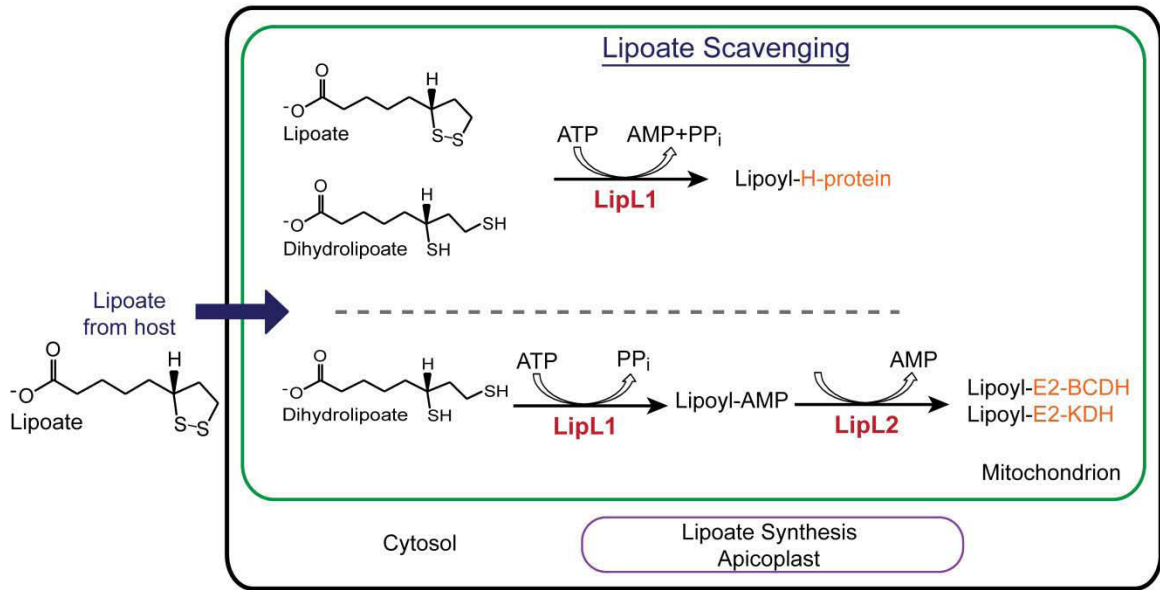


**Figure 7.** Updated scheme of mitochondrial lipoylate metabolism. Two routes exist to lipoylate the different substrates in the parasite mitochondrion. LipL1 is sufficient to lipoylate the H-protein in a ligation reaction using both lipoate and dihydrolipoate. LipL1 possesses a second function as lipoate activating enzyme to generate the conjugate, lipoyl-AMP. Lipoyl-AMP is used by a second enzyme, LipL2 which functions as a *N*-lysine lipoyltransferase to specifically lipoylate the BCDH and KDH.

### Scavenging Pathway

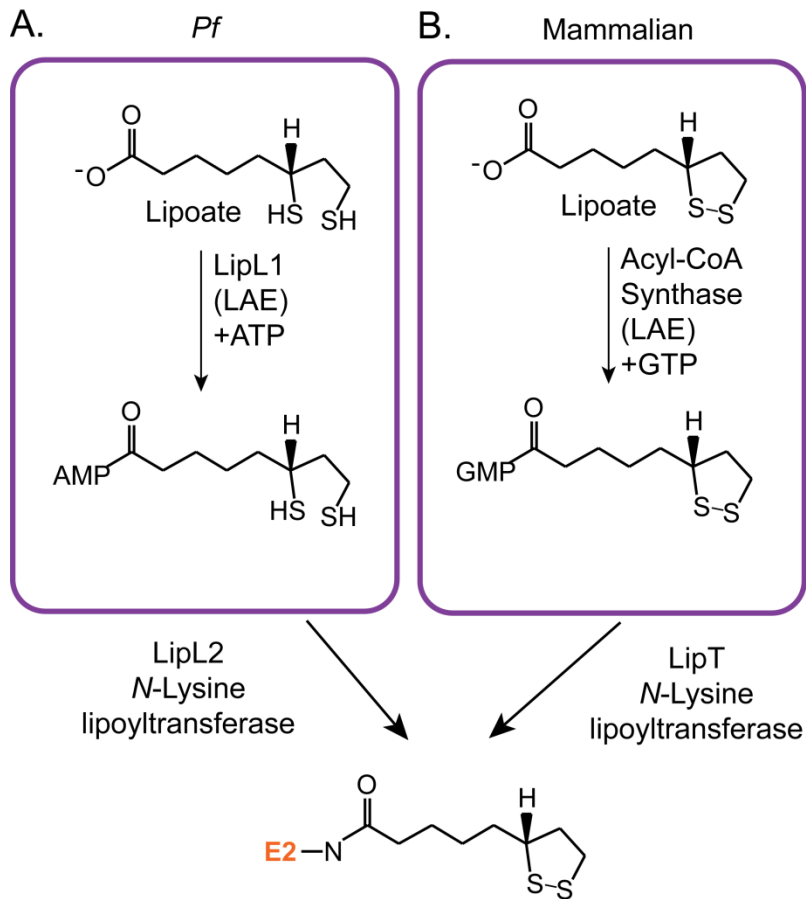


**Figure 8.** Comparison of parasite and mammalian lipoyl scavenging mechanisms. A) Dihydrolipoate is activated by LipL1, acting as a lipoyl activating enzyme (LAE) through an ATP dependent reaction. The formed dihydrolipoyl-AMP is taken by LipL2 which functions as a *N*-lysine lipoyl transferase to lipoylate the BCDH and KDH. B) In mammals, a lipoyl activating enzyme (identified to be a medium chain acyl-CoA synthase) catalyzes the GTP dependent activation of lipoyl. The formed conjugate, lipoyl-GMP, is taken by LipT which also functions as *N*-lysine lipoyl transferase to lipoylate all available substrates.

**Table 1.** Primers and plasmids used in this study.

Plasmid	Primer name	Primer sequence
pMALcHT-LipL1 <sub>K160A</sub>	LipL1K160A.fwd	<u>GAAACGATATTACAGTAAATGATCAAGCATG TTCAGGTTCTGCTTTTAAAAAAA</u>
	LipL1K160A.rev	<u>TTTTTTTAAAAGCAGAACCTGAACATGCTTGATCATTACTGTAATATCGTTTC</u>
pMALcHT-LipL2 <sub>C93A</sub>	LipL2C93A.fwd	<u>GTATCTTTAACAACAAGAAAGCTGTCATTCTGGGTATCAG</u>
	LipL2C93A.rev	<u>CTGATACCCAGAATGACAGCTTCTTGTTGTTAAAGATAC</u>
pMALcHT-LipL2 <sub>C276A</sub>	LipL2C276A.fwd	<u>CTTCAAAGCATAAAAAGCTGGCTCTTCATGATGATATTCAC</u>
	LipL2C276A.rev	<u>GTGAATATCATCATGAAGAGCCAGTTTTATGCTTTGAAG</u>
pMALcHT-LipL2 <sub>K219A</sub>	LipL2K219A.fwd	<u>GAACATAACAAAAACATAATCTGAAAAGCAGTCGGCGGTAACGCACAG</u>
	LipL2K219A.rev	<u>CTGTGCGTTACCGCCGACTGCTTTCAGGATTATGTTTTTGTATGTTTC</u>
pMALcHT-PbLipL2	PbLipL2.fwd	<u>GGTGGTGAATTC</u> <i>ATGGTGAAAAATGTAATGAAAAAATAGTTGG</i>
	PbLipL2.rev	<u>GGTGGTGTGAC</u> <i>TTAGTTAATAATAAAAAGAGTAAAAATTGAAAAAGGATTC</i>

The annealing portions of these sequences are underlined, endonuclease sites are marked by boldface type, and italics marks relevant start and stop codons.

**Table 2.** Changes in temperature of LipL1 in the presence of different ligands and reducing conditions as measured by thermal shift assay.

<b>Ligand</b>	<b>---</b>	<b>DTT</b>	<b>TCEP</b>
<b>LA-AMP</b>	6°C	3.8°C	0.1°C
<b>LA</b>	4.2°C	3.2°C	0°C
<b>6,8-diClO</b>	0.1°C	0.2°C	0.3°C

The thermal shift assay can help to calculate binding affinity of ligands to LipL1 in the presence or absence of reducing agents. The melting temperature of LipL1 is altered by binding of ligands that stabilize the protein. The increase in melting temperature can be correlated to the binding affinity as discussed in Chapter 3.<sup>24</sup> Oxidized lipoyl-AMP (LA-AMP) and lipoate (LA) show a higher melting temperature difference, with respect to the protein with no ligand, than reduced LA-AMP and LA. Based on this analysis, it appears that reduced LA and reduced LA-AMP bind poorly to LipL1, as does the reduced state analog 6,8-diClO.

**Table 3.** Sequence identity between known lipoate attachment enzymes.

	<i>PfLipL1</i>	<i>PfLipL2</i>	<i>PbLipL2</i>	<i>EcLplA</i>	<i>BtLipT</i>
<i>PfLipL1</i>	100%	21%	21%	29%	26%
<i>PfLipL2</i>	---	100%	44%	13%	15%

*Plasmodium falciparum* (*Pf*); *Plasmodium berghei* (*Pb*); *Escherichia coli* (*Ec*) lipoate ligase A; *Bos taurus* (*Bt*) N-lysine lipoyltransferase.

## **Chapter 6**

### **Conclusions**

During this work I have described human pathogens that affect millions of people, causing significant morbidity. My work focused on two Apicomplexan parasites: *Toxoplasma gondii* and *Plasmodium falciparum* (Pf). I made use of biochemical and biophysical methods to better understand fatty acid metabolic pathways that are essential for the survival of these parasites.

The first part of my work is a component of a multi-lab collaboration that has focused on optimizing the potency and drug-like properties of triclosan: a known biocide that targets the last step of Fatty Acid Synthesis type II (FAS-II) of *Toxoplasma gondii* with high specificity.<sup>1,2</sup> Several chemical modifications have been made to the rings of triclosan to make the molecule more “druggable”.<sup>3,4</sup> I have designed an assay to calculate inhibition and IC<sub>50</sub> values of triclosan and analogues in a 96-well plate using a plate reader.<sup>3-5</sup> This assay allowed us to compare the specificity of the analogues relative to triclosan and served as a guide for further modifications generated by our medicinal chemistry collaborators. For potent compounds, however, the enzymatic activity assay was not sensitive enough to discriminate between compounds. Our assay requires a final concentration of TgENR of 5 nM in order to achieve a robust signal to noise ratio. Thus, we will never be able to measure an IC<sub>50</sub> value of less than 2.5 nM.

To address the lack of sensitivity of the enzymatic assay, I developed a thermal shift assay<sup>6,7</sup> to calculate the binding affinity of the compounds to the enzyme.<sup>5</sup> In this assay we determine the melting temperature of the enzyme with or without ligands.<sup>5</sup> The melting temperature can be correlated to the relative binding affinity of the ligand to the enzyme. The assay has a great dynamic range, allowing for binding affinity calculations from millimolar to femtomolar values.<sup>5</sup> This allowed us to better discriminate between

potent compounds and added a second method to help decide what compounds are promising for further optimization. This assay also helped us to determine the mode of action of the compounds.<sup>5</sup> ENR enzymes have two binding sites, one for the cofactor NADH and one for the acyl-ACP (or acyl-CoA) species. Triclosan is known to occupy the acyl binding site of ENR enzymes, however, it does not bind to the enzyme alone. Instead, triclosan forms a ternary complex with the enzyme and a byproduct of catalysis, NAD<sup>+</sup>.<sup>5,8</sup> I tested whether the different analogues had a similar binding mode of action as triclosan does, and found that all compounds bind to the enzyme primarily in the presence of NAD<sup>+</sup>. I was able to measure the binding of one compound to *Tg*ENR in the absence of NAD<sup>+</sup> and found that the K<sub>d</sub> was too high to be physiologically relevant (0.8 mM). Furthermore, I found that the compounds appear to bind tighter to the enzyme as the concentration of NAD<sup>+</sup> increases.<sup>5</sup> The strong dependence on cofactor concentration could provide an explanation for why compounds that bind to *Tg*ENR very tightly do not perform very well in parasite growth inhibition experiments. If NAD(H) levels tend to be low in the apicoplast organelle, it would make it hard for triclosan or any analogue sharing its mechanism of action to inhibit the enzyme *in vivo* and reduce parasite growth.

The second and main part of my work focused on understanding lipoic acid metabolism in *Pf*. Lipoic acid or lipoate is an eight carbon fatty acid with sulfur atoms at positions 6 and 8. Lipoate is an essential cofactor, attached to a specific lysine of lipoate requiring enzymes.<sup>9</sup> From previous studies I knew that two organelles required lipoate in malaria parasites: the apicoplast and the mitochondrion.<sup>10,11</sup> These organelles are referred to in the singular since each parasite contains one apicoplast and one mitochondrion. The apicoplast relies on lipoate biosynthesis and contains only one enzyme that requires



lipoate, pyruvate dehydrogenase (PDH).<sup>12</sup> The PDH function is to generate acetyl-CoA, which feeds into FAS- II to elongate fatty acids.<sup>12, 13</sup> This is true for both *Plasmodium* spp. and *Toxoplasma gondii*.<sup>12, 14</sup> But contrary to the essentiality of these processes in *T. gondii*, both PDH and FAS-II are only essential in *Pf* liver stages; therefore I did not focus my work on lipoate biosynthesis.<sup>12, 15, 16</sup>

Contrary to the apicoplast, the mitochondrion relies on lipoate scavenged from the host.<sup>10</sup> These two pathways are non-redundant. My work focused on understanding the mechanism of action and specificity of two putative lipoate ligases involved in lipoate scavenging in the mitochondrion. I determined that after lipoate is trafficked to the mitochondrion, a known lipoate ligase (LipL1) can activate the cofactor through an ATP-dependent reaction to form lipoyl-AMP. Depending on the redox state of lipoate, oxidized or reduced (lipoate vs. dihydrolipoate, respectively), LipL1 can either only lipoylate the H-protein or transfer lipoyl-AMP to LipL2 in a concerted mechanism to lipoylate the BCDH and KDH. I determined that two routes exist in the mitochondrion for the lipoylation of the substrates: lipoate is used solely to lipoylate the H-protein; dihydrolipoate can be used to lipoylate all substrates. LipL2 is a second predicted lipoate ligase located in the mitochondrion, but it does not function as a ligase. Instead, it acts as an *N*-lysine lipoyltransferase, specifically against the BCDH and KDH. I also found that this enzyme belongs to a new family of lipoate attachment enzymes conserved throughout most species of the phylum Apicomplexa.

Lipoate scavenging is essential for the survival of malaria parasites in both blood and liver stages. Previous studies showed growth inhibition by treating parasites with a lipoate analog, 8-bromooctanoate (8BrO).<sup>10</sup> I found that the mode of action of this

analog is by irreversible modification of the mitochondrial substrates. Thus, 8BrO is a substrate of the lipoylation enzymes and an inhibitor of the mitochondrial enzymes to which it is attached. I also found the same to be true for a dihydrolipoate analog, 6,8-dichlorooctanoate (6,8-diClO), where we see modification of the protein substrates by Western blot in conjunction with parasite growth inhibition. Perhaps *in vivo*, the need for oxidized or reduced lipoate is a metabolic requirement for the parasite. Still, several questions remain unanswered.

How does LipL1 discriminate between oxidized and reduced lipoate? One possibility is that reduced dihydrolipoate and dihydrolipoyl-AMP binds loosely to LipL1 and the conjugate is more readily transferred to LipL2, as discussed in Chapter 5. A second possibility is that there is a conformational change in LipL1 upon binding or formation of dihydrolipoyl-AMP that allows LipL1 to interact with LipL2. Without this conformational change, LipL1 bound to oxidized lipoyl-AMP is only able to interact with the H-protein. It would be interesting to obtain an X-ray crystal structure of LipL1 in the presence of both lipoyl-AMP and 6,8-dichlorooctyl-AMP, which would give an insight to the mode of action of LipL1. I attempted to crystallize LipL1, but it presented challenges during purification and crystals that did not diffract beyond 4Å (see appendix).

I have mentioned that dihydrolipoate (reduced lipoate) is a requirement for the lipoylation of the BCDH and KDH. This raises the question of how is lipoate reduced after being scavenged to the mitochondrion? One possibility is that both lipoate and dihydrolipoate exist in the red blood cell and the parasite can scavenge both. It is more likely that the parasite scavenges only oxidized lipoate, since it has to cross several membranes and lipoate is more hydrophobic. In order to reduce lipoate the

mitochondrion environment could be reducing enough to reduce lipoate ( $<-.32\text{mV}$ ).<sup>17</sup> We may be able to demonstrate this by using a genetically modified green fluorescence protein (roGFP) that is sensitive to redox potential.<sup>18, 19</sup> This roGFP has been modified to have two cysteines near where the chromophore forms, changing the spectroscopic properties of the chromophore depending on the redox environment.<sup>18, 19</sup> The two cysteines can form disulfide bonds in more oxidizing environments or break the disulfide in more reducing environments. One can measure the emission ( $\lambda = 508 \text{ nM}$ ) of roGFP by exciting at two different wavelengths ( $\lambda = 400 \text{ nM}$  and  $475 \text{ nM}$ ). The emission ratio after excitation at  $400 \text{ nM}$  or  $475 \text{ nM}$  can be correlated to how reducing the environment is. I ordered this plasmid and in collaboration with Krista Matthews, we designed a transfection plasmid encoding roGFP with an amino-terminal mitochondrial transit peptide. Parasites transfected with this plasmid have fluorescent mitochondria, demonstrating that roGFP can be produced and trafficked to the parasite mitochondrion (work was done by a Krista Matthews). The next step is to calibrate the relative fluorescence under reducing and oxidizing conditions in order to make redox measurements. This work is still in progress.

Another possibility, as discussed in Chapter 4, is that the dihydrolipoamide (E3 subunit of lipoylated complexes) could reduce free lipoate.<sup>20, 21</sup> I cloned and purified the mitochondrial *Pf*E3 subunit and tested its activity on free lipoate. I found that the E3 can catalyze the reverse reaction, lipoate to dihydrolipoate using NADH (**Figure 1**). We can monitor this reaction at  $\lambda = 340 \text{ nm}$  and calculate  $k_{\text{cat}}$  and  $K_{\text{m}}$  for lipoate (**Figure 2**). The  $k_{\text{cat}}$  of  $288/\text{s}$  and  $k_{\text{m}}$  of  $1.8 \text{ mM}$ , similar to published values for E3 using lipoamide.<sup>22</sup>

While this is not conclusive evidence of what happens in the parasite, these *in vitro* data support the hypothesis that this process could happen in the mitochondrion.

The discovery that there are two routes for mitochondrial lipoylation in malaria parasites raises the question of why the mitochondrial substrates require different lipoylation mechanisms. To address this question, it is important to understand what roles the three mitochondrial substrates play in parasite biology. As mentioned in Chapter 4, only the KDH has been shown to have its canonical role as part of the citric acid cycle. Knockouts of the E1 subunit of the KDH were viable, showing that this role is not essential for parasite survival during the blood stage. The roles of the BCDH and H-protein are harder to discern because the parasite genome does not appear to encode partner enzymes necessary for their function. A possibility for all substrates is that they have moonlighting activity. There are several ways to approach this question. First, the genes encoding the different substrates could be knocked out in the parasite. This is a challenging kind of experiment to conduct in *Pf* since double crossover homologous recombination is a rare event and difficult to select for. An alternative approach is to use single crossover homologous recombination to attempt gene disruptions in the parasite and these attempts are currently ongoing. For technical reasons, gene deletion is more feasible in the rodent parasite *Plasmodium berghei*. An added value in doing gene knock outs in *P. berghei* is that the resulting strains can be examined in all life cycle stages (mosquito, liver and blood stage) using mice. This kind of experiment will address the essentiality of the lipoylated substrates and reveal lifecycle phenotypes for those that can be deleted. If the knock outs are viable one could perform metabolomics studies to look for aberrant product accumulation as done by other groups.<sup>23, 24</sup>

Last, *in vitro* experiments could be designed to address the question of whether the E2-KDH (or other lipoylated substrates) along with the E3 subunit can serve as the thioredoxin reductase as mentioned in Chapter 4. I have purified the E3 subunit and showed that it is active. I have *E. coli* clones containing expression plasmids of the E2-BCDH, E2-KDH and H-protein which will produce these proteins with an amino-terminal GST tag. These substrates can be expressed and purified in the holo form and tested to determine their roles as a reductase as done for other proteins.<sup>25-27</sup> The thioredoxin reductase dually localized to the mitochondrion and the cytosol, did not recognize downstream enzymes involved in the mitochondrial thioredoxin system in *in vitro* experiments.<sup>25</sup> It would be interesting to address whether the E3 along with a lipoylated substrate could act as such a thioredoxin reductase.

## References

1. Remington, J. S.; McLeod, R.; Thulliez, P.; Desmonts, G. *Toxoplasmosis*. 7th ed.; Elsevier Saunders: Philadelphia, 2011.
2. McLeod, R.; Muench, S. P.; Rafferty, J. B.; Kyle, D. E.; Mui, E. J.; Kirisits, M. J.; Mack, D. G.; Roberts, C. W.; Samuel, B. U.; Lyons, R. E.; Dorris, M.; Milhous, W. K.; Rice, D. W. Triclosan inhibits the growth of Plasmodium falciparum and Toxoplasma gondii by inhibition of apicomplexan Fab I. *Int J Parasitol* **2001**, 31, 109-13.
3. Cheng, G.; Muench, S. P.; Zhou, Y.; Afanador, G. A.; Mui, E. J.; Fomovska, A.; Lai, B. S.; Prigge, S. T.; Woods, S.; Roberts, C. W.; Hickman, M. R.; Lee, P. J.; Leed, S. E.; Auschwitz, J. M.; Rice, D. W.; McLeod, R. Design, synthesis, and biological activity

of diaryl ether inhibitors of *Toxoplasma gondii* enoyl reductase. *Bioorg Med Chem Lett* **2013**, 23, 2035-43.

4. Stec, J.; Fomovska, A.; Afanador, G. A.; Muench, S. P.; Zhou, Y.; Lai, B. S.; El Bissati, K.; Hickman, M. R.; Lee, P. J.; Leed, S. E.; Auschwitz, J. M.; Sommerville, C.; Woods, S.; Roberts, C. W.; Rice, D.; Prigge, S. T.; McLeod, R.; Kozikowski, A. P. Modification of triclosan scaffold in search of improved inhibitors for enoyl-acyl carrier protein (ACP) reductase in *Toxoplasma gondii*. *ChemMedChem* **2013**, 8, 1138-60.
5. Afanador, G. A.; Muench, S. P.; McPhillie, M.; Fomovska, A.; Schon, A.; Zhou, Y.; Cheng, G.; Stec, J.; Freundlich, J. S.; Shieh, H. M.; Anderson, J. W.; Jacobus, D. P.; Fidock, D. A.; Kozikowski, A. P.; Fishwick, C. W.; Rice, D. W.; Freire, E.; McLeod, R.; Prigge, S. T. Discrimination of Potent Inhibitors of *Toxoplasma gondii* Enoyl-Acyl Carrier Protein Reductase by a Thermal Shift Assay. *Biochemistry* **2013**, 52, 9155-66.
6. Lo, M. C.; Aulabaugh, A.; Jin, G.; Cowling, R.; Bard, J.; Malamas, M.; Ellestad, G. Evaluation of fluorescence-based thermal shift assays for hit identification in drug discovery. *Anal Biochem* **2004**, 332, 153-9.
7. Pantoliano, M. W.; Petrella, E. C.; Kwasnoski, J. D.; Lobanov, V. S.; Myslik, J.; Graf, E.; Carver, T.; Asel, E.; Springer, B. A.; Lane, P.; Salemme, F. R. High-density miniaturized thermal shift assays as a general strategy for drug discovery. *J Biomol Screen* **2001**, 6, 429-40.
8. Muench, S. P.; Prigge, S. T.; McLeod, R.; Rafferty, J. B.; Kirisits, M. J.; Roberts, C. W.; Mui, E. J.; Rice, D. W. Studies of *Toxoplasma gondii* and *Plasmodium falciparum* enoyl acyl carrier protein reductase and implications for the development of antiparasitic agents. *Acta Crystallogr D Biol Crystallogr* **2007**, 63, 328-38.

9. Spalding, M. D.; Prigge, S. T. Lipoic acid metabolism in microbial pathogens. *Microbiol Mol Biol Rev* **2010**, 74, 200-28.
10. Allary, M.; Lu, J. Z.; Zhu, L.; Prigge, S. T. Scavenging of the cofactor lipoate is essential for the survival of the malaria parasite *Plasmodium falciparum*. *Mol Microbiol* **2007**, 63, 1331-44.
11. Storm, J.; Muller, S. Lipoic acid metabolism of *Plasmodium*--a suitable drug target. *Curr Pharm Des* **2012**, 18, 3480-9.
12. Pei, Y.; Tarun, A. S.; Vaughan, A. M.; Herman, R. W.; Soliman, J. M.; Erickson-Wayman, A.; Kappe, S. H. *Plasmodium* pyruvate dehydrogenase activity is only essential for the parasite's progression from liver infection to blood infection. *Mol Microbiol* **2010**, 75, 957-71.
13. Prigge, S. T.; He, X.; Gerena, L.; Waters, N. C.; Reynolds, K. A. The initiating steps of a type II fatty acid synthase in *Plasmodium falciparum* are catalyzed by pfACP, pfMCAT, and pfKASIII. *Biochemistry* **2003**, 42, 1160-9.
14. Mazumdar, J.; E, H. W.; Masek, K.; C, A. H.; Striepen, B. Apicoplast fatty acid synthesis is essential for organelle biogenesis and parasite survival in *Toxoplasma gondii*. *Proc Natl Acad Sci U S A* **2006**, 103, 13192-7.
15. Yu, M.; Kumar, T. R.; Nkrumah, L. J.; Coppi, A.; Retzlaff, S.; Li, C. D.; Kelly, B. J.; Moura, P. A.; Lakshmanan, V.; Freundlich, J. S.; Valderramos, J. C.; Vilcheze, C.; Siedner, M.; Tsai, J. H.; Falkard, B.; Sidhu, A. B.; Purcell, L. A.; Gratraud, P.; Kremer, L.; Waters, A. P.; Schiehser, G.; Jacobus, D. P.; Janse, C. J.; Ager, A.; Jacobs, W. R., Jr.; Sacchettini, J. C.; Heussler, V.; Sinnis, P.; Fidock, D. A. The fatty acid biosynthesis

enzyme FabI plays a key role in the development of liver-stage malarial parasites. *Cell Host Microbe* **2008**, 4, 567-78.

16. Vaughan, A. M.; O'Neill, M. T.; Tarun, A. S.; Camargo, N.; Phuong, T. M.; Aly, A. S.; Cowman, A. F.; Kappe, S. H. Type II fatty acid synthesis is essential only for malaria parasite late liver stage development. *Cell Microbiol* **2009**, 11, 506-20.

17. Jocelyn, P. C. The standard redox potential of cysteine-cystine from the thiol-disulphide exchange reaction with glutathione and lipoic acid. *Eur J Biochem* **1967**, 2, 327-31.

18. Hanson, G. T.; Aggeler, R.; Oglesbee, D.; Cannon, M.; Capaldi, R. A.; Tsien, R. Y.; Remington, S. J. Investigating mitochondrial redox potential with redox-sensitive green fluorescent protein indicators. *J Biol Chem* **2004**, 279, 13044-53.

19. Dooley, C. T.; Dore, T. M.; Hanson, G. T.; Jackson, W. C.; Remington, S. J.; Tsien, R. Y. Imaging dynamic redox changes in mammalian cells with green fluorescent protein indicators. *J Biol Chem* **2004**, 279, 22284-93.

20. Constantinescu, A.; Pick, U.; Handelman, G. J.; Haramaki, N.; Han, D.; Podda, M.; Tritschler, H. J.; Packer, L. Reduction and transport of lipoic acid by human erythrocytes. *Biochem Pharmacol* **1995**, 50, 253-61.

21. Haramaki, N.; Han, D.; Handelman, G. J.; Tritschler, H. J.; Packer, L. Cytosolic and mitochondrial systems for NADH- and NADPH-dependent reduction of alpha-lipoic acid. *Free Radic Biol Med* **1997**, 22, 535-42.

22. McMillan, P. J.; Stimmler, L. M.; Foth, B. J.; McFadden, G. I.; Muller, S. The human malaria parasite *Plasmodium falciparum* possesses two distinct dihydrolipoamide dehydrogenases. *Mol Microbiol* **2005**, 55, 27-38.



23. Sheiner, L.; Vaidya, A. B.; McFadden, G. I. The metabolic roles of the endosymbiotic organelles of *Toxoplasma* and *Plasmodium* spp. *Curr Opin Microbiol* **2013**, 16, 452-8.
24. Cobbold, S. A.; Vaughan, A. M.; Lewis, I. A.; Painter, H. J.; Camargo, N.; Perlman, D. H.; Fishbaugher, M.; Healer, J.; Cowman, A. F.; Kappe, S. H.; Llinas, M. Kinetic flux profiling elucidates two independent acetyl-CoA biosynthetic pathways in *Plasmodium falciparum*. *J Biol Chem* **2013**.
25. Nickel, C.; Rahlfs, S.; Deponete, M.; Koncarevic, S.; Becker, K. Thioredoxin networks in the malarial parasite *Plasmodium falciparum*. *Antioxid Redox Signal* **2006**, 8, 1227-39.
26. Jortzik, E.; Becker, K. Thioredoxin and glutathione systems in *Plasmodium falciparum*. *Int J Med Microbiol* **2012**, 302, 187-94.
27. Kehr, S.; Sturm, N.; Rahlfs, S.; Przyborski, J. M.; Becker, K. Compartmentation of redox metabolism in malaria parasites. *PLoS Pathog* **2010**, 6, e1001242.

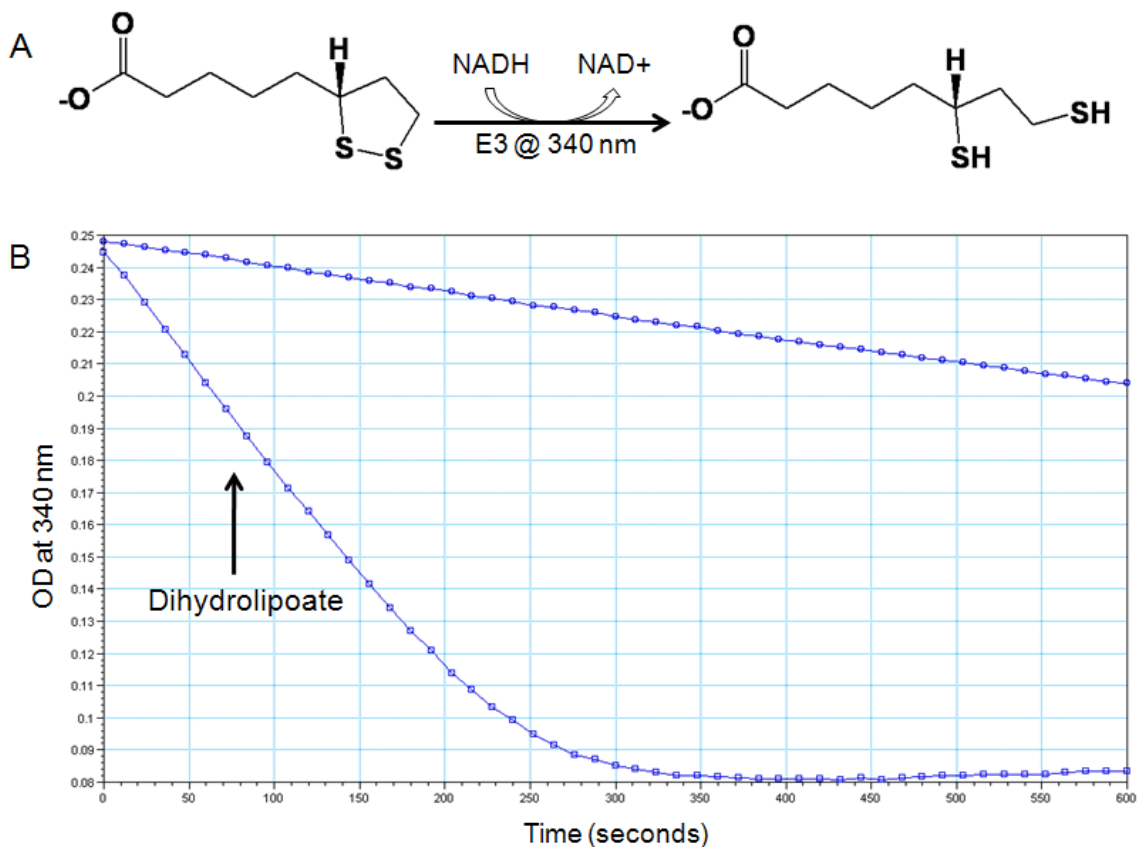


**Figure 1.** The dihydrolipoamide dehydrogenase (E3 subunit of lipoylated complexes) can catalyze the re-oxidation of the lipoyl moiety using  $\text{NAD}^+$ . A) A possible activity for this enzyme is that it could use free lipoate and reduce it, as shown for other systems.<sup>20, 21</sup> We can monitor the consumption of NADH by the E3 subunit in the presence of lipoate, which would mean that dihydrolipoate is being formed. B) An output from the SpectraMax M2 plate reader showing the consumption of NADH over time and formation of dihydrolipoate.

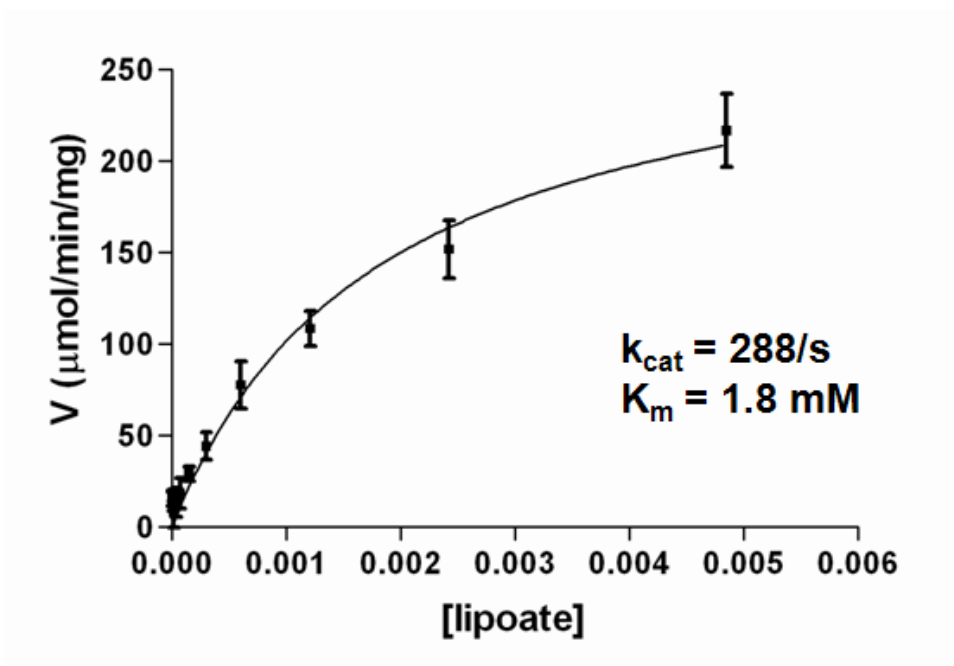


**Figure 2.** Kinetic analysis of E3 subunit using lipoate as a substrate. Initial velocity data were fit to the Michaelis-Menten equation using GraphPad Prism Software.

## **Appendix**

### **Crystallization Attempts of *Plasmodium falciparum* Lipoate Ligase 1**

*Plasmodium falciparum* lipoate ligase 1 (LipL1) appears to be the only lipoate ligase in the malaria parasite. Furthermore, it has two roles: as lipoate ligase only against the H-protein and as lipoate activating enzyme generating the intermediate lipoyl-AMP, which is subsequently used by *Plasmodium falciparum* lipoate ligase 2 (LipL2). These roles have distinct characteristics previously discussed, but one striking difference is the sensitivity to the lipoate redox state. When lipoate is oxidized or in the closed ring form, the H-protein is the only substrate lipoylated; whereas when lipoate is reduced or in the open ring form all substrates are lipoylated. Our data suggest that LipL1, upon activation of lipoate under different redox states, defines what substrates can be lipoylated. For this reason, among others, LipL1 X-ray crystal structure would be very informative to better understand mitochondrial lipoylation.

LipL1 is easily expressed and purified in *E. coli* with high yield. One challenge during purification of full-length LipL1 (fLipL1) is that it is cleaved during purification (**Figure 1A**). LipL1 contains a low complexity region, which is not conserved in other described lipoate ligases (**Figure 1B**). This region is found in other *Plasmodium* species, but with no conservation of sequence or size. Amino acid sequencing revealed that cleavage initially occurs between Lys264 and Glu265, which is found in this low complexity region. Mutation of this residue (K264A) did not prevent degradation during purification (**Figure 1C**). It appears that degradation occurs during expression in *E. coli* and it continues during purification. Use of protease inhibitors did not satisfactorily prevent degradation of LipL1. Still, LipL1 can be crystallized and the crystals diffract to low resolution (**Figure 2**). Crystallization of LipL1 was not always reproducible and crystals diffraction was not suitable for data collection. Taking all of this together, I decided to

create different mutants where I would reduce the size of the “low complexity” region and test the mutant LipL1 activity in JEG3 and in *in vitro* assays.

Four different mutants were made, deleting 11, 21, 31 or 37 residues from the low complexity region ( **Figure 3A**). Although all four deletion constructs removed the K264/E265 cut site, constructs d11LipL1, d21LipL1 and d31LipL1 still suffered from significant degradation. The best behaved construct was d37LipL1, which was generated by removing almost the entire 47 residue low complexity region. d37LipL1 still shows some minor degradation, but is far more stable than the full length construct (**Figure 3B**), allowing crystallization being more reproducible and yielding crystals that diffract close to 4 Å, with hexagonal unit cell. The truncated loop in d37LipL1 is not essential for lipoylate ligase activity. This construct lipoylates *E. coli* substrates when expressed in a lipoylation deficient *E. coli* cell line (**Figure 3C**) and lipoylates the H-protein in *in vitro* assays (**Figure 3D**). The following are conditions that were optimized to express, purify and crystallize LipL1.

1. flLipL1 (pMAL-LipL1) was mutated to generate pMAL-d11LipL1, pMAL-d21LipL1 and pMAL-d31LipL1 using the primers in **Table 1**. pMAL-d31LipL1 was mutated to generate pMAL-d37LipL1 using the primers in **Table 1**.
2. pMAL-d37 was transformed into BL21-Star (DE3) cells (Invitrogen) containing the pRIL plasmid isolated from BL21-CodonPlus-RIL cells (Agilent) and plasmid pRL586 encoding the Tobacco Etch Virus (TEV) protease.
3. 2L of LB media were inoculated with 20 mL of overnight culture containing 1% glucose and the antibiotics ampicillin, kanamycin and chloramphenicol.

The cells were grown to an OD<sub>600</sub> around 1.0-1.2. The temperature was dropped to 27°C and protein production was induced with 0.4 mM IPTG for 5 hours, and then the cultures were pelleted and stored at -20°C.

4. Cultures were lysed as described for fLipL1 (Chapter 4) and purified by metal chelate affinity, cation exchange, and gel filtration. One major consideration was to run all columns in the same day to avoid further degradation.

a. All buffers contained 20 mM HEPES at pH 7.5.

i. Buffers for the metal chelate affinity column (HiTrap Chelating HP, GE Healthcare) contained 100 mM NaCl. Impurities were eluted with two 10 mL steps containing 10 mM and 30 mM imidazole followed by elution with a gradient to 500 mM imidazole in 50 mL. LipL1 typically eluted around 160 mM imidazole.

ii. Elution fractions from the chelating column were loaded onto 2x 53 mL desalting columns (HiPrep Desalting 26/10, GE Healthcare) connected in tandem with a cation exchange column (HiTrap SP FF, GE Healthcare). After 65 mL, the desalting columns were disconnected and proteins were eluted from the cation exchange column with a gradient to 1 M NaCl in 50 mL. LipL1 typically eluted around 200 mM NaCl.

iii. Elution fractions from the cation exchange column were concentrated to a volume of 1-2 mL and loaded onto a gel

filtration column (S100 26/60, GE Healthcare). LipL1 typically eluted around 140 mL.

5. Purified LipL1 protein was concentrated to about 10 mg/mL. The usual yield for 2L of culture was between 15-20 mg.
6. Protein aliquots of 100  $\mu$ L were stored at -80°C.
7. Crystallization attempts were conducted by hanging drop. Two conditions were found for crystallization in the presence of two different ligands.
  - a. Ligands
    - i. 8-bromooctanoate
    - ii. 6,8-dichlorooctanoate
  - b. Conditions
    - i. Sodium Formate (2.6-3.6 M) pH 6.0 and 7.0
    - ii. Sodium Malonate (1.2-1.6 M) pH 7.0 and 7.5
8. The mother liquor contained 500  $\mu$ L of either of the above conditions with or without 3% ethanol or 3% DMSO. Glycerol did not help in crystallization.
9. d37LipL1 was mixed with 2x excess of ligand and excess of  $Mg^{+2}$ . The protein was allowed to bind to the ligand for 5 minutes at room temperature followed by a high speed spin at 4 degrees to remove particulates.
10. 1  $\mu$ L of d37LipL1 was mixed with 1  $\mu$ L of mother liquor and trays were stored at 20°C. Crystal formation was observed after 24 hours. Cold temperature (4°C) did not help in crystallization.
  - a. Micro- and macroseeding did not improve crystal quality.



11. Crystals formed after a few days (3-5 days) were tested for diffraction and typically resulted in 4-8 Å resolution diffraction.

a. Cryo conditions:

i. Crystals formed in Sodium Malonate can be transferred to a drop containing 3.4 M Sodium Malonate.

ii. Crystals formed in Sodium Formate can be transferred to a drop containing 5 M Sodium Formate.

iii. Mother liquor plus 15% or 20% glycerol can also be used.

iv. Ethylene glycol dissolves the crystals.

b. Crystals were flash frozen in either liquid nitrogen to ship to the synchrotron or in the cryo stream at our home source.

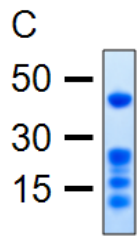
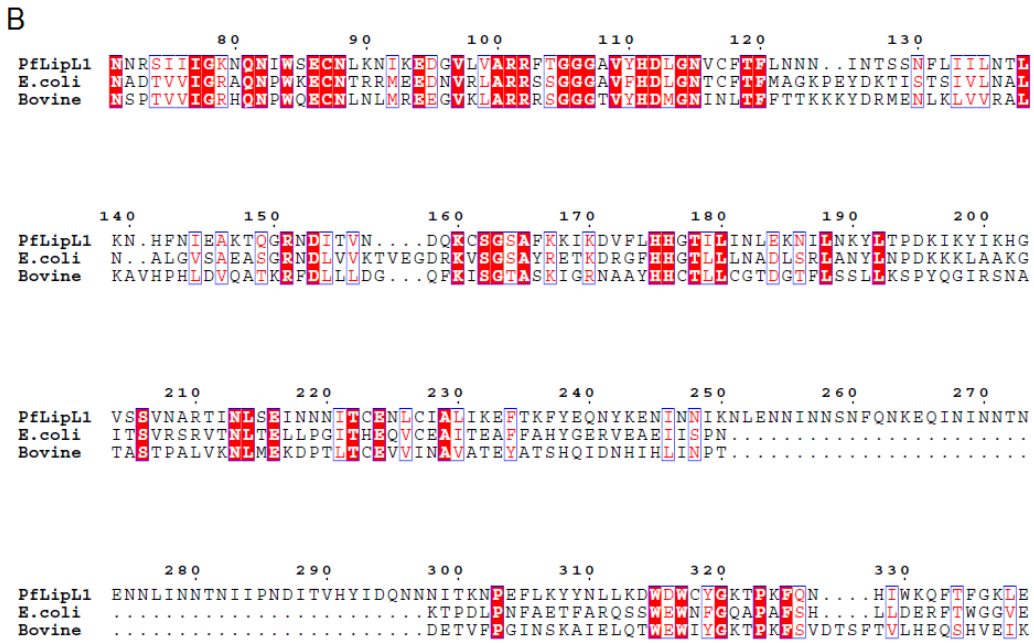
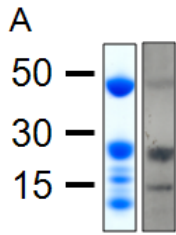


**Figure 1.** Expression and purification of full length LipL1. Full length LipL1 can be expressed and purified with high yield. However, some degradation occurs during purification, making crystallization attempts difficult. A) SDS-PAGE of purified fLipL1 after gel filtration. Western blot analysis of degraded fLipL1, probed with  $\alpha$ -His (antibody recognizes His-tag at N-terminus). B) Sequence alignment of *Pf*LipL1 with *E. coli* ligase and bovine homologues shows that the low complexity region is only present in *Pf*. C) Amino acid sequencing reveals that the primary degradation produce has the amino-terminal sequence EQININ.

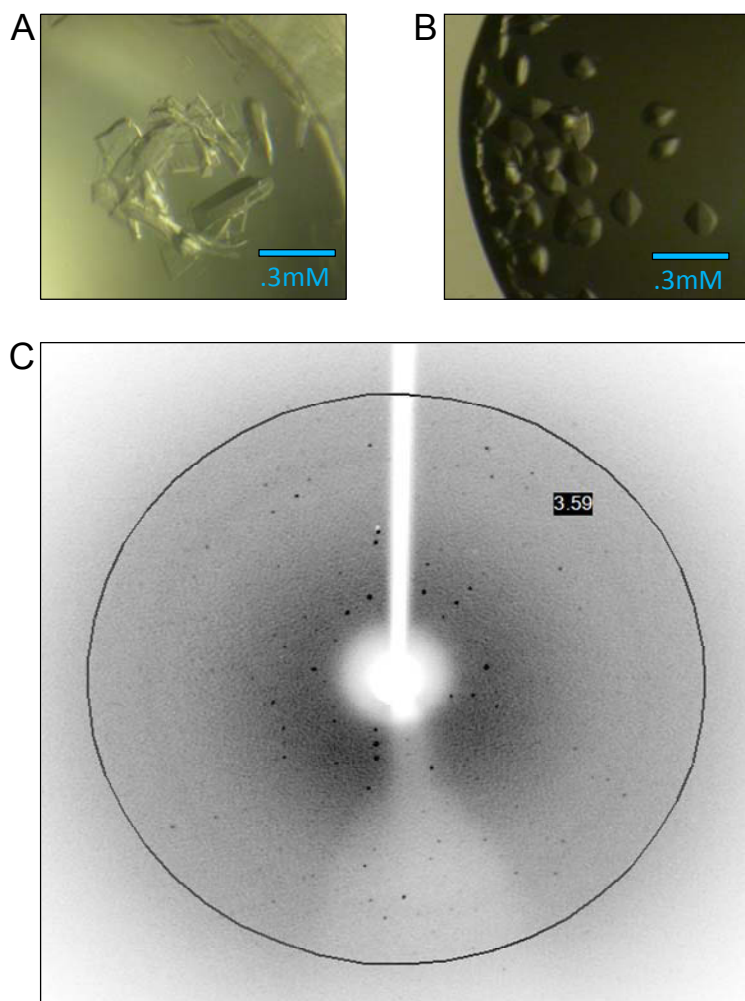


**Figure 2.** Crystallization attempts for fLipL1. In some instances we were able to purify fLipL1 rapidly avoiding major degradation. We found two conditions by which we can obtain crystals, both diffractable. A) Crystals are shown obtained for fLipL1, in the presence of 8-bromooctanoate, with 3.4 M Sodium Formate at pH 6.0. B) Crystals are shown obtained for fLipL1, in the presence of 8-bromooctanoate, with 1.2 M Sodium Malonate at pH 7.0. C) A diffraction pattern of the crystal shown in **Figure 1A**, with a triclinic unit cell.

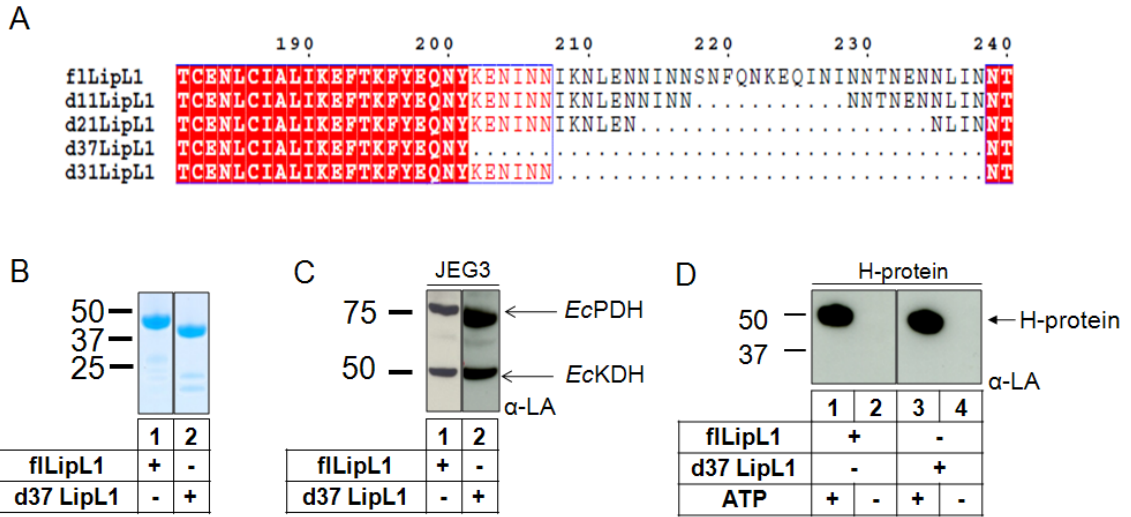


**Figure 3.** d37LipL1 expression and purification attempts. A) Sequence alignment of mutated region in LipL1: d11LipL1, d21LipL1, d31LipL1 and d37LipL1. B) SDS-PAGE of both flLipL1 (left panel) and d37LipL1 (right panel) after gel filtration. d37LipL1 shows minor degradation, but is consistently better behaved than flLipL1. C) Complementation of *E. coli* lipoylation deficient cell line (Chapter 4). Both flLipL1 and d37LipL1 are able to lipoylate endogenous *E. coli* substrates. D) Purified flLipL1 and d37LipL1 are active against the H-protein in an *in vitro* lipoylation assay in an ATP-dependent reaction.

**Table 1.** Primers used for LipL1 mutants construction.

<b>Plasmid</b>	<b>Primer name</b>	<b>Primer sequence</b>
pMAL-d11LipL1	d11LipL1.fwd	TTAGAAAATAATATAAATAATAACAATACAAATGAAAACAACCTTAATAAATAAC
	d11LipL1.rev	GTTATTTATTAAGTTGTTTTTCATTTGTATTGTTATTATTTATATTATTTTCTAA
pMAL-d21LipL1	d21LipL1.fwd	GAAAATATAAATAATATAAAAAATTTAGAAAACAACCTTAATAAATAACACCAAT
	d21LipL1.rev	ATTGGTGTATTATTATTAAGTTGTTTTCTAAATTTTTTATATTATTTATATTTTC
pMAL-d31LipL1	d31LipL1.fwd	CAAAATTATAAAGAAAATATAAATAATAACACCAATATAATACCTAATGATATTACG
	d31LipL1.rev	ATTAGGTATTATATTGGTGTATTATTATATTTTCTTTATAATTTTGTTTCATAAAA
pMAL-d37LipL1	d37LipL1.fwd	TTCACAAAATTTTATGAACAAAATTATAACACCAATATAATACCTAATGAT
	d37LipL1.rev	ATCATTAGGTATTATATTGGTGTATAATTTTGTTTCATAAAAATTTGTGAA

## GUSTAVO A. AFANADOR

### Personal Information

505 W. 28<sup>th</sup> Street  
Baltimore MD 21211  
Mobile: (787) 548-9422  
E-mail: gustavo.afanador@gmail.com

### Profile

Ph.D. student in Molecular Biophysics with focus in metabolism of infectious diseases. Researching essential metabolic pathways for survival of parasites *Plasmodium falciparum* and *Toxoplasma gondii* by using molecular, biochemical and biophysical techniques.

### Education

Ph.D. Molecular Biophysics March 2014  
Johns Hopkins University, School of Medicine

B.S. Industrial Biotechnology 2007  
University of Puerto Rico, Mayagüez Campus

### Research Experience

**2007-Present** Johns Hopkins School of Public Health, Department of Molecular Microbiology and Immunology, Baltimore, MD Dr. Sean Prigge  
“Function and specificity of mitochondrial lipoate attachment enzymes in *Plasmodium falciparum*”  
“Drug screening and affinity measurement against Enoyl-Acyl Carrier Protein Reductase of *Toxoplasma gondii*”

**2005-2007** University of Puerto Rico, Mayagüez Campus, Department of Chemistry, Dr. Juan López-Garriga  
“Over Expression of Hemoglobin I, II and Mutants in *Escherichia coli* from *Lucina pectinata*”

**Spring 2006** Institut National de la Santé et de la Recherche Médicale, Paris, France  
Dr. Michael Marden  
"Kinetic Studies of Hemoblobin II and Mutants from *Lucina pectinata*"

**Summer 2004** Massachusetts Institute of Technology, Department of Chemistry, Dr. JoAnne Stubbe  
“Studies on the *Bacillus subtilis* Formylglycinamide Ribonucleotide Amidotransferase”

## Publications

1. **G. A. Afanador**, K. A. Matthews, J. E. Gisselberg, M. S. Walters, C. Freel-Meyers, S. T. Prigge. Redox-dependent lipoylation of mitochondrial proteins in *Plasmodium falciparum*. *In revision*
2. C. Wilkinson, M. J. McPhillie, Y. Zhou, S. Woods, **G. A. Afanador**, S. Rawson, F. Khaliq, S. T. Prigge, C. W. Roberts, D. W. Rice, R. McLeod, C. W. Fishwick, S. P. Muench. The benziimidazole based drugs show good activity against *T. gondii* against its proposed enoyl reductase enzyme target. *Bioorg. Med. Chem. Lett.* 24, 911-916 (2014)
3. **G. A. Afanador**, S. P. Muench, A. Fomovska, Y. Zhou, M. McPhillie, C. Fishwick, A. Schon, G. Cheng, D. A. Fidock, D. Jacobus, D. W. Rice, E. Freire, R. McLeod, S. T. Prigge. Discrimination of Potent Inhibitors of *Toxoplasma gondii* Enoyl-Acyl Carrier Protein Reductase by Thermal Shift Assay. *Biochemistry.* 52, 9155-9166 (2013)
4. J. Stec\*, A. Fomovska\*, **G. A. Afanador\***, S. P. Muench\*, Y. Zhou\*, B.-S. Lai, K. E. Bissati, M. R. Hickman, P. J. Lee, S. E. Leed, J. M. Auschwitz, C. Sommerville, S. Woods, C. W. Roberts, D. Rice, S. T. Prigge, R. McLeod, A. P. Kozikowski. Modification of Triclosan Scaffold in Search of Improved Inhibitors for Enoyl-Acyl Carrier Protein (ACP) Reductase in *Toxoplasma gondii*. *Chem. Med. Chem.* 8, 1138-1160 (2013).
5. S. P. Muench, J. Stec, Y. Zhou, **G. A. Afanador**, M. J. McPhillie, M. R. Hickman, P. J. Lee, S. E. Leed, J. M. Auschwitz, S. T. Prigge, D. W. Rice, R. McLeod. Development of a triclosan scaffold which allows for adaptations on both the A- and B-ring for transport peptides. *Bioorg. Med. Chem. Lett.* 23, 3551-3555 (2013).
6. G. Cheng\*, S. P. Muench\*, Y. Zhou\*, **G. A. Afanador\***, E. Mui, A. Fomovska, B.-S. Lai, S. T. Prigge, S. Woods, C. W. Roberts, M. R. Hickman, P. J. Lee, S. E. Leed, J. M. Auschwitz, D. W. Rice, R. McLeod. Design, synthesis, and biological activity of diaryl ether inhibitors of *Toxoplasma gondii* enoyl Reductase. *Bioorg. Med. Chem. Lett.* 23, 2035-2043 (2013).
7. F. C. Schrader, S. Glinca, J. M. Sattler, H.-M. Dahse, **G. A. Afanador**, S. T. Prigge, M. Lanzer, A.K. Mueller, G. Klebe and M. Schlitzer. Novel Type II Fatty Acid Biosynthesis (FAS II) Inhibitors as Multistage Antimalarial Agents. *Chem. Med. Chem.* 8, 442-461 (2013).
8. A. Fomovska, Q. Huang, K. E. Bissati, E. J. Mui, W. H. Witola, G. Cheng, Y. Zhou, C. Sommerville, C. W. Roberts, S. Bettis, S. T. Prigge, **G. A. Afanador**, M. R. Hickman, P. J. Lee, S. E. Leed, J. M. Auschwitz, M. Pieroni, J. Stec, S. P. Muench, D. W. Rice, A. P. Kozikowski, R. McLeod, Novel *N*-Benzoyl-2-Hydroxybenzamide Disrupts Unique Parasite Secretory Pathway. *Antimicrob. Agents Chemother.* 56, 2666-2682 (2012).



\* co-first authors and contributed equally

### Abstracts and Presentations

1. **G.A. Afanador**, K. Matthews, J. Gisselberg, M. Spalding, C. Freel-Meyers, S. T. Prigge “Two redox sensitive routes for mitochondrial lipoate metabolism in *Plasmodium falciparum*” Oral Presentation Molecular Parasitology Meeting Woods Hole, MA 2013
2. **G.A. Afanador**, K. Matthews, J. Gisselberg, M. Spalding, C. Freel-Meyers, S. T. Prigge “Redox sensitive mitochondrial lipoate metabolism in *Plasmodium falciparum*” Oral Presentation Institute of Biophysics Retreat, Towson, MD 2013
3. **G. A. Afanador**, S. T. Prigge “Redox sensitive mitochondrial lipoate metabolism in *Plasmodium falciparum*” Oral Presentation Malaria Interest Group, Johns Hopkins School of Public Health, Baltimore, MD 2013
4. **G.A. Afanador**, M. Spalding, S. T. Prigge “Structure and function of lipoate cofactor ligases in *Plasmodium falciparum*” Poster Presentation Molecular Parasitology Meeting, Woods Hole, MA 2011
5. **G.A. Afanador**, T. Bohec, L. Kiger, M. Marden, J. Lopez-Garriga “Ligand binding kinetics of hemoglobin II and mutants from *Lucina pectinata* over expressed in *Escherichia coli*” Poster Presentation International Society for Pharmaceutical Engineering Annual Meeting, Orlando, FL 2006
6. **G.A. Afanador**, T. Bohec, L. Kiger, M. Marden, J. Lopez-Garriga XIV “Ligand binding kinetics of hemoglobin II and mutants from *Lucina pectinata* over expressed in *Escherichia coli*” Poster Presentation International Conference on Dioxygen Binding and Sensing Proteins, Naples, Italy 2006
7. **G.A. Afanador**, A. Hoskins, J. Stubbe “Studies on the *Bacillus subtilis* Formylglycinamide Ribonucleotide Amidotransferase” Poster Presentation Annual Biomedical Research Conference for Minority Students, Atlanta, GA 2005
8. **G.A. Afanador**, A. Hoskins, J. Stubbe “Studies on the *Bacillus subtilis* Formylglycinamide Ribonucleotide Amidotransferase” Poster Presentation 44<sup>th</sup> Annual Meeting of American Society for Cell Biology, Washington D.C. 2004

### Awards

- Poster Presentation Award at the Annual Biomedical Research Conference for Minority Students Anaheim, CA, 2006.
- IDEa Network for Biomedical Research Excellence in Puerto Rico Undergraduate Student Fellowship
- SLOAN program scholarship for outstanding students conducting research in biomedical science
- Pfizer Fellowship to conduct basic research in Pharmaceutical Sciences